School of Biological and Biomedical Sciences

An investigation into two photostable retinoids and their use as tools to study retinoid function *in vivo*.

Rachel Lopez-Real

PhD Thesis

2013

Declaration

The work described herein was carried out in the Department of Chemistry, University of Durham between October 2009 and October 2012. All of the work is my own, except where specifically stated otherwise. No part of this work has previously been submitted for a degree at this or any other university.

Statement of Copyright.

Abstract

All-*trans* retinoic acid (ATRA) is essential for embryonic development and adult homeostasis. Its study has been hindered by the fact that it can be converted to isomers upon exposure to light and because its metabolites are also bioactive molecules. Recent research has indicated that ATRA can also activate two different receptor pathways *in vitro* and *in vivo*.

The present study investigates the effects of these isomers and metabolites on chick wing development using two synthetic, photostable retinoids, EC23 and EC19. These retinoids have identical structures bar the position of the terminal carboxylic acid group but surprisingly, generate different effects *in vitro* and *in vivo,* and are differentially metabolised by metabolising enzymes. EC23 mimics most of the effects of ATRA *in vivo*, including the novel phenotype of scapula malformation, while EC19 does not. Their phenotypes are further characterised in the text but EC23 produces a novel retinoid phenotype characterised by duplications of solely forelimb digit 1.

The mechanisms behind the phenotypes generated by EC23 and EC19 are explored with respect to retinoid metabolism and localisation of ATRA binding proteins at the stage of application. Both ATRA signalling pathways are investigated at HH20 of chick embryonic development which improves our understanding of the role of retinoids in limb and embryonic development. Comparison of gene expression in response to ATRA and EC23 indicates that the metabolites and isomers of ATRA do not play a role in embryonic limb development, as well as highlighting avenues for further research into the development of the scapula and elbow. A major part of the retinoid response is to stall limb development while retinoid levels recover. By comparison with other teratogens, this may be part of a common response and be pertinent to the regulation of normal embryonic development by retinoids.

Acknowledgements

I would like to thank the following people for their help and support throughout the production of this work.

My supervisors, Dr Paul Hunt and Professor Stefan Przyborski, for their help and inspiration and particularly Dr Paul Hunt for instruction in embryology and *in ovo* microsurgery. Also members of the team in the Department of Chemistry, Durham University for their collaboration and support.

Heiko Peters at The Centre for Life, Newcastle and the team at the Roslin Institute, Edinburgh for microarray processing.

Simon Cockell at the Bioinformatics Unit, Newcastle University for the initial analysis of the microarray data.

All members of the research group during my time in Durham for the enjoyable times and support throughout. Particular thanks to James Budge for his previous investigations into the effects of EC23 and EC19 *in vivo* and Bridie Murray for instruction in qPCR. I would also like to thank my current employers and friends in Nottingham for their understanding and support.

My family for their support, encouragement and understanding throughout.

Finally, I would like to thank Mark for motivating me, being my rock through the challenging times and making me smile, without which this work would have been very difficult.

List of Publications.

Publications derived from the work presented in this thesis are outlined below.

Chapter 3 forms part of a manuscript accepted for publication by the Journal of Anatomy pending minor corrections[1].

The expression of FABP5 documented in chapter 4 will be investigated in more detail by Dr. P. Hunt, Dr. R. Hunt and Prof. S. A. Przyborski. Upon completion, this will also be submitted for publication.

All material from chapter 5 is being prepared to be submitted for publication. Any further work required will be carried forward by Dr. P. Hunt and Prof. S. A. Przyborski.

[1] R.E. Lopez-Real, J.J.R. Budge, T.B. Marder, A. Whiting, P.N. Hunt, and S.A. Przyborski. Application of Synthetic Photostable Retinoids Induces Novel Limb and Facial Phenotypes During Chick Embryogenesis *In Vivo.*

Table of Contents

Table of Figures

Table of Tables

Table of Appendices.

List of Abbreviations

13CRA	13-*cis* Retinoic Acid
9CRA	9-*cis* Retinoic Acid
AER	Apical Ectodermal Ridge
Alx	Aristaless homeobox
ANR	Anterior Neural Ridge
ANZ	Anterior Necrotic Zone
AP	Anterior-to-Posterior
ATRA	All-*trans* Retinoic Acid
BCCs	Boundary Cap Cells
BCIP	5-bromo-4-chloro-3-indolylphosphate toluidine salt
Blimp1	B-Lymphocyte-Inducing Maturation Protein 1
BMP	Bone Morphogenetic Protein
BMPR1B	Bone Morphogenetic Protein Receptor 1b
cDNA	complementary DNA
CO_2	Carbon Dioxide
COS-7	CV-1 in Origin, carrying SV40-7 Cell line
CRABP	Cellular Retinoic Acid Binding Protein
CRBP	Cellular Retinol Binding Protein
cRNA	Complementary RNA
CSPG	Chondroitin Sulphate Proteoglycan
CT	Cycle Threshold
CYP	Cytochrome P450 mono-oxidase family
DBD	DNA binding domain
DEAB	4-diethylaminobenzaldehyde
DEPC	Diethyl pyrocarbonate
Dhrs3	Dehydrogenase/reductase member 3
DIG	Digoxigenin
DiI	1,1'-Dioctadecyl-3,3,3',3'-Tetramethylindocarbocyanine Perchlorate
Dlx	Distalless homeobox family
DMSO	Dimethyl sulphoxide
DNA	Deoxyribonucleic Acid
DNase	Deoxyribonuclease

DPC	Days Post Coitum
DR1-5	Direct Repeat 1-5
DV	Dorsal-to-Ventral
ECM	Extracellular Matrix
EDTA	Ethylenediaminetetraacetic acid
Emx2	Empty Spiracles Homeobox 2
Enpp2	Ectonucleotide pyrophosphatase/phosphodiesterase 2 or Autotaxin
Eya2	Eyes absent homolog 2
FABP5	Fatty Acid Binding Protein 5
FEZ	Frontonasal Ectodermal Zone
FG	Fibroblast Growth Factor
FGFR	Fibroblast Growth Factor Receptor
FNM	Frontonasal Mass
GAPDH	Glyceraldehyde-3-phosphate Dehydrogenase
GC	guanine/cytosine
GC-RMA	Genechip-robust Multiarray Averaging
GDF	Growth and Differentiation Factor
Gli	GLI Family Zinc Finger
Gnot1	Gnot1 Homeodomain Protein
GNRH	Gonadotrophin Releasing Hormone
Gsc	Goosecoid Homeobox
H_2O	Water
Hand2	Heart and Neural Crest Derived 2
Hes1	HLH factor hairy and enhancer of split
Hey1	Hairy/enhancer of split related with YPWR motif 1
HH	Hamburger and Hamilton Stage
Hox	Homeobox
hoxb8	Homebox protein B8
HPLC	High-performance Liquid Chromatography
Hrs	Hours
HSPG	Heparan Sulphate Proteoglycans.
Id3	DNA binding protein Id-3
INZ	Interdigital Necrotic Zone
LBD	Ligand Binding Domain

Lhx9	LIM Homeobox 9
Lmx1b	LIM homeobox transcription factor 1 beta
LPM	Lateral Plate Mesoderm
Meis1/2	Myeloid ecotropic viral integration site (Meis) Homeobox 1/2
Msx1/2	Msh Homeobox 1/2
Myf5	Myogenic Factor 5
Myod1	Myogenic Differentiation 1
NBT	nitro-blue tetrazolium chloride
n-cadherin	Neural Cadherin/cadherin 2
NCBI	National Centre for Biotechnology Information
NCoR	Nuclear receptor co-repressor 1
NLS	Nuclear Localisation Sequence
OP	Opaque Patch
ORF	Open Reading Frame
Pax1/9	Paired Box 1/9
PBS	Phosphate Buffered Saline
Pbx1	Pre-B-Cell Leukaemia Homeobox 1
PCR	Polymerase Chain Reaction
PD	Proximal-to-Distal
PNZ	Posterior Necrotic Zone
POR	Cytochrome P450 Oxidoreductase
Postn	Periostin
PPAR	Peroxisome Proliferator-Activated Receptor
PRE	PPAR Response Element
PZ	Progress Zone
Raldh	Retinaldehyde Dehydrogenase
RAR	Retinoic Acid Receptor
RARE	Retinoic Acid Response Element
RBP	Retinol Binding Protein
RDH	Retinol Dehydrogenase
RIN	RNA Integrity Number
RNA	Ribonucleic Acid
RNase	Ribonuclease
ROR1	Receptor Tyrosine Kinase-like Orphan Receptor 1

RQ	Relative Quantification
rRNA	ribosomal RNA
RXR	Retinoid X Receptor
RXRE	Retinoid X response element
Sall1	Sall-like 1
SDS	Sodium Dodecyl Sulphate
SH3	Src Homology Domain 3
SHH	Sonic Hedgehog Homologue
Shox	Short Stature Homeobox
siRNA	Small interfering RNA
SMRT	Silencing Mediator of Retinoic Acid and Thyroid Hormone Receptor
Snai1/2	Snail homologue 1/2 (Drosophila)
Sox9	SRY (Sex Determining Region-Y)-box 9
SSC	Saline Sodium Citrate
Stra6	Stimulated by Retinoic Acid gene 6
Sulf1	Sulfatase 1
TAE	Tris-Acetate EDTA
TBE	Tris-Borate EDTA
TBS	Tris-buffered Saline
Tbx5	T-box 5
TE	Tris-EDTA
TFs	Transcription Factors
TGF	Transforming Growth Factor
TR	Thyroid Receptor
Tris	2-Amino-2-(hydroxymethyl)-1,3-propanediol
Tris-HCl	Tris-Hydrochloride
tRNA	transfer RNA
TTNPB	4-[(E)-2-(5,6,7,8-Tetrahydro-5,5,8,8-tetramethyl-2-naphthalenyl)-1-propenyl]benzoic acid
VAD	Vitamin A Deficiency
VDR	Vitamin D Receptor
Wnt	Wingless-type MMTV Integration Site
ZPA	Zone of Polarising Activity
αMEM	αMinimum essential medium

Chapter 1) Literature Review and Rationale for the present study.

Introduction.

Retinoids are known to be essential for the development of many organ systems in the developing vertebrate embryo. Their excess or deficiency can cause malformation to particular regions of the developing embryo in mouse and chick e.g. the limb (see p22). It has been shown that the most bioactive, naturally occurring retinoid is all-*trans* retinoic acid (ATRA) and excess or deficiency of this compound causes the most severe effects (see p4; (Abu-Abed et al., 2001; Cui et al., 2003; Lammer et al., 1985; Mic et al., 2004; Niederreither et al., 2002b; Yashiro et al., 2004)). The severity of the phenotype from excess retinoid depends on the stage and dose of exposure (Mark et al., 2006). Notably, severe malformations have been documented in human embryos exposed to retinoid during pregnancy. These are collectively known as retinoic acid embryopathy and include: microtia, micrognathia, cleft palate, heart, ocular and central nervous system malformations (Lammer et al., 1985). Vitamin A deficiency (VAD) can also generate embryonic malformations e.g. in avian embryos VAD is lethal at E3.5. These embryos exhibit: abnormal cardiac, ocular and central nervous system development, no large extra-embryonic blood vessels, shortened body and no axial rotation (Cui et al., 2003; Kostetskii et al., 1996). Vitamin A is also needed postnatal for correct growth, reproduction and vision (Mark et al., 2006).

Considering these effects *in vivo*, research has focused on how ATRA causes these phenotypes by investigating the ATRA signalling pathway and its effects on transcription. Considering that alteration of retinoid levels causes severe phenotypes, research has also investigated the control of its metabolism. The effects of retinoids have been well studied, as described in the following sections, and these compounds can be used for treatment of psoriasis as well as certain cancers (Njar et al., 2006). They have also been implicated in manipulation of stem cells which may have wide implications for future medicine (Christie et al., 2008; Maltman et al., 2009). However, some aspects of their role in development and their genetic targets are not well characterised. The presence and role of their metabolites and isomers during embryonic development is also poorly characterised. The aim of this review is to summarise the progress made to date in the study of ATRA signalling, its role in limb development and to introduce concepts pertinent to the present study.

The structure of ATRA.

The structure of ATRA is shown in figure 1.1 below. As can be seen, it can be split into three regions: hydrophobic domain (β-ionene ring; blue box), linker region (isoprene tail; bracket) and polar region (carboxylic acid tail; red circle). The precursors of ATRA are retinol (vitamin A) and retinal which have an alcohol or aldehyde group substituted in place of the carboxylic acid group. ATRA can also be converted into isomers 9-*cis* (9CRA) and 13-*cis* retinoic acid (13CRA; (Christie et al., 2008; Thaller et al., 1993)) or oxidative metabolites including: 4-*oxo*-retinoic acid, 4-*hydroxy*-retinoic acid, 5, 6-*epoxy*-retinoic acid, 16-*hydroxy*-retinoic acid and 18-*hydroxy*-retinoic acid (see p30; (Topletz et al., 2012)).

The production of synthetic retinoids is an area of important research to direct the differentiation of stem cells and to improve the action of retinoids for medical purposes. Synthetic retinoids share key structural features (Dawson et al., 1989) but can actually be very different, as shown by the structure of 4-[(E)-2-(5,6,7,8-Tetrahydro-5,5,8,8-tetramethyl-2-naphthalenyl)-1-propenyl]benzoic acid (TTNPB) in figure 1.1. Alteration of these major parts of the retinoids can affect retinoid activity, affinity with receptors, receptor specificity (Germain et al., 2004; Klaholz et al., 2000), affinity with binding proteins (Kleywegt et al., 1994) and metabolism *in vivo*.

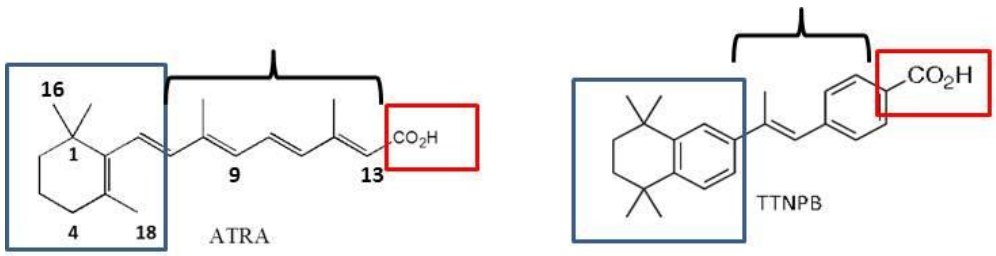

Figure 1.1: The structures of retinoids: ATRA and TTNPB.

Blue boxes correspond to the hydrophobic region (β-ionene ring in ATRA). Black brackets indicate the linker region. Red boxes indicate the polar region or carboxylic acid group. Numbers correspond to the carbon above. Abbreviations: ATRA, all-trans retinoic acid; TTNPB, 4-[(E)-2-(5,6,7,8-Tetrahydro-5,5,8,8-tetramethyl-2-naphthalenyl)-1-propenyl]benzoic acid.

Retinoid metabolism.

ATRA is produced from its precursors by the alcohol dehydrogenases and the retinaldehyde dehydrogenases (RALDHs). The alcohol dehydrogenases catalyse the production of retinal while the retinaldehyde dehydrogenases catalyse ATRA synthesis. Given the ubiquitous expression of the alcohol dehydrogenases, the RALDH enzymes are thought to control ATRA synthesis *in vivo* (Rhinn and Dolle, 2012). Despite their ubiquitous expression some alcohol dehydrogenases may be important for embryonic development. It is clear that retinal produced by retinol dehydrogenase 10 (RDH10) is important for correct limb, brain and craniofacial development from *Rdh10* knockout mice (Sandell et al., 2007). The importance of RALDH enzymes in ATRA production has been supported by the embryonic lethal *Raldh2* knock out mouse (Niederreither et al., 1999) as well as evidence that RALDH2 uses retinal as a substrate (Wang et al., 1996; Zhao et al., 1996). Other enzymes have been implicated in the production of ATRA from retinol including CYP1B1 which is a cytochrome oxidase but, unlike CYP26, it does not metabolise ATRA (Chambers et al., 2007; Choudhary et al., 2007). This enzyme is also present in vertebrate embryogenesis, expressed in the proximal wing bud and implicated in neural development similar to *Raldh2* (Chambers et al., 2007). The effects of ATRA are mediated by nuclear translocation to the retinoic acid receptors which alter transcription (see p6-7; (Mark et al., 2006)).

ATRA is then known to be metabolised by members of the P450 cytochrome oxidase superfamily (Roberts et al., 1980). These include CYP2C8, CYP2C9 and CYP3A4 demonstrated to be present in hepatic microsomes (Marill et al., 2000; McSorley and Daly, 2000; Nadin and Murray, 1999). However, ATRA is also metabolised by a group of retinoid specific P450 cytochrome mono-oxidases: CYP26A1, CYP26B1 and CYP26C1 (Taimi et al., 2004; White et al., 1997; White et al., 1996; White et al., 2000). The CYP26 enzymes are also known to be retinoid inducible (Loudig et al., 2000; Loudig et al., 2005; White et al., 1996) while *Raldh2* is down-regulated by retinoid administration at E8.5 (Niederreither et al., 1997; Swindell et al., 1999) providing a mechanism by which ATRA levels may be tightly controlled during development.

The structure of the CYP26 retinoid metabolising enzymes bound to ATRA has been difficult to elucidate. Previous research has relied on structural knowledge of other family

members and modelling studies but the research to date has indicated that the structure of the CYP active site is flexible to accommodate many different structures due to its role in xenobiotic metabolism. Oxidation by these enzymes requires residues from many regions of the enzyme, particularly helices I and K (Zeldin and Seubert, 2007). Modelling studies indicate that the active site of CYP26A1 is a hydrophobic tunnel similar to that of retinoic acid receptor (RAR) with a polar group for the carboxylic acid group to dock, involving R86. This work also suggests that ATRA binds to the active site with carbon 4 held 5.3A away from the heme group, favouring its oxidation (Gomaa et al., 2006)consistent with earlier work suggesting that these enzymes catalyse the 4-hydroxylation of ATRA to more polar derivatives (Frolik et al., 1979; Topletz et al., 2012; White et al., 1997).

Knockout mouse models of the *cyp26* enzymes exhibit the effects of retinoid excess and indicate that catabolism plays a major role in the control of ATRA during development (Abu-Abed et al., 2001; Yashiro et al., 2004). Whilst the oxidative derivatives of ATRA have been shown to bind to ATRA binding proteins including the receptors (Idres et al., 2002; Maden and Summerbell, 1986), they are not generally thought to be required for embryonic development (see p32; (Niederreither et al., 2002a; Williams et al., 1987)). Retinoid metabolism is also affected, indirectly, by cytochrome P450 oxidoreductase (POR) which is the electron acceptor for CYP enzymes. Knockout of this enzyme causes effects on the developing limb: reduced length, autopod and elbow malformations (Ribes et al., 2007; Schmidt et al., 2009). Correct regulation of ATRA levels may be very important in some disorders e.g. DiGeorge syndrome. This has been studied using *Tbx1* knockout mice and it has been shown that CYP26 enzymes are targets of TBX1. Inhibition of the CYP26 enzymes has phenocopied *Tbx1* null mice (Roberts et al., 2006).

The expression of ATRA synthesising and metabolising enzymes.

ATRA levels are tightly controlled during embryonic development by the restricted and complementary expression of synthesising enzymes (*Raldh1-3* and *cyp1b1*) and metabolising enzymes (*Cyp26A1-C1*) (Blentic et al., 2003; Chambers et al., 2007; MacLean et al., 2001; Niederreither et al., 1997; Reijntjes et al., 2003, 2004; Swindell et al., 1999). This ensures that areas of the developing embryo are maintained in areas of increased or decreased ATRA signalling which is important for the correct development of many organs e.g. the distal limb (Pennimpede et al., 2010a; Yashiro et al., 2004). *Raldh2* is

expressed in the posterior embryo at early stages and later is restricted to the somites and the proximal limb. It is also observed surrounding developing arteries in the forelimb and heart, interdigital regions and the ventral motor horns for forelimb innervation (Blentic et al., 2003; Niederreither et al., 1997). However, *Raldh2* expression does not completely correlate with areas of retinoid signalling indicating that other enzymes are involved in such as *Raldh1* and *Raldh3* (Blentic et al., 2003; Niederreither et al., 1997).

Cyp26 enzymes have been shown to be restricted and are observed in the anterior embryo at early stages, however, *Cyp26a1* is later seen in the tail bud and posterior embryo in mouse and chick (Blentic et al., 2003; MacLean et al., 2001; Swindell et al., 1999). C*yp26a1* and *cyp26b1* are expressed in complementary domains in the mouse branchial arches: *cyp26a1* is in neural crest cells while *cyp26B1* is in ectoderm and endoderm. This may reflect the need for differential turnover of ATRA in these tissues. *Cyp26b1* is involved in tail, rhombomere, somitic and heart development in chick and quail (Reijntjes et al., 2003). *Cyp26a1* and *Cyp26b1* are expressed in the distal limb from HH20: *cyp26a1* expression is in stripes adjacent to the AER and *cyp26b1* expression overlaps with the progress zone (PZ) in the mesenchyme, which is similar to mouse (Blentic et al., 2003; MacLean et al., 2001; Reijntjes et al., 2003; Swindell et al., 1999). *Cyp26c1* expression has also been documented in chick and has been observed in the anterior embryo, somites and then restricted to areas of the head including the frontonasal mass (Reijntjes et al., 2004). Altogether, it has been suggested that the RALDH and CYP26 enzymes can produce gradients of ATRA signalling across the embryo e.g. in the limb where ATRA production is high proximally and catabolism is high distally, indicating that a proximal-to-distal (PD) gradient may exist. This may also be important for development given that the CYP26 enzymes have different enzyme kinetics (Topletz et al., 2012) and their differential distribution provides another layer of complexity in that they can further influence ATRA levels during development.

Signalling pathway:

Retinoids enter vertebrates as retinyl esters or carotenoids from other animals or plants. It is thought that retinyl esters are carried to their site of action in the bloodstream via chylomicrons or protein-bound. They may also be metabolised to either ATRA or its derivatives via the CYP26 enzymes as mentioned in previous sections. On entering the

cell they are sequestered by cellular retinoic acid binding protein 1 (CRABP1) or channelled to nuclear receptors by CRABP2 as seen right in figure 1.2 (Blomhoff and Blomhoff, 2006; Budhu and Noy, 2002). The nuclear receptors for retinoids are heterodimers of RAR and retinoid X receptors (RXR) (Astrom et al., 1994; Leid et al., 1992b; Yu et al., 1991), which are a subgroup of the steroid receptor family (Rochette-Egly and Germain, 2009). These receptors are bound to retinoic acid response elements (RAREs) via their DNA binding domain and in the absence of ligand, recruit co-repressors. Upon binding ATRA or retinoids, there is a conformational change in the receptor causing the release of co-repressors and recruitment of co-activators such as p160 causing a change in transcription (Idres et al., 2002; Rochette-Egly and Germain, 2009). It has been established that most effects of ATRA are mediated by RAR given that RXR agonists cannot rescue *Raldh2* knockout mice (Mic et al., 2003). However, the function of RXR is not completely understood. Upon entering the cell ATRA may also be channelled to the nucleus by fatty acid binding protein 5 (FABP5) and activate an alternative pathway (see p20; figure 1.2, left side). I shall now review each of the components of the CRABP2/RAR mediated pathway in turn.

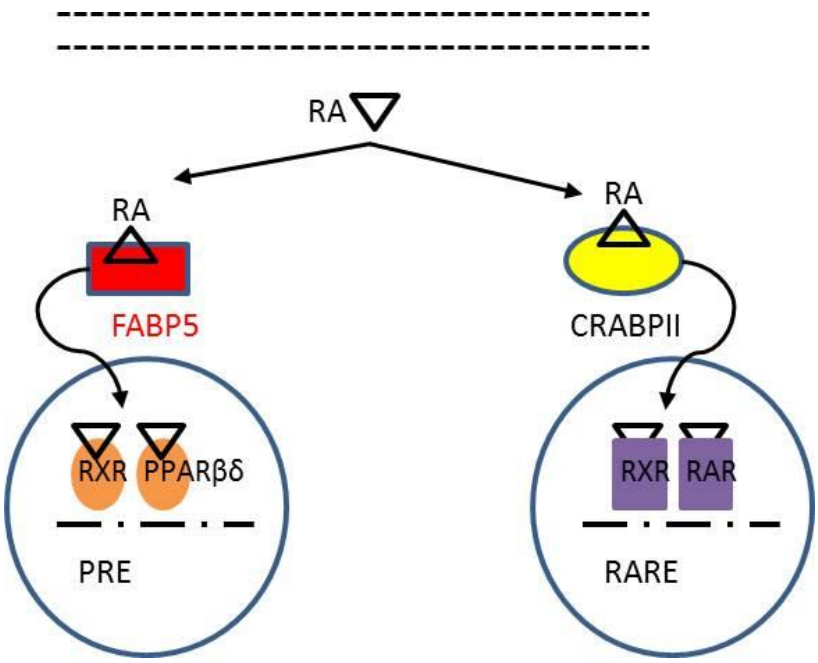

Figure 1.2: Two receptor pathways activated by ATRA.

Black dashed lines represent the cell membrane and blue circles represent the nucleus. Upon entering the cell, ATRA can be translocated to the nucleus by either CRABP2 or FABP5 which then causes activation of RAR or PPARβδ mediated transcription. Abbreviations: RA, ATRA; CRABPII, cellular retinoic acid binding protein 2; FABP5, fatty acid binding protein5; PPAR, peroxisome proliferator activated receptor; PRE, PPAR responsive element; RAR, retinoic acid receptor; RARE, retinoic acid response element; RXR, retinoid X receptor.

CRABP

Two CRABPs have been reported in chick and mouse: CRABP1 and CRABP2 (Kitamoto et al., 1989; Maden et al., 1988). CRABP2 translocates ATRA to the nucleus (Budhu and Noy, 2002) due to a nuclear localisation sequence (NLS) only apparent from its tertiary structure (Sessler and Noy, 2005). CRABP2 containing ATRA interacts with RARα and is particularly important at low retinoid concentrations (Budhu and Noy, 2002). Considering the importance of its role in retinoid signalling CRABP2 binding is important for retinoid activity as shown by those retinoids, e.g. 13CRA, which cannot bind to it and therefore exhibit diminished activity (Keeble and Maden, 1984; Maden and Summerbell, 1986; Maden et al., 1991). However, the role of CRABP1 is less clear. CRABP1 does not directly affect transcription or interact with RARα (Venepally et al., 1996). The affinity of ATRA for CRABP1 is higher than that of CRABP2 (Scott et al., 1994) and it has been implicated in sequestering ATRA from its receptors (see p16) or enhancing retinoid metabolism as it is shown to interact with the CYP26 enzymes (Dong et al., 1999; Fiorella and Napoli, 1991; Kleywegt et al., 1994).

The structure of the CRABP proteins has been investigated to determine how retinoids bind and why some retinoids have higher affinity. The ligand binding domain (LBD) is known to be narrow and hydrophobic to mimic the structure of ATRA. It also contains a polar region specifically containing Arg132, Tyr134 and Arg111 which interacts with the carboxylic acid group. 18 other amino acids interact with ATRA when bound. The structure of CRABP promotes binding of ATRA with the β-ionene ring in *cis* with the rest of the structure and suggests that the binding of 9CRA is therefore less favourable. Interestingly it has been noted that the β-ionene ring protrudes from the protein presumably allowing action of CYP26 mediated metabolism at carbons 4, 5, 6, 16 and 18 (Kleywegt et al., 1994). However, this does not explain the mechanism by which ATRA is shuttled between CRABP2 and RAR given that the carboxylic acid group is also bound to the centre of RAR LBD. However, it is known that residues Gln75, Pro81 and Lys102 are necessary for the transfer of ATRA (Budhu and Noy, 2002).

Despite their proposed importance in retinoid signalling *Crabp1* and *Crabp2* knockout mice were normal although a slight limb defect was noted in *Crabp2* null mice: extra post-axial bone in 45% of forelimbs. *Crabp1*/*Crabp2* double null mice exhibited this defect in 83% of forelimbs, but no other defect was seen. This defect was noted to be more severe in

double knockouts in that it resembled an additional digit (Lampron et al., 1995). Given that CRABP2 channelling has been implicated most at low retinoid concentrations characterisation of these mutants in VAD development would be of interest (Budhu and Noy, 2002; Lampron et al., 1995). However, investigation of this has not been published to date.

RARs.

The RARs are transcription factors which are known to bind DNA and change gene transcription in response to ligand binding. The RARs contain a LBD, a DNA binding domain (DBD) and dimerization regions for RXR binding. The RARs have a modular structure and can be split into A-F domains with the F domain specific to RARs. The A and B domains are involved in receptor activation independent of ligand binding. The C domain is the DBD while the E domain is the LBD and both C and E domains are involved in dimerization (Bastien and Rochette-Egly, 2004; Leid et al., 1992a; Michaille et al., 1995). The D domain is thought to be a hinge region containing a NLS and the function of the F domain is unknown but both it and the A domain are divergent between species and types of receptor. C and E regions are the most conserved suggesting that the function of retinoid signalling is highly conserved. Domains A and E are thought to interact on ligand binding to activate the receptor (Bastien and Rochette-Egly, 2004). Each of the receptors also has multiple phosphorylation sites and has been shown to be degraded by the ubiquitin-protease system. This may function to attenuate and regulate the retinoid response *in vivo* (Bastien and Rochette-Egly, 2004).

RARs have been shown to activate transcription of target genes and each RAR has a different affinity for ATRA as well as a different effect on gene induction: the biggest change in gene expression is caused by RARα binding (Astrom et al., 1990). The DBD in domain C is a zinc finger DBD which binds and recognises RAREs. RAREs are characterised by direct repeats of a consensus sequence: (G/A)G(G/T)TCA spaced by one, two or five nucleotides (DR1, DR2, DR5; (Bastien and Rochette-Egly, 2004)). The spacing of the direct repeats is thought to determine the orientation and function of the heterodimers which bind which, in turn, is thought to influence RAR/RXR action (Kurokawa et al., 1994). RARs usually bind 5’ on DR5 RAREs, however, RARs were thought to bind DR2 elements with reversed orientation i.e. binding 3’ causing gene repression rather than activation (Leid et al., 1992a). However, more recently, RARs have

also been shown to bind DR2 elements in a similar orientation to DR5 elements *in vitro* (Rochette-Egly and Germain, 2009). This reversal in orientation is also seen on RAREs with a DR1 spacer but DR1 elements (Rastinejad et al., 2000) have only been found on one vertebrate gene-*CRBPII* in rat (Mangelsdorf et al., 1991; Rochette-Egly and Germain, 2009). ATRA has been shown to activate the transcription of human and mouse *Crabp2 in vitro* via a DR5, and DR1 and DR2 elements respectively (Astrom et al., 1994). An *in silico* study of DR5 RARE containing genes conserved between 13 species has been carried out and shown that many genes contain multiple RAREs and their differential binding may allow complex regulation of retinoid genetic targets (Lalevee et al., 2011). In the absence of ATRA, RARs may still bind to DNA although more bind in the presence of ligand (de The et al., 1990; Lalevee et al., 2011). It has been reported that unliganded RARs repress gene expression: particularly during the development of the skeleton (Cash et al., 1997) and anterior structures in *Xenopus* (Koide et al., 2001). This is due to the fact that unliganded RARs bind co-repressors, such as silencing mediator of retinoid and thyroid hormone receptor (SMRT) and nuclear receptor co-repressor 1 (NCoR), but upon ligand binding, these co-repressors are released allowing co-activators to bind as the cofactor binding sites are overlapping (Benko et al., 2003).

There are three subtypes of RAR which are encoded on separate genes (α, β and γ) producing three isotypes (Zelent et al., 1989). Interestingly, the isotypes of the RARs have been shown to be more similar between species than to the other RARs within a species suggesting that their functions are highly conserved (Zelent et al., 1989). Multiple isoforms can be generated by alternative splicing and differential promoter activation (Bastien and Rochette-Egly, 2004). A number of RAR isoforms have been reported: RARα1, RARα2, RARβ1, RARβ2, RARγ1 and RARγ2 (Kastner et al., 1990; Zelent et al., 1989) but only one RARγ isoform appears to be characterised in chick corresponding to RARγ2 (Michaille et al., 1994; Michaille et al., 1995; Smith and Eichele, 1991; Smith et al., 1995). Other isoforms of *Rarγ* have been observed in chick and mouse. The seven isoforms isolated in mouse are thought to differ in 5' un-translated region while those in chick have not been characterised (Kastner et al., 1990; Michaille et al., 1994). It is believed, however, that *Rarγ1* and *Rarγ2* are the major isoforms involved in embryogenesis (Kastner et al., 1990).

It has been shown that the RARs have two promoters (Leid et al., 1992a), one of which is retinoid inducible. *Rarβ* has two promoters: one in the 5' un-translated region and the other in the intronic region proximal to exon 3 (Zelent et al., 1991). Differential promoter activation produces *Rarβ1* and *Rarβ2* with isoform specific exons in their A regions: *Rarβ1* contains exon 1 while *Rarβ2* contains exon 3. Both of these gene products can be alternately spliced in the A domain to generate *Rarβ3* (containing exons 1 and 2) and *Rarβ4* with an A domain containing only 4 amino acids (Kastner et al., 1990; Nagpal et al., 1992; Nohno et al., 1991). However, only *Rarβ2/4* is retinoid inducible as the *Rarβ2* promoter contains a retinoic acid response element (RARE) (Mendelsohn et al., 1994a; Nagpal et al., 1992). Similarly, *Rarα2* and *Rarγ2* have been documented to be retinoid responsive (Lampron et al., 1995; Lehmann et al., 1992; Leid et al., 1992b). These isoforms are often differentially expressed suggesting subtly different functions *in vivo* (Mollard et al., 2000; Nagpal et al., 1992; Smith et al., 1995).

RARs specifically respond to nanomolar concentrations of ATRA but it has been reported that RXR can bind both ATRA (micromolar concentrations) and its isomer, 9CRA, with higher affinity (Heyman et al., 1992; Levin et al., 1992; Yu et al., 1991). The ligand binding pocket of RAR is found in the E domain and consists of twelve α-helices separated by a β-sheet. Helix 12 of the LBD has been shown to be important for transcription and it is also known as activation function 2 (AF-2) (Mark et al., 2006). It is ligand dependent and interacts with the ligand independent activation function 1 (AF-1) (Bain et al., 2007) found in the A and B domains, which enhance the retinoic acid response. The AF-1 region is isoform specific as it is partially overlaps the A domain but the portion in the B region is more conserved and includes sites which become phosphorylated in response to ligand (Bain et al., 2007). These phosphorylation sites are important for the recruitment of SH3 or WW domain containing proteins and may regulate the function of these receptors or allow downstream signalling (Rochette-Egly and Germain, 2009). When ligand-bound, helix 12 undergoes a significant conformational change to form a hydrophobic cleft with helices 3 and 4 of the E domain. This causes the recruitment of co-activators such as the P160 subfamily of steroid receptor co-activators which contain the LXXLL motif (Rochette-Egly and Germain, 2009). Consequently there is a reprogramming of gene expression as co-activator and co-repressor binding are mutually exclusive (Bain et al., 2007). Less is known about gene regulation by RARβ and RARγ although a study has investigated the RARγ specific targets in mouse limb bud culture (Galdones and Hales,

2008). Some research has been carried out on the genetic targets of retinoids *in vitro* (Ali-Khan and Hales, 2006; Galdones and Hales, 2008; Williams et al., 2004) but the complete transcriptional response to retinoids has been little characterised *in vivo* bar the studies of retinoid on whole rat embryos (Feng et al., 2010; Luijten et al., 2010). This is an area for further work and which is addressed in the present study (see chapter 5 for more details). RAR binding clearly has potential to cause a great change in gene expression dependent on the distribution of these receptors (see p15).

The carboxylic acid group is important for RAR binding by an electrostatic guidance mechanism based on the attraction of this polar region to the LBD (Renaud et al., 1995) and, similarly, it is also important for the binding affinity for CRABP and CYP26 enzyme binding (Fiorella and Napoli, 1991; Gomaa et al., 2006; Kleywegt et al., 1994). There has been some investigation ligand specificity of the LBD in order that specific synthetic analogues could be synthesised (Lund et al., 2005; Piu et al., 2005). Ligand-bound RARγ has been crystallised either whole (Klaholz et al., 2000) or residues 178-723 only (Renaud et al., 1995), both of which indicated that three residues are important for carboxylic acid binding: Arg278, Ser289 and Leu233, with the equivalent residues shown for RARα and RARβ (table 1.1). The difference in these residues has been suggested to affect receptor selectivity as they are the only differences between the LBD of the receptors. The amino acids at positions 1 and 2 interact with the isoprene tail while the amino acid at position 3 interacts with the β-ionene ring. RARβ was thought to have a smaller LBD than the other RARs (Klaholz et al., 2000) but crystallisation of its structure indicates that it has an extra cavity which allows binding of agonists with a more bulky hydrophobic region (Germain et al., 2004).

Table 1.1: The different amino acids in the ligand binding domain of the retinoic acid receptor subtypes.

RAR	Amino Acid Position		
	1	2	3
RARγ	Ala234	Met272	Ala397
RAR α	Ser232	Ile270	Val395
RAR β	Ala225	Ile263	Val388

Amino acid position refers to the differences observed by Klaholz et al (2000). Abbreviations: RAR, retinoic acid receptor; Ala, alanine; Ile, isoleucine; Met, methionine; Ser, serine; Val, valine.

An electrostatic guidance mechanism has been suggested for RARγ ligand binding. The carboxylic acid group enters first and pulls the molecule down the electrostatic gradient, with the C-terminal helix 12 forming a lid on the LBD when bound. This leads to burial of ATRA in the hydrophobic binding site stabilised by hydrogen bonds and Van der Waals forces (Renaud et al., 1995).

The specific functions of the RARs are not well characterised but it appears that RARγ is highly involved in chondrogenesis and bone development from its expression during embryonic development (see p15) and its genetic targets in micromass cultures (Galdones and Hales, 2008) although RAR targets *in vivo* are unknown. Another source of information on receptor function could be mutant mice. However, comparison of the single receptor knockout mice and vitamin A deficiency (VAD) has indicated that the RARs are functionally redundant. *Rarα* knockout mice exhibit post-partum lethality, growth deficiency and testicular germinal epithelium degeneration (Lohnes et al., 1994). *Rarβ* knockout mice are fertile but exhibit eye malformations and transformation of certain vertebrae, but their limbs are normal suggesting that RARβ is not necessary for ATRA induced limb malformations (Ghyselinck et al., 1997; Luo et al., 1995). *Rarγ* null mutants are growth deficient, lethal early, infertile and exhibit vertebral transformations (Lohnes et al., 1993). Interestingly, they did show resistance to ATRA induced malformations (Iulianella and Lohnes, 1997; Lohnes et al., 1993). However, compound knockout of the RARs recapitulate the malformations exhibited in VAD embryos. RAR double knockouts do also exhibit some malformations which are not present in VAD embryos (Lohnes et al., 1994; Mendelsohn et al., 1994b). Despite the effects of ATRA on limb development (see p25) only one RAR double knockout combination caused a limb defect: *Rarα/γ* which exhibits scapula malformation, thickened humerus, shortened skeleton and delayed ossification (Lohnes et al., 1994).

RXR.

RXR is necessary for RAR function (Zhang et al., 1992) although its actual role in retinoid signalling has been debated. RAR mediated retinoid signalling is known to be most important for embryonic development as *Raldh2* knockouts were not rescued upon treatment with an RXR ligand (Mic et al., 2003). As mentioned previously, RXR binds

9CRA with higher affinity than ATRA and RAR which is thought to be due to the number of hydrogen bonds formed with the retinoid in the LBD: RXR forms two while RAR forms three (Heyman et al., 1992; Sussman and de Lera, 2005).

RXR homodimers can form and bind similar elements to RAR/RXR heterodimers but it has been shown that RAR/RXR heterodimers inhibit RXR homodimer binding. RAR is thought to allosterically inhibit ligand binding RXR through binding to the upstream half site of DR1, however other partners of RXR do not (Kurokawa et al., 1994). This has led to the hypothesis that RXR is submissive to RAR function. It has also been documented that an RXR selective ligand can bind when in RAR/RXR heterodimer but that the co-repressors on RAR/RXR are not released. Interaction of the co-activator p160 is enhanced with both RAR and RXR present indicating that activation of RAR or both are needed to contribute to cofactor binding (Germain et al., 2001).

Similar to RAR, it has been reported that there are three isotypes of RXR: RXRα, RXRβ and RXRγ (Mangelsdorf et al., 1992; Mangelsdorf et al., 1991). RXRs can also form homodimers or heterodimerise with other nuclear receptors such as peroxisome proliferator activated receptor (PPAR), vitamin D receptor (VDR) or thyroid receptor (TR) to mediate transcription, however, they have been shown to prefer different response elements (DR1, DR3 and DR4 elements respectively; (Kliewer et al., 1992; Leid et al., 1992b). *Rxrs* are expressed in developing embryo but levels of *Rxrγ* are much lower than the other isotypes. It has been documented that the *Rxrs* are not expressed in the developing limb (Mangelsdorf et al., 1992) but northern blotting has shown *Rxrγ* in the HH20 chick limb bud (Thaller et al., 1993). However, *Rxrα* expression has been documented from HH12-22 in chick: from rhombomere 6 to somite 9, roof plate, neural crest and limb bud. Unlike RAR, addition of ligand (9CRA) augments expression rather than expanding it (Hoover and Glover, 1998). The expression of *Rxrα* in the chick wing bud was further characterised as present in the ectoderm and mesenchyme and higher in the dorsal, anterior, proximal region (Seleiro et al., 1995). Consistent with the idea that RXRs are not essential for retinoid signalling *Rxrγ* null develop normally and are shown to be functionally redundant with *Rxrα/β* by compound mutants. *Rxrα* nulls, however, have similar ocular and cardiac defects to those seen in VAD as do compound *Rar*/*Rxr* nulls indicating that *Rxrα* is the most important for embryonic development (Krezel et al., 1996). *Rxrα* nulls develop normally until development arrests at E15.5 but exhibit normal limb development and are

resistant to retinoid induced limb malformations, indicating that this subtype is likely to be most important during limb development (Sucov et al., 1995).

The expression of *Rars* and *Crabp* during embryonic development.

The distribution of these receptors and CRABPs has been investigated during mouse development and in chick, to a lesser extent, mainly by sectioned *in situ* hybridisation with ^{35}S autoradiography (Mollard et al., 2000). Whilst this is important data, this technique has limitations in that it depends on the interpretation of 2D images to recreate a 3D expression pattern. The use of ^{35}S autoradiography generates a high signal to noise ratio and it can be difficult to detect expression in single cell layers due to sectioning and low resolution e.g. apical ectodermal ridge (AER). This suggests a need to re-examine the expression of these genes in intact embryos.

The expression of *Crabps* in development has been well characterised in the mouse model but is less characterised in the chick model. During development *Crabp* is expressed at the forebrain-midbrain boundary, cranial ganglia, branchial arch mesenchyme, frontonasal mass, limb and lateral plate mesoderm (Ruberte et al., 1991). *Crabp2* has been shown to be expressed in bone, tendon, muscle and skin throughout chick development by northern blotting (Kitamoto et al., 1989). To date, most research has focused on the localisation of CRABP2 and CRABP1 proteins in chick, however, investigations into transcript localisation have been characterised in mouse (summarised in table 1.2). CRABP1 is seen at high levels in the limb bud at E4 of chick development while CRABP2 is more widespread (Maden, 1994). CRABP1 is localised in a gradient anterior-posterior (AP) with levels highest at the anterior wing bud (Maden, 1994; Maden et al., 1988; Scott et al., 1994). CRABP2 is found in the developing limb bud between HH21-27 and is restricted to the distal limb bud or progress zone at HH23, specifically the middle and posterior progress zone as well as the dorsal and ventral muscle masses (Miyagawa-Tomita et al., 1992; Scott et al., 1994). However, this is contradictory with other studies which find no AP gradient of CRABP2 in the progress zone (Maden, 1994). These results are also distinct from those in mouse (compare tables 1.2 and 1.3) and indicate that these proteins may play distinct roles in these organisms.

The distribution of CRABP1 and CRABP2 proteins have been implicated in the production or exacerbation of the ATRA gradient in the limb bud described previously as increased ATRA in the posterior and low in the anterior wing (Thaller and Eichele, 1987). If the role of CRABP1 is to sequester ATRA in the anterior limb and present it to the CYP26 enzymes for metabolism (Dong et al., 1999; Fiorella and Napoli, 1991), this would account for the higher levels of free ATRA in the posterior limb. The CRABP2 present in the posterior progress zone would therefore indicate ATRA signalling would be important for limb patterning and growth, however, given the expression of reporter genes (discussed p27) this is unlikely to be the case. Despite being observed in bone tissue (Kitamoto et al., 1989), it is absent from the condensations in the developing limb similar to the distribution observed in mouse and is present in the interdigit mesenchyme in mouse (Dolle et al., 1989; Miyagawa-Tomita et al., 1992; Mollard et al., 2000).

The expression of the *Rar* isotypes has been well investigated in mouse embryonic development but few studies have investigated the expression of the isoforms in mouse development. In chick there is less data available and none in the intact embryo which represents an area of further study. Considering the role of the RARs in the retinoid signalling pathway and the alteration of the A domain caused by the production of the RAR isoforms described above, it ought to be further investigated and will be addressed in this work. This section summarises the expression of the RARs known to date with particular reference to the limb bud as it is pertinent to the present study.

According to previous research *Rarα* is ubiquitous, *Rarβ* is more tissue specific and *Rarγ* is specific to pre-cartilaginous regions and prospective squamous keratinising epithelia during embryonic development (Kastner et al., 1990; Ruberte et al., 1991). *Rarα* and *Rarγ* are mainly ubiquitous in the head region whereas *Rarβ2* is restricted to the frontonasal mass mesenchyme, periocular mesenchyme and anterior maxillary arch (Dolle, 2009; Dolle et al., 1990; Michaille et al., 1995). *Rarβ* was seen in the hindbrain at early stages (Smith, 1994) and intermediate mesoderm while *Rarγ* was expressed in the caudal embryo, neural tube, sclerotome and pre-vertebrae. Both *Rarβ* and *Rarγ* were also described to be present in the lateral plate mesoderm (Dolle et al., 1990; Michaille et al., 1994; Ruberte et al., 1991).

Rarα, *Rarβ* and *Rarγ* were expressed in the limb in both mouse and chick (summarised in tables 1.2 and 1.3 respectively). Generally in early limb development: *Rarα* and *Rarγ* are thought to be ubiquitous (Michaille et al., 1994; Mollard et al., 2000), *Rarβ1* is thought to be ubiquitous including the epithelium (Schofield et al., 1992; Smith et al., 1995) and *Rarβ2* is restricted to the proximal limb (Mollard et al., 2000; Smith et al., 1995). All RAR isoforms have been seen to be involved in the later stages of limb development but interestingly *Rarβ2* and *Rarγ2* are expressed in the apoptotic interdigit regions. *Rarγ1* was expressed in the developing cartilage and *Rarα* was ubiquitous but mutually exclusive with *Rarγ* (Dolle et al., 1989; Mollard et al., 2000).

Whilst all RARs bind ATRA their expression can be altered by ATRA and interestingly they differ in their responses: *Rarβ* is up-regulated or expanded (Rowe et al., 1991; Zelent et al., 1989), *Rarα* is unaffected and *Rarγ* expression decreases (Zelent et al., 1989). The expression ATRA inducible isoforms of *Rarα2* and *Rarβ2* (Kostetskii et al., 1996) is also dependent on vitamin A status as seen by their decreased expression in a comparison of normal and VAD quail up to HH10. This is reversed within 45 minutes upon addition of vitamin A or ATRA (Cui et al., 2003).

Table 1.2: The distribution of retinoic acid binding proteins and receptor isotypes in mouse limbs.

Stage	*Rarα*	*Rarβ*	*Rarγ*	*Crabp1*	*Crabp2*
10dpc	Ubiquitous, including AER (present in LPM)	Restricted (proximal limb and LPM)	Ubiquitous, mesoderm of limb only	Restricted distal, posterior and dorsal. Also AER.	Throughout but higher dorsally and low in PZ.
12.5dpc	Ubiquitous	Restricted (proximal to zeugopod blastema), opaque patch and AER.	Restricted (pre-cartilage blastemas proximally-including scapula and ubiquitous distally)	Restricted (surround blastemas and blood vessels. Not in distal mesenchyme)	
13.5 dpc	Ubiquitous	Restricted, interdigit mesenchyme.	Restricted, interdigit mesenchyme. Also in cartilage before ossification.	Restricted, distal and wrist elements.	Restricted, distal and interdigit mesenchyme.
14.5dpc	Restricted (everything but cartilage-complimentary to *Rarγ*)	Restricted (interdigit mesenchyme, *Rarβ1* at much lower levels)	Restricted (skin and cartilage-*Rarγ1*), *Rarγ2* is distal.	Restricted (periphery of cartilage and digit tips but not overlapping with *Rarβ*)	

Data summarised from studies using section *in situ* hybridisation and ^{35}S autoradiography (Dolle et al., 1989; Mendelsohn et al., 1992; Mollard et al., 2000; Ruberte et al., 1990a). Abbreviations: AER: apical ectodermal ridge; dpc: days post coitus; LPM: lateral plate mesoderm; PD: proximal-distal; PZ, proximal zone.

Table 1.3: The distribution of *Rarβ* and cellular retinoic acid binding protein in chick limb development.

Stage	*Rarβ1*	*Rarβ2*	CRABP	CRABP2
20-22	Ubiquitous (slightly higher dorsally)	Restricted (proximal limb bud and then localised to central core condensation)	Distal limb: high anterior low posterior.	+
24	Ubiquitous	Restricted (high in central proximal core condensation- overlaps with *Col1*)	Distal limb bud: PZ and more proximally but absent from the cartilage elements.	Distal limb in PZ, restricted to mid and posterior PZ.
25-27	Ubiquitous	As HH24 then high proximally to humerus/stylopod. Also in AER.	0	+
28-30	Restricted (cartilage and connective tissue. High in outer cartilage, low prehypertrophic cartilage)	Restricted (mainly to distal mesenchyme, lining digital plate and zeugopod)	0	0
36	Restricted (perichondrium cartilage and broader than *Rarβ2*)	Restricted (fibroblasts between digits)	0	0

Data was taken from (Kitamoto et al., 1989; Maden et al., 1988; Maden et al., 1989; Miyagawa-Tomita et al., 1992; Schofield et al., 1992; Smith and Eichele, 1991; Smith et al., 1995). Abbreviations: AER: apical ectodermal ridge; Col1: collagen1; HH, Hamburger and Hamilton staging; PZ, progress zone; +, present by Northern blot while other patterns are demonstrated as present by immunohistochemistry; 0, not investigated.

An alternative signalling pathway for ATRA.

It has recently been discovered that ATRA may bind to another intracellular binding protein: FABP5 (Shaw et al., 2003). FABP5 is essential for ligand translocation to peroxisome proliferator activated receptor β/δ (PPARβ/δ) in the nucleus and has been documented to contain the same NLS as CRABP2 in its tertiary structure (Sessler and Noy, 2005; Tan et al., 2002). FABP5 has been confirmed to channel ATRA to and activate PPARβδ *in vitro* (Schug et al., 2007; Shaw et al., 2003; Tan et al., 2005). PPARβδ is known to heterodimerise with RXR, which is necessary for transcriptional activation (Peters et al., 2000), and binds PPAR responsive elements, DR1 or DR2 RXR responsive elements (PRE or RXRE; (Hihi et al., 2002; Kliewer et al., 1992). As both RAR and PPAR/RXR heterodimers have been implicated in DR1 element binding, there may be competition between the PPAR and RAR pathways (Kliewer et al., 1992; Yu et al., 2012) consistent with findings of Schug et al (2007), although the significance of this is unclear. The formation of heterodimers with RXR allows PPARβδ/RXR heterodimers to respond to both 9CRA and PPARβδ specific ligands (Kliewer et al., 1992). Similar to RARs, in the absence of ligands it can activate or repress transcription (Adhikary et al., 2011; Shi et al., 2002; Tachibana et al., 2005). Although its action appears to mainly repress transcription as it binds co-repressors (Shi et al., 2002) and only 13 genetic targets are de-repressed in response to ligand and siRNA for *Pparβδ* using a human prostate cell line. It has been suggested that the genetic response is largely dependent on the PRE present and the function of the gene in question (Adhikary et al., 2011). Similarly PPARβδ has been shown to inhibit PPARα or PPARγ mediated transcription, thought to be via competitive binding to PREs, and it has been proposed to be a gateway receptor for correct activation of these pathways (Shi et al., 2002). PPARβδ is involved in barrier homeostasis through stimulation of keratinocyte differentiation, anti-inflammatory response, lipid metabolism, cholesterol transport, oligodendrocyte differentiation, wound healing and embryo implantation (Hihi et al., 2002; Michalik and Wahli, 1999; Schmuth et al., 2004; Tan et al., 2005).

ATRA has been used in the treatment of acute promyelocytic leukaemia but its use has been limited due to the fact that it can induce its own catabolism and the use of CYP26 inhibitors such as liarozole are now considered (Miller et al., 1994; Njar et al., 2006; Rigas et al., 1993). Therefore, retinoids resistant to metabolism could be of use in a clinical

context. It also causes contradictory effects of proliferation in some cancers but apoptosis in others (Schug et al., 2007). The ratio of FABP5:CRABP2 in the responding cells has been shown to direct ATRA to either PPARβδ or RAR and cause a proliferative or apoptotic response respectively (Schug et al., 2007; Schug et al., 2008). This differential response due to the ratio of FABP5:CRABP2 may aid future cancer treatment and also has implications for the role of ATRA in development.

Consistent with this, a recent study has suggested that the partitioning of ATRA between these two alternative pathways: PPARβδ and RAR is important for neurogenesis during development. It has been shown in P19 cells that ATRA acts via RAR mediated transcription early in differentiation but later acts via PPARβδ mediated transcription. The activation of PPARβδ mediated transcription inhibits RAR mediated transcription and, similar to RAR, PPARβδ is auto-regulated (Yu et al., 2012). *Pparβδ* is known to be expressed in the rat brain from GD11.5 as well as the adult (Abbott, 2009). Consistent with these observations, the *Fabp5* null mouse exhibits an accumulation of neuroprogenitor cells in the hippocampus and decreased neural maturation (Yu et al., 2012). However, the significance of this pathway remains to be seen as the *Fabp5* null mice are not documented to exhibit other malformations (Yu et al., 2012) and, similarly, the *Pparβδ* knockout mouse exhibited smaller foetuses but did not show any other embryonic malformations (Peters et al., 2000). However *Pparβδ* null adult mice do show abnormal wound response as cells move away from the wound instead of repair it (Tan et al., 2007).

The expression of *Fabp5* and *Pparβδ* has been little studied during embryonic development. However, *Pparβδ* is known to be expressed in the kidney, heart, liver, CNS and epidermis during rat, mouse and human embryonic development (Abbott, 2009; Braissant and Wahli, 1998; Michalik and Wahli, 1999). The sequences of chick *Fabp5* (Caldwell et al., 2005) and *Pparβδ* has been cloned and c*Pparβ* is closest to that of *Xenopus Pparβ* (Takada et al., 2000). To date, the expression of chicken *Pparβ* has only been reported as ubiquitous in the digestive tract (Hojo et al., 2006) and the expression of *Fabp5* has not been documented. Given their potential role in retinoid signalling *in vivo*, further characterisation of these genes is necessary to enhance our understanding of their role in development and will be addressed in this work.

The effect of altered ATRA levels *in vivo*.

As mentioned previously, ATRA excess and vitamin A deficiency cause malformations to the developing embryo and can be studied using mouse models. Mice null for *Cyp26a1* have been studied and exhibit similar phenotypes to those of ATRA excess in this model system including: absent genitalia, sirenomelia, spina bifida, abnormal kidney and posterior embryo development. *Cyp26a1* is also seen to be essential for normal hindbrain patterning including the trigeminal nerve and vertebral identity (Abu-Abed et al., 2001). Similarly, *Cyp26b1* knockout mice also exhibit effects associated with excess ATRA: limb malformations (meromelia and oligodactyly-see p26), micrognathia, malformation of neural crest derived structures, abnormalities of caudal cranial nerves and eyes open at birth (Maclean et al., 2009; Yashiro et al., 2004). This has led to the hypothesis that the CYP26 enzymes keep certain areas of the embryo in an ATRA depleted state for protection against teratogenesis. The level of ATRA has been shown to be important for development as these defects are rescued when mice are heterozygous for *Raldh2* knockout on a *Cyp26a1* knock out background (Niederreither et al., 2002a). Similarly mouse knockouts of the ATRA producing enzyme *Raldh2* exhibit no detectable ATRA signalling and development is arrested at E8.5-9.5 (Mic et al., 2003; Niederreither et al., 2002b), similar to VAD. These embryos exhibit cardiac defects, axial truncation and hindbrain defects (Niederreither et al., 2002b). *Raldh2* null embryos can be supplemented with ATRA to allow continued development and study the effect of ATRA deficiency on the limb (addressed p27).

ATRA and limb development.

One of the most studied regions affected by ATRA excess is the developing limb which will be addressed in this section. Limb outgrowth is initiated by the induction of the apical ectodermal ridge (AER) which secretes fibroblast growth factor 8 (FGF8) to maintain proliferation of the adjacent mesoderm (progress zone; PZ) and is thought to pattern the PD axis (Duboc and Logan, 2011). It has been well documented that cartilage differentiates in a proximal to distal sequence (Thorogood and Hinchliffe, 1975). The development of each PD segment (stylopod, zeugopod and autopod) is thought to be under the control of transcription factors marking each domain: *Homeobox d 9* (*Hoxd9)* and *Meis homeobox 2* (*Meis2*; stylopod), *Hoxa11* (zeugopod) and *Hoxa13* (autopod) (Pellegrini et

al., 2001; Pennimpede et al., 2010b). When the AER has been induced the limb is not polarised with respect to the AP axis. AP asymmetry and the production of digits is thought to be under the control of the zone of polarising activity (ZPA) and sonic hedgehog (SHH) produced in the posterior limb. This has been shown by the production of digit duplications from application or grafting of ZPA cells to the anterior wing bud, the severity of which is dependent on the number of cells and the stage at which the ZPA graft originated (Summerbell, 1974; Tickle, 1981). It was then shown that *Shh* was expressed in the ZPA and that SHH application to the anterior wing bud mimicked ZPA grafts (Riddle et al., 1993).

Once *Shh* in the ZPA has been induced, limb outgrowth is maintained by a SHH-gremlin-FGF feedback loop (Niswander et al., 1994; Scherz et al., 2004). It was also shown that bone morphogenetic protein (BMP) signalling inhibited the AER and a BMP antagonist, *Gremlin*, was essential for correct limb outgrowth (Capdevila et al., 1999; Pizette and Niswander, 1999). SHH causes proliferation and causes adjacent cells to express *gremlin* which allows the maintenance of FGF8 and FGF4 in the AER (Capdevila et al., 1999; Scherz et al., 2004). Once the ZPA cells and their descendants have proliferated significantly, they cannot induce *gremlin* expression adjacent to the AER, causing termination of limb bud outgrowth (Scherz et al., 2004). Consistent with this BMP antagonism in limb outgrowth, BMPs are also implicated in controlling the size of the *Shh* expression domain by a negative feedback loop and apoptosis caused by increased SHH in the posterior necrotic zone (PNZ; (Bastida et al., 2009; Sanz-Ezquerro and Tickle, 2000)). Death in the PNZ is therefore a buffer for the number of ZPA cells and may contribute to the control of limb outgrowth.

However, the AP axis is thought to be polarised before the induction of *Shh* in the ZPA. *Hoxb8* is seen to be expressed in the posterior mesoderm before restriction to the flank at early stages of limb development and overexpression can produce digit duplications, implicating it in the production of the ZPA (Charite et al., 1994). The expression of *heart and neural crest derived 2* (*Hand2*) and *Aristaless-like homeobox 4* (*Alx4*) is ubiquitous at early stages (Fernandez-Teran et al., 2000; Takahashi et al., 1998) but the action of Gli3R (repressor) causes *Hand2* to become restricted to the posterior limb and *Alx4* to be excluded from the posterior limb (te Welscher et al., 2002). *Hand2* is then able to induce *Shh* expression as shown by the misexpression of *hand2* in the anterior wing which results

in digit duplication (Fernandez-Teran et al., 2000). 5' *hoxd* genes are also implicated in the induction and positioning of *shh* (Hill, 2007) as are *T-box protein 2* (*Tbx2*) and *Tbx3* (Bastida et al., 2009). The 5' *hoxd* genes exhibit restricted expression during limb development and before ZPA induction but which appears to correlate with the AP segments of the limb rather than the PD segments like the 5' *hoxa* genes. *Hoxd11* and *hoxd12* are restricted to the posterior distal domain with an anterior limit of the radius. *Hoxd13* is expressed in the posterior distal limb and then becomes restricted to the posterior autopod with the 2nd metacarpal element as its anterior limit (Yokouchi et al., 1991b).

Digit identity, the manifestation of patterning in the AP axis, appears to be downstream of both *Shh* and *Gli3* considering that the polydactylous limb formed in *Shh*/*Gli3* double knockout mice exhibits identical digits (te Welscher et al., 2002). *Shh* has also been shown to be involved in digit identity given that *Talpid3* mutant embryos, which do not maintain *Shh* expression in the ZPA, exhibit severely polydactylous limbs of identical digit identity (Francis-West et al., 1995). The induction of anterior or digit 1 identity is thought to be dependent on Gli3R activity or SHH independent (Chiang et al., 2001). However, posterior identity (digit 2-5) is dependent on SHH (Chiang et al., 2001; Harfe et al., 2004; te Welscher et al., 2002) with more posterior digits thought to require increased levels for specification (Yang et al., 1997). The development of digits 2-5 is not dependent on a gradient of SHH as shown by the SHH responsiveness across the limb bud using the SHH target *Gli1*. The early response to SHH in the limb was graded: high posterior and low anterior with digit 2 as the anterior limit of expression but was absent from digit 1 producing region. Subsequently, the posterior limb stopped responding to SHH and the levels of *Gli1* in developing digits 3, 4 and 5 become equal indicating that digit identity is not solely due to a SHH gradient (Ahn and Joyner, 2004). Consistent with this, recent research has now implicated SHH dependent proliferation as important in the development of digits 3 and 4 as well as long range SHH signalling in digit 2 development (Drossopoulou et al., 2000; Harfe et al., 2004; Towers et al., 2008; Zhu et al., 2008a).

These findings are likely to have significance for chick digit development but there has been some debate over avian digit identity. Given that, during its formation, the most posterior digit of the chick wing is seen to overlap with the ZPA (Towers et al., 2008) and that it is homologous to the hindlimb posterior digit, it has been implied that this digit is

homologous to digit 4 in mice (Burke and Feduccia, 1997). However, recent research by Towers et al (Towers et al., 2011) has shown that the chick ZPA does not form any digits but instead contributes to soft tissue in the most posterior limb. This implies that the digit previously known as digit 4 in chick is in fact more similar to digit 3 in mouse which is the most posterior digit to contain non-*Shh* expressing cells (Harfe et al., 2004; Lewis et al., 2001). Therefore, the most anterior chick digit is more similar to murine digit 1 and may be SHH-independent.

ATRA has long been implicated in limb development since experiments indicating that excess ATRA applied to the anterior chick wing bud could mimic ZPA grafts and generate digit duplications (Tickle et al., 1982) and reductions in a dose dependent manner (Summerbell, 1983; Tickle et al., 1985). Earlier grafts of the ZPA can cause duplication of more proximal structures which is also seen with ATRA application earlier than HH20 (Summerbell, 1974, 1983). The effect of ATRA was later shown to be via the mesoderm and cause reorganisation of the AER (Tickle et al., 1989). Retinoids have also been shown to affect the development of axolotl limbs. Amputation of axolotl limb buds allows regeneration of the limb dependent on where the amputation occurred. Application of vitamin A to the blastemas causes regeneration of more proximal elements of the limb than expected from the site of amputation. Application of ATRA, increased exposure time or concentration can cause more proximal regenerations and can even include the limb girdle (Maden, 1983). ATRA application to mouse embryos has been shown to reduce forelimb length (Luo et al., 1995).

Excess ATRA is thought to mimic the early events of limb development when applied to the anterior chick wing bud as it induces *Hoxb8* which has been shown to induce *Shh* in the early steps of ZPA formation (Charite et al., 1994). Consistent with this ATRA then induces *Hand2* and *Shh* to form an ectopic anterior ZPA (Fernandez-Teran et al., 2000; Riddle et al., 1993; Wanek et al., 1991). The duplicated digits then develop under the control of the ectopic ZPA and if ATRA application occurs early enough the full digit pattern can be duplicated. Interestingly the wing appears to lose the ability to generate digit duplications after retinoid application at HH22 (Summerbell, 1983) and digit duplications are also not seen after ZPA graft later than HH25 (Summerbell, 1974). This may be due to a time lag between ATRA application and *Shh* induction.

In terms of the PD axis, ATRA has been shown to cause the up-regulation *Meis2* which is a marker of proximal fate, although, recent research shows that lack of ATRA via *Raldh2* and *Rdh10* does not affect *Meis1/2* expression and therefore ATRA is not necessary for endogenous PD patterning (Cunningham et al., 2013; Mercader et al., 2000). The up-regulation of *Meis2* and alteration of the PD axis after excess ATRA is likely to be due to suppression of FGF8 distally in the limb bud and then a subsequent down-regulation of *Meis* expression (Cunningham et al., 2013). Consistent with an effect on PD outgrowth and identity, excess application of ATRA has been shown to cause reduced skeletal elements along the PD axis at high concentrations (Summerbell, 1983), proximal relocation of limb bud cells (Mercader et al., 2000; Yashiro et al., 2004) and constitutive activation of RARα concurrent with increased Shh causes thickening of cartilage elements with increased proximal relocation (Ogura et al., 1996).

Cyp26 knockout can also be considered as a model of ATRA excess due to reduced ATRA metabolism. *Cyp26a1* knockout mice do not exhibit a forelimb phenotype, however, *Cyp26b1* knockout mice exhibit meromelia and oligodactyly, agenesis of the clavicle, fusion of the stylopod/zeugopod and lack the elbow joint (Maclean et al., 2009; Yashiro et al., 2004). Consistent with this, *Sox9* expression is not well separated in developing cartilage. Unexpectedly, analysis of markers indicates that the control of AP and dorsal-ventral (DV) patterning is normal. Expression of distal markers *hoxd12*, *hoxd13* and *hoxd13* is reduced and proximal marker *meis2* is expanded consistent with expansion of ATRA signalling in the limb and the relocation of distal cells to the proximal limb. Knockout limb buds also exhibited increased cell death at E12 over wild type and decreased chondrogenic maturation which was thought to cause the reduction in limb size (Yashiro et al., 2004).

A role for ATRA in limb development has been further supported by studies indicating that endogenous ATRA production is also important for limb initiation in chick (Stratford et al., 1996). VAD also affects chick limb development and these limbs have been shown to exhibit altered patterning of early markers of limb development: anterior *Hoxb8*, ventralised *Wnt7a* and down-regulation of *Shh*, *Fgf4* and *Bmp2* (Stratford et al., 1999). VAD has also been shown to affect the developing limb in rats but caused only a slight reduction in size concurrent with reduction of *Shh*, *fgf8* and *hox* expression consistent with impaired outgrowth (Power et al., 1999). *Raldh2* knockout mice lack forelimbs

(Niederreither et al., 1999) but supplementation with ATRA causes a dose dependent rescue of limb development and overcomes the heart defect in these mutants (Niederreither et al., 2002b). The best rescue was observed with supplementing with a low level of ATRA at E8.5 followed by higher levels until E14.5. These knockouts suggest that ATRA is necessary for forelimb initiation as well as subsequent patterning. Short ATRA supplementation caused development of a small scapula, no humerus, single zeugopod element and one digit. Increasing ATRA supplementation ameliorated the scapula and humerus but the zeugopod and autopod were still defective and the limb was truncated. These rescued forelimbs exhibited impaired *Shh-fgf4* signalling as they can be anteriorly expressed and the AER can be converted to a distal mound. They also show defective AP patterning: *Hand2* is ubiquitous while *Bmp2* and *Hox* are symmetrical (Mic et al., 2004; Niederreither et al., 2002b). Similarly application of an ATRA signalling antagonist to the limb in chick down-regulates *Hoxb8* expression and inhibits ZPA formation (Lu et al., 1997). This implies that a certain threshold of ATRA is necessary for correct limb development; however its genetic targets are unknown *in vitro* and *in vivo*. A study of retinoid targets on the developing mouse limb has indicated that retinoid excess impairs development by altering genes involved in differentiation (see chapter 5; (Ali-Khan and Hales, 2006)). This is an area which will be further explored in the current work.

ATRA signalling in the developing limb.

The study of ATRA distribution and signalling in the developing limb has yielded some conflicting data but would advance our understanding of the role of ATRA during limb development. Early experiments on ATRA indicated that it may be the morphogen produced from the ZPA to direct AP patterning during limb development (Tickle et al., 1982). Although subsequent experiments indicated that it is not the morphogen but acts to induce ZPA activity (Noji et al., 1991; Wanek et al., 1991), it has been documented from HPLC analysis that ATRA levels are higher in the posterior limb bud which has been confirmed using RARE::LACZ reporter cells (Maden et al., 1998; Thaller and Eichele, 1987). However, it was proposed that there was double the amount of ATRA in the posterior wing while other studies have indicated that the ratio of posterior: anterior ATRA is 1.33 which is unlikely to act as a developmental cue or to lead to the different responses seen with excess retinoid application (Martinez-Ceballos and Burdsal, 2001; Scott et al., 1994; Tickle et al., 1985). It has been suggested that HH23 limb buds can synthesise

ATRA despite the fact that they lack the ATRA synthesising enzyme *Raldh2* which may implicate other enzymes such as *Cyp1B1* in limb development, the importance of which are unknown (Chambers et al., 2007; Maden et al., 1998). This is also consistent with the observation that other areas of the developing *Raldh2* knockout mice demonstrate RARE::LACZ activity suggesting *Raldh1* and *Raldh3* are also important for aspects of embryonic development (Mic et al., 2004).

Measurement of endogenous ATRA by HPLC is challenging and therefore investigation into the location of ATRA has also been carried out by indirect methods: mapping the location of ATRA activity in the limb bud. This has exploited the production of transgenic mice containing the gene for *β-galactosidase* controlled by the RARE from *Rarβ* promoter (Sonneveld et al., 1999). The expression of *Raldh2* at the proximal limb bud and *Cyp26* at the distal limb bud has suggested a proximal-distal gradient of ATRA signalling in the developing limb (MacLean et al., 2001; Niederreither et al., 1997; Reijntjes et al., 2003, 2004; Swindell et al., 1999). Early in limb development ATRA signalling is ubiquitous across the limb although a PD difference is evident. Subsequently there is an area of increased ATRA signalling proximally and undetectable signalling distally rather than an AP gradient (Mendelsohn et al., 1991; Mic et al., 2004; Yashiro et al., 2004). Consistent with this FGF8, produced from the AER, is thought to have an antagonistic relationship with ATRA and controls distal identity confirmed by recent work in *Shh* deficient mice (Mercader et al., 2000; Probst et al., 2011).This may be responsible for the segmentation of the limb into RA high and low (FGF8 positive) domains and may be maintained and controlled by CYP26B1 activity at the distal wing (Probst et al., 2011). Oddly ATRA reporter activity has also been documented in the AER (Mendelsohn et al., 1991) which could account for *Cyp26* expression in this region. Later in limb development ATRA reporter activity is excluded from cartilage condensations and present in the INZ and opaque patch (Mendelsohn et al., 1991). Altogether these observations support a role for ATRA in PD limb development, although this is likely to be indirect via FGF8 suppression (Cunningham et al., 2013), and the formation of ATRA-low areas such as the distal limb. However, this does not explain the differential effect of ATRA on the posterior and anterior limb bud nor the differences in ATRA levels seen across the AP axis.

Hindering factors in the study of ATRA: the role of isomers and metabolites.

The study of ATRA can be hindered by the fact that ATRA has been documented to alter transcription by two separate receptor pathways dependent on the ratio of FABP5: CRABP2 present in the responding cell (Schug et al., 2007), as outlined in a previous section. Further characterisation of these proteins in development is necessary to advance our understanding. Two other hindering factors in the study of ATRA are based upon its structure and alteration *in vivo*. Firstly, it is known to isomerise upon exposure to light (Christie et al., 2008) which generates increased levels of other retinoids presumed to be 9-*cis* retinoic acid (9CRA) and 13-*cis* retinoic acid (13CRA). Secondly, ATRA is metabolised *in vivo* by the CYP26 enzymes which are known to produce more polar derivatives such as 4-*oxo*-retinoic acid, 4-*hydroxy*-retinoic acid, 5,6-*epoxy* retinoic acid, 16-*hydroxy*-retinoic acid and 18-*hydroxy*-retinoic acid (Taimi et al., 2004; Topletz et al., 2012; White et al., 1997; White et al., 2000). The structures of these isomers and metabolites can be seen in figures 1.3 and 1.4 respectively. Another retinoid, 3, 4-*didehydro*-retinoic acid has also been shown to generate phenotypes *in vivo*, is present in the chick limb but is absent from mouse, however, little further investigation has been published (Maden et al., 1998; Scott et al., 1994; Thaller et al., 1993).

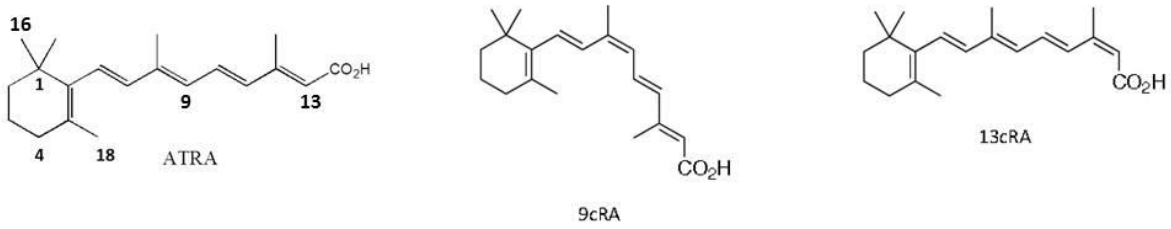

Figure 1.3: Naturally occurring ATRA and its isomers 9-*cis* and 13-*cis* retinoic acid.
Numbers on indicate carbon number. Abbreviations: ATRA, all trans retinoic acid; 9cRA, 9-*cis* retinoic acid; 13cRA, 13-*cis* retinoic acid.

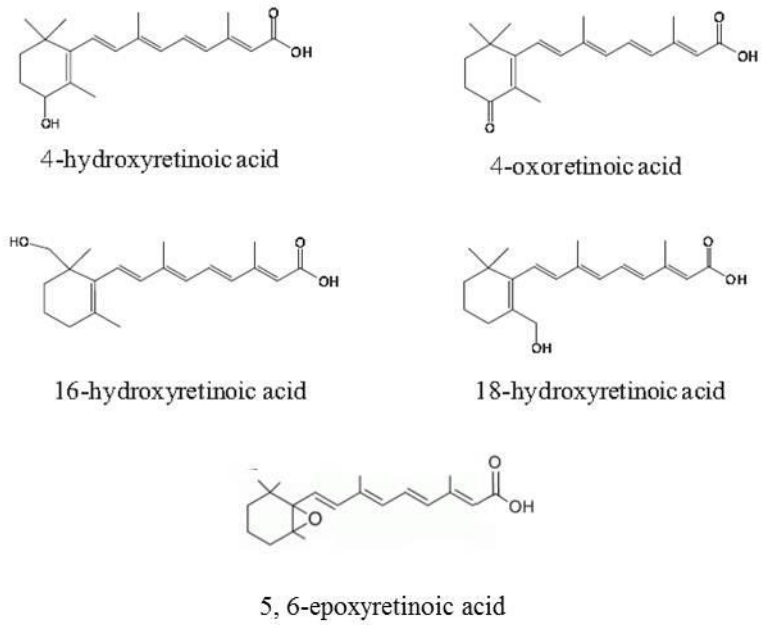

Figure 1.4: The oxidative derivatives of ATRA.

The Isomers.

As shown in figure 1.3, the isomerisation of ATRA to 13CRA and 9CRA causes a difference in retinoid structure and, given the importance of the carboxylic acid group, may alter their ability to bind RARs and CRABP (Kleywegt et al., 1994; Renaud et al., 1995). The precise effects of these isomers are unknown but they have been shown to be bioactive in limb bud cell culture (Kistler, 1987). Of the two isomers, 9CRA appears to be more bioactive than 13CRA as it is a high affinity ligand for RXR, being 40 times more potent than ATRA and can also activate RARs (Heyman et al., 1992; Levin et al., 1992; Zhang et al., 1992). It has been found to be metabolised specifically by *Cyp26c1* (Mark et al., 2006; Taimi et al., 2004). 9CRA has been documented to be 25 times more potent than ATRA at

generating digit duplications in the chick wing bud. It also affected upper beak growth similar to the phenotypes documented with ATRA (Thaller et al., 1993). As mentioned previously, 13CRA is less potent than ATRA which may be due to the fact that it cannot bind CRABP2 (Ruhl et al., 2001) and may therefore be less effective at activating the RAR:RXR heterodimer (Budhu and Noy, 2002). 13CRA also had a lower binding affinity to CRABP compared to ATRA (Fiorella and Napoli, 1991) and RAR activation by 13CRA needs significantly higher concentration: an order of magnitude (Astrom et al., 1990).

13CRA and 9CRA are thought to be produced by photo-isomerisation as mentioned previously (Christie et al., 2008). 13CRA has been shown to be found after excess ATRA application to E10.5 mice (Horton and Maden, 1995) and the occurrence of 9CRA *in vivo* is controversial (Kane, 2012). It has been found that bovine liver membranes can isomerise ATRA to 9CRA (Urbach and Rando, 1994) and this has been suggested to occur during chick limb development (Thaller et al., 1993). 9CRA was originally documented to be present in mouse kidney and liver (Heyman et al., 1992) but more recent reports have suggested that this was erroneous. Similar to 13CRA, it appears to be present after supraphysiological doses of ATRA suggesting that they are unlikely to mediate significant effects *in vivo*. This is consistent with the fact that high concentrations of 9CRA are needed to rescue *Raldh2* knockout mice and RXR specific agonists are unable to (Mic et al., 2003). Production of these isomers in response to light (Christie et al., 2008) or *in vivo* by the action of isomerases (Chen and Juchau, 1998; Urbach and Rando, 1994), leads to a decrease in the concentration of the bioactive molecule of interest, ATRA. These isomers may also affect transcription in a separate manner to that of ATRA: 9CRA is a high affinity ligand for RXR and could affect other pathways if generated *in vivo* (Heyman et al., 1992; Yu et al., 1991), masking the effect of ATRA.

The metabolites.

The metabolites are polar derivatives of ATRA derived from CYP mediated metabolism (see p3) as shown in figure 1.4 and their role in development is controversial. The oxidative derivative, 4-*oxo*-retinoic acid, has been documented to have similar binding affinity to CRABP as ATRA (Fiorella and Napoli, 1991). Interestingly, it has been shown that the RARs and CYP26 enzymes are responsive to particular enantiomers of the retinoids which may affect their activity *in vivo* and hinder their study (Klaholz et al.,

2000; Shimshoni et al., 2012). Similar to ATRA, the CYP26 enzymes are also known to act on 13CRA and 9CRA to produce the same polar derivatives including their 9-*cis* and 13-*cis* isomers (Fiorella and Napoli, 1991; Marill et al., 2002). Interestingly, other enzymes have also been documented to metabolise ATRA and its isomers: CYP3A7, CYP2C8 and CYP3A4 (Marill et al., 2002; Marill et al., 2000). The action of the metabolites may also mask the activity of ATRA during study of this molecule either by causing effects of their own or altering ATRA levels. Isomers and oxidative derivatives of ATRA can also induce RARE driven luciferase reporters at similar levels to ATRA. However, they exhibited different affinities to the three RARs. The retinoids with the highest affinity for RARα, RARβ and RARγ were: 9CRA, 4-*oxo*-retinoic acid and ATRA respectively (Astrom et al., 1990; Idres et al., 2002). However, it is unknown whether these compounds were maintained in their original state or if they were converted to ATRA itself via endogenous isomerases (Urbach and Rando, 1994) or other unknown enzymes. Nonetheless, the presence of oxidative derivatives and/or isomers could out-compete ATRA for RARα and RARγ mediated transcription and mask the true effect of ATRA on these receptors. The action of these metabolites *in vivo* is debated but it is believed that they are inactive products of ATRA and that the metabolising enzymes are necessary for the control of correct ATRA levels during development (Niederreither et al., 2002a). Opposition to this hypothesis stems from the fact that addition of the polar metabolites to VAD quails can cause partial rescue (Reijntjes et al., 2005) and they can pattern anterior structures of the Zebrafish head (Pijnappel et al., 1993).

Investigation of two photostable, synthetic retinoids.

Considering the isomerisation and metabolism of ATRA, the present study investigates two synthetic retinoids which should be resistant to these processes with a view to their use in cellular differentiation. It has been shown that ATRA can cause neural differentiation and decreasing its isomerisation and metabolism can optimise this process (Christie et al., 2008). EC23 and EC19, shown in figure 1.5, are two synthetic retinoids which have been shown to be stable upon exposure to light as they lack the isoprene tail of ATRA (Christie et al., 2008).

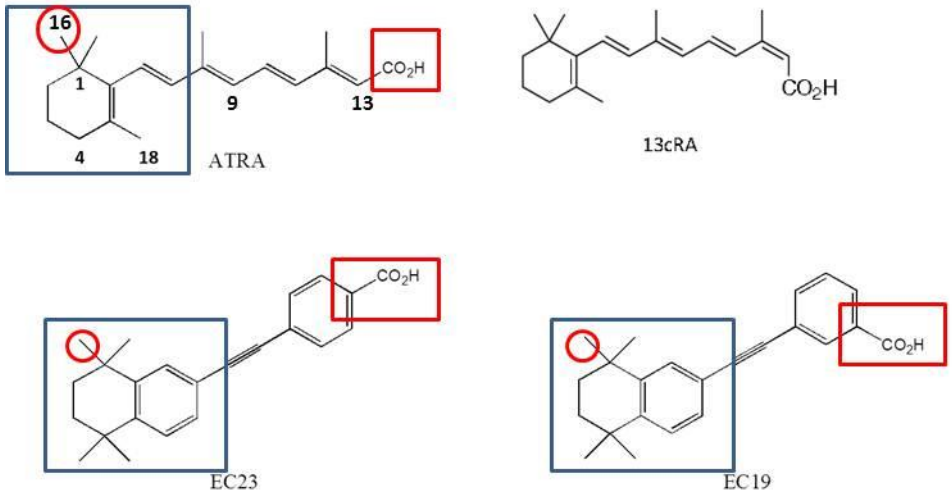

Figure 1.5: Structural comparison of the naturally occurring (ATRA and 13CRA) and photostable synthetic (EC23 and EC19) retinoids.

Blue boxes correspond to the hydrophobic (ATRA) or TMTN group (EC23 and EC19) which will block metabolism at C4, 5, 6 and 18. Red boxes highlight the differences between EC23 and EC19 being the position of the terminal carboxylic acid group. Red circles in EC23 and EC19 correspond to the carbon equivalent to C16 in ATRA which is the only known site where metabolism is possible (Topletz et al., 2012). Numbers correspond to the carbon above. Abbreviations: ATRA, all-trans retinoic acid; 9CRA, 9-cis retinoic acid; 13CRA, 13-cis retinoic acid; TMTN, 1,1,4,4-tetramethyl-1,2,3,4-tetrahydronapthalene.

EC23 has already been investigated with respect to its affinity for RAR subtypes and it has been suggested to activate all three at lower concentrations than ATRA and does not bind RXR. It also binds RARβ and RARγ with higher affinity than RARα (Gambone et al., 2002). However, the affinity of EC19 for these receptors is unknown. Given the known sites of retinoid metabolism: carbons 4, 5, 6, 16 and 18; it is proposed that EC23 and EC19 will be metabolised to a lesser extent than ATRA given that the only carbon similarly accessible compared to ATRA is in the position equivalent to carbon 16 (figure 1.5, red circle; (Henderson, 2011; Topletz et al., 2012)). They are also similar in structure to TTNPB (compare with figure 1.1). This synthetic retinoid has also been well studied and it has been shown to exhibit similar affinities for RAR and CRABP compared to ATRA despite its increased potency *in vivo* (Eichele et al., 1985; Kistler, 1987; Pignatello et al., 1997, 1999). However, this is thought to be explained by the increased resistance to CYP26-mediated metabolism (Eichele et al., 1985; Pignatello et al., 1997, 2002).

Interestingly, despite their similar structures, EC23 and EC19 have exhibited differential effects *in vitro* on NTER2.cl.SP12 cells. These cells undergo neural differentiation upon exposure to ATRA which is mimicked by EC23. EC19, however, causes more epithelioid

differentiation (Christie et al., 2008). The effects of EC23 on differentiation has been further characterised in this cell line by investigating the proteome in response to these retinoids. It was observed that ATRA and EC23 altered retinoic acid responsive proteins (CRABP1, CRABP2 and CRBP) as well as altering similar cytoskeletal targets (Maltman et al., 2009). The two photostable, synthetic retinoids EC23 and EC19 shown in figure 1.5 were then analysed in the chick limb bud and have been shown to cause differential effects *in vivo* (Budge, 2010). Varying concentrations of EC23 and EC19 were applied to anterior HH20 (Hamburger and Hamilton, 1951) chick wing buds using AG1-X2 beads (200-400 mesh size or 50-150μm diameter) and the phenotypes produced after 7 days were compared to those produced after ATRA treatment in the same manner. It was observed that the toxicity of the three retinoids was as follows: EC23, ATRA and EC19, with EC23 as the most toxic with 0 survival at 0.1mg/ml. EC23 was shown to mimic the effects of ATRA but generated mirror image digit duplications (321123) at concentrations two orders of magnitude lower than ATRA. EC19, however, had a more mild effect on the limb causing duplication of only the most anterior digit and required higher concentrations than EC23 (Budge, 2010). ATRA has also been documented to truncate the outgrowth of the upper beak (Tamarin et al., 1984). EC23 and EC19 were seen to mimic these effects however; although EC19 caused a higher frequency of this malformation, the phenotypes were not as severe as EC23 or ATRA treatment (Budge, 2010). Of particular interest, EC23 was also able to duplicate multiple additional digits of the most anterior identity (11123) at low frequency which was not observed with EC19 and has not been observed with ATRA previously (Budge, 2010; Tickle et al., 1985).

The present study aimed to further characterise the effects of these two retinoids in the chick limb bud model given the results previously described. Considering the additional digits of anterior identity duplicated at the highest level of EC23, experiments were carried out to further investigate this phenomenon by increasing the quantity of these retinoids applied. As summarised in this review, the effects of ATRA are well documented in chick wing development but there are gaps in our knowledge: the molecular mechanisms behind digit specification and retinoid response, the distribution of retinoic acid binding proteins in intact embryos and the role of ATRA metabolites and isomers *in vivo*. Therefore, the rationale for the present study was to address these gaps in our current understanding using the photostable synthetic retinoids EC23 and EC19. I aimed to particularly investigate the following:

- The effects of photostable, synthetic retinoids EC23 and EC19 *in vivo* which are theoretically resistant to metabolism by the CYP26 enzyme system.
- Characterisation of the metabolism of the photostable synthetic retinoids EC23 and EC19.
- Characterisation of components of the retinoid signalling pathway in chick given gaps in our current understanding.
- Genetic profiling of the anterior treated wing bud to elucidate the genetic targets of retinoids in chick *in vivo* and to improve our understanding of the mechanisms controlling limb development and response to teratogenic compounds.

Chapter 2) Materials and Methods.

Solutions:

Tyrode's Saline (10x; 500ml): 40g sodium chloride, 1g potassium chloride and 0.25g monobasic sodium phosphate dihydrate and then autoclaved. It is diluted to 50ml 1x on the day of use when 0.05g of both sodium bicarbonate and glucose, and add 500µl of 100x antibiotic/antimycotic (Sigma).

Phosphate Buffered Saline (10x; PBS): 80g sodium chloride (NaCl), 2g potassium chloride, 14.4g sodium phosphate (monobasic), 2 g potassium phosphate (dibasic) in 1l. This was treated with diethyl pyrocarbonate (DEPC; Sigma) and autoclaved if it was needed ribonuclease (RNase) free.

Ethanolic alcian blue: 80ml 96% ethanol, 20ml acetic acid, 15mg Alcian blue 8GX made fresh from a stock.

Alizarin Red S stain: 10mg alizarin red, 100ml 0.5% potassium hydroxide.

Alcian blue for cell culture: 0.5% aqueous alcian blue, 3% acetic acid pH 1 using acetic acid.

Tris hydrochloride (trisHCl; 2M): 121g Tris base into 350ml DEPC-water in baked glassware. pH was adjusted to 7.5, 8.0 or 9.5 using hydrochloric acid and water added to 500ml.

Buffered saline for TBS at 20x: 80g sodium chloride, 2g potassium chloride in 500ml water, add 0.5ml DEPC and autoclave.

Tris-buffered Saline (10x; TBS): Mix 125ml buffered saline and 31.25ml 2M trisHCl with 93.75ml DEPC water in baked glassware.

0.5M Ethylenediaminetetraacetic acid (EDTA): Dissolve 93.05 g $Na_2EDTA \cdot 2H_2O$ in 350 ml DEPC-H_2O. pH was adjusted with sodium hydroxide. DEPC-H_2O was added to 500 ml before autoclaving.

20x Sodium chloride sodium citrate (SSC): 17.53g sodium chloride, 8.523g sodium citrate dihydrate. Add water to 70ml and pH to 4.5 using citric acid pellets. Add water to 100ml, add 50µl DEPC and autoclave.

Sodium dodecyl sulphate (SDS; 10%): dissolve 10g into 100ml DEPC water. Add 50µl DEPC and heat to 60°C for 6hrs. Make up to 100ml with DEPC water.

NTMT (40ml): 800µl 5M sodium chloride, 4ml 1M trisHCl (pH 9.5), 1ml 1M magnesium chloride, 400µl 2M levamisole (Sigma), 40µl Tween20 (Sigma). Make up to 40ml with DEPC water.

Tris-acetate EDTA (TAE; 50x): 242 g Tris base, 57.1 ml acetic acid, 37.2 g $Na_2EDTA \cdot 2H_2O$. Add H_2O to 1L.

Tris-EDTA (TE; 10x): 100 mM TrisHCl (pH 8.0) and 10 mM EDTA, make up to 10ml.

Orange G loading dye: spatula of OrangeG, 30% glycerol and make up to 10ml water.

1M Triethanolamine pH8.0: dissolve 46.41g triethanolamine in 200ml water. pH to 8.0 using hydrochloric acid and make up to 250ml. Autoclave.

Methods pertinent to all chapters:

Eggs:

Eggs were obtained from PD Hook Hatcheries (Thirsk, North Yorkshire) of white leghorn chicks. They were kept at 10°C and then incubated at 38.4°C in 50% humidity (Brinsea Ova-Easy egg incubator).

Chemicals:

All-*trans* retinoic acid (ATRA) (Sigma) was dissolved in dimethyl sulphoxide (DMSO; Sigma). EC23 and EC19 were obtained from Reinnervate Ltd and dissolved in DMSO. Aliquots of ATRA, EC23 and EC19 were stored at -20°C. Liarozole (5-[(3-Chlorophenyl)-1***H***-imidazol-1-ylmethyl]-1***H***-benzimidazole hydrochloride; Tocris Biosciences) was stored in its powdered form at 4°C and was dissolved in DMSO on the day of use. 1,1'-Dioctadecyl-3,3,3',3'-Tetramethylindocarbocyanine Perchlorate (DiI; Life Technologies, Paisley UK) was obtained in aliquots and kept at -20°C until the day of use and then were used at 1mM.

In ovo microsurgery:

Eggs were incubated for 4 days and staged according to Hamburger and Hamilton (HH) and Fisher et al (Fisher et al., 2008; Hamburger and Hamilton, 1951). Eggs staged at

HH20-21 were then treated with retinoid or DMSO. Formate derived (see below) AG1-X2 beads (diameter 150-300μm; BioRad) were soaked in retinoid or DMSO for 30mins rinsed in Tyrode's saline similar to Tickle et al (Tickle et al., 1985) and then inserted into a slit in the anterior limb bud using fine forceps and tungsten needles. Embryos were prevented from dehydrating using Tyrode's saline solution. They were re-incubated for 7 days for phenotypic screens of the retinoids (chapter 3) or for 24hrs for microarray analysis (see chapter 5).

A modification of this protocol was used in chapter 5 to investigate the proximalisation of limb bud cells treated with EC23 in comparison to ATRA (Mercader et al., 2000). In this case, beads previously soaked in retinoid or DMSO as previously described, were then dipped into 1mM DiI and then dipped into Tyrode's saline solution to remove excess DiI. These beads were then implanted into a slit at the apex of the wing bud of HH23 chick embryos (Fisher et al., 2008; Hamburger and Hamilton, 1951). These were re-incubated for 48hrs and then analysed using a Nikon inverted fluorescence microscope at x10 magnification. These were imaged un-flattened or flattened. Subsequent analysis of limb bud cell relocation was carried out on fluorescent images using ImageJ and is described in more detail in chapter 5.

Bead Preparation:

Beads were placed into a falcon tube with 15ml sodium hydroxide and rocked for 10mins x2. Beads were then washed in 15ml deionised water for 10mins x4. Beads are then washed in 15ml formic acid for 10mins x2. Beads were then left to dry overnight in a fume cupboard. It had been found previously that beads were only stable in this condition for 1 month and therefore this was carried out once a month and for all *in ovo* microsurgeries.

Bead loading assay:

This was carried out similar to the method described by Eichele et al (Eichele et al., 1984). 20 AG1-X2 beads (150-300μm diameter) were placed into a microcentrifuge tube and collected by centrifugation at max speed for 2 minutes. 200μl of compound was added and the beads were re-centrifuged to remove any material from the supernatant. A 10μl aliquot was removed to determine the absorbance of the surrounding solution using a NanoDrop

spectrophotometer (ND1000) as the quantity of retinoid available was small. The beads were incubated in the dark between centrifugations and 10µl was removed at the following time points: 10, 20, 30, 40, 60, 120 and 180 minutes. A standard curve was then used to determine the amount of retinoid which had loaded per bead over 180mins.

Whole mount alcian Blue staining and photography

Embryos recovered after 7 days of incubation with retinoid are then stained with alcian blue and alizarin red to determine their phenotype. Briefly, embryos are fixed and stained in ethanolic acetic alcian blue for at least 3 days, followed by three washes in 100% ethanol over three days. Alcian blue stains for proteoglycans in the extracellular matrix (Kistler et al., 1985) to visualise cartilage. Embryos were imaged for limb and beak malformations using a camera (Idea, Spot) mounted to a Leica dissecting microscope. Embryos were imaged dry or surrounded by 100% ethanol on 3% agar plates. To allow for comparisons of beak length, the left eye was removed to allow the heads to lie flat. Embryos were then stained with Alizarin red in 1% aqueous potassium hydroxide for 45mins to stain for bone (Niswander, 2008). Embryos were cleared further in 1% potassium hydroxide (KOH). Embryos were then further cleared in 1% KOH, 25% glycerol and stored in 1% KOH, 50% glycerol or 80% glycerol. Embryos were then imaged using transmitted light.

Whole mount *in situ* hybridisation.

This was carried out according to Wilkinson and Acloque et al (Acloque et al., 1996; Acloque et al., 2008; Wilkinson, 1992) with some modifications. All solutions for whole mount *in situ* hybridisation were treated with 0.05% DEPC and autoclaved to denature RNases before use. Where this was not possible, RNase free solutions were made up using baked glassware and spatulas and RNase-free stocks were kept separately.

Ribonucleic acid (RNA) Isolation for whole mount in situ hybridisation:

Briefly, RNA was extracted from 30mg embryonic tissue using the Qiagen RNeasy kit (Dorking, UK) using manufacturer's recommendations. Embryos were dissected into ice cold PBS and placed into 600µl RLT where it was disrupted and homogenised by

vortexing and then syringed using a 21.5G needle. 70% molecular biology ethanol (Sigma) was added to the homogenised material to provide the correct conditions for RNA to bind to the column. The column was then washed with 350µl RW1 (Qiagen RNeasy kit). This was followed by on column digestion of DNA. 80µl of RNase free deoxyribonuclease (DNase) (Qiagen) was applied to the column for 15mins at room temperature. This was followed by one RW1 wash and 2 washes of 500µl RPE buffer (Qiagen RNeasy kit). The RNA was eluted into 30µl nuclease free water and stored at -80°C. Integrity was verified by electrophoresis on a 1% agarose (BioRad) TAE gel and concentration measured on the NanoDrop spectrophotometer (ND1500).

Reverse Transcription:

RNA was reverse transcribed using the High Capacity DNA Synthesis kit (Applied Biosystems, Paisley, UK) as per the instructions provided. Briefly, 2µg RNA in 10µl is added to 1µl 10x buffer, 0.4µl dNTP, 1µl random primers, 1µl reverse transcriptase and nuclease free water (Promega, Southampton, UK). This is then placed into a thermocycler (Biometra) with the following programme: 25°C 10mins, 2hours at 37°C and 85°C 10s.

Polymerase Chain Reaction (PCR)

Usually plasmid DNA is used to generate digoxigenin (DIG) labelled RNA probes but PCR is applicable to the rapid generation of a wide range of probes. In order to generate PCR products which could in turn be transcribed into labelled RNA probes, a T7 RNA polymerase binding site was added to each reverse primer (Frohman and Martin, 1989). This allowed the production of antisense probes for whole mount *in situ* hybridisation. Primers were designed using sequences from National Centre for Biotechnology Information (NCBI) and are shown below (table 2.1). Before designing primers which would generate specific probes, the sequence of interest was blasted to determine regions of homology and specificity. Primers and probes were then designed to the specific region, the A domain in the case of the RARs. The probes which would be generated for each gene were then blasted to ensure specificity.

The BLAST function on NCBI was used to design sequence specific primers ideally with the following conditions: 50% guanine-cytosine (GC) content and no more than 3/5 GC bases at the 3'end. For primer sequences see table 2.1 below. PCR was carried out using GoTaq Flexi DNA Polymerase kit (Promega). Briefly, 1µl DNA was added to: 2µl buffer, magnesium chloride at 1-4mM, 2mM nucleotides, 0.5mM primers (Sigma; Haverhill, UK) and 0.05µl GoTaq Flexi DNA Polymerase in a 20µl reaction volume. This was placed into a thermocycler (Eppendorf) with the following programme: 95°C 2mins, 95°C 30s, lowest melting temperature (Tm) -5°C 30s, and 72°C for 30s. This was cycled for 32 cycles followed by another extension step at 72°C for 2mins. PCR products were electrophoresed on 2% agarose TAE gel using a low range marker (Fermentas) to check band size.

Table 2.1: The sequences used to generate primers for PCR and subsequent whole mount *in situ* hybridisation.

Receptor Isoform	NCBI Sequence Number	Forward 5'-3'	Reverse 5'-3'
RARβ1(Smith and Eichele, 1991)	NM205326.1, X56674	AACTGAATGGTGGTCTGAGACACGGA	TGAGCTGGACTGTGTGATGGTGAAGA
RARβ2 (Smith and Eichele, 1991)	X57340.1, X59473.1	TGGGAAAAAGACCAACAGCCTACGT	TGTTTGTGCCAATCCACTGAAGCA
RARγ (Michaille et al., 1994)	X73973.2	AACAGCAAACCCAAGAAGCG	ATCGTCCCGCGCACC
Hand2 (Srivastava et al., 1995)	NM_204966.1	GCCGACACCAAGCTCTCTAAGATCAA	ATCGCTGCTGCTAACTGTGCTTT
PPARβδ (Takada et al., 2000)	NM_204728.1	AGCTGCGGAGAGGCTAGTGCAA	AGCTCTGCGAAAGGTCGGTGT
FABP5 (Caldwell et al., 2005)	NM_001006346.1	AATGGGAAGCATGGCGAAACCA	TCACATTCCACCACCAACTGTCCA
Pax1 (Barnes et al., 1996)	U22046.1	TGGAGCAGACGGGTGGGTA	TTCCTCGGCGGCTTTGTC
Shh (Riddle et al., 1993)	NM_204821.1	ATGAAGAGAACACGGGAGCTGACA	TCCTGATTTCGCTGCCACTGAGTT
T7 polymerase	AAGGATCCGTCGACATCGATAATACGACTCACTATAAGGGA		

References refer to first cloning of the gene. Abbreviations: NCBI. National Centre for Biotechnology Information; RAR, retinoic acid receptor; PPAR, peroxisome proliferator-activated receptor; FABP, fatty acid binding protein; Pax, Paired box gene; Shh, Sonic hedgehog.

Probe synthesis:

DIG labelled RNA probes were generated from total RNA from HH20 embryos. RNA was extracted and reverse transcribed as described earlier. The complementary DNA (cDNA) was used as a template for PCR to amplify the region of DNA specific to each probe using the primers in table 2.1 (note that reverse primers had the T7 polymerase binding site attached). The PCR product was then used as a template for *in vitro* transcription of DIG-labelled RNA probes for whole mount *in situ* hybridisation. The PCR fragments were transcribed into DIG labelled RNA using the method described by Wilkinson (Wilkinson, 1992). 1µl template was added to 2µl buffer, 0.2M dithriothreitol, 2µl nucleotides containing DIG-uracil triphosphate (Roche Applied Science; Burgess Hill, UK), 0.5µl recombinant ribonuclease inhibitor (RNasin) and 1µl T7 RNA polymerase (Promega) in 20µl reaction volume. This is incubated at 37-45°C for 2 hours and electrophoresed on a 2% agarose Tris-borate EDTA (TBE; Sigma) gel. The size of the product was checked against a low range DNA ladder (Fermentas). The probe was then ethanol precipitated by mixing with 100µl TE buffer, 300µl molecular biology ethanol and 10µl 4M DEPC treated lithium chloride and incubating at -20°C for at least 1hr. This was centrifuged at max speed for 10mins and washed twice with 80% ethanol before allowing to air dry. The probe was then re-suspended in 1xTE for quantification on the NanoDrop spectrophotometer (ND1000).

Pre-hybridisation, post-hybridisation and visualisation.

Embryos are incubated to desired stage and staged as Hamburger and Hamilton (Fisher et al., 2008; Hamburger and Hamilton, 1951). They are dissected into ice cold PBS and fixed overnight in 4% paraformaldehyde (Sigma)-DEPC treated PBS at 4°C. They were washed three times in DEPC-PBS containing 0.1% Tween20 (Sigma; PBT) and membranes were dissected off before dehydrating to 100% methanol (AnalaR VWR; Lutterworth, UK). Batches were stored in 100% methanol at -20°C. They were rehydrated to PBT and then bleached in 6% hydrogen peroxide (Sigma). This was rinsed off with PBT twice before digestion with proteinase K (Sigma): PBT to allow the probe access. Proteinase K was applied at 10µg/ml or 20µg/ml for 3 or 4 day old embryos respectively for 15 minutes (Acloque et al., 1996; Correia and Conlon, 2001). This enzyme was blocked using 2mg/ml

glycine (AnalaR VWR) and rinsed with PBT. Embryos were re-fixed in 0.2% glutaraldehyde: 4% paraformaldehyde: DEPC-PBS for 20 minutes followed by PBT. Embryos were then treated with 0.1M triethanolamine hydrochloride (pH 8) and 0.25% (v/v) acetic anhydride (Sigma) to reduce background. Hybridisation was carried out using highly stringent conditions. Embryos were equilibrated to the hybridisation solution and the temperature via three washes: firstly a 1:1 pre-hybridisation: PBT wash, followed by a wash in 100% pre-hybridisation solution at room temperature and one wash in 100% pre-hybridisation solution at 70°C for 1hour. Approximately 1µg DIG labelled RNA probe is then dissolved into 1ml pre-hybridisation buffer in which embryos are agitated at 70°C for 16hrs.

Pre-hybridisation buffer is: 50% formamide (Sigma), 5xSSC, 1%SDS, 50ug/ml heparin (Sigma) and 50ug/ml yeast transfer-RNA (tRNA; Sigma).

Embryos which were older than HH20 and had been treated with retinoid were processed slightly differently. Before dehydration they were dissected into three sections and then processed in bijoux tubes until pre-hybridisation. They then followed the same protocol as younger embryos. This was to minimise the loss of the bead and parts of the embryo.

Embryos were then washed with solution 1 at 70°C (50% formamide, 5xSSC, 1%SDS) and then with solution 3 (50% formamide, 2xSSC, 1%SDS) at 70°C. This was followed by TBST washes (1xTBS, 1% Tween20, 2mM levamisole (Sigma)) and then blocking with 10% sheep serum (Sigma): TBST. 1µl anti-DIG antibody (Roche Applied Science) was purified using embryo powder for 1hour in 1% sheep serum TBST at 4°C. The powder was then centrifuged to remove purified antibody in the supernatant and was applied to the embryos at 1:3000 dilution. This was rocked overnight at 4°C.

Antibody was removed and followed with 8 washes of TBST and left overnight at 4°C. The embryos were then placed in NTMT (100mM sodium chloride, 100mM TrisHCl pH9.5, 50mM Magnesium chloride, 0.1% tween20, 2mM levamisole). The DIG-antibody is conjugated to alkaline phosphatase which will catalyse a reaction between nitro-blue tetrazolium chloride (NBT) and 5-bromo-4-chloro-3-indolylphosphate toluidine salt (BCIP) to produce a purple precipitate. 4.5ul/ml NBT and 3.5ul/ml BCIP (Promega) were applied with NTMT and agitated in the dark for 20minutes and then left to develop. Once

the colour reaction had developed to the desired extent, embryos were washed 3 times with PBS and then fixed in 4% paraformaldehyde. Embryos were then imaged using the Idea (Spot) camera on the Leica dissecting microscope as described previously. Embryos were imaged on 3% agar plates so that they could be flat and pinned in place.

Chick limb bud cell culture (chapter 4).

Chick limb micromass cell cultures were set up using a modified method from Pignatello et al (Pignatello et al., 2002) to investigate the metabolism of EC23 and ATRA in comparison with the naturally occurring ATRA (chapter 4). Briefly, embryos were isolated after 4 days incubation and staged according to Hamburger and Hamilton (Fisher et al., 2008; Hamburger and Hamilton, 1951). Forelimb and hindlimb buds (Brown and Wiger, 1992) were isolated from HH20-21 embryos in Tyrode's saline solution. Cells were dissociated using 0.05% trypsin: EDTA for 30mins and then blocked with preheated medium: 10% foetal bovine serum (FBS; Lonza) α minimal essential medium (αMEM; Invitrogen), 5% glutamine (Lonza), antibiotic antimycotic (Sigma) and supplemented with 150µg/ml ascorbic acid (Sigma) (Jiang et al., 1995; Leboy et al., 1989). A single cell suspension was made and cells were passed through a 40µm cell strainer to remove epithelial fragments (Jiang et al., 1995). Trypan blue positive cells were counted using a haemocytometer (Kistler et al., 1985) and re-suspended so that 400,000 cells were plated in 20µl (Kochhar and Penner, 1992) onto 24 well plates (Nunc) to ensure the production of a high density culture (Nakanishi and Uyeki, 1985). This was incubated at 37°C 5% CO_2 for 1hr 45mins to allow cells to adhere (Kistler, 1987; Kistler et al., 1985). Wells were then flooded with 1ml media and this was taken as day 0 (Anderson et al., 2001). Cells were treated with combinations of DMSO, retinoid and/or liarozole on day 1. DMSO concentration was always of 0.1% in cell culture media except in cultures treated with high concentrations of liarozole and EC19 where it was 1.1%. Medium was changed on day 4 without addition of compounds tested and then incubated until day 7.

Fixation, Staining and Quantification of Chondrogenesis assays

Cells were rinsed with PBS and then fixed on day 7 using 10% formalin (Sigma), 0.5% cetyl pyridinium chloride (Sigma) for 30mins (Kochhar and Penner, 1992). Cells were then washed with 3% acetic acid and then left to stain in 0.5% aqueous alcian blue, 3%

acetic acid pH1 (Kistler et al., 1985) overnight while agitated. Cells were rinsed with 3% acetic acid and then imaged using a dissecting microscope as described previously but with an exposure time of 10.23ms. Alcian blue stain was then extracted with 300µl 4M guanidine hydrochloride (Sigma) to generate a quantitative measurement of chondrogenesis (Hassell and Horigan, 1982; Kistler, 1987; Kistler et al., 1985). The absorbance of the alcian blue staining was measured at 600nm using a Biotek ELX800 plate reader.

Methods for microarray analysis after retinoid treatment (chapter 5).

Embryo Dissection and RNA isolation for Microarray Analysis:

Embryos were exposed to retinoid or DMSO as described above by *in ovo* microsurgery (Figure 5.1A). 24hrs after operating, embryos were dissected into ice cold DEPC-PBS. Embryos whose limbs still had a bead attached and had developed as expected were included in the pool for RNA isolation. Torsos of embryos were dissected and pinned to 3% agar: Tyrode's plates to facilitate accurate dissection (figure 5.1C). The bead was removed and the anterior third of the limb bud was dissected using tungsten needles (Figure 5.1B, 5.1C). The anterior limb portion was transferred into an RNase free tube (Starlabs) in DEPC-PBS. After dissection, the limb portions were centrifuged for 15s to allow removal of DEPC-PBS. RLT (lysis buffer) was then placed on the limb portions. The limb portions were vortexed 4x10s and then passed through a 21.5G syringe needle 24 times to ensure complete lysis and homogenisation. Limb portion lysates were stored at -80°C until 16 limb portions were collected per repeat. They were then thawed on ice and RNA was isolated using the Qiagen RNeasy Kit (Dorking, UK) as described previously. RNA was quantified using the NanoDrop ND1000. If RNA met the requirements shown in table 2.2 it was used for microarray analysis otherwise they were cleaned up using the RNeasy Mini Kit (Qiagen) following manufacturer's instructions. The RNA pools hybridised at Newcastle University were ethanol precipitated to supply 5µg in 5µl but this was not carried out for pools sent to the Roslin Institute.

Table 2.2: Requirements for RNA for Microarray analysis.

Requirement	Threshold
Quantity	>5µg
260/280	Between 1.9-2.1
260/230	>1.8

Microarray hybridisation, scanning and analysis.

Production of labelled complementary RNA (cRNA), hybridisation and scanning of the microarray chip was carried out at Roslin Institute, University of Edinburgh and Centre for Life, University of Newcastle. RNA from pools treated with retinoid or DMSO was reverse transcribed into double stranded cDNA using the one cycle cDNA synthesis kit (Affymetrix). Labelled cRNA was then produced using an *in vitro* transcription reaction in the presence of biotinylated ribonucleotides. Quality and quantity of the fragmented cRNA was checked for quality control. Fragmented cRNA was then hybridised to a Genechip Chicken Genome Array (Affymetrix). The chip was then washed as manufacturers protocols to expose it to an antibody to biotin. This was then visualised with a secondary antibody conjugated to biotin and stained with streptavidin phycoerythrin. The stained chip was then scanned and .CEL files produced as per manufacturer's instructions. Analysis was then carried out at the Bioinformatics Support Unit in Newcastle University. Details of subsequent analysis are described in chapter 5.

qPCR.

qPCR was used to validate the microarray carried out for genetic targets of ATRA and EC23 (chapter 5). This was carried out using cDNA generated using the high capacity cDNA synthesis kit as described previously. qPCR was then carried out using the Applied Biosystems Real Time PCR 7500 System as per manufacturer's kits and instructions. The genes analysed and the assay IDs (Taqman Gene Expression Assays; Applied Biosystems) are shown in table 2.3.

Table 2.3: Taqman Gene Expression Assays used for qPCR validation of microarray analysis.

Gene name	Assay ID
Cyp26A1	Gg03345448_g1
Raldh2	Gg03348020_m1
Emx2	Gg03312130_m1
Hoxa13	Gg03813895_s1
Hoxb8	Gg03339343_m1
Meis2	Gg03338704_m1
Lhx9	Gg03340016_m1
Cdh2	Gg03345816_m1
Hgf	Gg03325663_m1
Col6 α3	Gg03340502_m1

Abbreviations: Cyp26A1, cytochrome P450 oxidase 26A1; Raldh2, retinaldehyde dehydrogenase 2; Emx2, empty spiracles homeobox 2; hox, homeobox; Meis2, meis homeobox 2; Lhx9, LIM homeobox 9; cdh2, cadherin 2/n-cadherin; hgf, hepatocyte growth factor; col6α3, collagen 6α3.

Briefly, DNA for analysis was diluted such that 20ng of DNA was added to each well of the 96 well plate used for qPCR in no more than 10µl RNase free water. 10µl 20xTaqman Universal Real Time PCR Master Mix (Applied Biosystems) was added to the assay for the gene in question (1µl 20x assay) and RNase free water added so that the volume of the reaction mix totalled 20µl. This was sealed and centrifuged and then placed into the Applied Biosystems Real Time PCR machine (7500-fast mode). The qPCR conditions were standard conditions supplied by Applied Biosystems and can be seen outlined in table 2.4. The PCR was run for 40 cycles and the progress monitored using Applied Biosystems software.

Table 2.4: Conditions used for qPCR analysis of microarray targets (chapter 5).

Temperature	Time	Reason
95°C	20s	Activating polymerase.
95°C	3s	Denaturing phase.
60°C	30s	Primer annealing and extension phase.

In all cases the assays were undetectable in the blank reaction. The change in gene expression was calculated as fold change using the ΔΔCT method. This calculates fold

change by calculating the change in cycle threshold (CT) compared to the endogenous control (*Gapdh* in this case) and then the difference in CT compared with a calibrator sample for that gene. In all cases DMSO sample 2 was used as the calibrator. The relative quantification (RQ) was then calculated using the formula: $RQ= 2^{-\Delta\Delta CT}$, standard deviations were then calculated for these values. The significance of the fold change in response to retinoid with respect to DMSO was calculated using an unpaired student's t-test.

Chapter 3) An investigation of the phenotypes produced with applications of high quantities of EC23 and EC19 to the anterior chick wing bud and their comparison with ATRA.

Introduction

The vertebrate limb develops from an area of limb forming mesoderm called the limb field. From this, the limb grows out under the control of three signalling centres: apical ectodermal ridge (AER), zone of polarising activity (ZPA) and dorsal ectoderm until it reaches the correct size (Scherz et al., 2004). During limb outgrowth the mesoderm must differentiate into cartilage, muscle and tendon to form a fully functioning limb. This process has been extensively studied in chick as it is affected in response to many teratogens e.g. ATRA and it is easily manipulated, hence will be used in the present study.

In chick, the limb field is specified between Hamburger and Hamilton stages 15-17 (HH15-17). By HH19 the AER has formed and the ZPA forms shortly after which together regulate limb outgrowth (see pages 22 and 55). During limb outgrowth the non-AER ectoderm patterns the DV structures (Parr and McMahon, 1995). The wing then develops to have three segments: stylopod (humerus), zeugopod (radius and ulna) and autopod (wrist, carpals, and digits). The development of cartilage is particularly important for limb development as the developing cartilage forms a template around which subsequent differentiation occurs. The first morphological sign of development is the formation of a cartilage condensation for the humerus at HH22 in chick with cells also forming myogenic condensations at a similar time. This condensation lengthens and then splits into two branches which will form the radius and ulna at HH24 (Searls et al., 1972; Singley and Solursh, 1981). During condensation and subsequent chondrogenesis the ECM surrounding these cartilage blastemas undergoes significant changes in the increased production of proteoglycans which can be stained with alcian blue (Hinchliffe, 1967; Summerbell, 1976). By HH26-27 the extracellular matrix (ECM) has changed significantly containing 25 times more sulphated proteoglycans than the previous stages (Cioffi et al., 1980). The opaque patch between the radius and ulna is also defined at this stage (Hinchliffe, 1967). By HH28 the wrist elements are beginning to condense and digit condensations can be observed with alcian blue (Summerbell, 1976). Previously it was thought that the progress of cartilage condensation was PD and posterior to anterior (as the ulna forms prior to the radius), however this is not true for the developing digits. The digit condensations have now been shown to form in the following order: 4, 2, 5, 3 and 1 via *Noggin* and *Sox9* expression in mouse (Zhu et al., 2008a).

Segmentation of the developing cartilage to produce the elements of the stylopod, zeugopod and autopod occurs via the formation of joints. This is thought to occur via a switch between chondrogenesis and joint differentiation. The joint is first morphologically distinguishable as the interzone, developing as a transverse stripe across cartilage elements at HH28 for the chick elbow. However, it has been shown to be determined by HH24 as a result of excision at HH24-26 (Holder, 1977) and can be regenerated if excised at HH26 (Ozpolat et al., 2012). The interzone is characterised by densely packed cells forming three layers. The outer two layers are densely packed cells which are become the articular layer on developing bones. The inner layer is less dense and undergoes cell death to form the joint and accumulate fluid (Storm and Kingsley, 1996, 1999).

The scapula or shoulder blade is important for correct limb function as the shoulder forms part of the pectoral girdle and is where the limb articulates with the appendicular skeleton. It is also important for muscle attachment. The scapula is a long thin bone spanning all ribs in chick consisting of a thicker head structure and the blade (figure 3.1). Chondrogenesis of the chick scapula begins at HH26 (embryonic day 5; E5) at the most caudal cervical vertebrae (C13-14) (Huang et al., 2000; Prols et al., 2004). The scapula then develops caudally so that at E6 (HH29) it spans 2 ribs, E7 it spans 3 ribs, E8 it spans 4 ribs, E9 it spans 5 ribs and it finally reaches the 7^{th} rib during adult life (Huang et al., 2000).

The scapula, as mentioned, is important for limb function but it is not traditionally thought of as part of the limb. Many manipulations can be made to the developing limbs which do not affect the scapula e.g. AER removal ablates limb outgrowth but has no effect on scapula formation. The origin of the scapula has been a subject of controversy since Chevalier (Chevallier, 1977) used quail-chick grafting to indicate that the scapula developed from the somites only. Other studies reported that it originated from lateral plate mesoderm (LPM) in Salamander and dual origin in chick with the blade originating from somitic mesoderm only (Huang et al., 2000). However, recent studies in mouse (Durland et al., 2008; Valasek et al., 2010) and chick (Shearman et al., 2011) show that the scapula does indeed have dual origin but the contributions of the somitic mesoderm and LPM are different to first thought. Shearman et al (2011) used a more rigorous technique than previous groups in that the quail-chick chimeras were sectioned and imaged completely to build up a 3D computer model of the scapula structure. This shows that in fact the cranial

two thirds of the chick scapula develops from the LPM, including the head structure, whereas the distal third develops from somites 18-24 (Shearman et al., 2011). Little is known about the mechanisms controlling scapula development as it has been studied less extensively than the limb but *pre-B-cell leukaemia homeobox 1-3* (*Pbx1-3*), *Paired box 1* (*Pax1*) and *empty spiracles 2* (*Emx2*) are thought to control genes involved in scapula patterning such as *Tbx15*, *Alx1*, *Alx4* and *Gli3* (Capellini et al., 2010; Timmons et al., 1994).

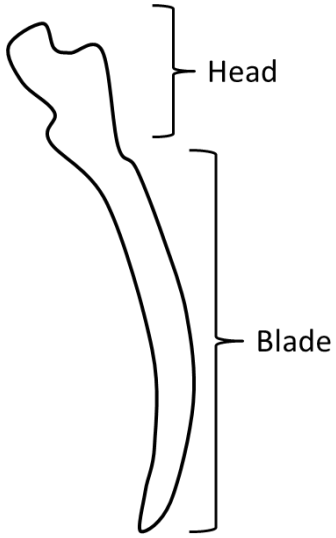

Figure 3.1: The structure of the scapula from the lateral view.
The scapula head and blade structures are marked. The scapula head includes both the head and neck designated by Huang et al, 2000 (Huang et al., 2000).

As mentioned the outgrowth and development of the limb is under the control of two main signalling centres: the AER and ZPA. The AER is situated at the distal wing tip and secretes FGFs. This is particularly important for PD patterning as removal of the AER at progressively earlier stages truncates the limb at more proximal regions (Niswander et al., 1993) which can also be seen with very high retinoid concentrations (Tickle et al., 1985). It is also thought that FGF8 has an antagonistic relationship with ATRA during limb development (Cunningham et al., 2013; Mercader et al., 2000). ATRA application causes an expansion of *Meis2* which is known to be proximally expressed in the developing limb and is has been used subsequently marker of stylopod development (Mercader et al., 2000; Pennimpede et al., 2010b; Yashiro et al., 2004). There is also a concomitant down-regulation of the autopodal marker genes *hoxa11* and *hoxa13* (Mercader et al., 2000) which indicates that ATRA treated cells contribute to more proximal structures.

The zone of polarising activity (ZPA) is formed shortly after the AER in the posterior wing and secretes SHH (Riddle et al., 1993). Formation of the ZPA is due to the sequential polarisation of the developing wing into anterior and posterior segments. This is achieved by the restriction of *HoxB8* to the posterior wing (Charite et al., 1994), followed by the sequential positioning of *Hand2* (Fernandez-Teran et al., 2000) in the posterior wing and *Alx4* in the anterior wing (Takahashi et al., 1998). Concomitant with *Shh* expression a gradient of Gli3R forms with highest levels anterior which may be important for digit identity. The ZPA is thought to form a positive feedback loop with the AER (Niswander et al., 1994) and this controls limb size via the BMP antagonist *gremlin* (Scherz et al., 2004).

SHH, whilst linked to PD patterning indirectly, has been linked to AP patterning more closely. The *Shh* knock out mouse generates a forelimb lacking digits and ulna and a hindlimb lacking all digits but digit 1 and the fibula (Chiang et al., 2001). This can also be seen in the *oligozeugodactyly* chick mutant who lacks SHH function (Ros et al., 2003). It has also been shown that application of excess SHH or ZPA grafts to the anterior wing bud generate ectopic digits/digit duplications (Yang et al., 1997). This effect has been mimicked by retinoids (Tickle et al., 1982; Tickle et al., 1985) which are thought to induce an ectopic ZPA in the anterior wing bud via *hoxb8*, *hand2* and *Shh* as previously mentioned (Fernandez-Teran et al., 2000; Wanek et al., 1991). Interestingly, concomitant with the retinoid malformation of the developing limb, application of excess ATRA can cause truncation to the upper beak (Tamarin et al., 1984) which, likewise, is thought to be due to an effect on SHH signalling ((Helms et al., 1997) addressed further in the discussion).

Digit differentiation has been shown to be partially dependent on SHH concentration and time of exposure as seen during application of increasing concentration of SHH: duplication of more posterior digits require a higher concentration of SHH than the duplication of anterior digits in chick (Yang et al., 1997). Given the phenotype of the *Shh* knock out mouse, it is widely thought that the murine digit 1 develops independently of SHH, at least in the hindlimb (Chiang et al., 2001). It has been more recently determined that cells which have been exposed to SHH during murine limb outgrowth contribute to digits 2 and 3 and that long range SHH signalling is important for their development (Ahn and Joyner, 2004; Drossopoulou et al., 2000). Digits 3, 4 and 5 consist of cells which were part of the ZPA (Harfe et al., 2004). Consistent with the importance of cell expansion in

digit development, Zhu et al (2008) showed that conditional knockout of *Shh* generated limbs with missing digits but that digit identity was not impaired. *Noggin* and *Sox9* expression showed that murine digit condensations form in the following sequence: 4, 2, 5, 3 and 1 (Zhu et al., 2008a). These studies highlight the importance of SHH dependent proliferation in the murine limb bud and this has also been observed in the chick wing (Towers et al., 2008). Inhibition of SHH signalling in the chick wing caused the formation of only the two most anterior digits, now designated 1 and 2. Inhibition of proliferation caused the formation of only the most posterior element, digit 3. This suggests that, similar to the mouse limb, digits 1 and 2 are produced from the SHH dependent expansion of digit progenitors while digit 3 is produced from *Shh* expressing cells as well as expansion. However, their study in 2011 (Towers et al., 2011) shows that digit 3 is also likely to be produced from purely non-*Shh* expressing cells as cells contributing to digit 3 never express *Shh* in chick.

Considering that the developing limb has been extensively studied and is known to be retinoid responsive, the limb bud was chosen as the model system to investigate EC23 and EC19.

Results

EC23 and EC19 have differential toxicity.

This aim of this work is to investigate the effects of EC23 and EC19 *in vivo* using the chick wing bud as a model system. The chick wing bud was chosen as the model as it is easily accessible and has been well characterised to investigate retinoid effects (Tickle et al, 1982; Tickle et al, 1985). EC23 and EC19 were applied to chick wing buds using ion exchange chromatography beads as previously described and their effects compared to ATRA. EC23 and EC19 have been shown to load onto ion exchange chromatography beads in a similar way to ATRA (Budge, 2010; Eichele et al., 1984). EC23 and EC19 have been shown to generate differential effects previously *in vitro* in the pluripotent stem cell line TERA2.cl.SP12 (Christie et al., 2008). Preliminary studies *in vivo* using the chick wing bud model system and smaller beads than the present study (50-150μm) have indicated that they also generate differential effects *in vivo* and have differential toxicity (Budge, 2010). This preliminary study showed that survival rate was lower after treatment with EC23 compared to either EC19 or ATRA. It also showed that EC23 mimicked the effects of ATRA in that it could generate digit duplications ranging from a single extra digit of the most anterior identity to complete mirror image duplication. EC19 was unable to produce these phenotypes but, similar to EC23 and ATRA, EC19 did truncate upper beak outgrowth. Interestingly, EC23 was seen to generate duplication of multiple additional digits of the most anterior identity i.e. 11123 or 111123 in 3.3% of embryos which survived till HH35 when applied to the anterior wing bud at 0.01mg/ml (Budge, 2010). The present study has further characterised the effects of EC23 and EC19 using beads with a diameter of 150-300μm to investigate the effects of increased quantities of these retinoids and the duplication of additional digits of the most anterior identity seen previously. 0.01mg/ml EC23 was chosen for further study as Budge (2010) had found that it generated the highest frequency of digit duplication, is the highest concentration of EC23 which allows survival and is the only retinoid concentration to duplicate multiple additional digit 1s. 1mg/ml ATRA was chosen for further comparison as it generated a similar frequency of phenotypes to 0.01mg/ml EC23.

Table 3.1 shows the percentage of embryos surviving after 7 days of EC23 and EC19 compared to ATRA. EC23 and ATRA have a similar survival rate at the concentrations chosen. ATRA exhibits a slightly lower survival rate indicating that it may be more toxic

than EC23. Interestingly there appears to be a difference in survival rate when EC23 is compared to EC19 at 0.01mg/ml. It can be seen that embryos treated with this concentration of EC19 exhibit a worse survival rate than those with EC23. This may also be due to the difference in number of operations performed as 38 fewer operations were performed with 0.01mg/ml EC19 than with EC23. However, it does appear that there is an increase in embryo survival at higher concentrations of EC19 as a similar number of operations were performed for both concentrations, yet there is a much higher survival rate with 0.1mg/ml EC19 than 0.01mg/ml EC19. This result is consistent with previous findings (Budge, 2010).

These results show that the survival rates are similar to those obtained previously (Budge, 2010). The fact that EC19 is less toxic than EC23 and demonstrates a similar toxicity to ATRA indicates that EC23 is more potent. This increased potency of EC23 may be due to a number of factors: enhanced CRABP2 binding, enhanced RAR binding or prolonged RAR activation due to differences in metabolism. Given the structural similarity with TTNPB, it is likely that these will all contribute to its increased potency (Pignatello et al., 1999, 2002). The low potency of EC19 is surprising as the structure of EC23 and EC19 are identical bar the position of the terminal carboxylic acid group (see figure 1.5).

Table 3.1: The toxicity of the synthetic retinoids EC23 and EC19 compared to ATRA.

Retinoid Concentration (mg/ml in DMSO)	Number of operations			% survival (number) surviving to 7 days		
	ATRA	EC23	EC19	ATRA	EC23	EC19
0.01	0	58	20	-	50 (29)	30 (6)
0.1	0	0	24	-	-	42 (10)
1	14	0	-	43 (6)	-	-

This shows the number of operations carried out at retinoid concentrations used. This is used to calculate the frequency/% survival 7 days after operation. % survival is presented as a percentage (number of embryos). % survival of DMSO only treated embryos was 44% (n=9).

Table 3.2 : The frequency and nature of limb phenotypes generated with ATRA and EC23.

Retinoid	Conc. (mg/ml)	Frequency (number) of limb phenotypes seen in embryos surviving to 7 days.									
		123	1123	11123	111123	2123	21123	1223	32123	Truncated	Other
EC23	0.01	35 (10)	24 (7)	17 (5)	3 (1)	0	0	0	0	10 (3)	7 (2)
ATRA	1	0 (0)	33 (2)	0	0	17(1)	17 (1)	17 (1)	17 (1)	0	0

Retinoids were used to treat HH20 chick embryos and phenotypes scored after 7 days of incubation. Normal limb development is referred to as 123 as shown on A) in accompanying figures e.g. figure 3.2. Extra digits are denoted by numbers before this and refer to the digit identity assigned by length of ectopic digits. "Truncated" refers to limbs which have extensively shortened or absent zeugopod and/or autopod elements (figure 3.2F). "Other limb defects" are those embryos which did not exhibit clear digit duplications (figures 3.2G-H). No limb phenotypes were seen when anterior wing buds were treated with DMSO alone. Abbreviations: conc, concentration.

EC23 mimics the effects of ATRA on limb development but EC19 has no effect at concentrations tested.

Consistent with the previous findings by Budge (2010) I have also found that EC23 and EC19 have differential effects *in vivo*. Budge (2010) found that EC23 caused digit duplications and facial phenotypes similar to ATRA but at concentrations 2 orders of magnitude lower than ATRA (Budge, 2010). EC19 was also found to cause similar facial phenotypes to ATRA but far fewer digit duplications. Digit duplications were only documented by Budge (2010) at 0.1mg/ml and 3mg/ml EC19. Despite the structural similarity of EC23 and EC19, I report that EC19 was not seen to generate digit duplications when using beads with a diameter of 150-300μm. In analysing the frequency of digit duplication and facial phenotypes, it was evident that EC23 and ATRA also affect other parts of wing development: cartilage element length, scapula and elbow development. These shall be addressed in order of their frequency.

EC23 causes duplication of multiple anterior digits whereas ATRA causes a wide range of duplications.

In the present study, the effect of a photostable retinoid, EC23 (Christie et al., 2008), has been investigated and compared to ATRA at one concentration. HH20 chick wings were treated with retinoid soaked beads and re-incubated for 7 days to study the digit duplications produced. Digit identity was assigned dependent on digit length, width and then finally on number of cartilage elements. The reason for this was that duplicated digits often did not form joints correctly and therefore the number of cartilage elements was not deemed a reliable method for determining digit identity. Wings designated as "truncations" were so assigned due to their appearance prior to clearing. These limbs appeared to lack autopodal elements concurrent with shortened zeugopod and stylopod elements. Recent research has demonstrated that the three digits in the developing avian wing correspond to digits 1, 2 and 3 of mammalian development (Towers et al., 2011) and therefore this nomenclature shall be used to identify and discuss the phenotypes seen.

Table 3.2 demonstrates the frequency of digit duplications and limb phenotypes seen with EC23 and ATRA. As can be seen EC23 generates a high frequency of digit duplications containing additional digits of the most anterior identity. However, ATRA generated a

range of digit duplications from the least severe (anterior digit duplication; 1123) to most severe (complete mirror image duplication; 32123). It can also be seen that ATRA never generated digit duplications containing multiples of the most anterior digit e.g. 11123 or 111123, both of which were seen with 0.01mg/ml EC23.

Figures 3.2 and 3.3 show examples of the range of limb phenotypes seen with 0.01mg/ml EC23 and 1mg/ml ATRA respectively ranging from the least to most severe. It can be seen from figure 3.2 and table 3.2 that the predominant duplication phenotype with EC23 is of multiple additional digit I. The differences between the types of duplication seen with ATRA and EC23 can be contrasted with when these are compared to the duplications seen in figure 3.3. Figure 3.3 shows that the full range of digit duplications can be generated with 1mg/ml ATRA from duplication of the most anterior digit (1123; figure 3.3B) to mirror image duplication (32123; figure 3.3E).

Some EC23 treated embryos can develop truncated limbs as seen in figure 3.2F which has been documented after application of high concentrations of ATRA (Tickle et al, 1985). Figures 3.2G and 3.2H show the two limbs classified as "other" in table 3.2. They were so assigned as they did not exhibit clearly identifiable digit identities. The wing in figure 3.2G could be classified as digit duplication or a proximalisation effect. The wing shown in figure 3.2H was so assigned as it shows an abnormal number of digits but assigning digit identity is difficult as all digits appear to have similar identity similar to digit pattern after experimental dysregulation of BMP signalling (Drossopoulou et al., 2000).

These data are consistent with the finding that EC23 mimics the effect of ATRA *in vitro* (Christie et al., 2008) and previous data *in vivo* (Budge, 2010). The ability of ATRA to generate digit duplications at the current concentration is consistent with data documented by Budge (2010) and previous literature (Tickle et al., 1985). The fact that EC19 did not generate any digit duplications is consistent with its lower potency *in vitro* (Christie et al., 2008). Interestingly EC23 was able to generate phenotypes of multiple additional digits of anterior identity not seen by Budge (2010) or Tickle et al (1985). Therefore, EC23 application at this concentration and quantity could be used as a tool to study anterior digit development.

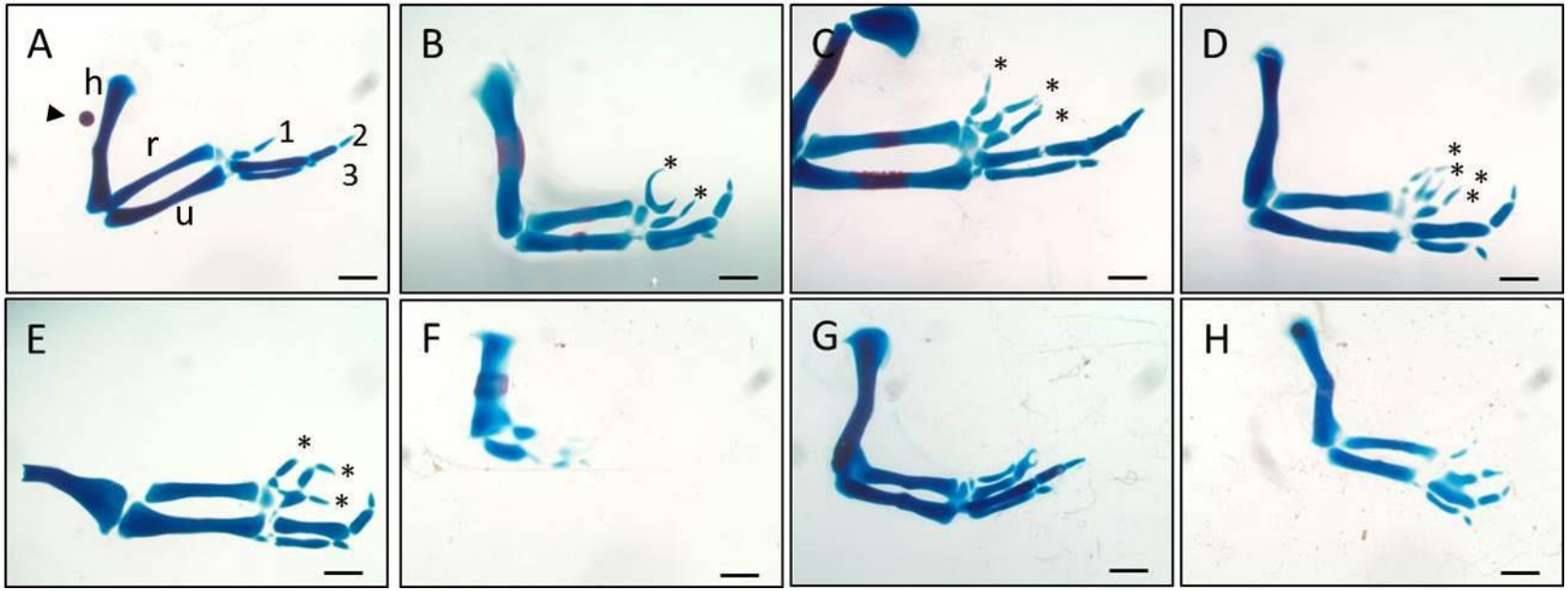

Figure 3.2: The effect of 0.01mg/ml EC23 on chick wing development.

Dorsal views of whole mount skeletal preparations of isolated retinoid treated wings are shown. A) shows the effect of DMSO with normal digit development shown by numbers 1, 2, 3. The arrowhead indicates the bead. B) to F) show the digit duplications generated with EC23 ranging from least to most severe: B) 1123, C) 11123, D) 111123, E) 11123, F) truncation. G and H) do not exhibit clear digit duplications and have been designated "other". Multiple digit 1's are highlighted by asterisks. Abbreviations: h; humerus, r; radius and u; ulna. Scale bars are 1mm.

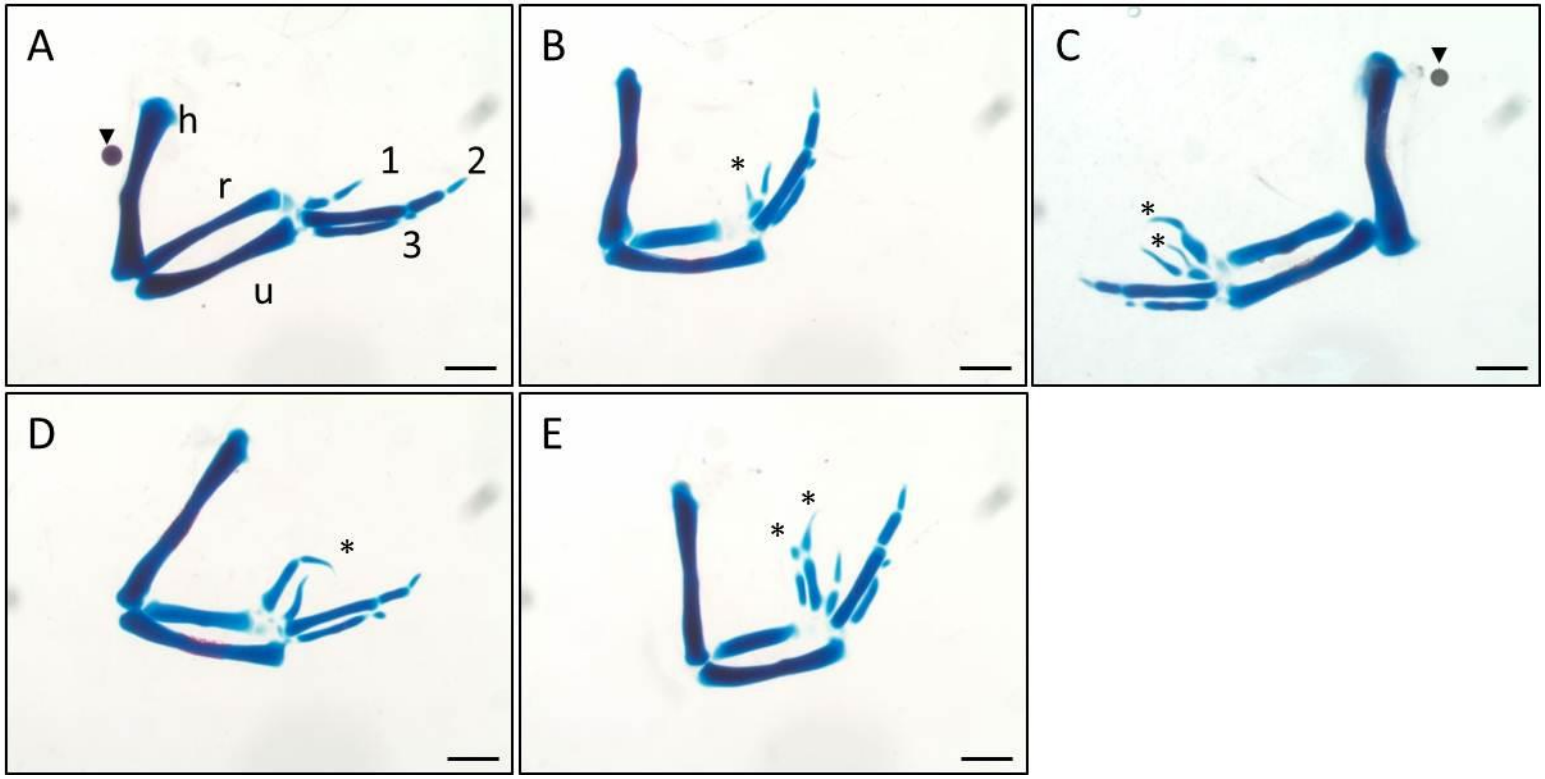

Figure 3.3: The effect of 1mg/ml ATRA on chick wing development.

Whole mount skeletal preparations of isolated retinoid treated wings are shown. A) shows the effect of DMSO. Digits 1, 2 and 3 are indicated to show normal digit development. B) to E) show the digit duplications generated with ATRA ranging from least to most severe. B) 1123, C) 21123, D) 2123, E) 32123. Arrowheads in A) and C) indicate the bead. Asterisks indicate additional digits. Abbreviations: h, humerus; r, radius; u, ulna. Scale bars are 1mm.

Both EC23 and ATRA affect cartilage element size of the humerus, radius and ulna.

The development of the different cartilage elements is the first morphological sign of differentiation in the developing limb and muscles, tendons and nerves develop subsequently (Thorogood and Hinchliffe, 1975). Cartilage development is connected to overall limb size and patterning as removal of the AER causes limb reductions dependent on the time of removal (Niswander et al., 1993). Knock out or dysregulation of signalling pathways such as BMP, growth and differentiation factor 5 (GDF5) or transforming growth factor β (TGFβ) (Brunet et al., 1998; Spagnoli et al., 2007; Storm and Kingsley, 1996; Yi et al., 2000) can cause reductions to limb element length and exogenous BMP can generate longer elements and increase humerus width (Macias et al., 1997). Changes to the ECM have also been shown to affect limb length (Choocheep et al., 2010; Hudson et al., 2010; Shepard et al., 2008; Wilson et al., 2012). Retinoids have been shown to affect members of these pathways. High concentrations of retinoids can truncate limb development and depending on the position of application on the PD axis, they can affect proximal elements (Tickle and Crawley, 1988). Application of ATRA to the posterior proximal wing can affect length of the zeugopod and autopod elements (Tickle et al., 1985) as can application of extremely high concentrations of ATRA to the anterior wing bud at earlier stages than the present study (Summerbell, 1983). Consistent with a role for retinoids in element length it has been affected in both *Rarα/γ* null mice (Lohnes et al., 1994) and *cyp26b1* knockout mice (Pennimpede et al., 2010b; Yashiro et al., 2004). Given these previous results, cartilage element size was analysed in the present study.

It can be seen from table 3.3 that EC23 and ATRA cause malformation to the zeugopod (radius and ulna) and stylopod (humerus) of the wing. The frequency of digit duplication was 65% in EC23 treated wings and 100% ATRA treated wings, which is similar to the frequency of effects on zeugopod element size: 69% in EC23 treated wings and 100% in ATRA treated wings. Both EC23 and ATRA also affected the humerus but with differential frequencies: ATRA causing a higher frequency of phenotypes. Interestingly, EC23 and ATRA showed differential effects on development of the humerus, radius and ulna.

Table 3.3: the effect of EC23 and ATRA on development of humerus, radius and ulna.

Retinoid	Concentration (mg/ml)	% of embryos (number) surviving after 7 days treatment with malformations to humerus, radius or ulna cartilage			
		RU change	Small Radius	Small Ulna	Humerus
EC23	0.01	69 (20)	48 (14)	48 (14)	48 (14)
ATRA	1	100 (6)	100 (6)	17 (1)	83 (5)

This shows the frequency of phenotypes and number of examples with a smaller length: width ratio of radius, ulna or humerus. Note that embryos exhibiting smaller radius or ulna are both included in the column designated RU change. Some embryos show changes to one or both elements. Abbreviations: R, radius; U, ulna.

Table 3.4 : The effect of EC23 and ATRA on size of radius, ulna and humerus.

Retinoid	Concentration (mg/ml)	Average LW ratio of radius, ulna and humerus 7 days after treatment.		
		Radius	Ulna	Humerus
DMSO/untreated	N/A	12.6 (±2.5)	13.2 (±2.2)	11.9 (±1.0)
EC23	0.01	**8.6 (±2.5) *****	**9.2 (±3.1) *****	**9.4 (±2.3) *****
ATRA	1	**7.4 (±1.1) *****	**10.8 (±2.1) ***	12.4 (±1.8) NS

This shows average length: width ratio of these cartilage elements (±standard deviation). Significance was tested using an unpaired student t-test to compare retinoid treated to DMSO treated cartilage elements. * $p<0.05$, ** $p<0.01$, *** $p<0.001$, NS indicates not significant.

Both EC23 and ATRA application at HH20 decreased the humerus length: width ratio (L: W) which is characterised phenotypically by a thickened and shorter humerus (compare figure 3.5A with 3.5C and 3.5H). It can be seen from table 3.3 that ATRA causes this phenotype at twice the frequency of EC23. However, it appears from table 3.4 that EC23 generates a more severe effect on humerus size than ATRA supported by the fact that the humerus L: W ratio of untreated embryos vs. ATRA treated embryos was not significant. This is contrasted with the highly significant drop in length: width ratio seen when EC23 treated and untreated humerus is compared. It can be seen from figure 3.4B and 3.4C) that the correlation between length and length: width of the humerus is reduced with retinoid treatment supporting the observation that there is a change to the width of the humerus. The fact that this correlation is markedly reduced in ATRA treated embryos but there is no significant change in humerus L: W ratio reflects the fact that there is a greater range in the phenotypes of the ATRA treated embryos than the EC23 treated embryos.

Table 3.3 shows that 69% of embryos treated with 0.01mg/ml EC23 exhibit a change in the L: W ratio of the radius and/or the ulna and these effects occur at equal frequencies (table 3.4). This can be contrasted with ATRA which affects the radius in all embryos treated but only affects in ulna in a subset (table 3.4), consistent with previous literature (Summerbell, 1983). Figure 3.5 shows examples where EC23 or ATRA have affected the length of the zeugopod elements equally (figure 3.5B, 3.5D, 3.5F and 3.5H) or one element more than the other (figure 3.5C, 3.5E and 3.5G) in a single embryo. Graphs plotting the radius L:W against ulna L:W show that there is less correlation between the development of these two elements in the presence of retinoid indicating that they are both sensitive to retinoid treatment (Figure 3.6). The correlation between radius and ulna in response to EC23 is more similar to untreated wings consistent with observations that the radius and ulna can be equally affected. The further decrease in correlation in response to ATRA is consistent with the observation that ATRA affects the radius at a higher frequency than the ulna (tables 3.3 and 3.4; figures 3.6C and 3.6B).

Radius and humerus L: W ratios co-vary less in retinoid treatment consistent with the observations that one or both are malformed after retinoid treatment and that this effect is independent of the other element (figure 3.7 and Table 3.3). Ulna and humerus L: W co-vary to a similar extent in DMSO and ATRA treatments consistent with the fact that ATRA has little effect on these elements (Figure 3.8, table 3.3). However there is much less correlation in response to EC23 treatment consistent with the fact that one or both elements are often significantly malformed in response to EC23 (figure 3.8, table 3.3).

Due to the fact that element size increases during outgrowth of the limb and that embryos were not at the exact same developmental stage, age of the embryos recovered could explain the changes to element length: width ratio. Therefore humerus length was plotted against humerus length: width ratio to discount the fact that differences in age may cause the differences seen in cartilage size. As can be seen from figure 3.4A, there is no significant correlation between the two in untreated wings indicating that age at harvest is unlikely to be a factor contributing to the phenotypes observed.

This shows that EC23 and ATRA both affect the entire PD axis. Therefore retinoids can affect the entire PD axis during limb development.

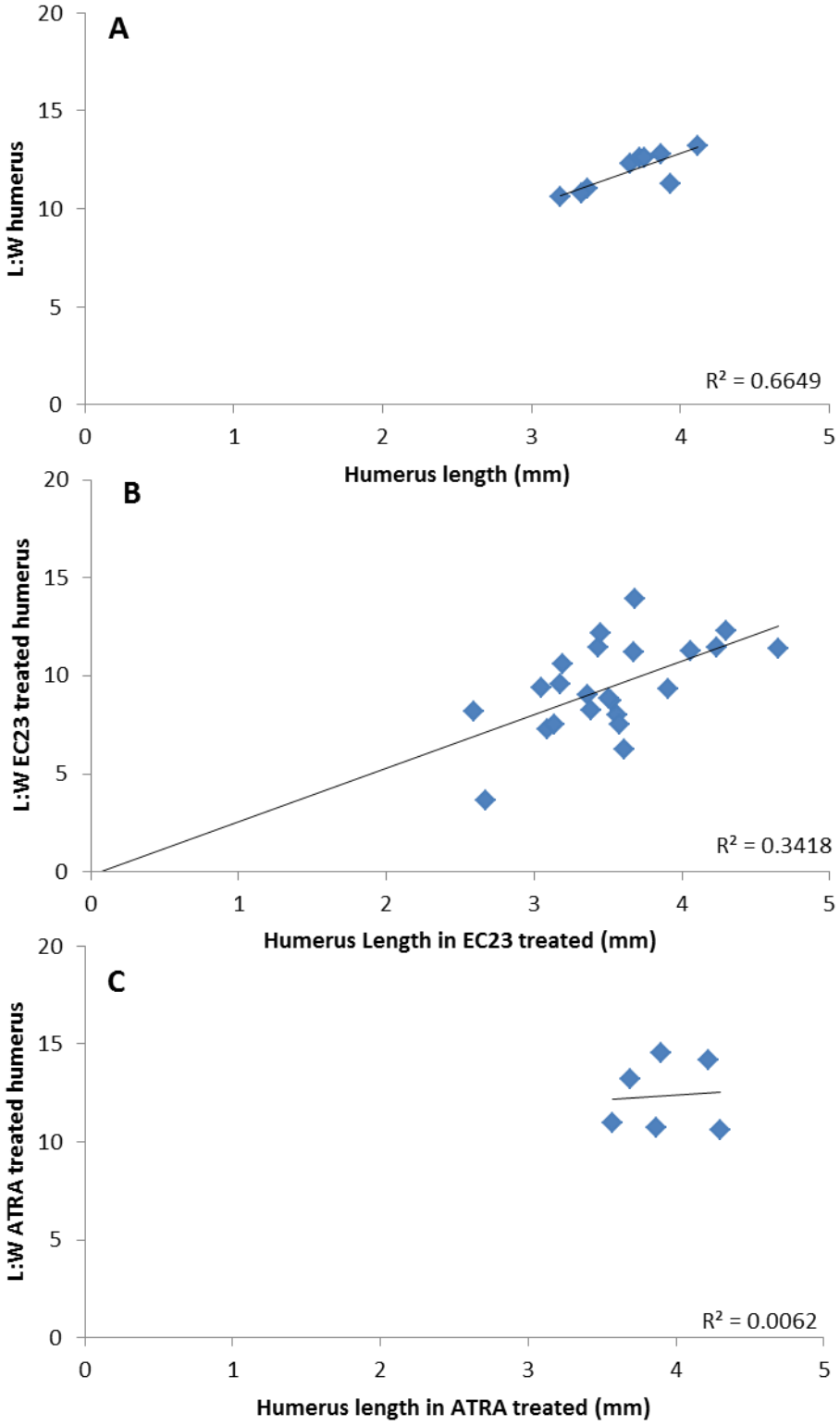

Figure 3.4 : The effect of ATRA and EC23 on the relationship between humerus length and length: width ratio.

A) shows the relationship between humerus length and length: width (L:W) ratio of the humerus in untreated/DMSO treated embryos. B) and C) show the same relationship in EC23 and ATRA treated embryos respectively. R^2 values are for the trendlines shown.

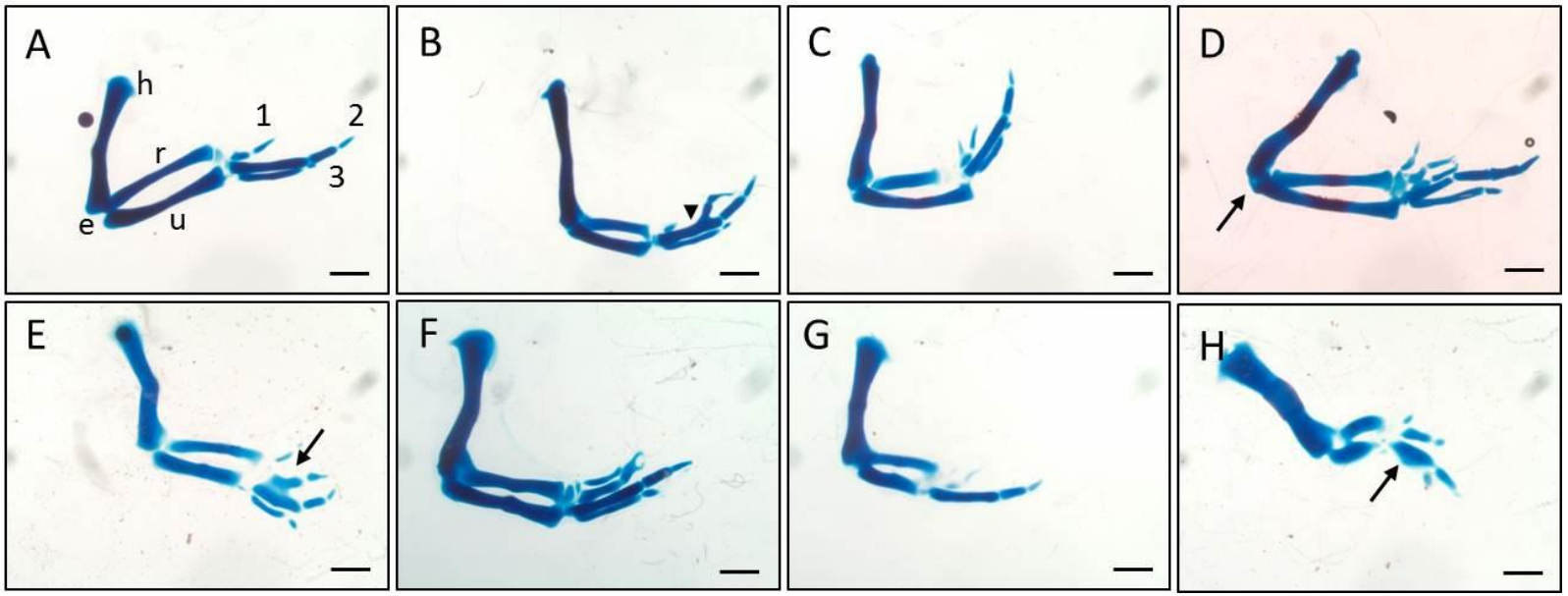

Figure 3.5 : Changes to length: width ratios of humerus, radius and ulna caused by EC23 and ATRA.

Whole mount skeletal preparations of isolated retinoid treated wings are shown. A) shows normal development of the wing in response to DMSO. B) and C) show the effect of 1mg/ml ATRA. B) shows 1223 duplication with the proximal cartilage elements of digit 3s fused (arrowhead). C) shows a 1123 digit duplication with the two digit 1s fused at the proximal element. B) and C) also exhibit shortened radius and ulna elements. D-H) show the effects of 0.01mg/ml EC23. D) shows normal length of the humerus, radius and ulna. The arrow indicates a humerus-radius fusion. E-H) show shortened radius and ulna elements as well as thickened humerus elements. The arrow in E) indicates a fusion between the 1st and 2nd digits. F) shows one of the wings with a digit duplication designated as "other" with severe thickening of the humerus and shortening of the zeugopod. G) shows severe effects on humerus, radius and ulna lengths. H) shows a severely truncated limb with abnormal development of the humerus, radius and ulna. The arrow in H) indicates a fusion between proximal elements of digits 2 and 3 of the 1123 duplication. Abbreviations: h, humerus; e, elbow; r, radius; u, ulna. Scale bars are 1mm.

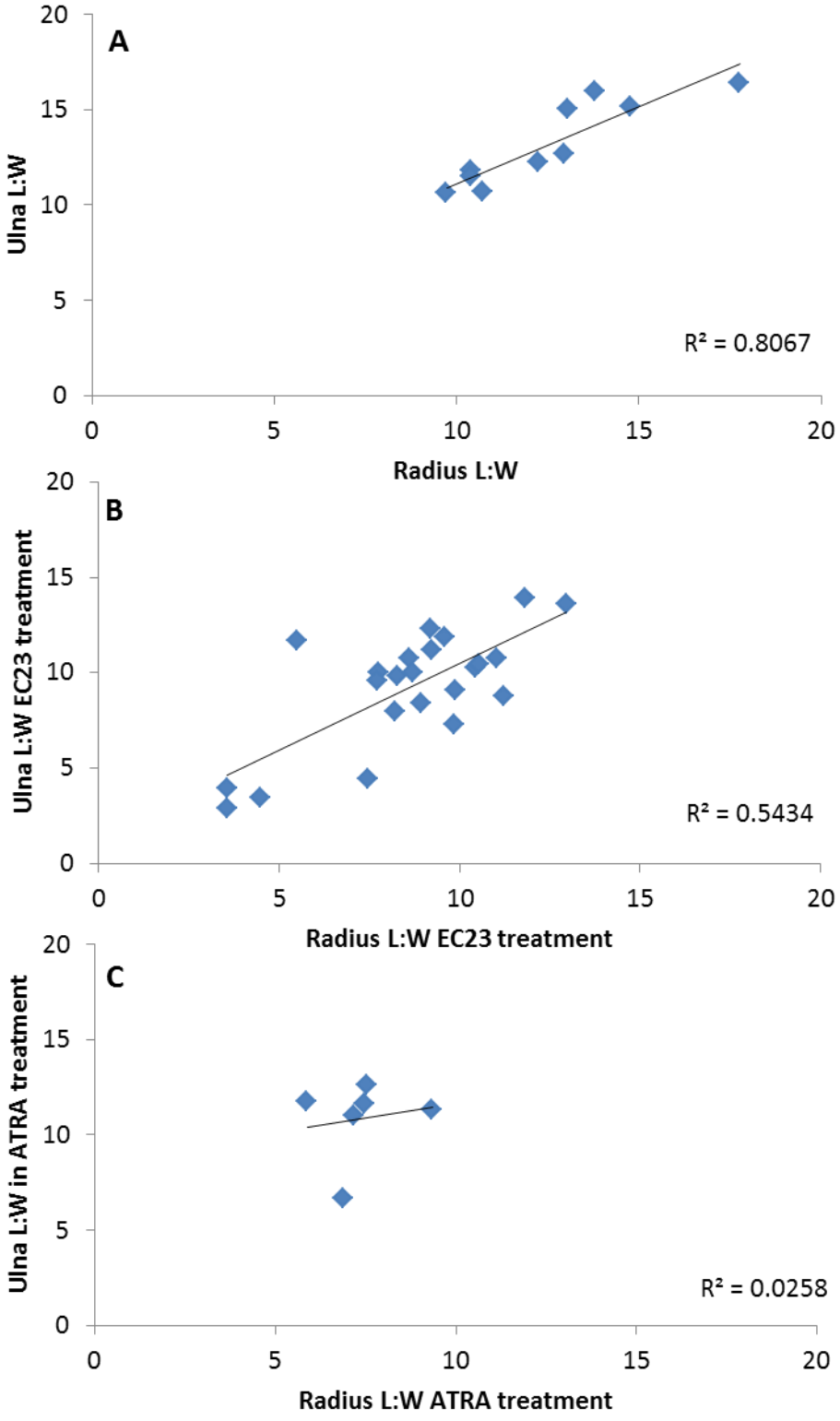

Figure 3.6 : The effect of retinoid on the relationship between radius and ulna length: width ratios. A) shows the relationship in DMSO/untreated wings. B) and C) show the relationship in response to EC23 and ATRA respectfully. The R^2 values shown correspond to the trendlines plotted. Abbreviations: L:W, length : width ratio.

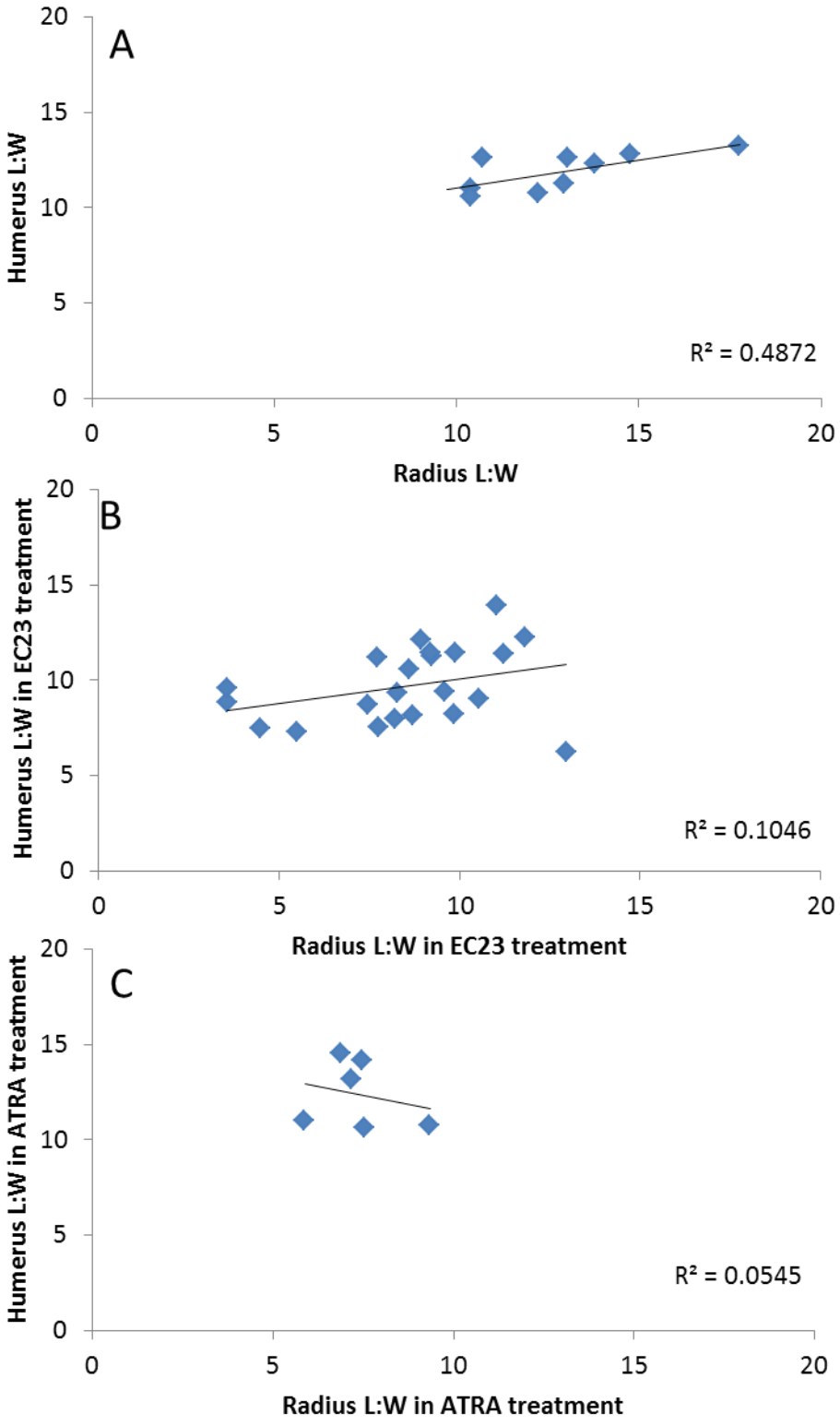

Figure 3.7 : The effect of retinoid on the relationship between radius and humerus length: width ratios.

A) shows the relationship in DMSO/untreated wings. B) and C) show the relationship in response to EC23 and ATRA respectfully. R^2 values shown correspond to the trendlines plotted. Abbreviations: L:W, length : width ratio.

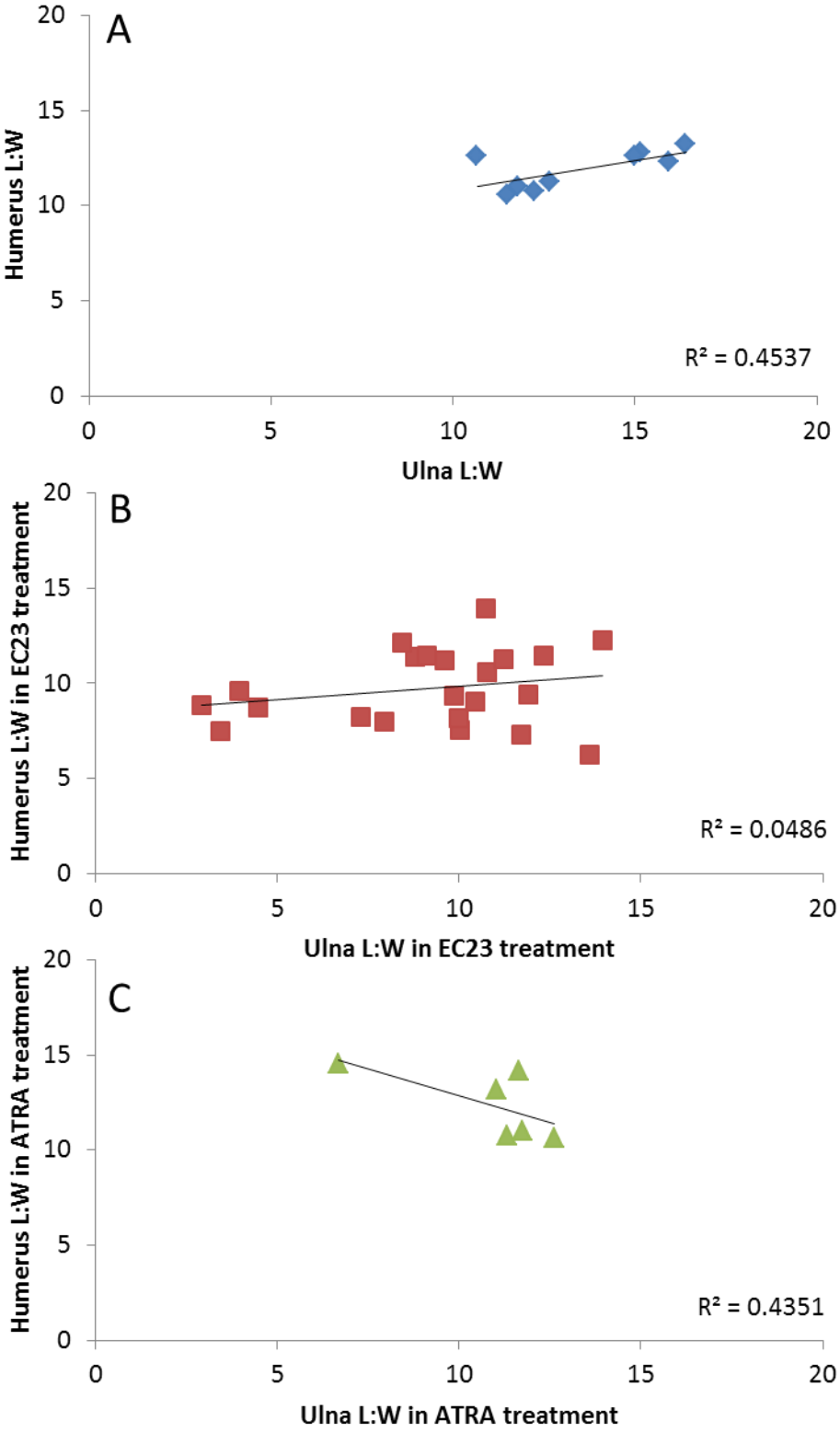

Figure 3.8 : The effect of retinoid on the relationship between ulna and humerus length: width ratios. A) shows the relationship in DMSO/untreated wings. B) and C) show the relationship in response to EC23 and ATRA respectfully. The R^2 values shown correspond to the trendlines plotted. Abbreviations: L:W, length: width ratio.

Both EC23 and ATRA affect scapula development.

The limb is characterised as having 3 segments: stylopod, zeugopod and autopod. Previous sections have addressed the effects on all of these segments. The limb girdle is also an important part of the limb in that it is necessary to connect the limb to the axial skeleton and important for subsequent function. However, compared to the rest of the wing skeleton, this region has been less extensively studied as it is not considered to be part of the wing skeleton. This is due to the fact that manipulations which cause dramatic malformation to the wing skeleton e.g. AER removal or high concentrations of ATRA at HH20 are not documented to affect the limb girdle (Niswander et al., 1993; Tickle et al., 1985). Its origins are also controversial: previous research has suggested that it develops entirely from the somites (Chevallier, 1977), from a mixture of the somites and LPM while research in Salamander indicated that it was purely derived from LPM (Huang et al., 2000). Latest research suggests that the scapula develops from a mixture of somite and LPM derived cells: head and proximal 2/3 of blade is LPM and distal portion is somite derived (Shearman et al., 2011). Previous research has shown that retinoids can affect the shoulder girdle if applied at HH18-20 in chick and showed that retinoid caused production of ectopic cartilage or duplication of the coracoid (Oliver et al., 1990).

Table 3.5 : The effect of EC23 and ATRA on scapula development.

A)

Retinoid	**Conc. (mg/ml)**	**% (number) of embryos surviving 7 days after treatment**	
		Normal	Malformed
EC23	0.01	24 (7)	66 (19)
ATRA	1	0	100 (6)

B)

Retinoid	**Conc. (mg/ml)**	**% embryos (number) with one or more scapula malformations surviving for 7 days**				
		Reduced	Foramen	Bend	Ectopic cartilage	Absent head
EC23	0.01	59 (17)	0	7 (2)	14 (4)	48 (14)
ATRA	1	83 (5)	17 (1)	0	17 (1)	67 (4)

HH20 chick wing buds were treated EC23 and ATRA. A) shows the frequency of embryos (number) surviving for 7 days after treatment with a normal or malformed scapula on the operated side. B) shows the frequency (number) of embryos with scapula malformations: reductions, foramen, bending, ectopic cartilage or absent head structure. Note that some examples exhibited more than one of these phenotypes and therefore an embryo can contribute to more than one total.

As mentioned previously, EC23 and ATRA affect the entire PD axis of the limb and they also affect the scapula. Malformation to the scapula occurs at a similar frequency to digit duplication and to changes to the zeugopod elements (compare Tables 3.2, 3.3 and 3.5A). As can be seen, all embryos treated with 1mg/ml ATRA that survived for 7 days exhibited a scapula malformation whereas 0.01mg/ml EC23 caused scapula malformations at a lower frequency. In the limited number of operations performed scapula phenotypes were always seen with digit duplications in response to 1mg/ml ATRA. Scapula phenotypes were not always concurrent with digit duplication in response to 0.01mg/ml EC23: 24% scapula malformations seen were with normal digit development. This indicates that some data may have been lost as embryos were not fixed without an obvious external phenotype. However, in most cases of EC23 treatment if there was a digit phenotype there was also a malformation of the scapula: 78% limb phenotypes had a malformed scapula and 67% scapula malformations were seen with digit duplication. 67% scapula phenotypes are seen concomitant with a change in the size of the radius and/or ulna. 52% scapula malformations are seen with a change in the size of the humerus.

As can be seen from table 3.5B, the scapula malformations generated ranged in severity. The most frequent scapula malformation seen with either EC23 or ATRA was a shortening of the scapula blade (figures 3.9C-D and 3.10C-D respectively). This was often concurrent with absence of the scapula head in EC23 and ATRA treated embryos (figure 3.9E and figure 3.10C-D respectively). There was a range in the severity of the scapula blade shortening in either EC23 or ATRA treated embryos (compare 3.10B with 3.10D for ATRA; 3.9D and 3.9E for EC23).

The least severe phenotypes are those of ectopic cartilage, bending and a foramen (figures 3.9 and 3.10). Both EC23 and ATRA can generate ectopic cartilage around the scapula as seen in figure 3.9D’ and 3.10C. This phenotype is consistent with previous literature although the ectopic cartilage has been documented to be a duplicated coracoid (Oliver et al., 1990). Duplication of the coracoid was never seen with EC23 and ATRA. Only EC23 was seen to have any effect on the coracoid causing one embryo to develop with a thickened coracoid (not shown). Significant bending of the scapula blade was only seen in response to treatment with 0.01mg/ml EC23 (figure 3.9C’). The development of a foramen in the scapula was only seen once in response to 1mg/ml ATRA (figure 3.10B’).

EC23 and ATRA are shown to affect the limb girdle as well as the entire PD axis of the wing. They both appear to affect regions of the scapula derived from both the LPM and the somitic mesoderm and therefore it is worth considering mechanisms affecting the development of both of these regions in determining their mechanism of action. Retinoids have been documented to affect shoulder girdle development if applied at HH18-20 or at high concentrations. Unlike the present findings, previously they have induced formation of ectopic cartilage (Oliver et al., 1990). The mechanism behind this shortening of the scapula was investigated by analysing the effect of retinoid on *Pax1* expression.

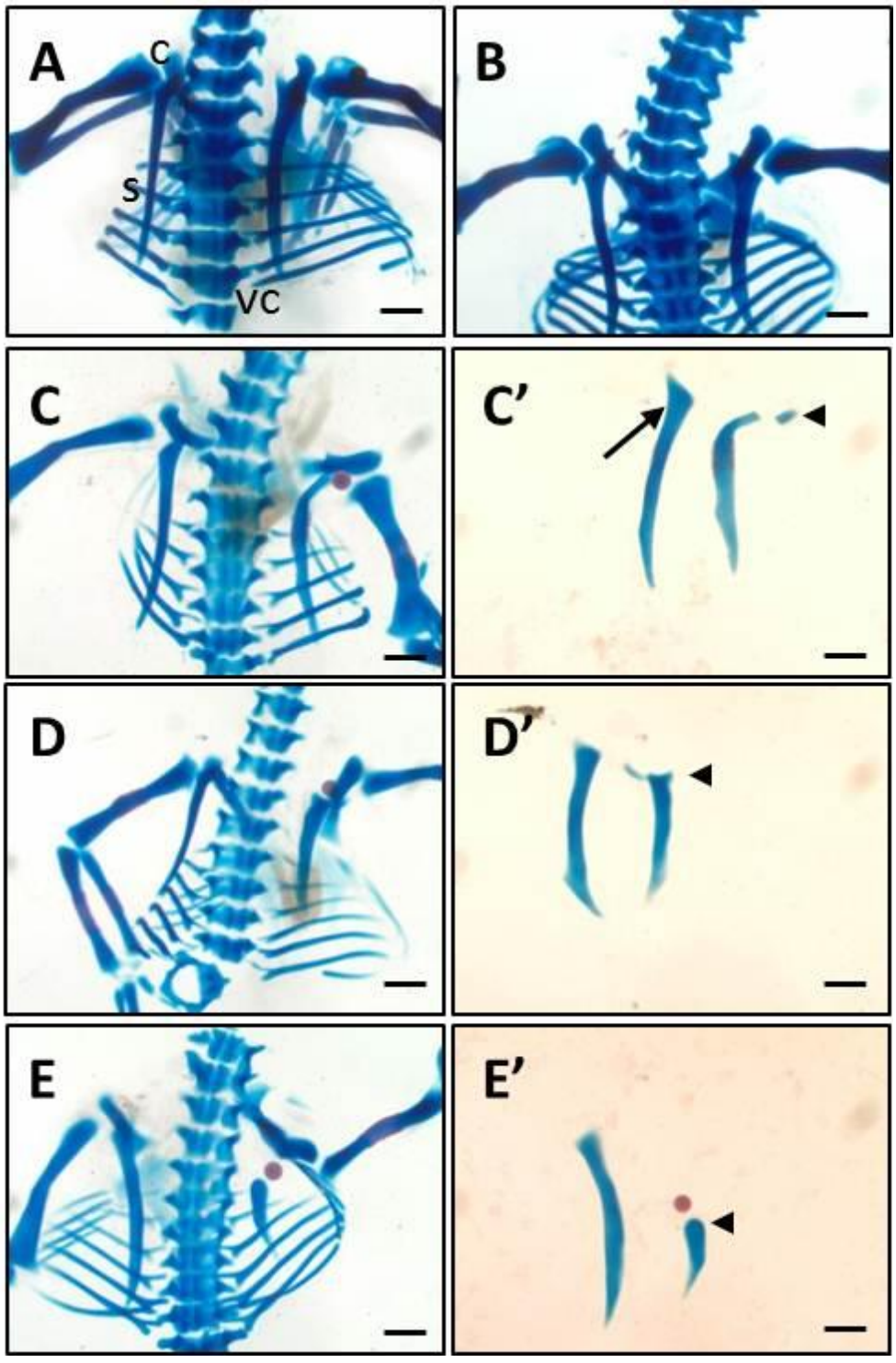

Figure 3.9 : The effect of 0.01mg/ml EC23 on scapula development.

Whole mount skeletal preparations of isolated retinoid treated torsos and scapulae are shown. A, B, C, D and E) are dorsal views of the torso with the operated wing on the right and anterior is top. C', D' and E') are flat views of both scapulae from the adjacent embryo: right is operated. A) shows the effect of DMSO. B) to E') show the scapula phenotypes generated with EC23 ranging from least to most severe. C) shows an example of scapula blade bending. D) shows an example of ectopic cartilage and E) shows an example of scapula blade truncation. C', D' and E') also exhibit absence of the scapular head. Arrow in C') indicates the scapular head on the un-operated wing. Arrowheads in C', D' and E') indicate absence of the scapular head on the operated side. Abbreviations: s, scapula; c, coracoid; vc, vertebral column. Scale bars are 1mm.

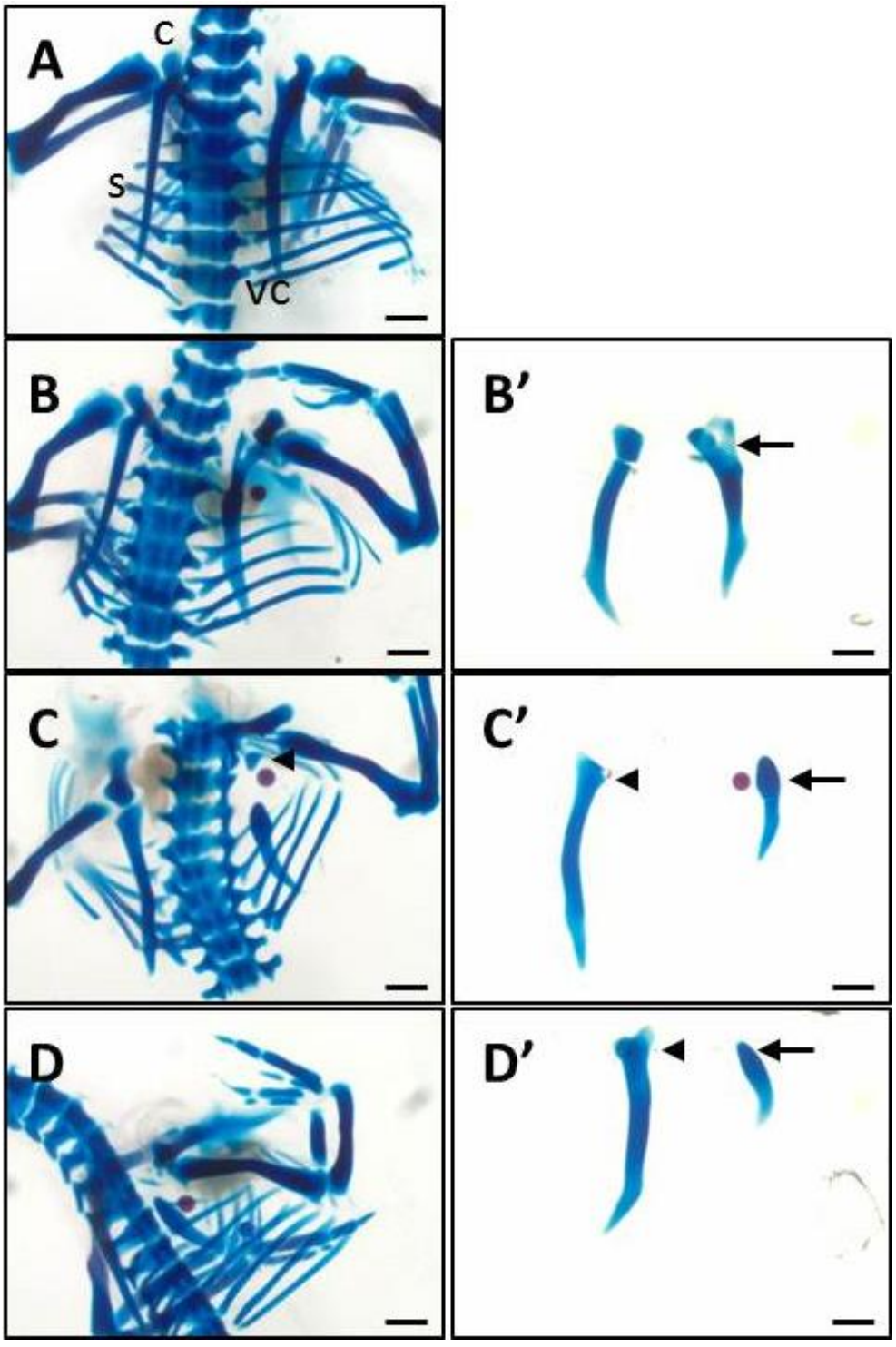

Figure 3.10 : The effect of application of 1mg/ml ATRA at HH20 on scapula development.

Whole mount skeletal preparations of isolated retinoid treated torsos and scapulae are shown. A,B,C and D) are dorsal views of the torso with the operated wing on the right and anterior is top. B', C' and D') are ventral views of both scapulae from the torsos shown: right is operated. A) shows the effect of DMSO. B) to D') show the scapula phenotypes generated with 1mg/ml ATRA ranging from least to most severe. B) shows the scapula can develop a foramen (arrow in B') in the presence of ATRA. C) shows the presence of ectopic cartilage indicated by the arrowhead. C, C', D and D') show reduction to the scapula blade in the presence of ATRA. They also show that scapula head formation can be inhibited in the presence of ATRA (arrow compared to arrowhead in C' and D'). Abbreviations: s, scapula; c, coracoid; vc, vertebral column. Scale bars are 1mm.

Both ATRA and EC23 affect expression of the scapula marker *Pax1*.

The mechanisms controlling scapula development are still largely unknown. *Pax1* has been implicated in scapula development as the *Pax1* knock out mouse (*undulated*) shows malformations in the structures which articulate with the clavicle (acromion and spina scapula-see figure 3.17; (Timmons et al., 1994). Its expression pattern has also been documented in mouse and chick development (Huang et al., 2000; LeClair et al., 1999). *Pax1* expression in chick has been shown to precede scapula cartilage development and is the only marker for scapula development (Huang et al., 2000). *Pax1* has been documented as a marker of chondrogenic cells in the dermomyotome (Huang et al., 2006) and as a marker of the scapula although it is absent from condensations (Huang et al., 2000; LeClair et al., 1999; Timmons et al., 1994). Therefore, the mechanism behind the scapula reductions in EC23 and ATRA treated embryos was investigated by investigating the effect of these retinoids on *Pax1* expression.

Pax1 expression is seen in chick from HH21 as a crescent shaped band at the proximal dorsal wing as well as in a domain in the anterior wing. This band then extends caudally between HH22-25 and at HH23 it could be found cranial and ventral to the shoulder. By HH26-27 it is found at the cranial edge of the shoulder and dorsal to the shoulder there is a pronounced cranio-caudal stripe of expression. At HH28 there is a new spot of expression in the dorsal posterior limb bud which later becomes a stripe of posterior expression. By HH29 *Pax1* is seen at the cranial parts of the scapula at the scapula-humeral joint as well as caudally along the dorsal margin of the scapula (Huang et al., 2000; LeClair et al., 1999).

Figure 3.11 shows whole mount *in situ* hybridisation for *Pax1* expression in the wing after 48hrs of retinoid treatment. The solid arrows indicate normal expression of *Pax1* in untreated wings. It is seen to be expressed in a domain at the anterior, proximal wing and on the ventral side. This is similar to that reported at HH24-26 (Huang et al., 2000; Timmons et al., 1994). It can be seen that both EC23 and ATRA down-regulate *Pax1* expression. This down-regulation can be complete as shown in figure 3.11 (n=2/6 ATRA or n=3/5 EC23) or a reduction in *Pax1* levels (n=3/6 ATRA or n=1/5 EC23; not shown). These data are consistent with the idea that retinoids cause the scapula phenotype via a

down-regulation of *Pax1* and highlights the fact that retinoids can affect the entire PD axis of the limb.

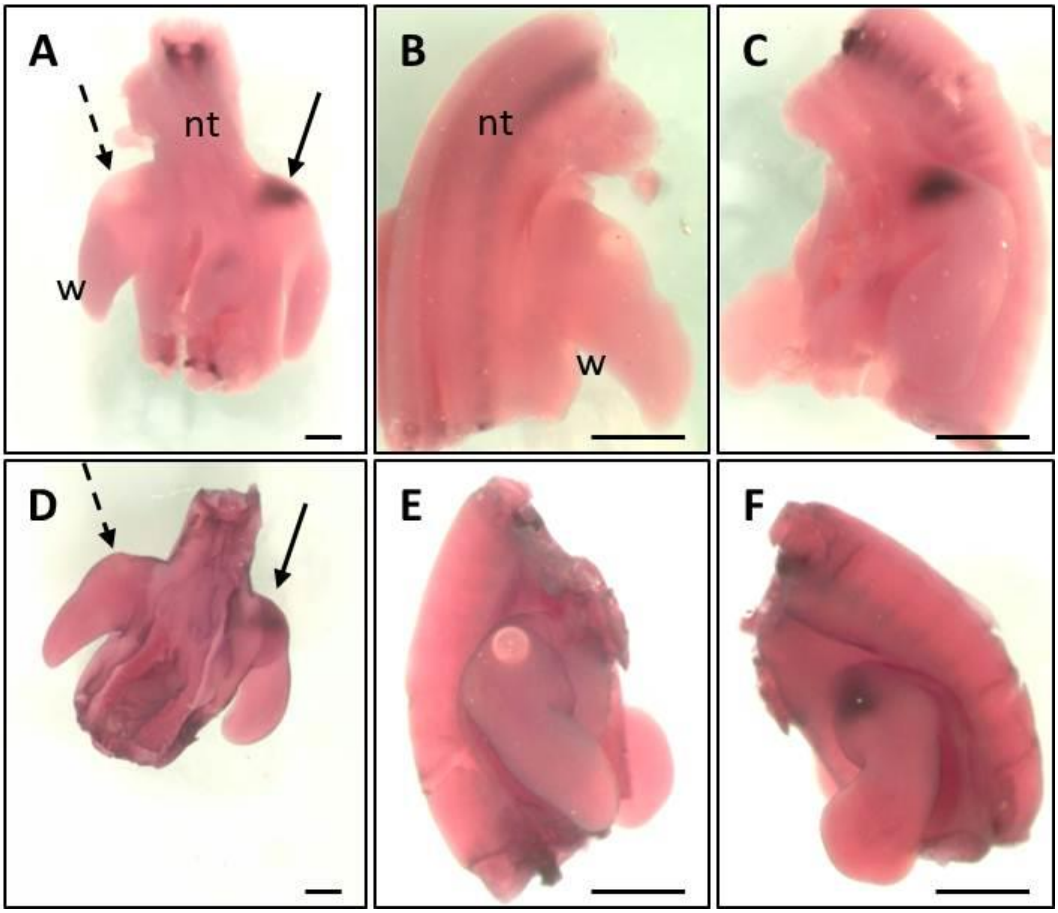

Figure 3.11 : The expression pattern of *Pax1* in response to retinoids.

Embryos were treated with retinoid dissolved in DMSO at HH20 and allowed to develop for 48hrs. *Pax1* expression was investigated using whole mount *in situ* hybridisation. A and D) are ventral views while B,C,E and F) are lateral, dorsal views of chick wings after 48hrs of retinoid treatment. A-C) were treated with 1mg/ml ATRA and D-F) were treated with 0.01mg/ml EC23. B and E) show *Pax1* expression is absent in the presence of retinoid. This is also shown by the dashed arrows in A) and D). C and F) show normal expression of *Pax1* on the contralateral side of the embryo. This is also shown by the solid arrows in A) and D). Abbreviations: nt, neural tube; w, wing. Scale bars are 1mm.

Both EC23 and ATRA affect elbow development and cause digit fusions.

As mentioned previously both EC23 and ATRA can be seen to generate fusions to the elbow joint or between digits during wing development (table 3.6 and figures 3.12 and 3.13). Table 3.6 shows that the frequencies of elbow phenotypes seen are similar between EC23 and ATRA. EC23 has not been observed to cause fusion of the humerus-ulna and ATRA has not been observed to cause fusion of the humerus-radius elements. However, EC23 can fuse humerus-radius (figures 3.12B and 3.13D) and ATRA can fuse humerus-ulna (figure 3.12F and 3.13B). Both EC23 and ATRA can generate fusion of all three elements at varying severity. Fusion of the three elements by 0.01mg/ml EC23 can occur with varying degrees of severity (compare figure 3.12C and 3.12D). This can also be seen more clearly by comparing figure 3.13C and 3.13E. The degree of severity was not seen to be as wide with ATRA (data not shown) but this could be due to number of operations performed.

As seen from table 3.6, EC23 and ATRA cause fusions to developing digits at similar frequencies. Figure 3.12E and 3.12F show examples of digit fusions in response to 0.01mg/ml EC23. These are between cartilage elements of digit 1s. 0.01mg/ml EC23 can also generate fusions between other digits as seen in figure 3.5E and 3.5H. 0.01mg/ml EC23 also caused bifurcation of a duplicated digit 1 as seen in figure 3.12G. 1mg/ml ATRA was also able to generate digit fusions (figure 3.5B).

Table 3.6 : The frequency and nature of cartilage element fusion in wing development after treatment with EC23 and ATRA.

Retinoid	Conc. (mg/ml)	% of embryos (number) surviving after 7 days treatment with fusions			
		HR	HU	HRU	Digit
EC23	0.01	17 (5)	0	21 (6)	10 (3)
ATRA	1	0	17 (1)	17 (1)	33 (2)

Note that some examples with digit fusions also exhibited more proximal fusions, and are included in the HR, HU and HRU frequencies. Abbreviations: conc, concentration; HR, humerus-radius; HU, humerus-ulna; HRU, humerus-radius-ulna.

Both EC23 and ATRA can cause digit fusions and elbow fusions. It can be seen that more severe effects on elbow fusion are seen with EC23 rather than ATRA confirming that it is a more potent retinoid than ATRA. EC23 and ATRA appear to differentially affect fusion of humerus and radius or ulna although both retinoids can cause the fusion of all three elements.

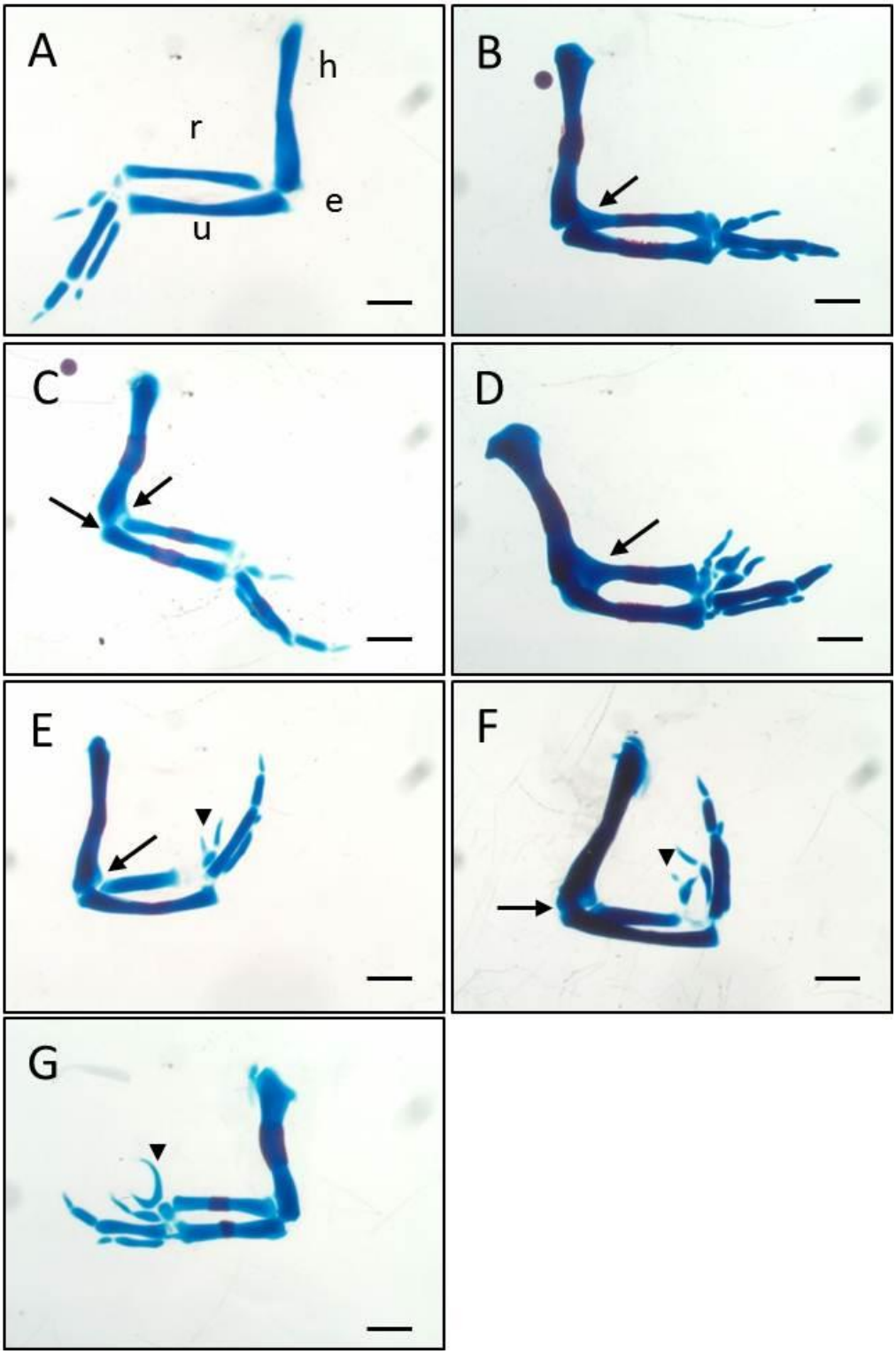

Figure 3.12 The effect of EC23 and ATRA on elbow and digit development.

Whole mount skeletal preparations of isolated retinoid treated wings are shown. A and G) show ventral views and B-F) show dorsal views. A) shows an untreated wing with normal digit and elbow development. B-D) show the effects of 0.01mg/ml EC23 on development of the elbow joint ranging from least to most severe. The arrow in B) shows a humerus-radius fusion. The arrows in C) show a mild humerus-radius-ulna fusion. D) shows a complete fusion of humerus-radius-ulna (arrow). E and F) show the effect of 1mg/ml ATRA on elbow development. E) shows a mild humerus-radius-ulna fusion (arrow). F) shows a humerus-ulna fusion (arrow). The arrowheads in E) and F) also indicate fusion between digit 1s in these duplications. G) shows a 1123 duplication with a bifurcation (arrowhead) in the most anterior digit with 0.01mg/ml EC23. Abbreviations: h, humerus; e, elbow; r, radius; u, ulna. Scale bars are 1mm.

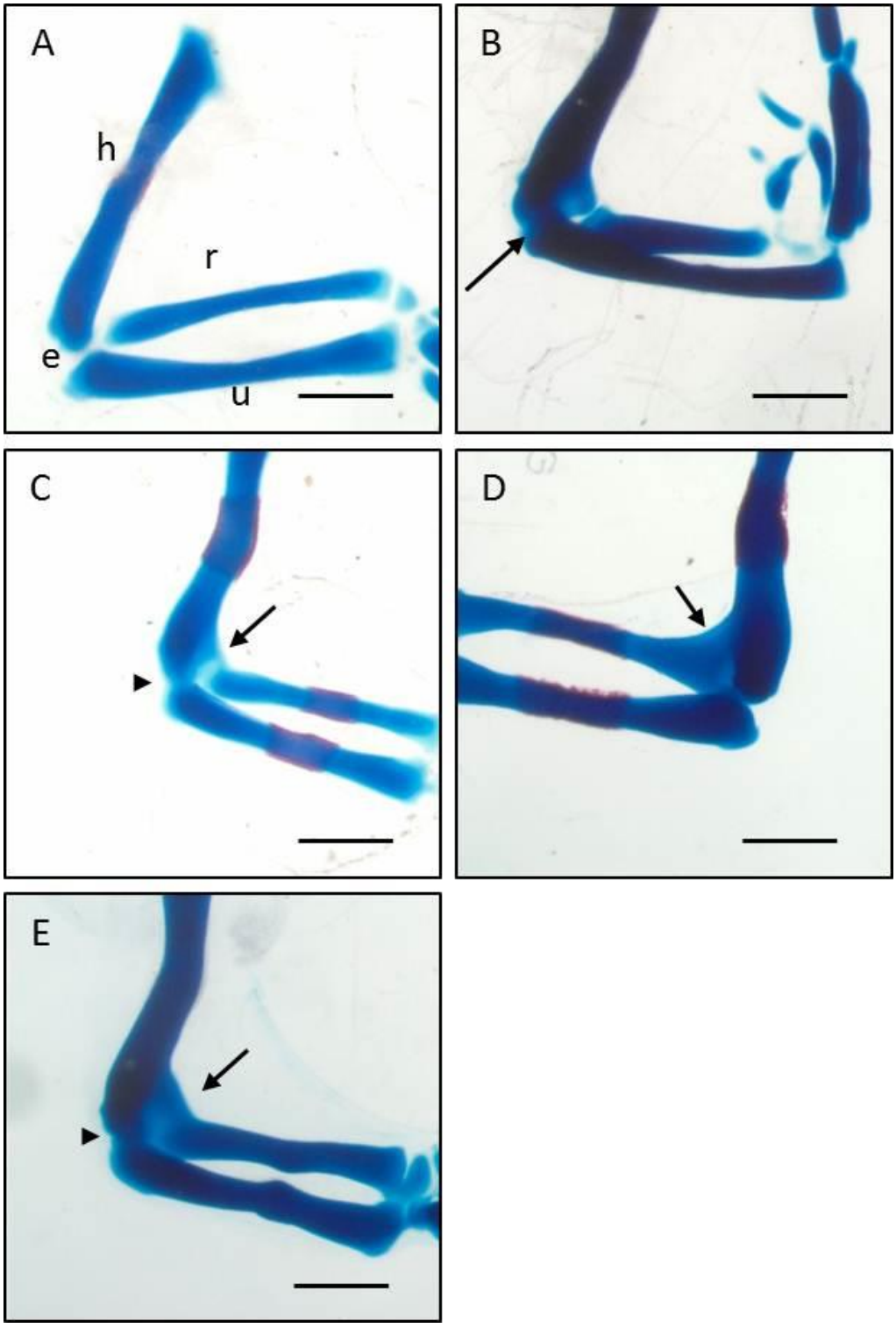

Figure 3.13 The effect of EC23 and ATRA on elbow development.

Whole mount skeletal preparations of isolated retinoid treated wings are shown. All images are dorsal views except A and D) which are ventral. A) shows an untreated wing with normal elbow development. B) shows an embryo treated with 1mg/ml ATRA and the arrow indicates a humerus-ulna fusion. C-E) represent phenotypes seen with 0.01mg/ml EC23. C) shows a mild humerus-radius-ulna fusion. The arrow and arrowhead indicate additional cartilage between humerus-radius and humerus-ulna respectively. D) shows a humerus-radius fusion with the additional cartilage indicated by an arrow. E) shows a complete fusion between humerus-radius and ulna. Extra cartilage is indicated between humerus-radius and humerus-ulna by an arrow and arrowhead. Abbreviations: h, humerus; e, elbow; r, radius; u, ulna. Scale bars are 1mm.

Effect of EC23, EC19 and ATRA on upper beak outgrowth.

Retinoids are also known to affect the development of the upper beak when applied to the anterior chick wing at HH20 (Tamarin et al., 1984). Therefore the effect of EC23, EC19 and ATRA on upper beak development was also compared. Table 3.7 shows the frequencies of facial phenotypes at concentrations chosen for EC23 and ATRA and 2 concentrations of EC19. EC23 and ATRA generated a range of facial phenotypes (figures 3.14 and 3.15). ATRA generated a mild reduction of upper beak outgrowth in 50% of embryos (see figure 3.14C) and the more severe truncated upper beak in 33% of embryos (figure 3.14D). 0.01mg/ml EC23 caused both reduced and truncated upper beak outgrowth in 38% and 14% of embryos respectively (figure 3.15G-H and 3.15I-J). EC23 was also able to cause asymmetric upper beak outgrowth (3% of embryos; figure 3.15C-D) and the production of an overbite (3% of embryos; figure 3.15E-F).

Interestingly EC19 was able to generate mild effects on upper beak outgrowth (table 3.7 and figure 3.16). At 0.01mg/ml EC19 only 17% of embryos exhibited a facial phenotype which was reduced upper beak outgrowth (table 3.7; data not shown). However, at 0.1mg/ml EC19 reduced upper beak outgrowth in a similar frequency to EC23 (table 3.7; figure 3.16G-H). 0.1mg/ml EC19 also generated a high frequency of asymmetric upper beak outgrowth (60%; figures 3.16C-D and 3.16E-F). The frequency of this phenotype is higher than the frequency seen with 0.01mg/ml EC23. It is also notable from comparing figure 3.16C-D with figure 3.16E-F that the asymmetry can be either towards or away from the source of retinoid (retinoid was always applied to the right wing). In the most severe phenotype generated by 0.1mg/ml EC19, there is both reduced and asymmetric upper beak outgrowth (figure 3.16G-H).

These data indicate that EC23 is more potent than EC19 *in vivo*. EC23 is able to generate more severe phenotypes at lower concentrations than EC19. This is consistent with previous findings by Budge (2010) and Christie et al (2008).

Table 3.7: The effect of ATRA, EC23 and EC19 on upper beak development in embryos surviving for 7 days after treatment.

Retinoid	Conc. (mg/ml)	Frequency of embryos surviving with facial phenotypes after 7 days treatment. %(number)				
		Normal	Asymmetric	Reduced	Truncated	Overbite
EC23	0.01	41 (12)	3 (1)	38 (11)	14 (4)	3 (1)
ATRA	1	17 (1)	0	50 (3)	33 (2)	0
EC19	0.01	83 (5)	0	17 (1)	0	0
EC19	0.1	10 (1)	60 (6)	40 (4)	0	0

Shows the frequency of embryos which survived for 7 days with either normal, asymmetric, reduced, truncated or overbite facial phenotypes. Reduction is characterised as decreased upper beak outgrowth whereas truncation is complete absence of the upper beak (see figures 3.14-16 for examples of all phenotypes). Numbers are presented as percentages of embryos surviving to 7 days (number surviving). Abbreviations: conc, concentration.

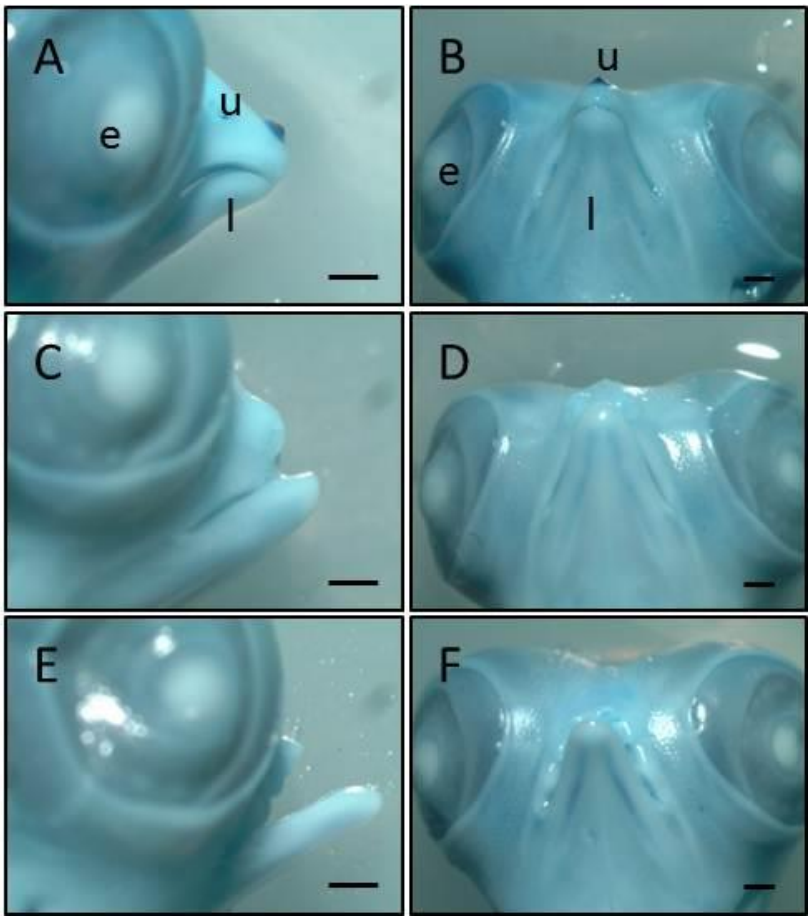

Figure 3.14: The effects of 1mg/ml ATRA on upper beak outgrowth.

A, C and E) show lateral views of embryos stained with Alcian Blue and B, D and F) show frontal views of the same embryo. A) and B) indicate the effect of DMSO on upper beak outgrowth. C) to H) show the phenotypes produced with 1mg/ml ATRA in increasing severity. C, D) show reduced upper beak outgrowth. E, F) show complete truncation of upper beak outgrowth. Abbreviations: e, eye; l, lower beak; u, upper beak. Scale bars are 1mm.

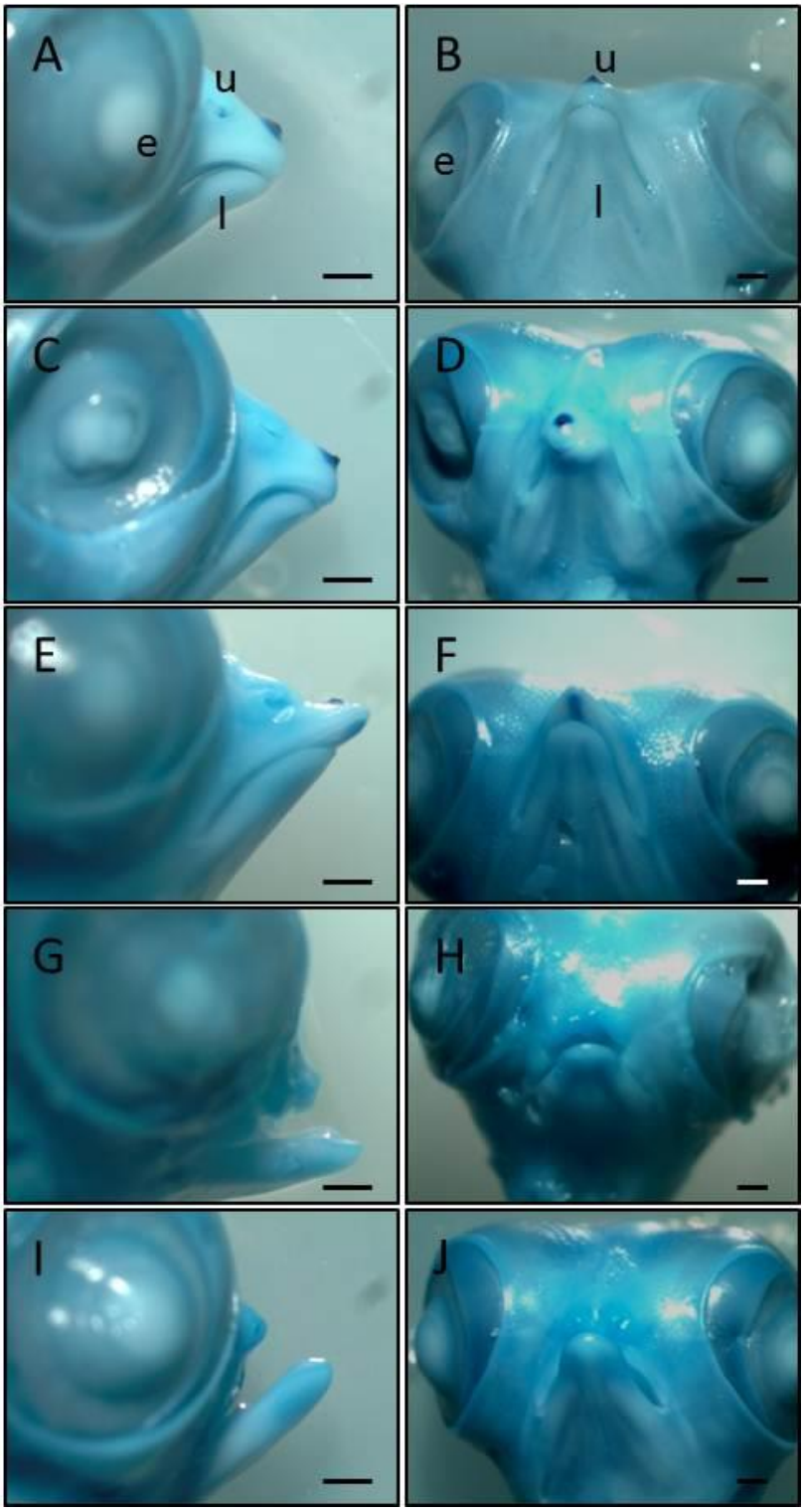

Figure 3.15: The effects of 0.01mg/ml EC23 on upper beak outgrowth.
A, C, E,G and I) show lateral views of embryos stained with Alcian Blue and B, D, F, H and J) show frontal views of the same embryo. A) and B) indicate the effect of DMSO on upper beak outgrowth. C) to J) show the phenotypes produced with 0.01mg/ml EC23 in increasing severity. C, D) show asymmetric upper beak outgrowth. E, F) show production of an overbite. G, H) show reduction in upper beak outgrowth. I, J) show complete truncation of the upper beak. Abbreviations: e, eye; l, lower beak; u, upper beak. Scale bars 1mm.

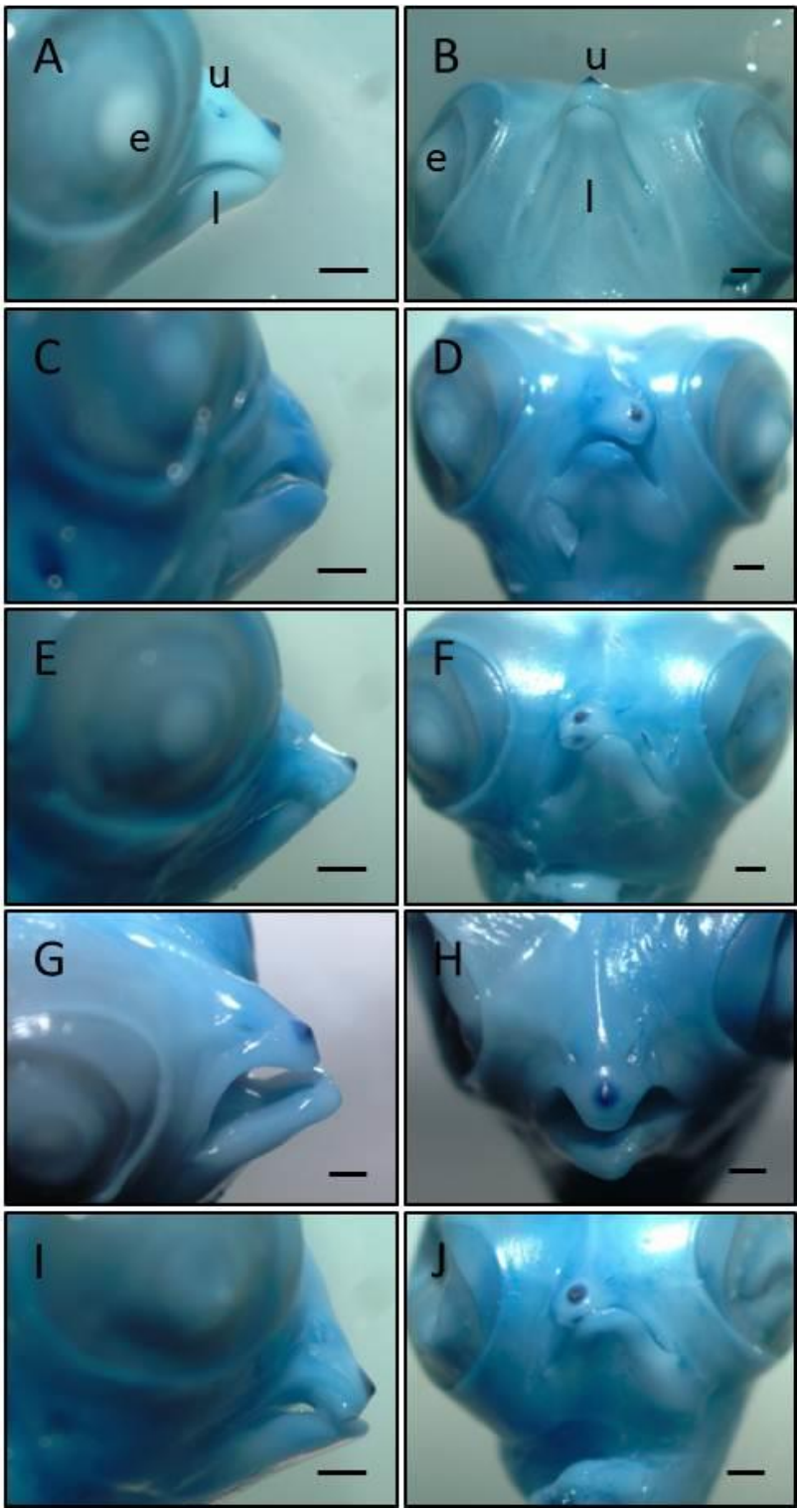

Figure 3.16: The effects of 0.1mg/ml EC19 on upper beak outgrowth.

A, C, E and G) show lateral views of embryos stained with Alcian Blue and B, D, F and H) show frontal views of the same embryo. A) and B) indicate the effect of DMSO on upper beak outgrowth. C) to H) show the phenotypes produced with 0.1mg/ml EC19 in increasing severity. C, D) show asymmetric upper beak outgrowth with the upper beak skewed to the un-operated side. E, F) asymmetric upper beak outgrowth with the upper beak skewed towards the operated side. G, H) show reduction in upper beak outgrowth. I, J) shows both reduced and asymmetric upper beak outgrowth. Abbreviations: e, eye; l, lower beak; u, upper beak. Scale bars 1mm.

Discussion:

EC23 and EC19 on toxicity and limb development:

The two synthetic retinoids analysed in the present study generate different phenotypes as well as effects on toxicity (table 3.1 and 3.2) consistent with data obtained by Budge (2010). This is also consistent with the observation that these retinoids generate different effects on TERA2.cl.SP12 cells *in vitro* (Christie et al., 2008). The differential effects of these retinoids raises the question of how two such similar compounds could cause such different effects and potencies. Given the position of the terminal carboxylic acid group, EC23 was designed to be an analogue of ATRA whereas EC19 was designed to be an analogue of 13CRA. Therefore, perhaps it is unsurprising that these cause such differential effects *in vivo* and *in vitro*. 13CRA has been shown to be present at low concentrations *in vivo*, like 9CRA, and is increased after the application of excess amounts of ATRA (Horton and Maden, 1995). 13CRA has been shown to be less potent than ATRA (Kistler, 1987) and its effects have been attributed to its inter-conversion with ATRA by isomerases (Chen and Juchau, 1998). Considering the differences in structure of the synthetic retinoids used here compared to naturally occurring retinoids, it is unlikely that these isomerases can act on EC23 and EC19 hence generating a dramatic difference in their effects.

Equally, there may be other causes of these differential effects on limb development and toxicity by EC23 and EC19. The increased toxicity of EC23 could be hypothesised to be due to decreased CYP26 mediated metabolism: considering its structural similarity to TTNPB and the fact that almost all known sites of metabolism are blocked (Eichele et al., 1985; Henderson, 2011; Pignatello et al., 2002; Topletz et al., 2012). This potential decrease in metabolism may cause an inhibition of limb development and also the duplication of multiple digit 1s as well as the severe cartilage element shortening and truncations observed with EC23. This is supported by the fact that some of these phenotypes are seen in *Cyp26b1* knockout mouse limbs ((Yashiro et al., 2004); see later). However, these phenotypes are not documented with TTNPB (Eichele et al., 1985).

Given the similar structures of EC23 and EC19 this potential resistance to metabolism should also apply to EC19 however it exhibits lower potency than ATRA *in vivo*. Therefore, the mechanism behind these effects could also be due to differential binding of CRABP2 as seen between ATRA and 13CRA (Maden and Summerbell, 1986) or

differential RAR binding and activation as investigated for TTNPB (Pignatello et al., 1997). The mechanisms behind the differential effects on limb and upper beak development observed with these two synthetic retinoids will be investigated and further discussed in chapter 4.

Retinoids and digit development.

Application of ATRA or EC23 to the anterior wing bud at HH20 has generated digit duplications and a more limited number of truncations to the limb in the present study. Truncations have been seen previously in response to 1-10mg/ml of ATRA in chick (Tickle et al., 1985), or in excess ATRA after *Cyp26b1* knock out in mouse (Yashiro et al., 2004). The increased numbers of truncations seen with 1mg/ml ATRA compared with previous results (Budge, 2010) are consistent with the fact that the beads in this study load larger quantities of retinoid (up to 300μm diameter compared to 150μm used previously). Similarly, ATRA has been previously shown to generate duplications (Tickle et al., 1985) as has the synthetic retinoid TTNPB (Eichele et al., 1985), which has a similar structure to EC23. These early experiments on the developing limb showed that retinoids could posteriorize the anterior wing bud at this developmental stage by inducing an ectopic ZPA (Wanek et al., 1991). This is supported by studies showing that ATRA up-regulated *Hoxb8* (Stratford et al., 1997), *Hand2* (Fernandez-Teran et al., 2000) and *Shh* (Riddle et al., 1993). SHH is secreted by cells of the ZPA (Riddle et al., 1993) and involved in AP axis patterning after the stylopod/zeugopod transition (Chiang et al., 2001). Therefore, up-regulation of *Shh* in the anterior wing after EC23 treatment could be the mechanism behind the duplications seen.

EC23 does generate digit duplications similar to those of ATRA in that extra digits are formed but, unlike ATRA, those which are formed are of the most anterior identity. The duplication of multiple additional digit 1s has not been described previously after ATRA treatment ((Budge, 2010; Tickle et al., 1985) and table 3.2). This, combined with the fact that it is observed at low frequency with 0.01mg/ml EC23 (table 3.2; (Budge, 2010)), indicates that it is a specific property of this retinoid. This also supports the fact that increased EC23 concentrations were achieved in this study given the increased frequency of this type of duplication as well as the increased range of examples seen.

This phenotype has been described in response to application of 0.75mg/ml SHH to the anterior chick wing bud (Yang et al., 1997) and is consistent with subsequent studies in mice suggesting that the hindlimb digit 1 develops independent of SHH signalling (Chiang et al., 2001). Increased SHH concentrations or numbers of ZPA cells are known to generate the development of more posterior digits in chick (Tickle, 1981; Yang et al., 1997). Similarly, *Shh* expressing cells have been described to contribute to digits 3, 4 and 5 while part of digit 3 and all of digit 2 are produced from long range SHH signalling in mouse (Harfe et al., 2004; Lewis et al., 2001). Interestingly, longer SHH exposure has been shown to be important for digit 4 compared to more anterior digits, while a pulse of SHH signalling is important for digit 5 development (Ahn and Joyner, 2004). SHH-deficient mice have shown that SHH dependent proliferation of these progenitors controls digit number but not identity (Zhu et al., 2008a).

A similar relationship between SHH concentration, exposure time and proliferation has also been postulated for chick digit development. Given that chick ZPA cells contribute to soft tissue at the posterior wing rather than the most posterior digit itself, the wing digits can be re-named 1, 2 and 3 (Towers et al., 2011). Inhibition of SHH signalling by cyclopamine caused the loss of digit 3 suggesting that, consistent with previous studies, digit 3 requires high concentrations of SHH (Towers et al., 2008; Yang et al., 1997). Interestingly, inhibition of proliferation using trichostatin A caused the loss of anterior digits 1 and 2 consistent with the fact that proliferation is important for development of digits 1 and 2 as seen in mice (Harfe et al., 2004; Towers et al., 2008; Zhu et al., 2008a). Given the phenotypes observed, ATRA may cause an increase in proliferation as well as *Shh* expression in the anterior wing to enable mirror image duplications. However, considering that digit 1 is SHH-independent in mouse (Chiang et al., 2001), it is possible that the duplication of additional digit 1s after increased quantity of EC23 as seen here, may not induce *Shh* expression in the anterior wing bud at all but still allow increased proliferation. Considering that mirror image duplications are observed at lower concentrations and quantities of EC23 (Budge, 2010), EC23 is likely to be able to induce *Shh* in the anterior wing bud. Instead the increased quantity of EC23 may stimulate proliferation in the wing bud but not up-regulate *Shh* expression in the anterior wing, which could produce multiple additional digit 1's.

Considering that retinoid treatment after HH22 and ZPA grafting after HH25 cannot generate digit duplications (Summerbell, 1974, 1983), it could be further postulated that this quantity of EC23 may not be able to up-regulate *Shh* within the duplication window. This could be due to its potential resistance to metabolism in the wing bud. It has been suggested that excess retinoid generates digit duplication in two phases: a lag phase followed by a duplication phase (Eichele et al., 1985). If EC23 were more resistant to metabolism, the lag phase may be extended to metabolise the excess retinoid resulting in the duplication phase occurring later in development. Due to the extended time over which this could occur, the resulting duplication phase may result in a smaller or absent ectopic ZPA. Lower levels of SHH would then be produced in the anterior limb, compared to ATRA treatment, which would lead to the duplication of only anterior digits (Towers et al., 2008; Yang et al., 1997). Altogether, it can be observed that EC23 can generate similar limb phenotypes to ATRA but the differences in digit identity produced suggests the potential for a differential effect on *Shh* expression in the anterior treated wing bud.

Retinoids and cartilage element size.

ATRA and EC23 have been observed to reduce the length of the humerus, radius and ulna during limb development. They have also been seen to differentially affect these elements: ATRA affects the humerus and ulna to a lesser extent than EC23 (Figure 3.5 and Table 3.4). Both EC23 and ATRA can affect cartilage elements of the entire PD axis which may occur via the alteration of limb outgrowth, patterning or progression of chondrogenesis. This has not been previously documented after anterior application of retinoid. Previous research indicated that retinoid application to the **posterior** wing could shorten the zeugopod and autopod (Tickle et al., 1985) and that the *Rarα/γ* knockout mouse exhibited shortening of the limb including the elements of the stylopod and zeugopod (Lohnes et al., 1994). Very high concentrations of retinoic acid have also been documented to cause shortening of cartilage elements however it was not documented at HH20 with 1mg/ml (Summerbell, 1983). Increased resistance to metabolism may also affect cartilage element size as aberrant retinoid signalling may occur at later developmental stages e.g. during the specification and development of the stylopod and zeugopod (Pignatello et al., 1997; Searls et al., 1972). In the following section, some mechanisms behind the shortening of the limb cartilage elements and the differential effects of these retinoids are explored.

It has been seen that exogenous application of BMPs can alter cartilage element length in the developing limb but depending on the member of the BMP family applied and its position, they affect the radius or ulna (Macias et al., 1997)and will be discussed later. *BMP receptor 1B* (*Bmpr1b*) and *Gdf5* single or double knock outs, however, affect cartilage element length along the entire PD axis (Yi et al., 2000). BMP7 signalling through BMPR1B is vital for regulating element length as *Bmp7*/*Bmpr1b* double knockout mice exhibit more severe reductions to the length of skeletal elements along the entire PD axis. Interestingly *Bmp7* knockout mice also exhibit preaxial polydactyly (Yi et al., 2000), mimicking another retinoid phenotype seen here.

Components of the ECM are also implicated in regulating cartilage size and width along the PD axis. One of the major components of the ECM during limb development is the chondroitin sulphate proteoglycan (CSPG) *Versican* which can be alternately spliced and cleaved during development (Capehart, 2010). The different isoforms have been shown to be present in distinct locations in the limb and may provide a method for regulating joint development and limb length over a growing 3D object (Hudson et al., 2010). Reduction of *versican* has been shown to reduce limb element length in chick and mouse (Choocheep et al., 2010; Shepard et al., 2008; Shepard et al., 2007) causing alteration of the elbow joint and increase the width of the humerus (Hudson et al., 2010). Similarly, enzymes which modify ECM proteins e.g. chondroitin sulphate synthase 1 (*chsy1*) are also implicated in the control of element size. *Chsy1* knockout mice exhibit chondrodysplasia, decreased bone length and density in all limb elements due to a delay in chondrogenesis (Wilson et al., 2012).

Alteration of limb outgrowth may also affect cartilage element length. Limb outgrowth occurs under the control of the ZPA and AER which are mutually dependent (Niswander et al., 1994). The AER secretes several FGFs which maintains survival of the undifferentiated mesenchyme adjacent to it (Niswander et al., 1993)while the ZPA confers AP patterning by the secretion of SHH (Riddle et al., 1993). It has been shown that AER removal affects cartilage element development depending on the stage of removal. If removed at HH20-21 the radius and ulna are completely truncated but development can be partially rescued with FGF4 to produce a shortened radius and ulna (Niswander et al., 1993). Both retinoids could cause a transient down-regulation of AER FGFs and cause decreased proliferation of progenitors. This could particularly affect the zeugopod and

stylopod if this down-regulation occurred before their differentiation which, based on morphological observations, is HH24 (Summerbell, 1976; Thorogood and Hinchliffe, 1975).

Given the positive feedback between FGFs and SHH in the developing limb (Niswander et al., 1994), there could also be a transient down-regulation of endogenous *Shh* (see chapter 5). The development of the limb in the absence of *Shh* function leads to the development of the humerus and radius alone (Ros et al., 2003). Transient down-regulation of *Fgf4* and *Shh* could therefore affect the length of the ulna if the expression of *Fgf4* and *Shh* were to recover. However, this is not consistent with previous studies showing that retinoids up-regulate *Shh* expression in the anterior wing (Riddle et al., 1993) nor explains the differential effects seen on the radius. Also this would not be consistent with research showing that grafting P19 cells expressing *Shh* and constitutively active RARα exhibit polarising activity in the anterior wing bud and also cause the development of thicker cartilage elements, similar to the phenotypes seen here (Ogura et al., 1996).

Another transcription factor expressed in the AER is *Msh homeobox 1* (*Msx1*) (Yokouchi et al., 1991a). It has been shown that *Msx1* and *Msx2* are required for the correct development of the anterior limb as *Msx1*/*Msx2* knockout mice exhibit shortening or absence of the radius concurrent with preaxial polydactyly (Bensoussan-Trigano et al., 2011; Lallemand et al., 2005). Similar to *Shh* and *Msx1*, BMPs have been shown to differentially affect the development of the radius and ulna. Retinoids have been shown to interact with BMP signalling in the control of chondrocyte differentiation (Weston et al., 2000) and can induce *Bmp2* expression (Francis et al., 1994). Exogenous BMP can shorten zeugopod elements if applied to the chick wing between HH19-21: anterior application of BMP2 inhibited radius development while posterior application of BMP7 inhibited ulna development. Interestingly application of either BMP2 or BMP7 to the dorsal wing between HH22-25 caused thickening to the humerus element. These phenotypes were proposed to be due to the role of BMP in the amount and position of chondrocyte precursors (Macias et al., 1997) and could also occur here.

An effect on areas of cell death could also be proposed to be the mechanism behind the shortening of cartilage elements. There are three regions of apoptosis in the early stages of normal wing development: anterior necrotic zone (ANZ), PNZ and the opaque patch (OP)

(Dawd and Hinchliffe, 1971).The ANZ and PNZ have been suggested to sculpt the limb bud while the OP is involved in the separation of zeugopod elements (Zuzarte-Luis and Hurle, 2002). It is unlikely that either retinoid causes aberrant apoptosis in the OP given that both the radius and ulna are not fused in response to retinoid treatment. Removal of the presumptive ANZ and PNZ can reduce limb cartilage length (Rizgeliene, 1996) presumably due to decreased cell number. It has been suggested that lower concentrations of ATRA than are used in the present study are able to decrease apoptosis in the ANZ (Tickle et al., 1985) consistent with a down-regulation of a marker of apoptosis, *Msx1*(Yokouchi et al., 1991a). As the concentration of EC23 used is the highest non-toxic concentration in the developing chick embryo and the concentration of ATRA is higher than that discussed in Tickle et al (1985) these quantities may be cytotoxic or cause a further decrease in apoptosis. If the retinoids were cytotoxic increased apoptosis could deplete zeugopod progenitors given that the presumptive zeugopod has been mapped to be in close proximity to the site of bead implantation (Vargesson et al., 1997). This could provide a mechanism behind cartilage element shortening; however, it would not explain the increased width of the humerus also observed. ATRA could be proposed affect the ANZ whereas as EC23 as a more potent retinoid could also affect the PNZ, causing an effect on both elements of the zeugopod. However, if the retinoids decreased apoptosis and *Msx1* expression in the limb bud their effects could be linked to the phenotypes observed as *Msx1*/*Msx2* knockout mice exhibit shortening or absence of the radius concurrent with preaxial polydactyly (see chapter 5;(Bensoussan-Trigano et al., 2011; Lallemand et al., 2005)).

Considering the previous studies described here, it is proposed that both retinoids alter the expression of BMPs early in the retinoid response. This may then cause a negative effect on the AER and the control of limb bud outgrowth (Pizette and Niswander, 1999). As discussed this would indirectly decrease *Shh* in the limb and could contribute to the inhibition of limb bud outgrowth and development of the ulna. Alteration of BMP and application of retinoid has been documented to lead to decreased *Msx1* and *Msx2* during limb development (Pizette and Niswander, 1999) which may contribute to the effects on the radius (Bensoussan-Trigano et al., 2011; Lallemand et al., 2005). This in turn may also affect apoptosis in the ANZ and PNZ and contribute to the effects on the ulna and/or radius (Rizgeliene, 1996). The differential effect of EC23 and ATRA on the zeugopodal elements could also be proposed to be due to differences in their effects on members of the BMP

signalling or due to a retinoid effect on the ANZ via *Msx1* (Macias et al., 1997; Yokouchi et al., 1991a).

Retinoids and scapula development:

In a similar manner, EC23 and ATRA are both observed to cause malformation of the most proximal element of the limb: the scapula. They caused shortening to the scapula blade and absence of the scapula head at high frequency as well as formation of ectopic cartilage, bending of the scapula and development of a foramen (see figures 3.9 and 3.10; table 3.5). This indicates that they affect both LPM and somitic mesoderm derived portions of the scapula and therefore mechanisms involved in the development of the entire scapula are discussed. The retinoid signalling antagonist AGN193190 (Prols et al., 2004) and *Rarα/γ* null mice (Lohnes et al., 1994), indicate that the loss of retinoid signalling appears to truncate scapula blade development. The results presented in this study appear to contradict these studies, given that excess retinoid is applied here, as well as early data suggesting that retinoid application could induce changes to the coracoid rather than the scapula (Oliver et al., 1990). However, considering that more retinoid was applied to the limb in the present study, it seems most likely that the correct level of retinoid signalling is important for correct development of the scapula and deviations from these cause scapula malformations. Some of the mechanisms behind the retinoid effect on scapula development are explored in the following section and are further discussed in chapter 5.

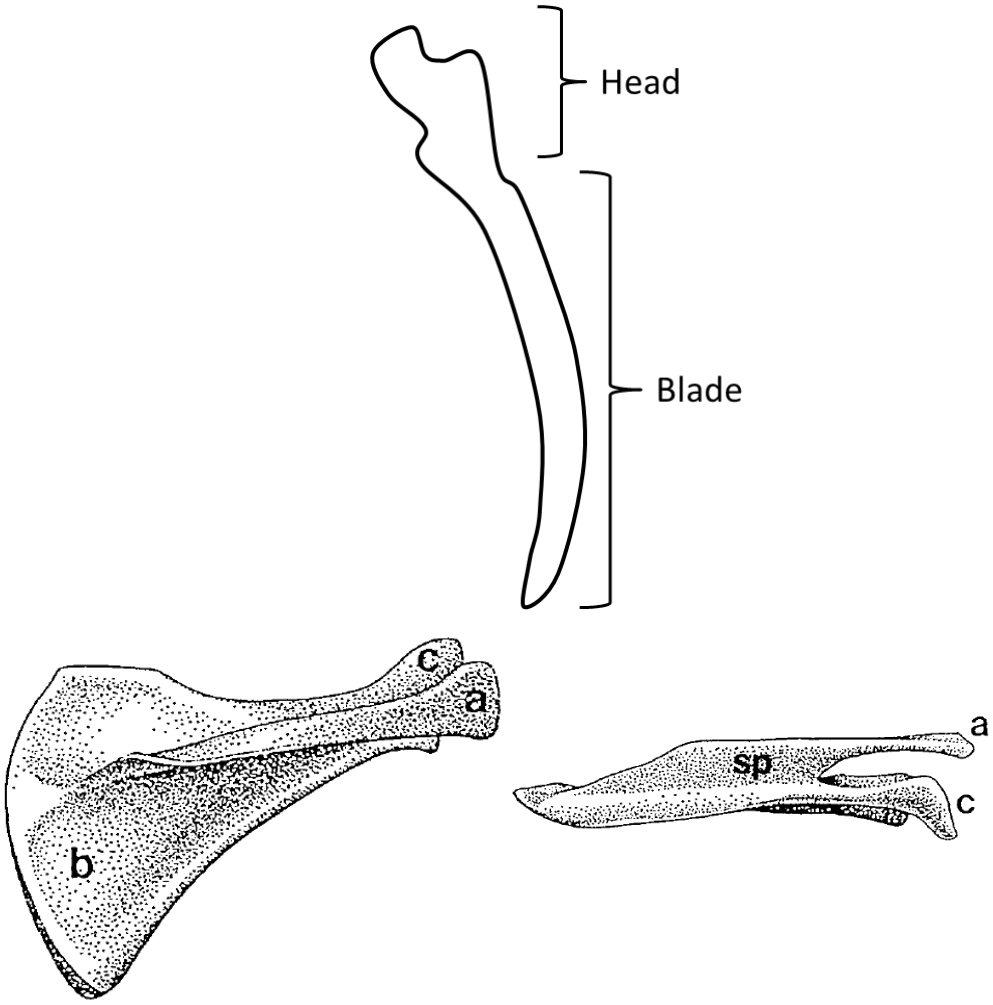

Figure 3.17: Comparison of the chick (top) and mouse (below) scapula.
Abbreviations: A, acromion; b, blade; c, coracoid process; sp, scapula spina. Bottom panel shows lateral view of a right scapula (left) and anterior view of the left scapula (right) taken from Timmons et al (1994).

Compared to limb development far less is known of the control of scapula development however BMP signalling and the following transcription factors have been implicated: *Pax1*, *Emx2* and *Pbx1-3* in early stages of development while *Alx1*, *Alx4*, *Tbx15* and *Gli3* in its correct patterning (Capellini et al., 2010; Kuijper et al., 2005; Pellegrini et al., 2001; Prols et al., 2004; Timmons et al., 1994; Wang et al., 2005). The structure of the mouse scapula compared to the chick scapula is shown in figure 3.17. It can be seen that the structures are similar in that they have a head (acromion and coracoid process) and a blade (Timmons et al., 1994). However, in chick the coracoid is a separate bone connecting to the wishbone and the acromion and scapula spina in mouse are raised with respect to the scapula blade (Huang et al., 2000). The factors implicated will be discussed with reference to the phenotypes observed with EC23 and ATRA.

Interestingly ATRA and EC23 both affect the development of the scapula head. The development of the scapular head has been proposed to be dependent on the AER (Prols et al., 2004). ATRA is known to have an antagonistic relationship with FGF and excess ATRA causes expansion of proximal markers *Meis1/2* although endogenous ATRA is not thought to be necessary for their expression (Cunningham et al., 2013; Mercader et al., 2000). The down-regulation AER-FGFs could therefore be a mechanism behind this phenotype. Reduction to FGF signalling is shown in microarray analysis after retinoid treatment (chapter 5) and may be consistent with the effect on scapular head development as proposed by Prols et al (2004). *Pax1* mutant mice (*undulated*) have been shown to exhibit malformations in the shoulder girdle particularly the absence of the acromion or its fusion with the scapula blade (Capellini et al., 2010; Timmons et al., 1994). *Pax1* has been proposed to be a marker of scapula forming cells and is expressed marking the extension of the scapula blade later in development (Huang et al., 2000). Analysis of compound *Pbx* mutants has showed that all *Pbx* genes are also necessary for correct formation of the acromion as are *Tbx15, Gli3, Alx1* and *Alx4* (Capellini et al., 2010; Kuijper et al., 2005) potentially implicating them in the correct development of the chick scapula head.

Increased BMP signalling has been implicated in scapula malformation and inhibits *Pax1* expression if applied between HH19-25 (Hofmann et al., 1998) consistent with a subsequent study showing NOGGIN injection at varying somite levels between HH20-22 caused lack of scapula blade development in the corresponding region (Wang et al., 2005). *Emx2* is a transcription factor expressed at the anterior-proximal limb bud, overlapping *pax1* expression and has been proposed to have a role in shoulder girdle development (Pellegrini et al., 2001; Prols et al., 2004). *Emx2* null mice exhibit scapula agenesis although the shoulder joint and acromion develop correctly (Pellegrini et al., 2001). This suggests that *Emx2* is involved in scapula blade development unlike *Pax1* which mainly controls acromion development (Pellegrini et al., 2001; Timmons et al., 1994). Another transcription factor, *Pbx1*, has also been implicated in the control of scapula development given its expression pattern and its knockout mouse exhibiting reduction of the scapula blade (Capellini et al., 2010; Selleri et al., 2001).

Considering the studies described previously and the present data, the reduction in *Pax1* expression in response to retinoids (figure 3.11) is consistent with the absence of the scapula head (figures 3.9 and 3.10; (Capellini et al., 2010; Timmons et al., 1994)). Given

that *Pax1* expression is seen subsequently extending over the scapula blade (Huang et al., 2000) it is likely that retinoids also inhibit *Pax1* expression in the development of the scapula blade in chick. However investigation of the effect of EC23 and ATRA on *Pax1* expression over the scapula blade requires further investigation. Given the scapula truncations generated after NOGGIN injection (Wang et al., 2005) and the truncations seen after BMP application (Hofmann et al., 1998) it is likely that the retinoids used may truncate the development of the scapula via a dysregulation of BMP signalling (see chapter 5).

Unexpectedly, some of the genes implicated to be involved in scapula blade development are seen to be up-regulated in response to retinoids: *Emx2* (Prols et al., 2004) and *Pbx1* ((Qin et al., 2002); see also chapter 5). This may indicate that aberrant up-regulation of these transcription factors in either the incorrect location, developmental stage or above a certain threshold may cause the scapula malformations observed. Interestingly alteration of other genes may be the mechanism behind the less frequently observed phenotypes: e.g. *Tbx15* and *Gli3* knockouts exhibit scapulae with foramina (Kuijper et al., 2005) although these are not altered after 24hrs retinoid treatment (chapter 5). Application of EC23 and ATRA at these concentrations and quantities provides a useful method for the subsequent investigation of scapula development in chick.

Retinoids and elbow development:

As shown in figures 3.12 and 3.13 as well as table 3.6, EC23 and ATRA can cause fusion of the elbow joint. This has not been seen previously although fusion of the knee joint has been seen after retinoid application to mice at E12 (Abu-Hijleh and Padmanabhan, 1997). Little is known about the mechanisms controlling elbow development as much research has concentrated on the developing digits, however, the potential mechanisms behind this retinoid phenotype are discussed in the following section. Joints were thought to develop from the cartilage condensations by dedifferentiating from chondrocytes into pre-joint cells but pre-joint cells are now thought to differentiate from undifferentiated mesenchyme (Cortina-Ramirez and Chimal-Monroy, 2007; Fell and Canti, 1934). This forms an interzone structure: a central domain of cell death surrounded by two layers of highly dense cells (Storm and Kingsley, 1996, 1999). This can undergo cavitation later in development to form the joint. It has been proposed that *Bmp2*, *Bmp4*, *Chordin*, *Gdf5* and

Wnt14 (*wingless-type MMTV integration site, family member 14*) are expressed in the joint interzones in chick limb development while *bagpipe homeobox homologue 1* (*bapx1*), *Collagen type 2α1* (*Col2α1*), *Noggin* and *sex determining region Y-box 9* (*Sox9*) are expressed in the digits (Crotwell and Mabee, 2007).

Interactions between these signalling pathways are thought to control joint development. Considering that BMP family members are highly expressed in the developing limb and that one of the earliest markers of joint development is *gdf5*, it could be proposed that the elbow fusions are due to retinoid action on members of the BMP signalling family. Overexpression of *gdf5* has been shown to cause lengthening of the humerus (as previously discussed) and fusion of the digit joints (Francis-West et al., 1999). GDF5 has also been shown to act upstream of BMPR1B and when both are lost they cause malformation to the elbow joint (Yi et al., 2000). Previous studies have indicated that application of BMP2/7 to the dorsal wing between HH22-25 can cause elbow fusions (Macias et al., 1997) and that retinoic acid can up-regulate *Bmp2* and *Bmp7* (Francis et al., 1994). Retinoids could therefore be generating elbow fusions via BMPR1B, up-regulation of *Bmp7*, aberrant *Ggf5* expression (as seen in Zebrafish;(Bruneau et al., 1997)) or a mixture of these. This is supported by the observation that after microarray analysis *Bmpr1b* is down-regulated (see chapter 5). Similarly other early markers of elbow development are *Dlx5* and *Dlx6* which may also be altered by retinoid signalling ((Ferrari and Kosher, 2006); chapter 5).

Shh has also been documented to affect elbow development: in *Shh* nulls the elbow joint chondrifies and the element fails to segment (Chiang et al., 2001) implying a role in facilitating the correct position and development of the joint either directly or indirectly. Retinoids have been shown to induce *Shh* expression in the anterior wing after 30hrs ((Riddle et al., 1993); see chapter 5). However, consistent with *Shh* null phenotypes is the observation that both retinoids do not induce *Shh* anteriorly and there appears to be a slight down-regulation of the expression of endogenous *Shh* which could cause elbow fusion (see chapter 5). WNTs are known to be involved in limb development and they have also been implicated in joint development. *Wnt4* and *Wnt14* have been shown to be expressed in both elbow and digit joint forming regions suggesting that they are important for elbow development (Loganathan et al., 2005). Thus investigation into the expression of these genes may elucidate the mechanism behind the effect of retinoid on elbow development. Excess VEGF application can cause elbow fusion in chick wing development via increased

chondrocyte differentiation and inhibited joint formation (Cortina-Ramirez and Chimal-Monroy, 2007) and may provide another mechanism by which retinoids could affect elbow joint formation. Overexpression of the *Versican1* and *3* in chick between HH19-25 can reduce olecranon/elbow development (Hudson et al., 2010). Morpholino knock down of *Versican* expression in the chick wing at HH22-25 also reduced olecranon process (Shepard et al., 2008; Shepard et al., 2007) suggesting that the correct threshold of *versican* in the ECM is necessary for correct elbow development and may be affected by retinoids.

Muscle and elbow development

During limb development other tissue types develop using the cartilage as a template e.g. muscle. Early experiments by Fell and Canti (Fell and Canti, 1934), Holder (Holder, 1977) and, more recently, analysis of Muscleless mutants (Nowlan et al., 2010) have shown that muscle is important for correct limb development. Muscleless mutants (*Myf5*/*MyoD* and *Splotch*) particularly reduced scapula, humerus and ulna length, similar to the present study, while heterozygotes exhibited a less severe phenotype (Nowlan et al., 2010). Concurrent with decreased cartilage element size, fusion of the elbow and shoulder joint was also seen. Therefore, it appears that the many events occurring during limb development are inter-dependent and regulate the final size and shape of the limb to ensure the production of a correctly functioning appendage. Considering the similarity in phenotypes generated in the present study, retinoids may affect the development of these three elements and the elbow joint by interfering with muscle development. Similarly, it has been shown that lack of chick embryonic movement after E8 from treatment with a neuromuscular blocking agent inhibits joint cavitation (Persson, 1983). This could be investigated by analysing the effect of retinoid on muscle markers e.g. *Pax3* or *MyoD* (chapter 5). The difference in severity of phenotypes between EC23 and ATRA treated embryos may be explained by the fact that EC23 is a more potent retinoid and should be more resistant to metabolism. Therefore it could be concluded that EC23 and ATRA may inhibit muscle development or movement at later stages which then affects joint development.

Altogether the effect of retinoid on elbow development may be via BMP, SHH or VEGF signalling. However, both the composition of the ECM and the development of embryonic

muscle have also been implicated in correct development of this structure and therefore are avenues for further investigation.

Retinoids and upper beak outgrowth.

ATRA and EC23 can be seen to reduce or truncate upper beak outgrowth (figures 3.14 and 3.15). These results are consistent with those reported previously for ATRA (Tamarin et al., 1984). Upper beak outgrowth and DV polarity are controlled by a region called the frontonasal ectodermal zone (FEZ) which develops at HH20 in chick. The FEZ is two expression domains of *Shh* and *Fgf8* which are adjacent in the ectoderm and expressed in the ventral and dorsal parts respectively (Hu et al., 2003). SHH and FGF8 are essential for outgrowth and morphogenesis of the upper beak as removal of the FEZ or inhibition of FGF8 at HH17 causes truncation of the upper beak (Hu and Marcucio, 2009). Inhibition of SHH signalling has been documented to cause truncation (Hu and Marcucio, 2009) but it has been shown that the epithelium can re-specify itself after FEZ excision at HH20 to produce normal upper beak development (Hu and Helms, 1999).

Both EC23 and ATRA may cause decreased upper beak outgrowth by interfering with the FEZ. Consistent with this it has been documented that *Shh* expression is absent from 30hrs after ATRA treatment in the developing frontonasal mass (FNM) while *Fgf8* is unaltered (Helms et al., 1997). The timing of this response is also consistent with previous data suggesting that ATRA affects mesenchyme as its primary target tissue (Wedden, 1987). ATRA has been shown to decrease *Msx* expression in the developing facial processes which leads to decreased outgrowth of the FNM (Brown et al., 1997; Song et al., 2004) and has been seen in the limb in this study (see chapter 5). Given the similarity of the phenotypes seen, it is likely that EC23 mimics the effects of ATRA on the expression of *Shh* but this would require further verification. However, work to investigate the state of the FEZ after ATRA or EC23 treatment would be necessary to draw conclusions on the molecular mechanisms by which retinoids affect upper beak development.

EC19 treatment can also produce facial phenotypes (figure 3.16 and table 3.7); however, those observed appear to be distinct from those produced by ATRA or EC23 in that the outgrowth of the FNM is reduced or asymmetric. EC19 may be a less potent isomer of EC23 or act via a different mechanism to cause its differential effects. EC23 causes no effect at concentrations lower than 0.01mg/ml rather than inducing similar facial

phenotypes to EC19, indicating that this is unlikely (Budge, 2010). This is also supported by data showing that the frequency of digit duplications generated by EC19 is not increased in a concentration dependent manner: approximately 40% 1123 duplications at 0.01mg/ml EC23 against 10% 1123 duplications at 3mg/ml EC19 and no limb phenotypes at all with 10mg/ml EC19(Budge, 2010). This is further supported by the fact that in the present study no duplications were generated with EC19 despite more retinoid being loaded than Budge (2010). The idea that EC19 is a less effective isomer is therefore unlikely and further investigation of this phenotype is not addressed here.

Conclusions.

From the data presented here it can be observed that EC23 and EC19 exhibit differential effects on toxicity, limb and craniofacial development *in vivo*. EC23 mimics ATRA to an extent in the production of digit duplications, shortening of the cartilage elements and malformation of the scapula but also generates novel digit duplication in the production of multiple digit 1s. EC19 however, is never seen to generate digit duplications at the concentrations tested here. EC23 mimics the effects of ATRA on upper beak outgrowth while EC19 causes far more mild effects: reductions and asymmetrical outgrowth.

Chapter 4) Further characterisation of EC23 and EC19: investigation of their metabolism *in vitro* and the localisation of retinoid signalling pathway components with respect to the phenotypes observed.

Introduction:

As presented in chapter 3, EC23 and EC19 generate differential phenotypes *in vivo* as *in vitro* (Christie et al., 2008) despite their similar structures. EC19 is far less potent than EC23 *in vivo* consistent with the previous study *in vitro* (Christie et al., 2008). EC23 mimics ATRA *in vivo*: truncating upper beak outgrowth, shortening limb cartilage element size, reducing scapula blade development and generating digit duplications. Despite the fact that EC23 was designed to be an ATRA analogue, EC23 generates different types of digit duplications to ATRA in the production of multiple additional digits of digit 1 identity. EC19, however, causes very limited effects on limb development and mild effects on craniofacial development. Considering that their structures are identical bar the position of the terminal carboxylic acid group, it is intriguing that they should cause such different effects.

There may be many mechanisms behind the differential effects of these retinoids and their differences with ATRA. It has been documented that similar retinoids have limited affinity for parts of the retinoid signalling pathway. TTNPB has been documented to have decreased affinity for all RARs, decreased activation of all RARs but similar affinity for CRABPs compared to ATRA (Maden and Summerbell, 1986; Pignatello et al., 1997, 1999). Meanwhile 13CRA has less affinity for CRABPs than ATRA (Maden and Summerbell, 1986). Given the role of FABP5 proposed in retinoid signalling *in vitro* (Schug et al., 2007), affinity for this binding protein may also affect retinoid signalling during development. Differences in potency and phenotype seen may also be due to differences in retinoid metabolism: the closely related retinoid, TTNPB, has been shown to be more potent than ATRA due to its resistance to metabolism by the CYP26 enzymes (Pignatello et al., 2002). Considering the structure of EC23 and EC19 both retinoids would be hypothesised to be potentially resistant to metabolism by the CYP26 enzymes as all bar the site equivalent to C16 in ATRA are blocked (red circle; figure 1.5). However, other enzymes have been documented to metabolise ATRA in humans, as mentioned previously, and include CYP2C8, CYP2C9 and CYP3A4 (McSorley and Daly, 2000; Nadin and Murray, 1999). RAR specificity may also provide a mechanism behind the differential effects: if one receptor is restricted to the developing wing bud, this may provide the mechanism behind EC23 effects and indicate that EC19 cannot activate this receptor. This

chapter investigates the potency and differential effects generated by EC23 and EC19 by investigating: metabolism likely to be mediated by the CYP26 enzymes and distribution of *Rarβ1*, *Rarβ2*, *Rarγ*, *Fabp5* and *Pparβ* at HH20 of chick development. Given that the expression of *Rarα1*, *Rarα2* and *Crabp2* are not investigated, this study is not yet complete and is an avenue for further work.

Results:

TTNPB, a retinoid with a similar structure to EC23 and EC19, has been shown to be resistant to metabolism by the CYP26 enzymes *in vitro* using the CYP26 inhibitor liarozole. Although liarozole only inhibited ATRA metabolism by 10%, it was shown to enhance the activity of ATRA to a similar level to that of TTNPB (Pignatello et al., 2002). A similar approach was considered here as a mechanism to explain the differential effects of EC23 and EC19 *in vivo*. It could be hypothesised that EC23 and EC19 are potentially resistant to metabolism by the CYP26 enzymes. The 1, 1, 4, 4-Tetramethyl-1, 2, 3, 4-tetrahydronapthalene (TMTN) group blocks almost all known sites of CYP26 action (Henderson, 2011; Topletz et al., 2012) and may contribute towards their differential phenotypes and potencies *in vivo* and *in vitro*. Given that the phenotypes described in chapter 3 were generated after *in ovo* microsurgery applying retinoid to the anterior wing bud at HH20, application of both liarozole and retinoid *in vivo* was attempted to investigate the effect of liarozole and the metabolism of these retinoids. However, this was unsuccessful as liarozole would not load onto the beads in question and an alternative approach was taken.

EC23 and EC19 inhibit chondrogenesis in chick limb bud cell culture but exhibit different potencies.

It is known that limb bud cells can be cultured at high density (micromass) for seven days and during this time they will undergo chondrogenesis. The degree to which they undergo chondrogenesis can be quantified using alcian blue staining of sulphated glycosaminoglycans and proteoglycans present in the cartilaginous ECM (Hassell and Horigan, 1982; Paulsen and Solursh, 1988). The extracted alcian blue stain can be quantified by measuring its absorbance at 600nm or image analysis (Anderson et al., 2001; Kistler, 1987). Many teratogens have been assayed using this system including ATRA and its derivatives (Kistler, 1987). It has been shown that ATRA and TTNPB (Kistler, 1987; Kochhar and Penner, 1992; Pignatello et al., 2002) can decrease alcian blue staining and hence inhibit chondrogenesis.

It can be seen from figure 4.1A that chick limb bud cells can be cultured in the presence of 0.1% DMSO (vehicle) and will undergo chondrogenesis shown by the presence of alcian

blue staining. Chondrogenesis is also evident from the presence of densely packed cells in cartilage nodules (see asterisk in figure 4.4A). In all subsequent analyses DMSO treatment was included so that chondrogenesis seen could be calculated as a percentage of the chondrogenesis seen in DMSO treatment.

The effects of ATRA, EC19 and EC23 on chick limb bud chondrogenesis can be seen from figures 4.1, 4.2 and 4.3 (top panels) respectively with quantification of staining level by measurement of absorbance at 600nm shown in figure 4.7. As can be seen ATRA inhibits chondrogenesis completely at 10^{-6}M (figure 4.1B), partially at 10^{-7}M (figure 4.1C) but has little effect on chondrogenesis at lower concentrations (figure 4.7A and figure 4.1D-E). EC19 is less potent than ATRA in this system as it completely inhibits at 10^{-5}M rather than 10^{-6}M with ATRA (compare figures 4.1B and 4.2B; figure 4.7A and 4.7B). EC19 partially inhibits chondrogenesis at 10^{-6}M (figure 4.2C) and has little effect on chondrogenesis at lower concentrations (figure 4.2D-E, figure 4.7B). EC23 is more potent than ATRA in this system as chondrogenesis is completely inhibited at 10^{-9}M rather than 10^{-6}M (compare figure 4.3A with 4.1B). Interestingly it is three orders of magnitude more potent in the limb bud assay compared to two orders of magnitude more potent *in vivo* (see chapter 3). It can be seen that at 10^{-10}M EC23 partially inhibits chondrogenesis (figure 4.3B and 4.7C) but at concentrations lower than this EC23 has little effect on chondrogenesis (figure 4.3C-D and 4.7C).

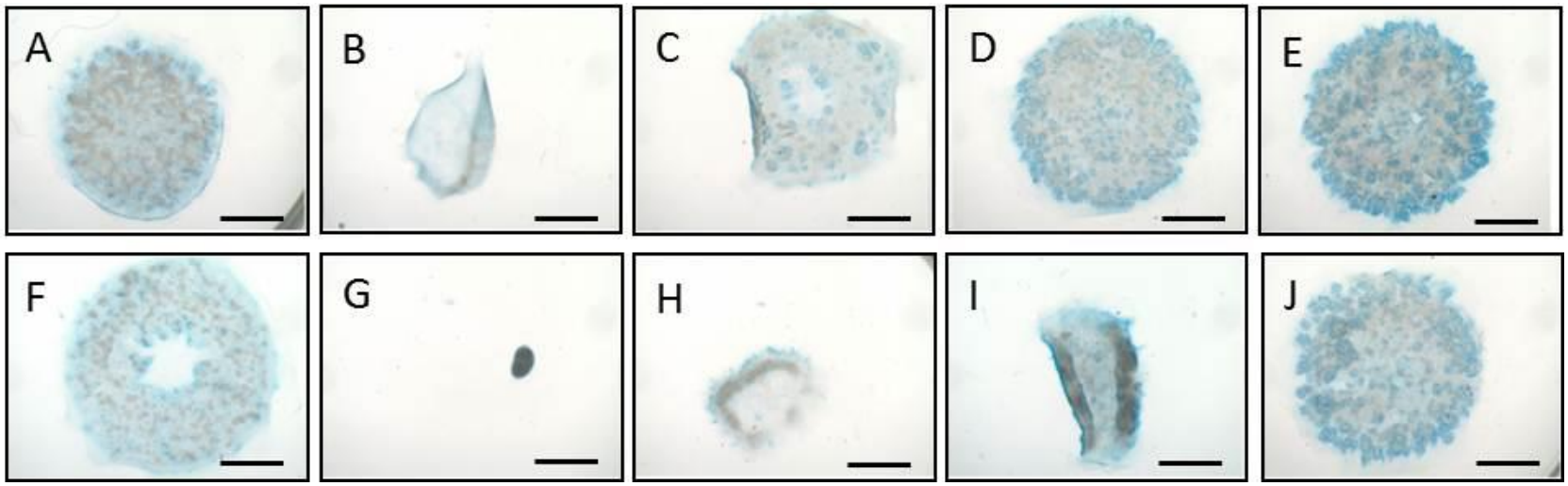

Figure 4.1: The effect of ATRA on chondrogenesis in chick limb cell cultures.

Chick limb bud cells were cultured at high density and treated with varying concentrations of ATRA: B,G) 10^{-6}M; C,H) 10^{-7}M; D,I) 10^{-8}M; E,J) 10^{-9}M. (A-E) were cultured in the absence of liarozole and (F-J) in the presence of 10^{-7}M Liarozole. A,F) represent control cultures treated with 0.1% DMSO. Cultures were stained with Alcian Blue and photographed at x11. Scale bars =2mm.

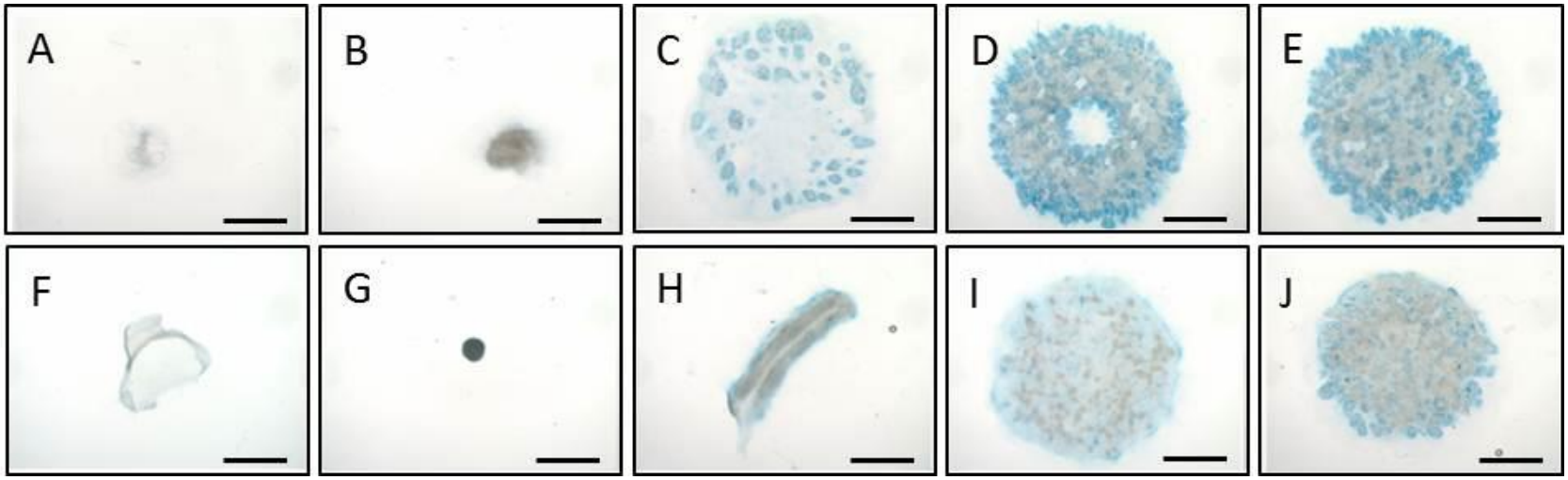

Figure 4.2: The effect of EC19 on chondrogenesis in chick limb bud cell culture.

Cultures were treated with varying concentrations of EC19: A,F) 10^{-4}M; B,G) 10^{-5}M; C,H)10^{-6}M; D,I) 10^{-7}M and E,J) 10^{-8}M. Chick limb bud cells were cultured at high density for 7 days in the absence (A-D) or presence (F-J) of 10^{-7}M liarozole and stained with alcian blue. Photographed at x11 magnification with scale bars=2mm.

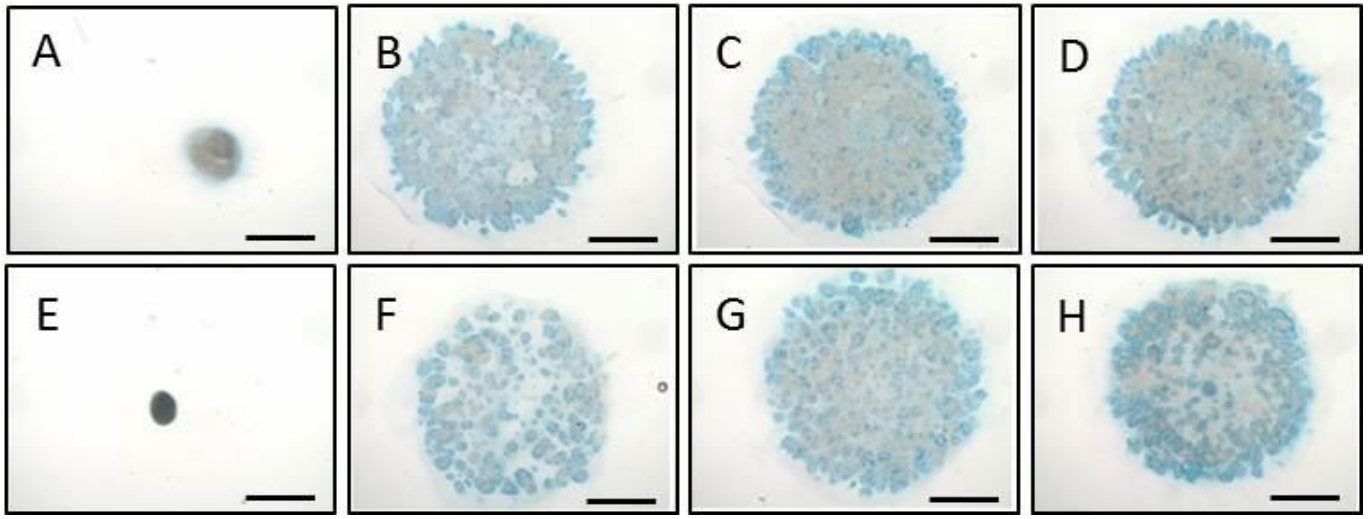

Figure 4.3: The effect of EC23 on chondrogenesis in chick limb bud cell culture.

Cultures were treated with varying concentrations of EC23: A,E) 10^{-9}M; B,F) 10^{-10}M; C,G)10^{-11}M; and D,H) 10^{-12}M. Chick limb bud cells were cultured at high density for 7 days in the absence (A-D) or presence (F-J) of 10^{-7}M liarozole and stained with alcian blue. Photographed at x11 magnification with scale bars=2mm.

Cell death is unlikely to be the cause of the different potencies seen with EC23 and EC19.

It is possible that the inhibition of chondrogenesis is due to cell death rather than inhibiting chondrogenesis. Figure 4.4 shows the appearance of chick limb bud cell cultures at day 4. By day 4 the cells have been cultured in retinoid at concentrations sufficient to completely inhibit chondrogenesis for 3 days. As can be seen from figure 4.4B-D, cells are present at high density and alive. This is consistent with the idea that retinoids do not immediately cause apoptosis and therefore the effects are due to inhibition of chondrogenesis alone. However, cell death at later stages cannot be ruled out.

The inhibition of chondrogenesis described previously with retinoid is notable by the decrease in alcian blue staining shown from figures 4.1, 4.2, 4.3 and 4.7 at day 7. However, it can also be observed in phase images at day 4 shown in figure 4.4. From this time it can be seen that the retinoids negatively affect chondrogenesis due to the absence of cartilage condensations after retinoid treatment. Figure 4.4A shows the appearance of cultures after treatment with 0.1% DMSO. The asterisk indicates the presence of a large condensation which later will secrete cartilaginous ECM. There are also other differentiated cell types indicated by the arrow, which are most likely to be muscle fibres. However, in cultures treated with high concentrations of retinoid, the appearance of the cultures is very different. There is a decrease in the number and size of cartilage nodules (figure 4.4B-D, particularly compare asterisks in A and C). Likewise there is also a decrease in the number of differentiated cells (arrows). In response to the more potent retinoids, ATRA and EC23, there does not appear to be differentiated cells present (figure 4.4B and 4.4D). Therefore, it can be seen that chick limb bud cells appear to survive until at least day 4 and that the response to retinoid is not due to immediate apoptosis. It can also be concluded that all retinoids tested inhibit chondrogenesis by inhibiting the earliest stage: cartilage condensation.

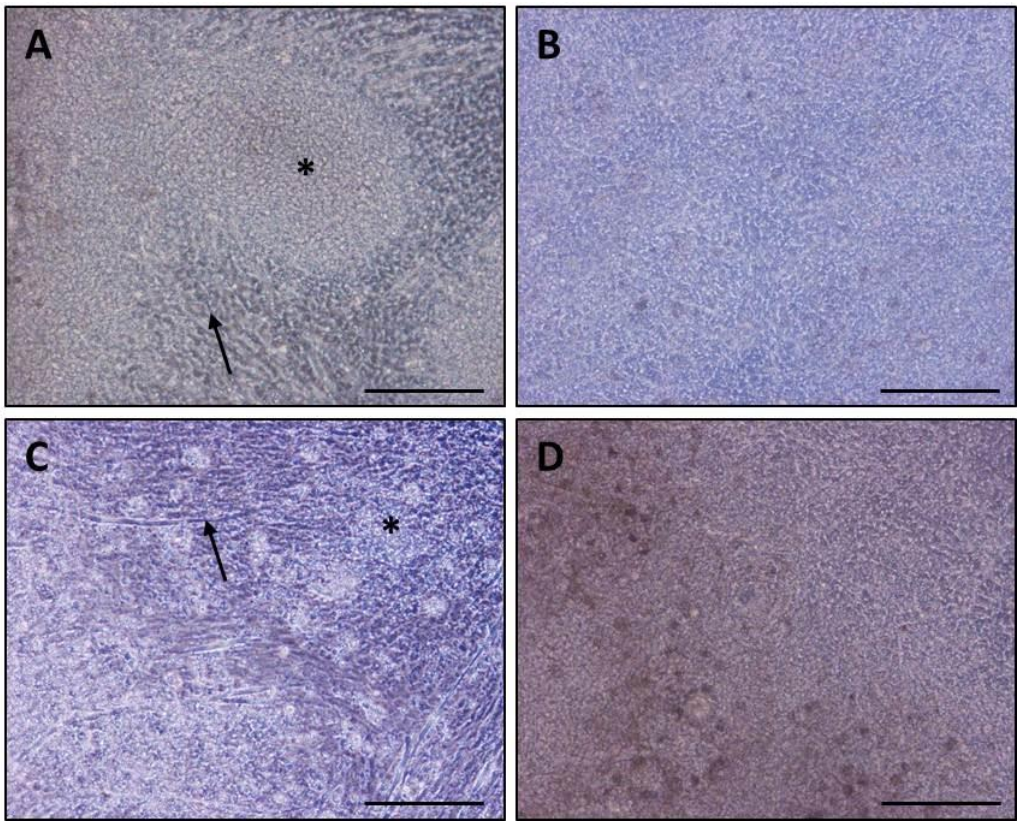

Figure 4.4: The appearance of chick limb bud cell cultures after treatment with high concentrations of retinoids.

Chick limb bud cells were plated at high density and then treated with 0.1% DMSO (A), 10^{-6}M ATRA (B), 10^{-5}M EC19 (C) or 10^{-9}M EC23. Cells were then cultured and photographed on day 4 at x10 magnification . * in A and C indicates the presence of cellular condensations. Arrows indicate other differentiated cell types. Scale bars are 200μm.

Liarozole can inhibit chondrogenesis in micromass cultures in a dose dependent manner.

As previously mentioned, Pignatello et al (Pignatello et al., 2002) used the CYP26 inhibitor liarozole to indicate that TTNPB was metabolised to a lesser extent than ATRA. Upon addition of liarozole ATRA activity was enhanced such that lower concentrations of ATRA could achieve inhibition of chondrogenesis such that alcian blue staining was 50% lower than controls (50% inhibition). The concentration at which 50% inhibition was achieved with ATRA and liarozole was similar to the concentration of TTNPB needed for 50% inhibition. This suggests that TTNPB is resistant to metabolism by the CYP26 enzymes and contributes to its increased potency (Pignatello et al., 2002). As mentioned previously, this method was to be used to investigate metabolism of EC23 and EC19. However, as liarozole is used as a poison it may itself affect chondrogenesis in this assay. The effect of liarozole was therefore investigated so that the highest ineffective concentration could be used in subsequent analysis.

As hypothesised liarozole inhibits chondrogenesis in a dose dependent manner (figures 4.5 and 4.6). Liarozole is able to completely inhibit chondrogenesis at concentrations higher than 10^{-5}M (figures 4.5C and 4.5D and 4.6) and partially inhibit chondrogenesis at 10^{-6}M (Figure 4.5E). There is no significant difference in chondrogenesis at 10^{-7}M and 10^{-8}M liarozole (figure 4.5F, 4.5G and 4.6). The concentration used for subsequent studies was chosen to be 10^{-7}M liarozole as it caused no measurable effect on chondrogenesis and was the highest ineffective concentration which would enable any effects on EC23, EC19 and ATRA activity to be highlighted.

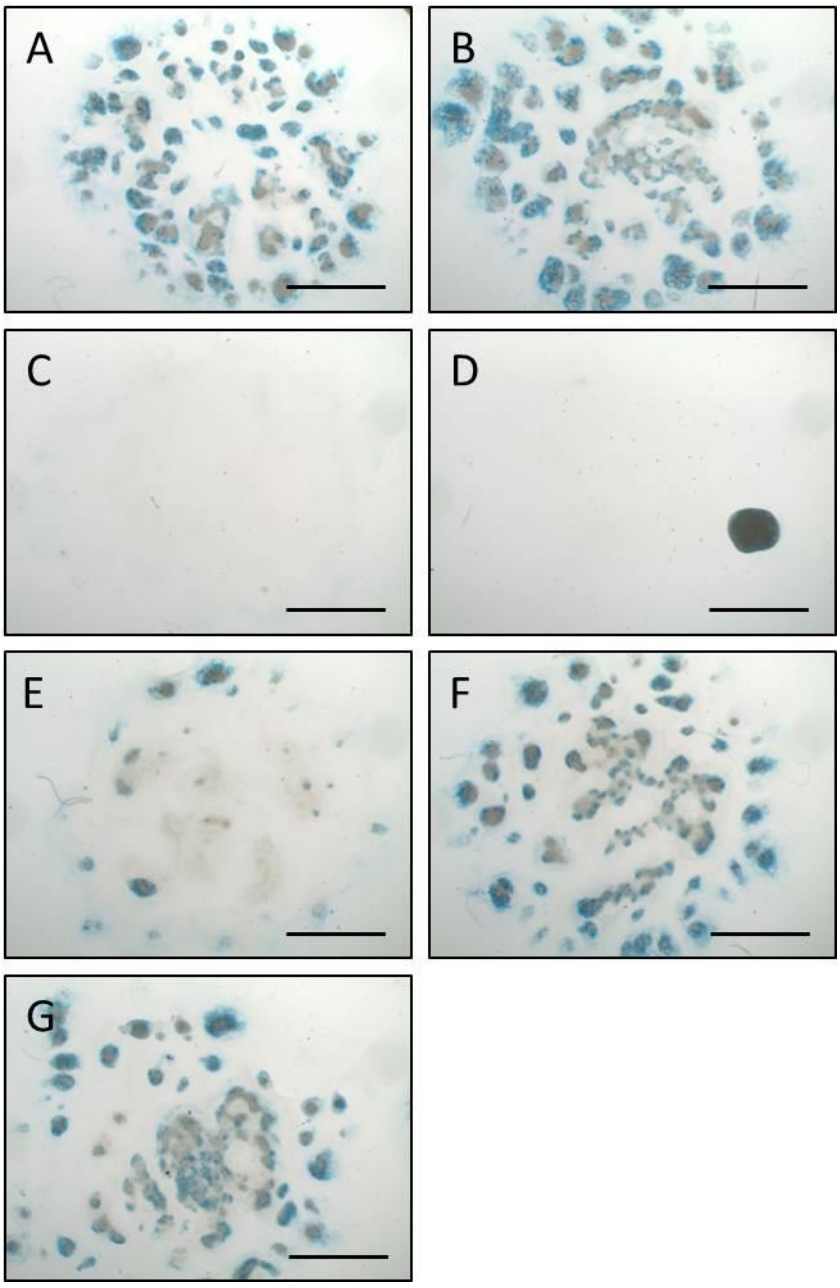

Figure 4.5: The effect of liarozole on chondrogenesis in chick limb bud cell cultures.

Chick limb bud cells were cultured at high density and treated with varying concentrations of liarozole before being fixed and stained with alcian blue for cartilage. C-G) were treated with varying concentrations of liarozole: C) 10^{-4}M, D) 10^{-5}M, E) 10^{-6}M, F) 10^{-7}M and G) 10^{-8}M. A and B) represent control cultures treated with 0.1% and 1.1% DMSO respectively. Cultures were stained with Alcian Blue and photographed at x11. Scale bars =2mm.

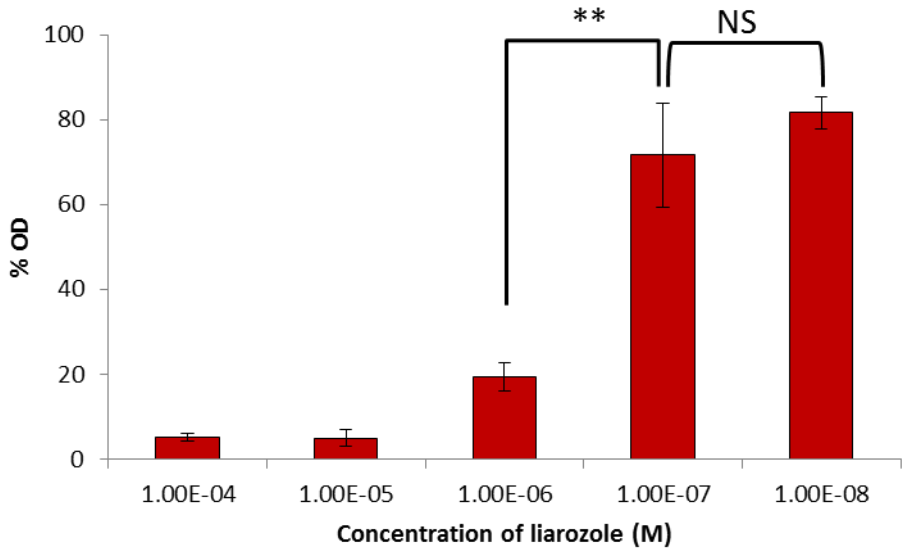

Figure 4.6: Quantification of the effect of liarozole on chondrogenesis in chick limb bud cell culture.

Extent of chondrogenesis in response to varying concentrations of liarozole was measured by alcian blue staining. The Alcian Blue stain was extracted and its absorbance measured at 600nm. %OD is a measure of chondrogenesis. %OD is the absorbance in response to liarozole as a percentage of equivalent DMSO treated cultures. DMSO concentration never exceeded 1.1% in culture media. N=4 wells, error bars ±standard deviation. Statistical significance was used to determine the concentration of liarozole to be used subsequently. Significance was calculated using an unpaired t-test. * $p<0.05$, ** $p<0.01$, *** $p<0.001$, NS indicates not significant.

ATRA and EC19 are metabolised by chick limb bud cells but EC23 is not.

As ATRA is metabolised by the CYP26 enzymes, it acts as a positive control (see figures 4.1 and 4.7A). Combination of ATRA with liarozole treatment inhibits CYP26 activity and increases the concentration of ATRA present, thus decreasing chondrogenesis more than ATRA alone at the retinoid concentrations tested except 10^{-9}M (figure 4.7A red bars, figure 4.1G-I). It can be proposed that were EC23 and EC19 metabolised in chick limb bud cells, the chondrogenesis profile when their treatment was combined with liarozole would be similar to that of ATRA.

Combination of EC19 and liarozole further decreases chondrogenesis at all concentrations tested (figure 4.2G-J) and which is statistically significant ($p<0.05$ or lower; figure 4.7B). There was a 57% decrease in alcian blue staining in response to ATRA and liarozole combined when compared to ATRA treatments alone (at 10^{-7}M retinoid). However, there was only a 34% decrease in alcian blue staining in EC19 combined with liarozole when compared to EC19 treatment alone (at 10^{-6}M EC19). This decrease in alcian blue staining upon addition of liarozole at 10^{-6}M EC19 was statistically significant ($p<0.01$) and similarly the decrease in alcian blue staining at lower concentrations was also statistically significant ($p<0.05$) although to a lesser extent. It can therefore be concluded that at the concentrations tested, EC19 is metabolised *in vitro* although to a lesser extent than ATRA.

However, combination of EC23 with liarozole does not decrease alcian blue staining when compared to EC23 alone, unlike EC19 and ATRA (compare figures 4.1, 4.2 and 4.3). Interestingly, addition of liarozole can cause a statistically significant increase in alcian blue staining at 10^{-10}M and 10^{-12}M EC23 ($p<0.05$; figure 4.7C). As this effect is opposite to the positive control of ATRA, this indicates that EC23 is potentially resistant to metabolism by the CYP26 enzymes. Altogether, this indicates that EC23 is more resistant to metabolism by the CYP26 enzymes as previously proposed while EC19 is metabolised by the CYP26 enzymes.

Increased resistance to metabolism by the CYP26 enzymes would allow longer signalling period as seen with TTNPB (Pignatello et al., 1999) which could account for the greater potency of EC23 and even generate different phenotypes. This is particularly pertinent for the effects of EC23 on the limb bud compared to EC19. It has been shown that retinoid signalling for 14hrs is necessary for complete digit duplication in the chick wing (Eichele

et al., 1985). Given that the signalling centre for upper beak outgrowth forms at HH20 but that the ectoderm can re-specify if the FEZ is removed at this stage while it cannot at later stages (Hu and Helms, 1999), increased resistance to metabolism may contribute to the upper beak truncations seen. This difference in metabolism cannot be the sole mechanism for the differential effects and potencies seen with EC23 and EC19 due to the fact that EC19 would mimic ATRA at higher concentrations, which is not the case.

Upon combination of liarozole with retinoids it is also noted that the appearance of the limb bud cell cultures is altered. It can be seen that the increased level of retinoid causes cultures to roll up (figures 4.1D+1I and 4.2C+2H). This can also be seen upon increasing concentrations of ATRA: compare figure 4.1B with 4.1C-D. The cells present are still alive given the presence of cartilage nodules and a micromass culture present in the well. This indicates that the increased level of retinoid is causing limb bud cells to change their cell: cell adhesion, given the decreased number of cartilage condensations observed, but also adhesion to the cell culture plasticware. Interestingly, this effect is not seen upon combination of EC23 and liarozole indicating that there is not an appreciable increase in retinoid present due to the fact that EC23 is more resistant to metabolism. However, this does beg the question why this rolling of cell cultures is not observed at high levels of EC23. It could be proposed that EC23 does not affect genes involved in the control of adhesion to the same extent that ATRA does (see chapter 5).

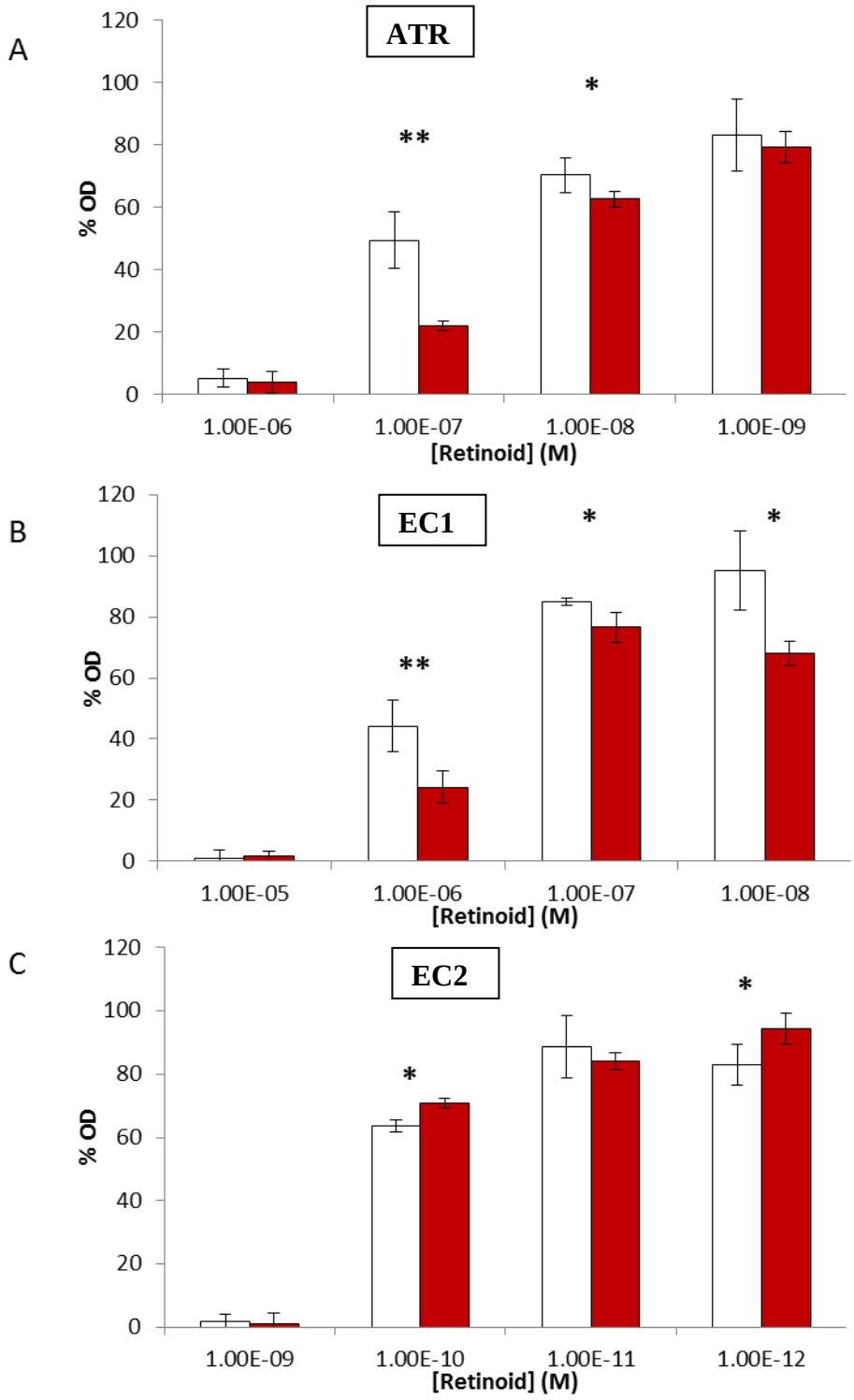

Figure 4.7: Quantification of the effect of ATRA, EC19 and EC23 on chondrogenesis in the absence and presence of 10^{-7}M liarozole.

A-C) show quantification of chondrogenesis by extraction of alcian blue and extract absorbance measured at 600nm for cells cultured as in figures 4.1-3). Cultures were treated with A) ATRA, B) EC19 and C) EC23. White bars are treated with retinoid only and red bars were treated with retinoid in the presence of 10^{-7}M liarozole. %OD was calculated as the absorbance as a percentage of the corresponding control (DMSO or 10^{-7}M liarozole). DMSO treatment never exceeded 1.1%. Statistical significance was tested using the students t-test and * $p<0.05$, ** $p<0.01$, *** $p<0.001$, NS indicates not significant.(n=3, error bars ±SEM).

Retinoic acid receptor specificity as a mechanism behind differential effects of ATRA, EC23 and EC19.

Retinoids are known to alter gene expression by binding to nuclear RAR: RXR heterodimers bound to DNA at RAREs (Astrom et al., 1990; Idres et al., 2002). ATRA is thought to activate transcription by binding to all RARs whereas 9CRA can activate both RARs and RXRs (Heyman et al., 1992; Idres et al., 2002). As ATRA only binds RARs, these receptors will be considered here. There are three isotypes of RAR: RARα, RARβ and RARγ (Michaille et al., 1994; Michaille et al., 1995; Smith et al., 1995), which produce the following isoforms: RARα1, RARα2, RARβ1, RARβ2 and RARγ2 by differential promoter activation and alternative splicing given their similarities with the mouse isoforms (Kastner et al., 1990; Leroy et al., 1991; Zelent et al., 1991). It has been shown that the potency of TTNPB is also due to the fact that it can activate RARs at similar concentrations to ATRA and it is a pan-agonist (Pignatello et al., 1999). Previous research has suggested that EC23 is also a pan-agonist although it binds RARβ and RARγ with higher affinity than RARα (Gambone et al., 2002). Given that EC23 and EC19 have similar structures to each other and TTNPB, it is proposed that EC19 is also a pan-agonist of the RARs. If they were to be specific to a receptor isotype, the differential expression of RARs in the limb and facial processes may provide a mechanism behind their differential effects. Considering the limited existing data in chick, this chapter further investigates the expression of *Rarβ1*, *Rarβ2* and *Rarγ2* at HH20.

The expression of the RARs has been investigated in mouse by section *in situ* hybridisation (Mollard et al., 2000; Ruberte et al., 1991) and partially in chick (Michaille et al., 1994; Rowe et al., 1991; Schofield et al., 1992; Smith et al., 1995). The present study uses whole mount *in situ* hybridisation for *Rarβ1*, *Rarβ2* and *Rarγ2* to determine whether EC23 or EC19 might explain the differential phenotypes observed via differential expression of RARs in the limb and facial processes. I also attempt to elucidate novel expression patterns of *Rarβ1* and *Rarβ2* as well as describe the expression of *Rarγ2* in the intact chick embryo. Considering that EC23 and EC19 cause different effects: EC23 mimics ATRA in craniofacial and limb development while EC19 only affects the face; expression of a RAR isoform in the facial processes which is absent from the limb may suggest EC19 is specific for this receptor and vice versa.

Figure 4.8 shows the expression of *Rarβ1*, *Rarβ2* and *Rarγ2* in the developing facial prominences at HH20. As can be seen all *Rars* investigated are expressed in the facial processes. *Rarβ1* is expressed in the FEZ (figure 4.8B, white arrow), the distal maxillary arch and anterior distal mandibular arch (arrows in figure 4.8A and 4.8B). *Rarβ2* is expressed in the anterior half of the maxillary arch (figure 4.8C); the nasal pits and the FNM (figure 4.8D). Expression in the FNM is lower in the medial FNM corresponding with the anterior neural ridge (ANR; figure 4.8D, asterisk). *Rarγ2* is expressed in the posterior maxillary and 2nd arches, anterior distal mandibular arch, mandibular-2nd arch cleft, the FEZ and mesenchyme at the midline adjacent to the FEZ (figure 4.8E and 4.8F). Considering that upper beak outgrowth is controlled by the FEZ (Hu et al., 2003) and that both EC23 and EC19 affect upper beak development (see chapter 3) it is likely that both EC23 and EC19 can bind and activate RARβ1 and RARγ2. Both EC23 and EC19 may also bind and activate RARβ2.

Figure 4.9 shows the expression of *Rarβ1*, *Rarβ2* and *Rarγ2* in the wing bud at HH20. All *Rars* investigated are seen to be expressed in the wing bud. *Rarβ1* is expressed in the wing bud ectoderm including the AER (arrow figure 4.9A). *Rarβ2* is expressed in the proximal wing bud but is absent from the distal wing bud (arrow figure 4.9B) as previously described (Smith et al., 1995). *Rarγ2* appears to be expressed throughout the bud wing as described for *Rarγ* (Michaille et al., 1994) but is more highly expressed in the distal wing bud adjacent to and including the AER (arrow, figure 4.9C). Considering that the known molecular events of digit duplication and limb patterning centre around the posterior mesoderm (ZPA) and that the effects of ATRA in the limb have been proposed to be via induction of another ZPA and lengthening of the AER via the mesenchyme (Tickle et al., 1989; Wanek et al., 1991), it seems likely that EC23 is able to activate RARβ2. As EC19 does not affect wing development in the present study it is possible that EC19 is not a RARβ2 agonist. Therefore the receptor expression patterns from this investigation are consistent with the idea that EC23 appears to be a pan-RAR agonist whereas EC19 could activate both RARβ1 and RARγ2 but not RARβ2.

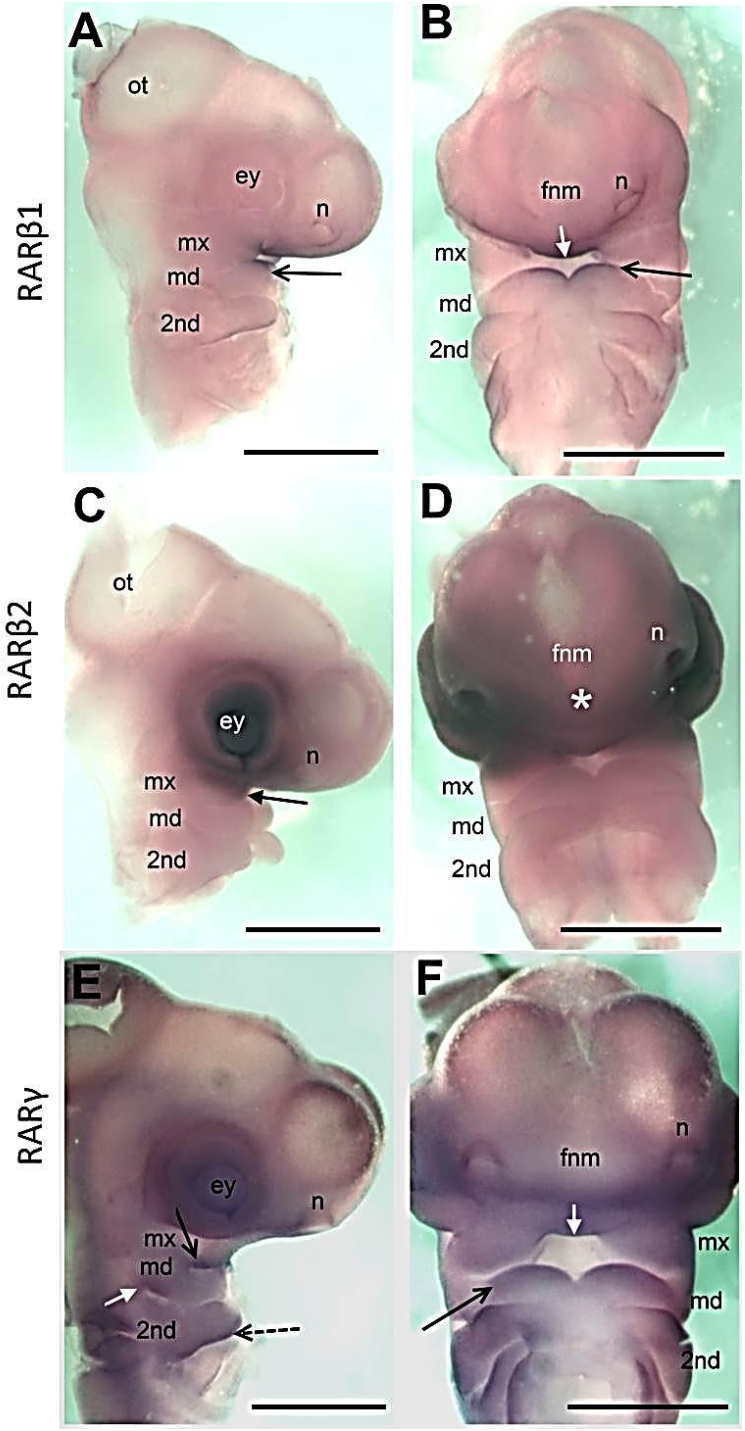

Figure 4.8: The expression of *Rarβ1*, *Rarβ2* and *Rarγ2* in the facial processes at HH20.

A, C and E) are right lateral views, dorsal is left and B, D and F) are frontal views, anterior is top. A and B) show whole mount *in situ* hybridisation for *Rarβ1*. C and D) show whole mount *in situ* hybridisation for *Rarβ2*. E and F) show whole mount *in situ* hybridisation for *Rarγ*. The black arrows in A and B) indicate higher levels of *Rarβ1* expression in the anterior mandibular arch. The white arrow in B) indicates higher levels of *Rarβ1* in the frontonasal ectodermal zone (FEZ). The arrow in C) indicates *Rarβ2* expression in the anterior maxillary arch. D) shows lower levels of *Rarβ2* in the middle of the FNM (white asterisk) flanked by higher levels of expression laterally. E) shows expression of *Rarγ2* in the posterior maxillary arch (arrow), proximal posterior mandibular arch adjacent to the pouch (white arrow) and posterior 2nd arch (dashed arrow). F) shows *Rarγ2* is expressed at higher levels in the anterior distal mandibular arch (black arrow) and expression is seen in the FEZ (white arrow). Abbreviations: ey, eye; fnm, frontonasal mass; md, mandibular arch; mx, maxillary arch; n, nasal pits; ot, optic tectum; 2nd, 2nd branchial arch. Scale bars are 1mm.

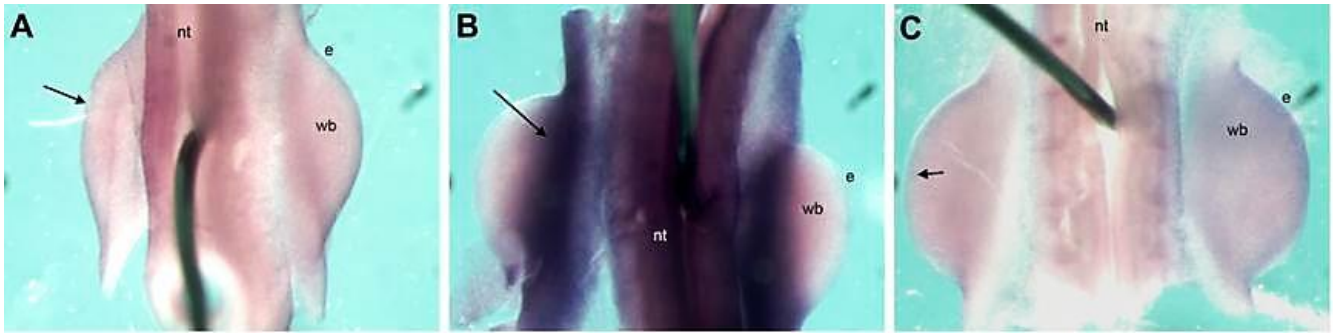

Figure 4.9: The expression of *Rarβ1, Rarβ2* and *Rarγ2* in the wing bud at HH20.

A-C) are dorsal views pinned on agar with tungsten wire. A-C) shows dorsal views of whole mount *in situ* hybridisation for A) *Rarβ1*, B) *Rarβ2* and C) *Rarγ2* where anterior is top. The arrow in A) indicates *Rarβ1* expression in the ectoderm over the wing bud. The arrow in B) indicates *Rarβ2* in the proximal wing bud. The arrow in C) indicates expression of *Rarγ2* in the distal wing bud. Abbreviations: e, ectoderm; nt, neural tube; wb, wing bud. Scale bars are 500μm.

Novel Expression of *Rarβ1*, *Rarβ2* and *Rarγ2*.

As mentioned, previous investigations into RAR distribution in chick have been limited and have mainly focused on *Rarβ* in limb (Schofield et al., 1992; Smith et al., 1995) and craniofacial development (Rowe et al., 1992). An investigation of the *Rarγ* isoforms in chick was performed and the expression of the *Rarγ* isotype was described at HH21 using section *in situ* hybridisation (Michaille et al., 1994). Investigation into *Rar* expression domains is further complicated by the fact that many studies, including many in mouse, did not carry out isoform specific investigations. *Rarβ1* and *Rarβ2* differ in the length and sequence of the A region due to differential splicing and promoter activity (Smith et al., 1995; Zelent et al., 1991). The difference between the two isoforms is illustrated below (figure 4.10). The probes used in the present study to differentiate between *Rarβ1* and *Rarβ2* were directed towards the specific sequences in the A domains.

Figure 4.10: Illustration of *Rarβ1* and *Rarβ2* isoforms.

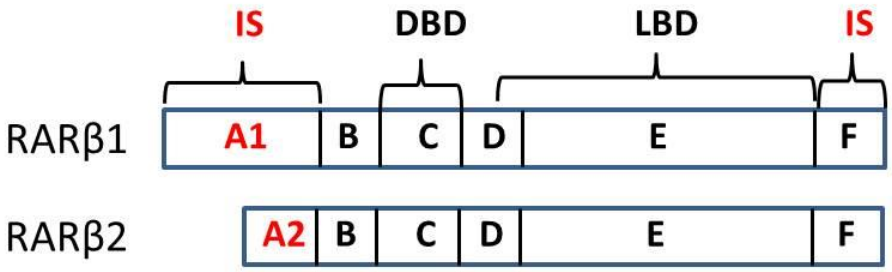

Abbreviations: IS, isoform specific; DBD, DNA binding domain; LBD, ligand binding domain.

Most studies address the expression of *Rarβ* but often relate to *Rarβ2*. They describe *Rarβ1* as ubiquitously expressed in the limb and *Rarβ2* restricted to the proximal third of the limb (Smith and Eichele, 1991; Smith et al., 1995). *Rarβ* also appears to be expressed in the limb ectoderm which is likely to be *Rarβ1* (Schofield et al., 1992). The study of *Rarβ* expression in the facial processes describes *Rarβ* expression in the anterior maxillary process and periocular mesenchyme at HH20 which is likely to be *Rarβ2* given its similarity with the expression domain in mouse (Mollard et al., 2000; Rowe et al., 1991; Smith and Eichele, 1991). *Rarγ* expression has been less characterised during chick embryonic development compared to *Rarβ* but it has been described in: the ectoderm, anterior midbrain, eye, neural tube, caudal region and limb buds as well as characterised during skin development (Michaille et al., 1994; Michaille et al., 1995). *Rarγ1* and *Rarγ2* are documented in the limb buds, frontonasal process and branchial arches at E10.5 in

mouse with expression of *Rarγ1* being more restricted than *Rarγ2*. It is also documented to be expressed in cartilaginous condensations later in limb development (Mollard et al., 2000). *Rarγ1* has not been isolated from chick at present and therefore the expression domain investigated in the present study is that of *Rarγ2* due to its similarity with the mouse gene sequence (Michaille et al., 1994). It must also be noted that none of the previous studies have investigated expression of *Rarβ1*, *Rarβ2* or *Rarγ2* in intact chick embryos (Michaille et al., 1994; Michaille et al., 1995; Smith et al., 1995). As introduced in the previous section, the distribution of *Rarβ1*, *Rarβ2* and *Rarγ2* was investigated at HH20 to infer a mechanism for the differences in phenotypes observed with EC23 and EC19. This is the first investigation into *Rarβ1*, *Rarβ2* and *Rarγ2* using both whole mount *in situ* hybridisation and isoform specific probes. This section describes some of the expression domains which were observed except the limb and facial process which was addressed in the previous section.

Figure 4.11 shows the expression of *Rarβ1* in the embryo at HH20. *Rarβ1* can be seen to be expressed at a high level over the entire embryo (figure 4.11A). Although particularly high levels of expression appear in the eye, branchial arches, gut (white bracket) and limbs (figure 4.11A). The expression in the eye is due to expression in the choroid fissure and otherwise may include trapping (figure 4.11B). Figure 4.11C shows that *Rarβ1* is absent from the hindbrain at this stage. From a partial dissection of the wing bud (arrow figure 4.11D) *Rarβ1* appears to be restricted to the ectodermal layer similar to previous literature (Schofield et al., 1992).

Figure 4.12 shows the expression of *Rarβ2* in chick at HH20. Figure 4.12A and 4.12B show *Rarβ2* expression in the periocular mesenchyme and the anterior half of the maxillary arch as documented previously (Rowe et al., 1991; Smith and Eichele, 1991). Figure 4.12B also demonstrates *Rarβ2* expression in the developing gut region (bracket), caudal to the 6th branchial arch and reaching the anterior wing, which is a region of novel expression. It can be seen that *Rarβ2* is expressed in the proximal third of the developing wing (figure 4.9) and the proximal hindlimb (figure 4.12D) at this stage which is consistent with previous reports (Schofield et al., 1992; Smith et al., 1995). *Rarβ2* was also observed to be expressed in the lateral plate mesoderm between the wings and hindlimbs (arrow figure 4.12C) and in two stripes within the neural tube (white arrow figure 4.12D). *Rarβ2*

is absent from the medial frontonasal mass (asterisk figure 4.12F) as reported (Rowe et al., 1992) as well as the novel finding that it is absent from the hindbrain (figure 4.12E).

Figure 4.13 shows the expression of *Rarγ2* in chick at HH20. *Rarγ2* is expressed at low levels in the intersomitic clefts (black arrow) and the neural crest derived regions of the trigeminal ganglion (figure 4.13A, white arrow). Interestingly, it is also expressed in the hindbrain demarcating the posterior boundary of rhombomeres 2-5 (arrows figure 4.13B) which was not documented previously (Michaille et al., 1994; Mollard et al., 2000). *Rarγ2* has been documented to be expressed in the mouse and chick limbs (Michaille et al., 1994) as well as the FNM and branchial arches in mouse (Mollard et al., 2000; Pennimpede et al., 2010b) which has been described in the present study in chick (figure 4.8). However, it was not documented to be expressed in the trigeminal ganglion, hindbrain or intersomitic clefts although it was shown to be expressed in the pre-vertebrae at later stages of development (Mollard et al., 2000). These differences may be due to differences in methodology, developmental stage, species or isoform assayed.

The analysis of *Rarβ1*, *Rarβ2* and *Rarγ2* at HH20 of chick embryonic development has demonstrated some novel domains as well as the documentation of these *Rars* in intact chick embryos. The domains observed implicate *Rarβ1*, *Rarβ2* and *Rarγ2* in ectoderm development; gut and neural tube development; and neural, somite, limb and craniofacial development respectively. The expression domains are summarised in tables 4.1 and 4.2.

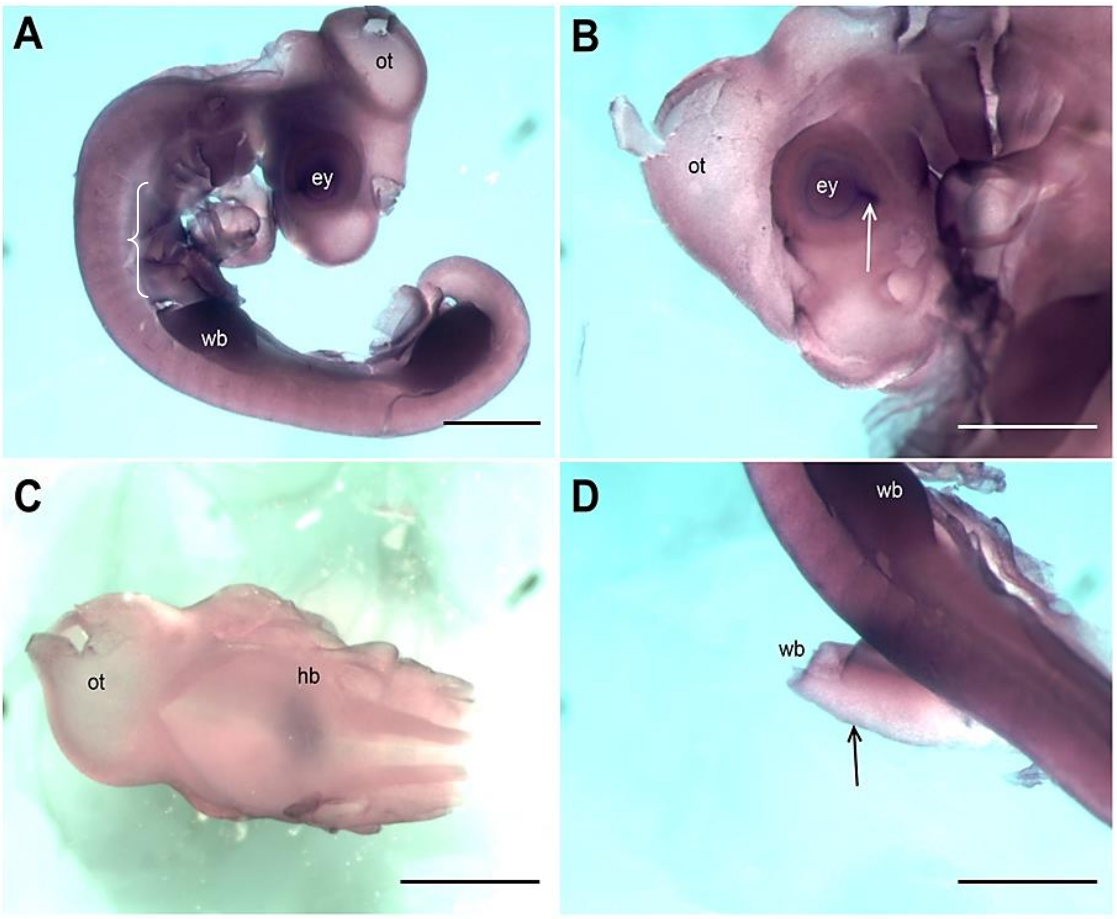

Figure 4.11: The expression of *Rarβ1* in the embryo at HH20.

A) is a right lateral view of an embryo anterior top showing generalised expression of *Rarβ1*. White bracket indicates expression in the developing gut. B) is the left side of an embryo showing *Rarβ1* expression in the head. The arrow indicates expression in the choroid fissure. C) shows dorsal view of the hindbrain, anterior left. Expression of *Rarβ1* is absent from the rhombomeres. D) shows medial view of a partially dissected left wing bud, anterior top and dorsal left. The arrow indicates expression of *Rarβ1* is ectodermal in the wing bud. Abbreviations: ey, eye; hb, hindbrain; ot, optic tectum; wb, wing bud. Scale bars are 1mm.

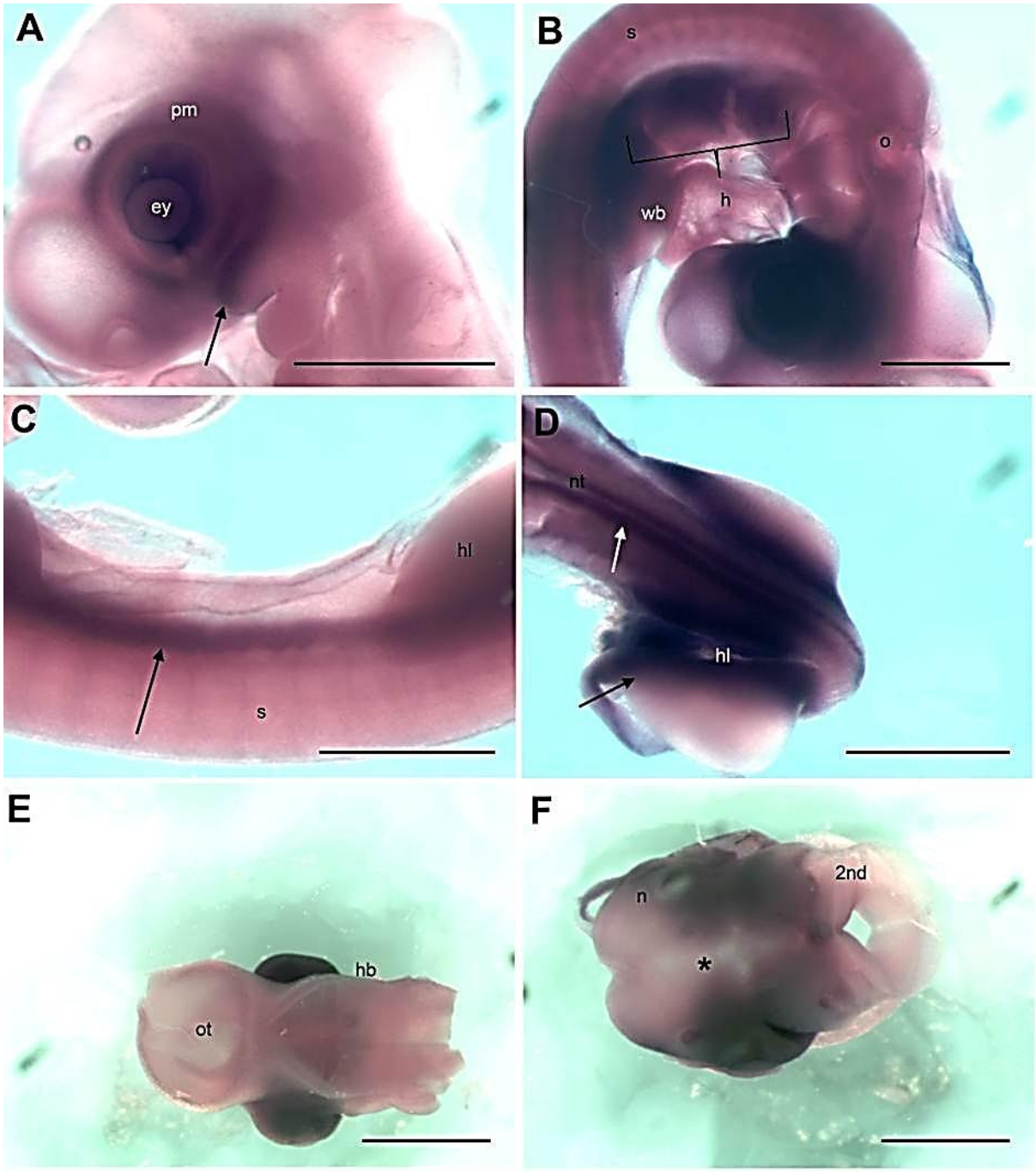

Figure 4.12: The expression of *Rarβ2* in the embryo at HH20.

A) is a left view of the head, anterior top and dorsal right, showing expression of *Rarβ2* in the periocular mesenchyme (pm) and an anterior stripe of the maxillary arch (arrow). B) shows the right side of embryo. The bracket indicates expression of *Rarβ2* from the posterior 6th arch to the anterior wing bud. C) shows expression of *Rarβ2* in the lateral plate between the limbs (arrow), anterior left dorsal bottom. D) shows dorsal view of the hindlimbs showing *Rarβ2* expression in the proximal hindlimb (black arrow) and expression in the neural tube (white arrow). E) shows dorsal view of the hindbrain, anterior right showing that *Rarβ2* is absent from the rhombomeres. F) is a ventral view of the frontonasal mass showing lower levels of *Rarβ2* expression at the midline (asterisk) and higher levels lateral to this. Abbreviations: ey, eye; h, heart; hb, hindbrain; hl, hindlimb; n, nasal pit; nt, neural tube; o, otocyst; ot, optic tectum; pm, periocular mesenchyme; s, somite; wb, wing bud; 2nd, 2nd branchial arch. Scale bars are 1mm.

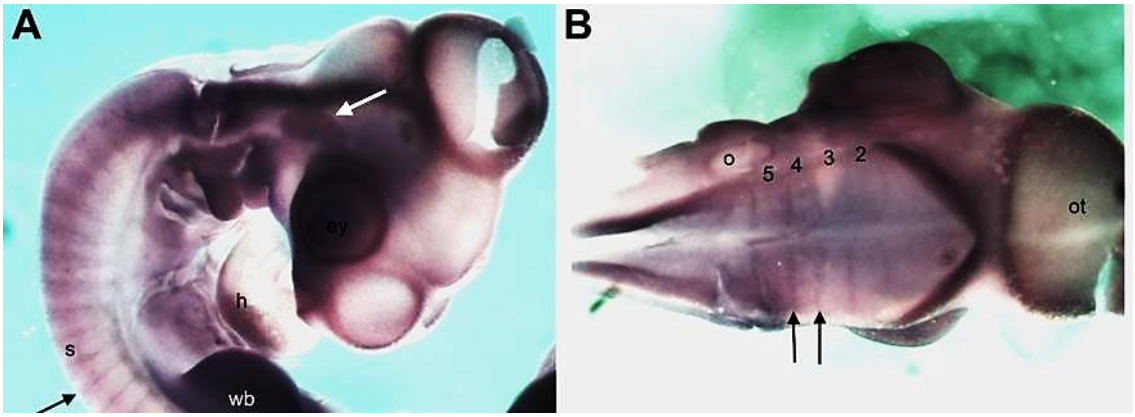

Figure 4.13: The expression of *Rarγ* in the embryo at HH20.

A) right lateral view and B) dorsal view of the hindbrain with anterior right. A) shows general expression of *Rarγ*. It is expressed at higher levels in the limb buds and the branchial arch region but is expressed at lower levels in the optic tectum and forebrain. *Rarγ* also exhibits a regular expression pattern in the somites (black arrow) and the placode derived trigeminal ganglion (white arrow). B) shows the expression of *Rarγ* at the boundaries of rhombomeres 2-5 (arrows) . Abbreviations: ey, eye; h, heart; o, otocyst; ot, optic tectum; s, somite; wb, wing bud; numbers indicate rhombomeres 2-5. Scale bars are 1mm.

Differential activation of the PPARβδ/FABP5 pathways as a mechanism for differential effects of EC23 and EC19.

As described previously, ATRA binds to CRABP2 which translocates ATRA to the nucleus and allows it to bind and activate RAR:RXR heterodimers (Budhu and Noy, 2002). It has been proposed recently that ATRA can also bind to FABP5 which channels ATRA to the nucleus to activate PPARβδ (Schug et al., 2007; Shaw et al., 2003). The activation of this receptor pathway would activate different target genes and the ratio of FABP5:CRABP2 is thought to be the mechanism behind the contradictory effects seen with ATRA (Schug et al., 2007). To investigate the hypothesis that EC23 and EC19 could differentially activate this pathway and generate the phenotypes seen in chapter 3, the expression of *Fabp5* and its receptor *Pparβ* was investigated in chick at HH20. This may also give novel insights into retinoid function by localisation of where this receptor pathway may be activated in the entire embryo and its comparison with RAR/CRABP2 domains. The expression of *Fabp5* and *Pparβ* in the wing and facial processes is addressed here.

Figure 4.14 shows the expression of *Fabp5* and *Pparβ* in the facial processes (4.14A-D) and the developing wing buds at HH20 (4.14E-F). *Fabp5* is seen to be absent from the branchial arches and other facial processes, although it is present in other areas of the head which will be addressed later (figure 4.15A and 4.15C). The arrow in figure 4.14E shows expression of *Fabp5* in the mesoderm of the posterior half of the wing bud but which is absent from the ZPA region. *Pparβ* is expressed at low levels in the head but at higher levels in the posterior maxillary process, anterior distal mandibular process and posterior 2nd arch. It is also expressed in the FNM and FEZ (figure 4.14B and 4.14D). It appears to be ubiquitously expressed in the wing bud mesenchyme bar a region in the posterior wing where it is expressed at lower levels and which may correspond to the ZPA. It is also absent from the AER (figure 4.14F-arrow). From these expression patterns it appears that PPARβ may have a role in both upper beak and limb development whereas FABP5 appears to be involved in limb development alone at HH20. The differential expression of *Fabp5* with respect to *Pparβ* may support previous research suggesting that unliganded PPARβδ has an important role as a repressor of transcription (Shi et al., 2002), similar to unliganded RARs (Damm et al., 1993; Koide et al., 2001), or that another channelling protein may deliver a different ligand to the receptor in this region. With respect to EC23 and EC19, as

Fabp5 is restricted to the wing bud and EC23 affects wing development while EC19 does not, this suggests that EC23 may bind FABP5 and activate PPARβ while EC19 may not.

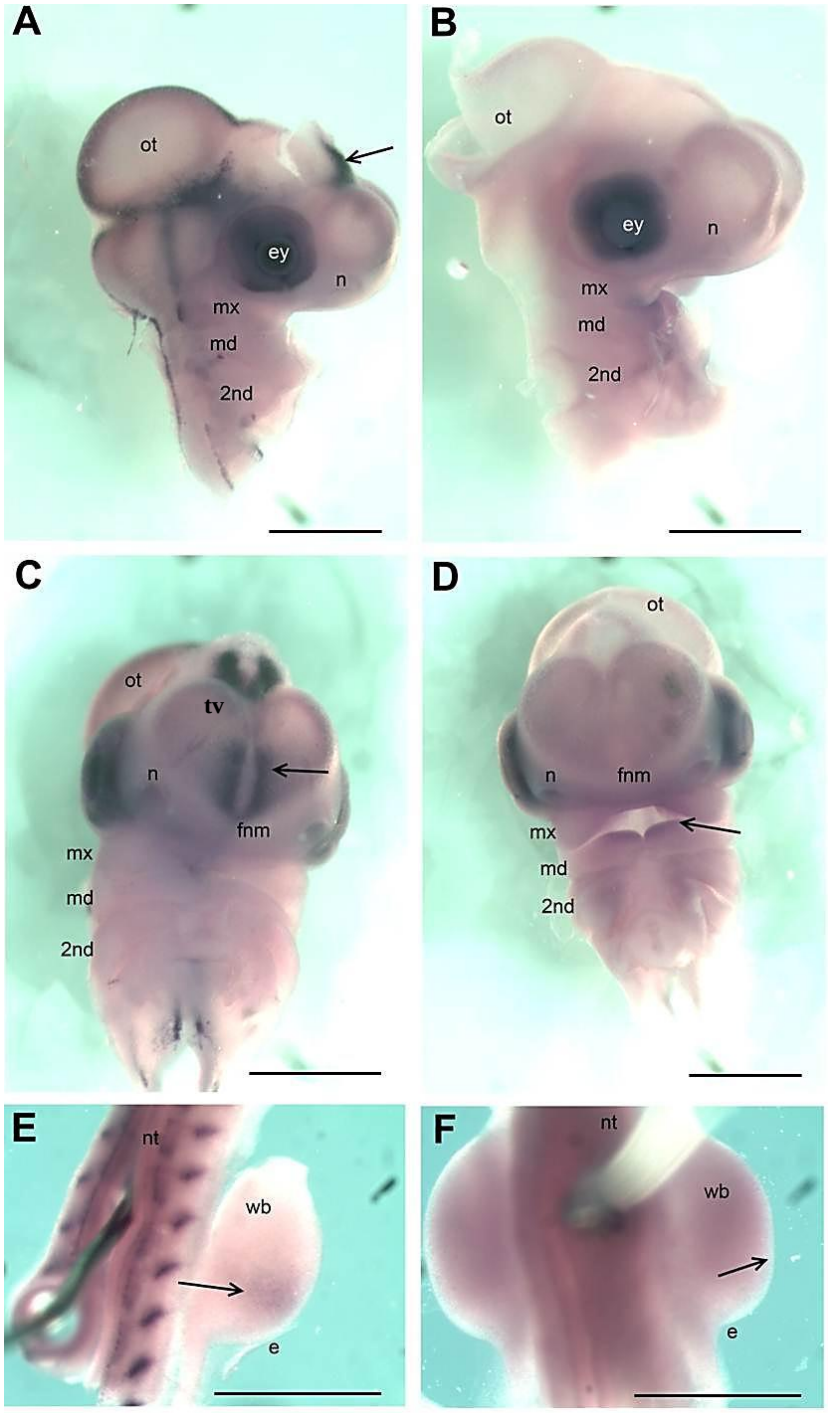

Figure 4.14: The expression of *Fabp5* and *Pparβ* in the facial processes and wing buds at HH20.

A) and B) are right lateral views of the head, anterior top. C and D) are frontal views of the facial processes, anterior top. E and F) are dorsal views of wing buds pinned to agar, anterior top. A, C, E) show expression of *Fabp5* and B, D, F) show expression of *Pparβ*. A and C) show absence of *Fabp5* expression from the branchial arches and frontonasal mass. The arrow in A) indicates expression flanking the pineal gland. The arrow in C) indicates expression between the cerebral hemispheres. E) shows expression of *Fabp5* in the posterior wing bud (arrow) but anterior to the zone of polarizing activity. B and D) show *Pparβ* is expressed generally in the developing facial processes with higher levels in the anterior proximal mandibular arch (arrow in D). F) shows expression of *Pparβ* in the mesoderm of the wing bud but is absent from the ectoderm (arrow). Abbreviations: e, ectoderm; ey, eye; fnm, frontonasal mass; md, mandibular arch; mx, maxillary arch; n, nasal pit; nt, neural tube; ot, optic tectum; s, somite; tv, telencephalic vesicles; wb, wing bud. Scale bars are 1mm.

Expression of *Fabp5* and *Pparβ* in the entire embryo at HH20.

The expression patterns of *Fabp5* and *Pparβ* have not been documented in chick embryonic development and this section addresses their expression patterns in the rest of the embryo. Figure 4.15 shows the expression of *Fabp5* in other areas of interest at HH20. It can be seen that *Fabp5* appears to be expressed in a pattern consistent with a role in neural development. Figure 4.15A-D exhibits the expression of *Fabp5* in the developing brain and eye and it is expressed in two lines demarcating the un-segmented floor plate of the hindbrain (figure 4.15A; solid arrow). There are also projections of *Fabp5* expression extending into the hindbrain which appear to follow rhombomere boundaries (dashed arrow). This expression in the hindbrain is reminiscent of that of *Islet1* which is expressed in developing motor neurons (Chambers et al., 2007). Expression is also seen in the rhombic lips marking the boundary between non-neural tissue and neural tube (figure 4.15A and 4.15E). Figure 4.14C, 4.15B, 4.15C and 4.15D show that the expression of *Fabp5* in the head is complex and restricted. Figures 4.14C, 4.15B (black arrow) and 4.15D (white arrow) show that *Fabp5* is expressed in two stripes flanking the midline of the dorsal telencephalon and lies between the posterior third of the telencephalic vesicles and the FNM. This is similar to the expression of *Fgf8* between HH19 and HH23 marking the ANR (Fuchs et al., 2010; Halilagic et al., 2007). There is also a stripe of *Fabp5* expression visible connecting the nasal pits to the telencephalic vesicles (black arrow, figure 4.15D). Figure 4.15B and 4.15C show that *Fabp5* is also expressed in the dorsal diencephalon particularly surrounding the developing pineal gland (white arrow and p respectively). There are also two stripes of expression flanking the midline of the dorsal midbrain. These stripes of expression at the midline are not completely connected with those in the forebrain (see figure 4.15B) although it is a common theme for *Fabp5* expression within the developing brain. Interestingly it is also seen in embryos hybridised with *Raldh2* (GEISHA, March 2013). *Fabp5* is therefore expressed in the head at HH20 including: the developing eye and in two stripes at the midline of the hindbrain, midbrain and forebrain.

Figure 4.15C shows the most strongly expressing domains of *Fabp5* expression: ventral retina (solid arrow), lens and, likely, the fourth cranial nerve (dashed arrow and figure 4.15E; (Guthrie, 2007)). The expression of *Fabp5* in the ventral retina is also seen in a similar region to *Raldh3* in mouse and chick at earlier stages of development (GEISHA, March 2013; Mic et al., 2000; Reijntjes et al., 2005). It can also be seen that *Fabp5* is

expressed in restricted areas of the developing cranial nerves: trigeminal (V), geniculate (VII), vestibular (acoustic VIII), petrosal (IX), nodose/vagus(X) and accessory (XI). Figure 15G and 15H show *Fabp5* in the proximal V^{th} ganglion which are known to be a population of neural crest derived boundary cap cells (bc in figure 4.15H; (Wilkinson et al., 1989)). It also appears to be expressed in the boundary cap cells of cranial nerve VII (fa in figure 4.15H). It is also expressed in two spots in the 2^{nd} and 3^{rd} branchial clefts which correspond to the placode derived exit points of cranial nerves VII and IX (geniculate and petrosal; white dashed arrows in figure 4.15H) as well as part of cranial nerve X (nodose or vagus; white and black arrows in 4.15F and 4.15H respectively). As mentioned previously, *Fabp5* is also expressed in neural crest corresponding to the developing cranial nerve XI (white dashed arrow, figure 4.15F). Figure 4.15E and 4.15F also indicate that *Fabp5* is expressed at the intersomitic boundary (solid black arrows, figure 4.15F) which is expressed in a progressively more ventralised portion caudal to the wing. This also appears to spread to include anterior and posterior somites in the posterior embryo. Taken together, the expression pattern of *Fabp5* indicates a role in neural development as it is highly restricted in the developing brain and cranial nerves.

The expression of *Pparβ* at HH20 is shown in figure 4.16. Figure 4.16A shows ubiquitous expression of *Pparβ* as reported previously in rat (Braissant and Wahli, 1998), with regions of higher expression in the following areas: limb buds, eye, branchial arches and telencephalic vesicles. *Pparβ* is absent from the hindbrain (figure 4.16B). The expression of *Pparβ* is consistent with a role for this pathway in limb and face development. It must be noted that the differences between *Pparβ* and *Fabp5* expression patterns, particularly in the developing facial processes where they are marked, are puzzling as it has been shown from manipulation of cancer cell lines that FABP5 can channel ATRA to PPARβδ to activate this pathway (Schug et al., 2007; Shaw et al., 2003). However, it may be proposed that in these regions, as in the anterior wing, the primary function of PPARβ may be to act as an unliganded repressor of transcription in a similar manner to the RARs and described for this receptor (Cash et al., 1997; Koide et al., 2001; Shi et al., 2002).

Table 4.1 and 4.2 show a summary of the expression of the receptors investigated in this study, the implications of which are discussed in the following section.

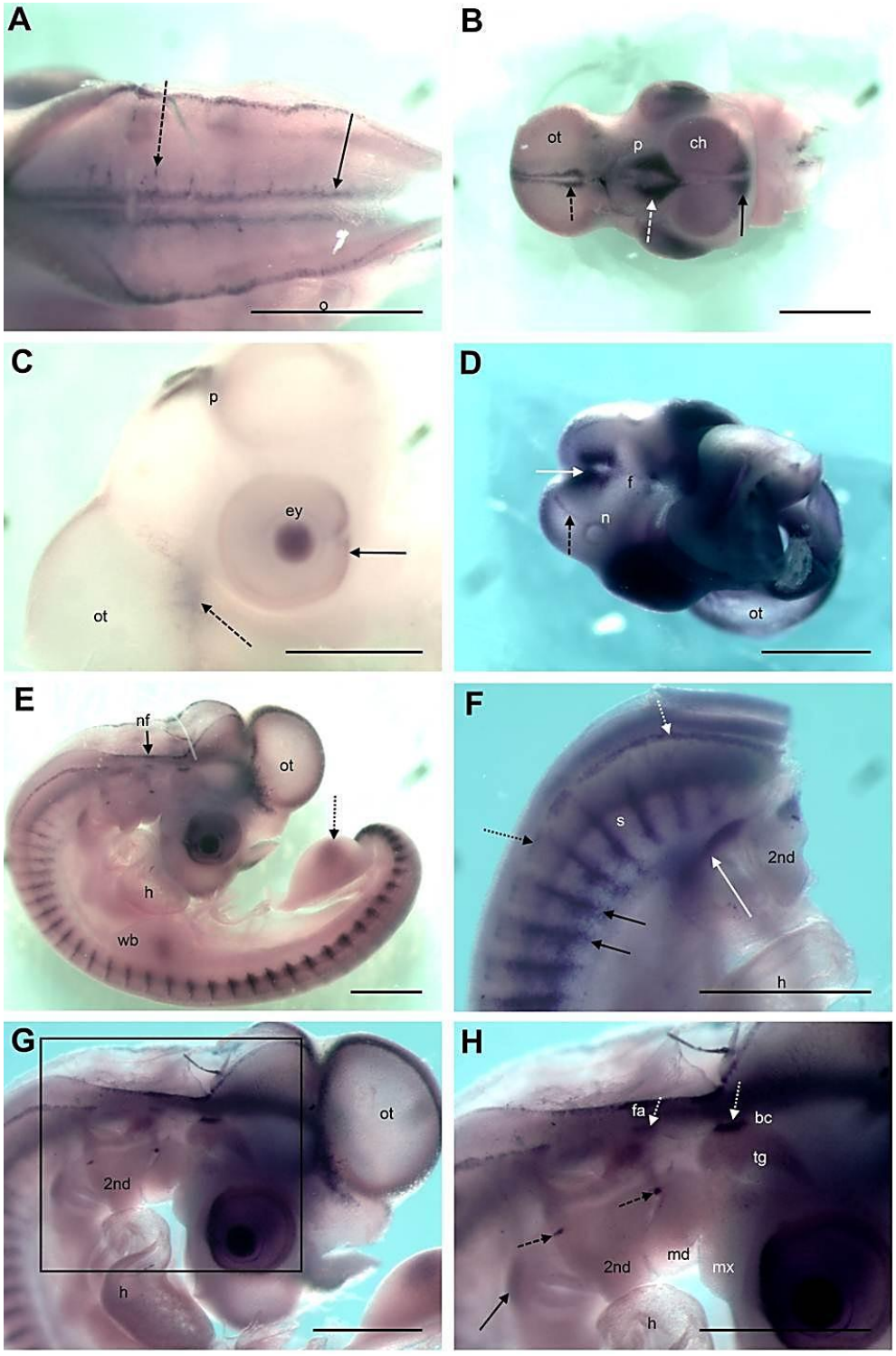

Figure 4.15: The expression of *Fabp5* in the embryo at HH20.

See following page for figure legend.

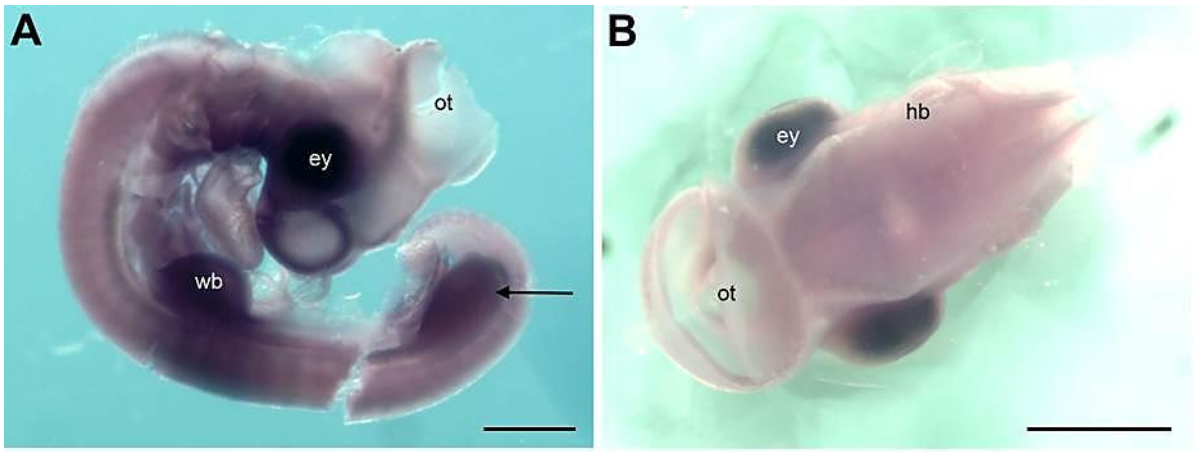

Figure 4.16: The expression of *Pparβ* in the embryo at HH20.
A) is a right lateral view of the whole embryo showing general expression of *Pparβ* but higher levels at the branchial arches and cerebral hemispheres (bracket) and leg bud (arrow). Expression is lower in the optic tectum. B) shows a dorsal view of the hindbrain with anterior left showing absence of *Pparβ* expression from the rhombomeres. Abbreviations: ey, eye; hb, hindbrain; ot, optic tectum; wb, wing bud. Scale bars are 1mm.

Legend for Figure 4.15: The expression of *Fabp5* in the embryo at HH20.

A-D) anterior is left, E-H) anterior top. A) is a dorsal view of the hindbrain showing *Fabp5* expression in the floor plate (arrow) and at rhombomere boundaries (dashed arrow). B) shows ventral view of the forebrain showing *Fabp5* expression in two stripes flanking the midline of the optic tectum (dashed black arrow), pineal gland (dashed white arrow) and cerebral hemispheres (black arrow). C) shows right lateral view of the head showing *Fabp5* expression flanking the pineal gland (p), in developing neurons (CNIV; dashed arrow) and at the ventral eye (solid arrow). D) shows *Fabp5* expression between the cerebral hemispheres (white arrow) and a stripe of expression from the nasal pits (dashed arrow). E) shows a right lateral view of the whole embryo to show areas of high expression levels: somites (close up F), cranial ganglia (close up G and H), posterior limb bud (dashed arrow) and neural folds (arrow). F) shows lateral right view of *Fabp5* expression at the posterior somite boundaries (black solid arrows), also expression adjacent to branchial arches 3-6 (white arrow), vagus nerve (CNX; white dashed arrow) and chain ganglia (black dashed arrow). G) shows a right lateral view of the branchial arches. Box indicated the area shown in H) at higher magnification. H) shows right lateral view of the head showing *Fabp5* expression in the boundary caps of the trigeminal and facioacoustic ganglia (white arrows), exit points for other cranial nerves seen as spots of expression in the mandibular-2nd cleft and 2nd-3rd cleft (black dashed arrows) and adjacent to arches 3-6 (black arrow). Abbreviations: bc, boundary cap; ch, cerebral hemispheres; ey, eye; f, frontonasal mass; fa, facioacoustic ganglion; h, heart; md, mandibular arch; mx, maxillary arch; n, nasal pit; nf, neural folds; o, otocyst; ot, optic tectum; p, pineal gland; s, somite; tg, trigeminal ganglion; v, vagus nerve; wb, wing bud; 2nd, 2nd branchial arch. Scale bars are 1mm.

Table 4.1: A comparison of *Rarβ1*, *Rarβ2*, *Rarγ2*, *Fabp5* and *Pparβ* expression in the developing chick wing and face at HH20.

Gene	Limb	Face
Rarβ1	Ectoderm Inc. AER.	Distal maxillary arch and anterior mandibular arch. FEZ
Rarβ2	Proximal limb and lateral plate mesoderm between wings.	Periocular mesenchyme and anterior half of maxillary arch. FNM but lower expression at the midline. Absent from the FEZ.
Rarγ2	Distal wing adjacent to the AER and within it.	Generally high. Elevated in the posterior distal maxillary arch and anterior proximal mandibular arch. Also seen flanking 2nd and anterior 3rd branchial pouches. Distal FNM and FEZ.
Fabp5	Mesoderm region in both wing and hindlimb anterior to the ZPA.	-
Pparβ	+ ubiquitous bar AER	Higher expression in proximal and posterior maxillary arch, distal anterior mandibular arch and posterior distal 2nd. FNM and FEZ.

Abbreviations: AER, apical ectodermal ridge; FNM, frontonasal mass; FEZ, frontonasal ectodermal zone; md, mandibular arch; mx, maxillary arch; ZPA, zone of polarizing activity. + denotes expression and – denotes absence of expression.

Table 4.2: A comparison of *Rarβ1, Rarβ2, Rarγ2, Fabp5* and *Pparβ* expression in the embryo at HH20 excluding the limbs and facial processes.

Gene	Brain	Head	Nerves and NT	Somites and Other
Rarβ1	-	Expressed in the choroid fissure.	-	Ectodermal *
Rarβ2	-	Periocular mesenchyme and choroid fissure.	Expressed in two stripes adjacent to the neural tube.	6th arch to the anterior wing-developing gut.
Rarγ2	Posterior boundaries of rhombomeres 2-5. Neuroepithelium of the rhombic lips.	Increased expression in the head compared to the rest of the embryo.	Seen in neural crest derived region of CN V.	Intersomitic clefts at low levels.
Fabp5	2 stripes of expression adjacent to the floor plate in the hindbrain (MNs). Some medio-lateral expression corresponding to rhombomere boundaries. 2 stripes flank roof plate of hindbrain, midbrain and forebrain (pineal and ANR).	A stripe of expression is seen from NP to FNM. Ventral retina and choroid fissure.	BCCs of CN V and VII. Spots indicating exit points of CN VII and IX. CN X and IX (placode derived).	Entire intersomitic clefts cranial to the wing. Caudal somites exhibit ventralised expression also spreading anterior and posterior.
Pparβ	Forebrain.	Expressed in choroid fissure.	-	Very faint expression in somitic clefts.

Abbreviations: BCCs, boundary cap cells; CN, cranial nerve; FNM, frontonasal mass; MNs, motor neurons; NP, nasal pit; NT, neural tube; RAR, retinoic acid receptor. Roman numerals refer to the cranial nerves: V, trigeminal; VII, geniculate; IX, petrosal; X, nodose and vagus; XI, spinal accessory.* indicates partial dissection.

Discussion:

EC23 and EC19 have been shown to generate differential effects *in vivo* (chapter 3) and *in vitro* (Christie et al., 2008). This is intriguing as these retinoids are identical except in the position of the carboxylic acid group (see chapter 1). This has led to the production of two photostable retinoids which may mimic ATRA and, given the position of the carboxylic acid group in EC19, 13CRA. This chapter has investigated the mechanisms behind these differential effects by exploring the metabolism of these retinoids and whether the location of their binding proteins may correlate with the differential phenotypes generated. Their metabolism was investigated using an *in vitro* chondrogenesis system which has been used previously in the investigation of teratogenic compounds (Jiang et al., 1995; Kistler, 1987; Pignatello et al., 2002) and will be addressed first.

Differential metabolism of EC23 and EC19 as part of the mechanism behind their differential effects *in vivo* and *in vitro*.

As described, EC23 is relatively more potent in this *in vitro* system than it is *in vivo* as well as demonstrating increased potency over ATRA (figures 4.1, 4.3 and 4.7). This is most likely to be due to the fact that retinoid treatment of the *in vitro* system is direct whereas retinoid treatment of the chick limb can be dissipated to the rest of the embryo via the vascular system. EC19, however, is less potent than ATRA (figure 4.2). It has been documented that excess ATRA inhibits chondrogenesis in chick limb bud micromass cultures while 13CRA is less potent (Kistler, 1987; Kistler et al., 1985). This inhibition is due to a decrease in cartilage condensations formed, also seen in response to EC23 and EC19 (figures 4.2, 4.3 and 4.4), and may occur via inhibition of cell: cell adhesion or signalling factors such as TGFβ (see chapter 5; (Cho et al., 2003; Miura and Shiota, 2000)). The decreased potency of EC19 observed provides further evidence that EC19 is an analogue of 13CRA. TTNPB is a retinoid of similar structure to EC23 and EC19 which has also been investigated (Kistler, 1987; Kochhar and Penner, 1992; Pignatello et al., 1997, 1999, 2002). It has been shown that the action of TTNPB is similar to the action of ATRA when it cannot be metabolised indicating that TTNPB is resistant to metabolism (Pignatello et al., 2002). Similarly the action of ATRA is enhanced here with an inhibitor of metabolism while it has no effect on EC23 indicating that EC23 is potentially resistant to metabolism. Oddly, EC19 is apparently metabolised despite their similar structures.

Considering that metabolism of EC23 and EC19 to 4-*hydroxy*-, 4-*oxo*, 5,6-*epoxy*- and 18-*hydroxy*-derivatives are blocked by the TMTN unit ((Henderson, 2011) chapter 1), both retinoids should theoretically be resistant to metabolism by the CYP26 enzymes at these sites. Some potential explanations for these differences are discussed below.

As previously mentioned, EC19 can be thought of as an analogue of 13CRA. The action of 13CRA *in vivo* has been studied as it is also a potent teratogen and has been used as a treatment for dermatological diseases. It has been described as being metabolised *in vitro* at a similar rate to ATRA (Klaassen et al., 2001) but no studies have characterised it further. 13CRA levels *in vivo* are low indicating that it is present due to the application of excess ATRA and interconverted by isomerases (Horton and Maden, 1995). It is thought that these isomerases can convert 13CRA to ATRA which cause the teratogenic effects of 13CRA given that its affinities for CRABP and RAR are very low (Klaassen et al., 2001; Maden and Summerbell, 1986; Ruhl et al., 2001). EC19, however, is unlikely to be converted to ATRA or its analogue EC23 *in vivo* as the terminal carboxylic acid is linked to a conjugated ring structure rather than a polyene chain. EC19 may therefore be useful as a tool to investigate the relative lack of teratogenicity of 13CRA compared to ATRA.

ATRA is thought to be metabolised to 4-*hydroxy*-retinoic acid (RA), 4-*oxo*-RA, 18-*hydroxy*-RA and 16-*hydroxy*-RA (primary) and then sequentially to their more polar derivatives such as 4, 16- *hydroxy*-RA; 4, 18-*hydroxy* RA; 4-*oxo*, 16-*hydroxy*-RA and 18-*oxo*, 4-*hydroxy* RA by the CYP26 enzymes in humans (Topletz et al., 2012). A recent study has shown that the primary and secondary metabolism of ATRA may also depend on the chirality of the compound present. CYP26A1 metabolises ATRA predominantly to the enantiomer 4S-*oxo* RA as binding to the active site favours this. CYP26 enzymes have also been shown to catalyse this to 4-*hydroxy* RA and this occurs three times faster if the 4S-*oxo* RA enantiomer is present (Shimshoni et al., 2012). Similarly, it has been documented that different enantiomers of synthetic retinoids bind preferentially to the CYP26 enzymes (Kleywegt et al., 1994). Further investigation into the chirality of the metabolites produced from EC23 and EC19 metabolism as well as CRABP binding for EC23, EC19 and their metabolites may provide a mechanism behind their differential metabolism and phenotypes despite their similar structures.

CYP26 enzymes have been documented to carry out primary and secondary metabolism of ATRA *in vivo* (Taimi et al., 2004; Topletz et al., 2012; White et al., 1997; White et al., 2000) but retinoids have also been documented to be metabolised to glucoronide derivatives *in vivo* although the enzyme responsible for this conversion is unknown (Barua and Sidell, 2004). This pathway could be another mechanism for the differential metabolism of EC23 and EC19. It could be proposed that binding of EC23 or EC19 to CYP26 is hindered. CYP26A1 is the major enzyme involved in ATRA metabolism. Interestingly its active site is thought to be narrow after modelling studies (Gomaa et al., 2006; Shimshoni et al., 2012) which may result in neither EC23 nor EC19 binding to CYP26 enzymes. Other cytochrome P450 oxidase enzymes are capable of catabolising ATRA and its isomers in human liver: CYP2C8, CYP2C9, CYP3A4, CYP3A5 and CYP3A7 (Marill et al., 2002; Marill et al., 2000; McSorley and Daly, 2000; Shimshoni et al., 2012; Thatcher and Isoherranen, 2009) although their activity during embryonic development is unknown. Unlike CYP26 enzymes, these enzymes may have a larger active site, as documented for CYP3A4 (Shimshoni et al., 2012), which may allow some metabolism of EC23 and EC19. However, considering that fewer enzymes would be involved, metabolism of EC23 and EC19 would be decreased.

Given that the only difference between these molecules is the position of the carboxylic acid group (red box; figure 1.5); this may also suggest an area for further research. It could be proposed that the position of the carboxylic acid in EC19 favours its metabolism by stabilising the molecule in the CYP26 active site whereas the planar structure of EC23 may not allow this. This may be significant as it has been shown that the carboxylic acid group interacts with an arginine residue when bound to the active site of CYP26A1 or to three residues in CYP26B1 (Gomaa et al., 2006; Karlsson et al., 2008). Equally, it could be proposed that EC23 and EC19 bind the CYP26 active site in a different conformation than expected. When ATRA is bound, the β-ionene ring is closest to the heme group (Karlsson et al., 2008). As the carboxylic end of EC23 and EC19 is very similar to this β-ionene ring, this could bind closest to the heme group to allow oxidation of these residues. It could then be proposed that metabolism could occur in EC19 at the carboxylated carbon of EC23. If this were true it would explain why EC19 is metabolised and EC23 is not and could be an interesting avenue for further work. Also, as all other sites for metabolism are still blocked in EC19 and EC23 bar the equivalent position to carbon 16 in ATRA (red

circle; figure 1.5), this would be consistent with the fact that EC19 is metabolised to a lesser extent than ATRA and that EC23 is metabolised even less.

Interestingly, it can be seen that 10^{-10}M and 10^{-12}M EC23 cause a slight decrease in chondrogenesis but when combined with liarozole, chondrogenesis is enhanced (figures 4.3 and 4.7C). It has been shown that the CYP26 enzymes are highly retinoid responsive (Loudig et al., 2000; Loudig et al., 2005; Reijntjes et al., 2005; White et al., 1996) and that EC23 induces them *in vivo* (see chapter 5). The concentrations of EC23 used here may induce the CYP26 enzymes more strongly than ATRA or EC19 causing them to metabolise all ATRA present in the limb bud cells or in cell culture medium. RALDH2 is known to synthesise ATRA (Wang et al., 1996; Zhao et al., 1996) and could also be down-regulated in order to maintain correct retinoid levels in culture (chapter 5; (Niederreither et al., 1997)). In these low levels of ATRA the concentration of EC23 alone may not be high enough to inhibit chondrogenesis in this system and would disinhibit chondrogenesis by reducing ATRA concentrations to lower than normal.

Overall it can be concluded that EC23 and EC19 are differentially metabolised *in vivo* which may partially explain the differential phenotypes generated with these compounds. The increased metabolism of EC19 compared to EC23 suggests that EC19 may be metabolised at the carbon which is carboxylated in EC23 by other unknown enzymes *in vivo* while the presence of the carboxylic acid group in EC23 inhibits this. As ATRA can be metabolised to 16-*hydroxy* RA (Topletz et al., 2012), it can be proposed that the metabolism of EC23 and EC19 seen occurs at the equivalent carbon on the TMTN group (red circle; figure 1.5). The differences between EC23 and EC19 may then be due to differences in binding to the CYP26 or other enzymes via their terminal carboxylic acid groups. Given the similarities with 13CRA it may be proposed that EC19 may not bind CRABP or RAR *in vivo* which would also explain the differential phenotypes seen. As EC23 is metabolised to a lesser extent *in vivo* it can be used as an experimental tool to investigate ATRA function. The fact that EC23 is metabolised less but not isomerised *in vivo* and mimics the phenotypes of ATRA bar digit specification suggests that the metabolites are unlikely to be involved in signalling during development consistent with previous literature (Niederreither et al., 2002a). This suggests that exogenously applied metabolites such as 4-*oxo*-RA to VAD quail may be converted to ATRA for use in development and hence can rescue the VAD phenotype (Reijntjes et al., 2005).

Differential activation of the RARs or PPARβδ as a mechanism for the differential effects of EC23 and EC19.

The expression of some receptors linked to retinoic acid signalling was investigated here to determine whether differential expression of *Rarβ1*, *Rarβ2, Rarγ2*, and *Pparβ* as well as its channelling protein *Fabp5*, in the developing limb and facial processes may provide a mechanism for the differential effects generated by EC23 and EC19. From the investigations presented in chapter 3, it can be seen that EC23 generates severe effects on the developing wing while EC19 does not. Both EC23 and EC19 inhibit upper beak outgrowth but the effects of EC23 are more severe than EC19. The expression patterns of *Rarβ1*, *Rarβ2* and *Rarγ2* were presented in figures 4.8-13, the expression patterns of *Pparβ* and *Fabp5* were presented in figures 4.14-16 and all expression patterns studied are summarised in table 4.1 and 4.2. All receptors were found to be expressed in the developing facial processes and wing.

***Rarβ1, Rarβ2, Rarγ2, Fabp5* and *Pparβ* in the developing facial processes and wing.**

Rarβ1 and *Rarγ2* are expressed in the FEZ (and FNM mesenchyme) while *Rarβ2* is expressed in the FNM bar a region at the midline (figure 4.8). Upper beak development and outgrowth is directed by the FEZ present from HH20 and consists of a boundary of *Fgf8* and *Shh* expression in the ventral and dorsal facial ectoderm respectively (Hu et al., 2003). Expression of *Rarβ1* and *Rarγ2* in the FEZ suggests that they may be involved in the control and regulation of this structure at HH20. Altered ATRA signalling via these receptors could lead to the down-regulation of *Shh* signalling observed previously resulting in truncation of the upper beak (Helms et al., 1997). Retinoids have been shown to alter *Fgf8* signalling in pharyngeal ectoderm in mice (Abe et al., 2008) and requires further investigation. Whilst the FEZ is known to direct upper beak outgrowth, it has been shown that the effects of ATRA on the upper beak result from effects on the mesenchyme rather than the ectoderm (Wedden, 1987). Therefore the expression of *Rarβ2* and *Rarγ2* in the FNM mesoderm is equally important in the production of upper beak abnormalities.

It has been shown in chick and mouse that ATRA can affect the proliferation of the developing FNM by altering its direction in excess (McGonnell et al., 1998) and causing

apoptosis in *Rarα/γ* knockout models (Lohnes et al., 1994). The proliferating region in the distal FNM corresponds to a region of *Rarγ2* and *Rarβ2* expression (figure 4.8). This is consistent with a role for *Rarγ2* and *Rarβ2* in the regulation of proliferation in the FNM. This is also consistent with previous research showing that signalling via *Rarβ2* has mediated other teratogenic effects of ATRA in the branchial arches (Matt et al., 2003). Considering these observations, it could be proposed that EC19 is *Rarβ1* specific given its expression in the FEZ providing a mechanism for the inhibition of *Shh* signalling after ATRA treatment (Helms et al., 1997). This alteration at the FEZ may indirectly affect proliferation in the FNM (McGonnell et al., 1998) which would lead to the asymmetrical phenotypes seen in chapter 3. However, this may also involve *Rarγ2* given its expression pattern.

Interestingly, *Fabp5* is not expressed in the developing facial processes unlike *Pparβ*. As PPARβδ requires FABP5 to translocate ATRA to the nucleus (Schug et al., 2007; Shaw et al., 2003; Tan et al., 2002), the ubiquitous expression of *Pparβ* in this region suggests that, similar to the RARs in other areas (Cash et al., 1997; Koide et al., 2001), it may function as an unliganded repressor in the development of the facial processes. Consistent with this it has been documented to function as an unliganded repressor and to repress the transcription of other PPAR target genes (Adhikary et al., 2011; Shi et al., 2002). However, in these regions it could be activated by another ligand. This is unlikely as although it has been suggested that polyunsaturated fatty acids may be another endogenous ligand for PPARβδ, they also require FABP5 for nuclear translocation (Michalik and Wahli, 1999; Tan et al., 2002).

With respect to wing development, *Rarβ1* and *Rarγ2* are expressed in the AER but they are also expressed in the surface ectoderm and the adjacent distal mesenchyme respectively, while *Rarβ2* is restricted to the proximal wing mesenchyme (figure 4.9). Given their expression in the AER, *Rarβ1* and *Rarγ2* may be involved in the control of PD outgrowth and patterning. Considering that *Rarγ* knockout mice exhibit no abnormalities of limb development it is likely to be redundant with other receptors expressed in the limb in this function e.g. *Rarα* (Lohnes et al., 1993; Lohnes et al., 1994). The role for *Rarγ2* in the distal limb mesenchyme may be to mediate the effects of RA induced teratogenesis since *Rarγ* knockout in the *Cyp26b1* knockout background, rescues some limb defects (Pennimpede et al., 2010b). Considering that EC23 generates similar phenotypes to the

Cyp26b1 knockout mouse: shortening of the cartilage elements and alteration to digit development (Pennimpede et al., 2010b), it may be considered that EC23 is signalling via *Rarγ2* in the chick wing while EC19 may not. However, EC23 and ATRA have been shown to cause proximalisation of cells in the developing wing (chapter 5; (Mercader et al., 2000)). As ATRA is known to cause an expansion of *Rarβ2* and *Meis2* (Mercader et al., 2000) expression it is likely that the effects of EC23 on the wing occur via *Rarβ2*. This is consistent with the idea that the retinoid response induces changes to the wing mesoderm (Tickle et al., 1989) although this does not rule out EC23 acting via *Rarγ2* in the distal limb or *Rarα* which is documented to be ubiquitously expressed in the mouse (Mollard et al., 2000).

As in the facial processes, *Pparβ* is expressed ubiquitously through the limb bud mesoderm bar the ZPA region (figure 4.14) and *Fabp5* expression must therefore determine retinoid signalling via this receptor. *Fabp5* expression is seen in the mesoderm of the posterior half of the wing but is absent from the ZPA (figure 4.14). Given that *Fabp5* is only expressed in the wing, where EC19 has significantly less effect, it could be proposed that EC19 cannot bind to FABP5 and activate PPARβ while EC23 can. These results imply that EC23 is a pan-agonist and EC19 may be specific to *Rarβ1* as EC19 does not generate a limb phenotype and therefore it cannot affect the mesenchyme.

Therefore, it can be surmised that EC23 is likely to be a pan-agonist of the RARs and that EC19 may be specific to RARβ1 or RARα. However, this cannot be determined conclusively as the expression of *Rarα1* and *Rarα2* in the limb have not been determined in chick. Previous research in mouse has elucidated that they are ubiquitously expressed at early stages, although they are restricted later, particularly in limb development (Mollard et al., 2000). Given that *RARα/γ* knockout mice exhibit many of the phenotypes seen with EC23: scapula and radius malformations as well as alteration to digit number (Lohnes et al., 1994), this would be consistent with the idea that EC23 is a pan-agonist of the RARs. It would also fit with the idea that EC19 may be a RARβ1 agonist rather than RARα given that *Rarα* is expressed in the mesoderm (Mollard et al., 2000) and the fact that RARα specific ligands cause limb malformations (Elmazar et al., 1996) does not correlate with the absence of a limb phenotype after EC19 treatment. If true, the fact that EC19 would only affect one receptor in the developing facial processes would cause a far milder

phenotype consistent with results seen in chapter 3. Considering the presence of *Fabp5* in the developing wing bud mesoderm but its absence from the FNM, this supports the idea that EC19 is unable to activate PPARβ in the limb. It could be proposed that EC23 can activate both RAR and PPARβ while EC19 can only activate RARβ1 during limb development and this may contribute to the differential effects seen with EC23 and EC19.

Retinoid signalling is not just confined to activation of the RARs but also involved binding to intracellular binding proteins, receptors and degradation enzymes, all of which could provide a mechanism behind the effects seen (Pignatello et al., 2002) and refs therein). Indeed, the expression of *Fabp5* in the limb but not the facial processes provides one such mechanism: it is possible that EC23 may bind FABP5 as well as CRABP2 while EC19 may have lowered affinity for FABP5. This in conjunction with differential receptor activation may lead to the dramatic difference in limb phenotypes generated by these two retinoids of such similar structure. Further investigation into binding affinity of EC23 and EC19 is necessary to conclusively reveal the mechanism behind the different phenotypes seen with these similar retinoids. Their degradation has also been investigated in the previous section and the finding that EC23 is potentially resistant to metabolism unlike EC19 and ATRA suggests that further investigation of RARs may be necessary for the mechanism behind the EC23 phenotype. It must be concluded that EC23 may activate receptors for an increased period of time over both EC19 and ATRA and therefore exploring RAR expression at later time points may be equally important in determining receptor activation of EC23.

Novel findings from the investigation of *Rarβ1*, *Rarβ2* and *RARγ2* expression at HH20 of chick embryonic development.

The RARs have been a subject of research since the late 1980s and their expression patterns were analysed in mouse and chick development early on (Dolle et al., 1989; Dolle et al., 1990; Michaille et al., 1994; Michaille et al., 1995; Mollard et al., 2000; Rowe et al., 1991; Smith et al., 1995). Since then, their knockout phenotypes (Lohnes et al., 1993; Lohnes et al., 1994; Mendelsohn et al., 1994b) and investigation into ATRA metabolism (Mic et al., 2004; Niederreither et al., 2002a; Pennimpede et al., 2010b; Reijntjes et al., 2005; Yashiro et al., 2004) has become the focus of research into retinoids in the developing embryo. Many investigations researched the expression of the receptor

subtypes but not their isoforms and are reported in that fashion (Dolle, 2009). The expression of the RARs are still not fully characterised in chick embryonic development although they have been studied in skin development (Michaille et al., 1995) and this has left gaps in our knowledge and understanding of ATRA in development. The present study reports the expression of *Rarβ1*, *Rarβ2* and *Rarγ2* using whole mount *in situ* hybridisation rather than section *in situ* hybridisation and notes some novel areas of expression.

Rarβ1 and *Rarβ2* are perhaps the most studied of the RARs during embryonic development. It has been shown that *Rarβ2* is highly retinoid inducible; its promoter is well characterised and used as a retinoid signalling reporter (Mercader et al., 2000; Sonneveld et al., 1999; Yashiro et al., 2004). Previous studies of *Rarβ* have often described the expression of *Rarβ2* as it is more restricted during development (Schofield et al., 1992; Smith and Eichele, 1991). The expression of *Rarβ2* has been documented previously as restricted to the proximal limb during development (Mollard et al., 2000; Schofield et al., 1992; Smith et al., 1995). *Rarβ2* is also restricted to the anterior maxillary process at HH20 as presented in this chapter (Rowe et al., 1991; Smith and Eichele, 1991).

Interestingly, it is also expressed in the periocular mesenchyme and the FNM as shown by Smith and Eichele (1991) but as can be seen from the present study it is also seen in the choroid fissure and more particularly the FNM mesenchyme bar a central T shaped region which is discussed in the previous section (figure 4.8). The area of *Rarβ2* expression in the FNM is also complementary to that of *Fabp5* (discussed below) and may delineate the boundary between the forebrain and the facial mesenchyme. *Rarβ2* can also be seen to be expressed in two stripes flanking the neural tube in the spinal cord similar to *Fabp5* and is discussed in more detail later (figures 4.12 and 4.15). This is also a region of *Raldh2* expression (GEISHA, March 2013) indicating that the balance between *Rarβ2* and *Fabp5* mediated pathways may be important for developmental control. This is thought to delineate a boundary with the roof plate at this point or a subset of differentiating motor neurons, given its similarity to *Islet1* (Chambers et al., 2007; GEISHA, March 2013). A domain of expression is also noted caudal to the branchial arches to the cranial forelimb. This expression domain encompasses the developing gut and is also a region of *Raldh2* expression (GEISHA, March 2013; Swindell et al., 1999). Interestingly, *Raldh2* knockout mice exhibit agenesis of the enteric nervous system (Niederreither et al., 2003), and *Fabp5* is also documented to be expressed in the cranial nerve X (discussed later) indicating that

Rarβ2 and *Fabp5* may have complementary roles in its development. The LPM between wing and hindlimb also expresses *Rarβ2* and is another region of *Raldh2* expression (GEISHA, March 2013; Swindell et al., 1999). Altogether this indicates that RARβ2 is likely to be the main receptor for ATRA during this period of embryonic development.

Given the highly restricted pattern of *Rarβ2*, it has been investigated more than *Rarβ1* and when *in situ* hybridisation was performed for the *Rarβ* subtype, the expression of *Rarβ1* may have been missed. This is likely considering the expression of *Rarβ1* presented here. *Rarβ1* has been described as ubiquitously expressed in the developing wing at HH20 (Smith and Eichele, 1991; Smith et al., 1995) and it can be seen to be highly expressed in the developing limbs here, but partial dissection reveals that this is restricted to the wing bud ectoderm. Considering the high levels of background staining which could be seen with section *in situ* hybridisation, this ectoderm specific expression may not have been recognised in previous studies although it is noted with *Rarβ* probes (Schofield et al., 1992). This implies that ATRA signalling can occur in the surface ectoderm of the limb which has not been discussed previously and may provide an interesting avenue for new research. Considering that it is also expressed in the AER it could be proposed to be involved in the maintenance of an ATRA-negative distal limb in that it may up-regulate *Cyp26a1*, also expressed in this region (Pennimpede et al., 2010b; Reijntjes et al., 2004; Swindell et al., 1999). Similar to *Rarγ*, the *Rarβ1* knockout mouse does not exhibit limb malformations (Ghyselinck et al., 1997; Lohnes et al., 1993). As discussed earlier, it also has a restricted expression pattern in the FEZ and anterior-distal maxillary arch (figure 4.8). It may be that the close proximity of *Rarβ1* and *Rarβ2* expression domains are necessary to provide a unified response to ATRA in the developing facial processes.

Rarγ2 is the third and final RAR investigated here. This receptor has been documented to have two isoforms in mouse (Kastner et al., 1990; Zelent et al., 1989) but as yet only one isoform has been documented in chick embryonic development. It is thought to be homologous to the *Rarγ2* receptor in mouse (Michaille et al., 1994). Its expression at HH20 is documented here for the first time and is similar to that documented at HH21 for *Rarγ* (Michaille et al., 1994). *Rarγ2* has been documented to be expressed in the mesoderm of the: developing FNM, branchial arches and limb buds in mouse (Mollard et al., 2000; Pennimpede et al., 2010b; Ruberte et al., 1990b) as well as the anterior and middle brain, neural tube, eye and caudal region for *Rarγ* in chick (Michaille et al., 1994). The

expression pattern presented here demonstrates that *Rarγ2* is expressed in the distal limb bud, AER, intersomitic clefts, branchial arches, trigeminal ganglion (placode derived region), rhombic lips and the boundaries of rhombomeres 2-5 in chick (see figures 4.8, 4.9, 4.13 and table 4.2). The expression pattern for chick *Rarγ2* confirms regions already observed however, the following domains have not been previously observed in mouse or chick: intersomitic clefts, rhombic lips and rhombomere boundaries. These may reflect species specific differences or differences in methodology.

The expression of *Rarγ2* in the intersomitic clefts is intriguing. *Fabp5* is also expressed in the intersomitic clefts and expression in this region is discussed later. It may be possible that these pathways both regulate the development of the somites and their derivatives. It is documented that cervical vertebrae are affected in *Rarγ* knock outs but, after dosing these knockouts with ATRA, lumbosacral vertebrae are also affected (Ghyselinck et al., 1997; Lohnes et al., 1993; Lohnes et al., 1994). *Rarγ2* is seen to be expressed in intersomitic clefts along the entire embryo and therefore may play a role in the correct development of the axial skeleton. This hypothesis is further supported by the inhibition of cervical and thoracic vertebrae ossification after treatment with a RARγ-specific agonist (Elmazar et al., 1996).

The expression of *Rarγ2* in the trigeminal ganglion and the rhombic lips is complementary to *Fabp5* in that *Rarγ2* is expressed in the placode derived region of the trigeminal ganglion (rather than the boundary cap cells-BCCs) and in the developing neuroepithelium of the rhombic lips rather than the boundary (compare figures 4.13A and 4.15H). The differential location of these retinoid transduction pathways provide further support for the hypothesis that FABP5 mediated signalling is necessary for boundary formation or in regions of proliferation and that activation of RAR in other regions is involved in the control of neural differentiation. The balance between these pathways may be important for correct neural development (see later for further discussion).

Interestingly, *Rarγ2* is also seen to be expressed in the posterior boundary of rhombomeres 2-5 (figure 4.13B). The hindbrain is split into segments or rhombomeres from early in hindbrain development (beginning at HH7) and they are crucial for the correct development and patterning of the cranial nerves as well as branchial arch derived structures (Kontges and Lumsden, 1996; Mahmood et al., 1995). During rhombomere

formation a boundary is also formed which comprises of morphologically distinct, slowly proliferating cells with a distinct cell matrix containing high levels of CSPG (Sela-Donenfeld et al., 2009; Theodorakis et al., 2002). The expression of *Rarγ2* at rhombomere boundaries in slowly proliferating cells may be consistent with previous research indicating that RARs are involved in differentiation while PPARβδ controls the proliferative response to ATRA (Schug et al., 2007) in that its role here may be to suppress proliferation and maintain the rhombomere boundary. This may indicate a role for RAR vs. PPARβ mediated retinoid signalling *in vivo*. However, a role for FABP5 and PPARβδ signalling is just one possible explanation of the expression patterns presented here and further experiments are required to ascertain the role for this pathway in development.

One of these possibilities is that FABP5/PPARβδ signalling is involved in coordinating the development of cells forming the rhombomere boundary. Other genes have been documented to be expressed in rhombomere boundary cells at similar developmental stages: *neurological stem cell leukaemia* (*NSCL1*), *promyelocytic leukaemia zinc finger ortholog* (*PLZF*), *Pax6* (Theodorakis et al., 2002), *Fgf3* (Mahmood et al., 1995; Powles et al., 2004; Weisinger et al., 2008), *Fgf19*, *radical fringe* (*rfng*; (Sela-Donenfeld et al., 2009)), *Wnts* (Riley et al., 2004), *follistatin* (Weisinger et al., 2008) and *notch* receptors (Qiu et al., 2009). Further investigation has highlighted a role for *fgf3* and *notch* in the maintenance of rhombomere boundaries (Qiu et al., 2009; Riley et al., 2004; Weisinger et al., 2008). *Fgf3* is expressed in the posterior boundaries of rhombomeres 2-5 at HH20 of chick development (Weisinger et al., 2008) which would overlap with *Rarγ2* expression indicating that these genes may function as part of a boundary maintenance pathway. Earlier in hindbrain development, *Fgf3* is documented to be restricted rhombomeres 4 and 5 (Mahmood et al., 1995) and ectopic expression can induce otic placode formation (Powles et al., 2004), its expression is then reorganised by a signal from the boundary cells (Sela-Donenfeld et al., 2009). Conversely, *Fgf3* knockout mice exhibit no rhombomere abnormalities indicating that it is functionally redundant, possibly with *Fgf19* (Weisinger et al., 2008). *Follistatin* expression has been shown to be necessary for the expression of *Fgf3* in the boundaries at earlier stages in development and their correct patterning.

The presence of these expression domains and boundaries at HH20 (Weisinger et al., 2008) and their overlap with *Rarγ2* in rhombomeres 2-5, suggest that they may form a pathway segregating rhombomeres and boundary cells. *Notch1a* and *notch3* have been shown to be

necessary for boundary maintenance and correct neural development in Zebrafish (Qiu et al., 2009) as have *Wnt: notch* signalling (Riley et al., 2004) indicating that RARγ2 may also function to regulate these. However, only cranial nerve IV is aberrant in *Rarα/γ* knockout mice (Dickman et al., 1997) indicating that it may be functionally redundant with another receptor and the action of RARγ in the hindbrain requires further investigation.

It can be seen from this study that the expression of *Rarβ1, Rarβ2* and *Rarγ2* in the intact chick embryo has been described for the first time as well as novel expression domains for these receptors (summarised in tables 4.1 and 4.2). These expression patterns raise many new avenues of research: *Rarβ2* in Hirschsprung's Disease, role of *Rarβ1* in the ectoderm and the role of *Rarγ2* during chick embryonic development. *Rarγ2* may be implicated in correct facial, somitic and neural development. Despite the implications of this work, it must be noted that the expression of *Rarα1* and *Rarα2* in chick embryonic development is still uncharacterised. The expression patterns reported here require validation by sectioning and it would also be of interest to investigate their expression patterns at earlier and later stages of development.

Expression of *Fabp5*/*Pparβ* reveals implications for ATRA signalling in neural, limb and somite development.

As previously described, recent research has indicated that the contradictory effects seen with ATRA in different cancer cell lines may be due to activation of the receptor PPARβδ via FABP5 (Schug et al., 2007). FABP5 is an intracellular binding protein which is thought to channel ATRA to this receptor (Shaw et al., 2003; Tan et al., 2002). This could reconcile the different spatiotemporal responses to ATRA during development. More specifically, it has been proposed that the ratio of CRABP2:FABP5 in responding cells is crucial to determine whether ATRA will cause cells to proliferate, differentiate or undergo apoptosis. Manipulation of these levels in responding cells has supported this conclusion (Schug et al., 2007; Schug et al., 2008). Considering the implications this could have for ATRA signalling in the developing embryo, the expression of *Fabp5* and *Pparβ* at HH20 have been described here.

Although the effect of PPARβδ/FABP5 signalling has not been tested on limb development, it has been suggested that PPARβδ is involved in many processes including

embryo implantation and neural development during mouse development (Hihi et al., 2002). *Fabp5* is known be expressed during skin development (Collins and Watt, 2008) but has not been studied in embryonic development in depth. As described in the results section of this chapter, it appears that *Pparβ* is expressed ubiquitously at HH20 but with decreased levels in the rhombic lips, roof plate and midbrain. However, it is expressed at higher levels in the developing limb buds, branchial arches, periocular mesenchyme and telencephalic vesicles indicating the possibility that it is involved in many aspects of development (figures 4.14, 4.16, tables 4.1 and 4.2). *Fabp5*, however, is expressed in a far more restricted pattern (figures 4.14, 4.15, tables 4.1 and 4.2) and therefore must determine the response of PPARβ to ATRA in the developing embryo and will be the focus of this discussion. As previously mentioned, PPARβ may therefore function as an unliganded repressor in areas where *Fabp5* is not expressed during embryonic development (Shi et al., 2002; Tachibana et al., 2005), or another ligand and binding protein exits but is as yet undiscovered. Interestingly, FABP5 appears to be involved in the control of differentiation and proliferation in the chick embryo.

FABP5 and development of the Cranial Ganglia.

Fabp5 is seen to be expressed in cranial ganglia V, VII, IX, X and XI (figure 4.15G and 4.15H). These ganglia arise from placode derived cells or neural crest and dependent on their origin, the location of *Fabp5* expression is different. Unlike the other ganglia, the trigeminal and facial ganglia consists of neural crest derived BCCs in the proximal region as well as cells of placodal origin in the distal portion (Niederlander and Lumsden, 1996; Wilkinson et al., 1989). Interestingly, *Fabp5* is seen to be expressed in the neural crest derived BCCs which have been documented at the entry and exit points of spinal ganglia (Hjerling-Leffler et al., 2005; Maro et al., 2004). BCCs proliferate and maintain an undifferentiated state (Altman and Bayer, 1984; Aquino et al., 2006; d'Amico-Martel and Noden, 1980; Kim et al., 2003; Zujovic et al., 2011) before they differentiate into all associated glia and some peptidergic nociceptive or thermoreceptive neurons later in development (Coulpier et al., 2009; Hjerling-Leffler et al., 2005; Marmigere and Ernfors, 2007; Maro et al., 2004). As they are actively proliferating at HH20, *Fabp5* expression in these cells is consistent with a role for ATRA in maintaining proliferation as proposed by Schug et al (Schug et al., 2007). If BCCs are ablated there are no effects on nerve patterning but their somata migrate out of the CNS (Vermeren et al., 2003). This border

control is thought to be due to interactions between semaforin and plexin proteins (Bron et al., 2007; Golding and Cohen, 1997). When neural crest is removed earlier in development, the cranial nerve develops closer to the midline indicating an early role in positioning of the ganglion ((Shigetani et al., 2008) and refs therein). Therefore, BCCs are of paramount importance in defining the position and trajectory of developing neurons. Furthermore, FABP5 may be implicated in BCC maintenance and hence correct development of the nervous system at HH20.

The first gene shown to be expressed in BCCs was *Krox20* (Voiculescu et al., 2001; Wilkinson et al., 1989) but recent microarray and expression analyses have indicated that *cadherin 7* (Bravo-Ambrosio and Kaprielian, 2011; Maro et al., 2004), *Dapper2* (Alvares et al., 2009), *sox10* (Aquino et al., 2006), *Lingo1* (Okafuji and Tanaka, 2005), erythropoietin receptor (Bravo-Ambrosio and Kaprielian, 2011) *L20* and *Wnt inhibitory factor-1* (*Wif1*) (Coulpier et al., 2009) are also markers of BCCs. *Krox20* is involved in maintaining the identity of the motor column (Coulpier et al., 2009; Vermeren et al., 2003) indicating a role for FABP5 in motor-neuron development whether as a border control in the BCCs or in regulating their differentiation (see later discussion of expression in the hindbrain). Manipulation of *krox20* generates shorter, de-fasciculated neurons (Maro et al., 2004) and can also cause fusion of cranial nerves V and VII (Schneider-Maunoury et al., 1993) indicating a role for BCCs in correct path-finding. Interestingly, excess ATRA decreases *Krox20* expression in the hindbrain at early stages (Conlon and Rossant, 1992; Morriss-Kay et al., 1991) while *Raldh2* knockout mice demonstrate altered *krox20* expression in the rhombomeres at earlier time points (Niederreither et al., 2000). Excess or deficiency of ATRA has been shown to decrease the nerves present in the trigeminal ganglion and cause deranged projections (Gale et al., 1996; Lee et al., 1995; Reijntjes et al., 2007). Altogether, this implies that incorrect levels of ATRA may inhibit proliferation in the BCCs via *Krox20* and the FABP5/PPAR pathway and inhibit differentiation via the CRABP2/RAR pathway. This is supported by the fact that *Crabp2* has been shown to be expressed in the entire V^{th} cranial nerve (Ruberte et al., 1991) indicating that the ratio of CRABP2:FABP5 and hence differential activation of the PPARβδ/RAR pathways would be pertinent to development of the BCCs.

The nodose, geniculate, vagal and spinal accessory ganglia (IX, X and XI) are also seen to express *Fabp5*. However, these cranial ganglia are purely placodal in origin (Watari-

Goshima and Chisaka, 2011). Interestingly, it has been documented that *Crabp2* is also expressed in cranial nerves VII, IX and X (Ruberte et al., 1991) indicating that the level of FABP5:CRABP2 in retinoid responsive cells is likely to be important for the development of these cranial nerves. Spots of *Fabp5* expression are also seen in the mandibular-2nd branchial cleft and the 2^{nd}-3^{rd} branchial cleft corresponding to the exit points for cranial nerves VII and IX (figure 4.15G and 4.15H). The widespread expression of *Fabp5* in these cranial nerves indicates that it is involved the control of neuron development, trajectory and survival rather than solely the control of neuron trajectory as in the BCCs of cranial nerves V and VII. The areas of higher *Fabp5* expression may indicate an important role in proliferation in these cranial nerves.

ATRA and the cranial nerves:

Interestingly, ATRA levels have been shown to affect the development of all cranial nerves (Dickman et al., 1997; Reijntjes et al., 2007). VAD rats have defective cranial nerve development: hypoplastic nerve V, apoptotic cranial nerves VII and VIII and absence of cranial nerve X (Dickman et al., 1997). This suggests that ATRA is necessary to maintain proliferation and neuronal development in the cranial nerves which would be consistent with activation of both FABP5/PPARβδ and CRABP2/RAR pathways. The VAD rat exhibits many phenotypes also seen in RAR mutants, the most similar of which is the *Rarα/γ* double knock out mouse, exhibits a hypoplastic or absent cranial nerve IV (Dickman et al., 1997). The fact that the nuclei affected in VAD and RAR mutant mice are different and that these correlate with *Fabp5* expression indicates a role for FABP5 in development and possibly proliferation of these nerves. The retinoid effects seen in developing mice are accepted to be due to RAR:RXRα heterodimers considering that the *Rxrα* knockout mouse recapitulates many of the phenotypes seen in the *Rar* knockouts and are resistant to ATRA induced malformations (Kastner et al., 1997; Sucov et al., 1995). It may be interesting to investigate the expression of *Fabp5* and *Pparβ* at earlier time points as it has been documented that *Rxrγ* is expressed in cranial nerves V, VII, IX and X at earlier time points (Rowe and Brickell, 1995) and could be a binding partner for PPARβ.

Similar to VAD rats, knockout of genes involved in retinoid metabolism generates defects of murine cranial nerve development (Maclean et al., 2009; Niederreither et al., 2003; Reijntjes et al., 2007; Sandell et al., 2007). *Raldh2* null mice exhibit aberrant connections

of cranial nerves XI and X with the hindbrain or, in more severe cases, these nerves have fused (Niederreither et al., 2003) while *Rdh10* nulls affect cranial nerves V, VII, VIII, IX and X and they note an absence of the proximal ganglia in particular (Sandell et al., 2007). Morpholino directed manipulation of *Cyp26b1* in zebrafish decreased neuron production in cranial nerves V, VII and X and well as retarding their projections into the branchial arches. As reported previously, the manipulation of ATRA levels affected the vagus nerve more than those more rostral to it (Reijntjes et al., 2007). Similar effects are seen on cranial nerves IX and X in the *Cyp26b1* knock out mouse (Maclean et al., 2009). Given that these effects mimic inhibition of retinoid synthesis with 4-diethylaminobenzaldehyde (DEAB) treatment more closely that excess ATRA levels (Reijntjes et al., 2007) this suggests that a minimum threshold of ATRA is necessary for cranial nerve development. Furthermore, lack of the murine ATRA induced gene *neuron navigator 2* (*nav2*) can cause deranged connections of the IXth cranial nerve or fusion of it with Xth cranial nerve (McNeill et al., 2010).

Altogether, this implies that path-finding and survival in cranial nerves V, VII, IX and X are defective in the absence of ATRA. As these phenotypes and their worsening severity correlate with relative levels of *Fabp5* expression in these cranial nerves, the FABP5/PPARβ pathway may be important for proliferation (survival) and path-finding in the development of cranial nerves V, VII, IX, X and XI in chick. Interestingly, the vagus nerve (X) has been documented as more severely affected by altered ATRA levels (Reijntjes et al., 2007) and agenesis of this nerve can generate a Hirschsprung's like phenotype in mouse due to vagal crest deficiency and subsequent agenesis (Niederreither et al., 2003). FABP5 may provide part of the mechanism behind agenesis of this nerve in low levels of ATRA and may be an interesting avenue of research for the development of Hirschsprung's Disease.

FABP5/PPARβ and the development of the CNS.

As well as its restricted expression in the cranial ganglia, *Fabp5* also exhibits restricted expression domains in the developing brain: *Fabp5* is seen to be expressed in two stripes adjacent to the floor plate of the hindbrain and also to the roof plate of the hindbrain, midbrain and forebrain (figure 4.15A-D and table 4.2). Each region of the brain will be addressed in turn.

Hindbrain:

The expression of *Fabp5* in the hindbrain is in two similar regions: two stripes (adjacent to the floor plate; figure 4.15A) and both rhombic lips (adjacent to the roof plate; Figure 4.15H). Its expression pattern is compared to that of genes involved in hindbrain patterning and retinoid signalling discussed in the following section in the schematic shown in figure 4.17. The expression of *Fabp5* in the cranial nerves and later the limb indicate that FABP5 may be involved in a proliferative response to ATRA. However, the expression domains that are seen in the hindbrain could indicate a role in delineating boundaries. The dorsal rhombic lips are known to be the boundary between neural and non-neural tissue (roof plate) during embryonic development (Wilson et al., 2007). The floor plate of HH17 chicks has been shown to produce ATRA and exhibit polarising activity when transplanted to the anterior chick wing (Wagner et al., 1990). Considering these it could be proposed that FABP5 provides a barrier between differentiating and non-differentiating regions for cellular protection and proliferation at important developmental boundaries. However, at HH20 no enzymes involved in retinoid synthesis are expressed in the floor plate (Wilson et al., 2007) and figure 4.17) indicating that it does not produce ATRA at this time. It has been observed that *Cyp1b1*, another enzyme involved in retinoid synthesis, may be expressed in the notochord at earlier stages to provide ATRA to the floor plate (Chambers et al., 2007).

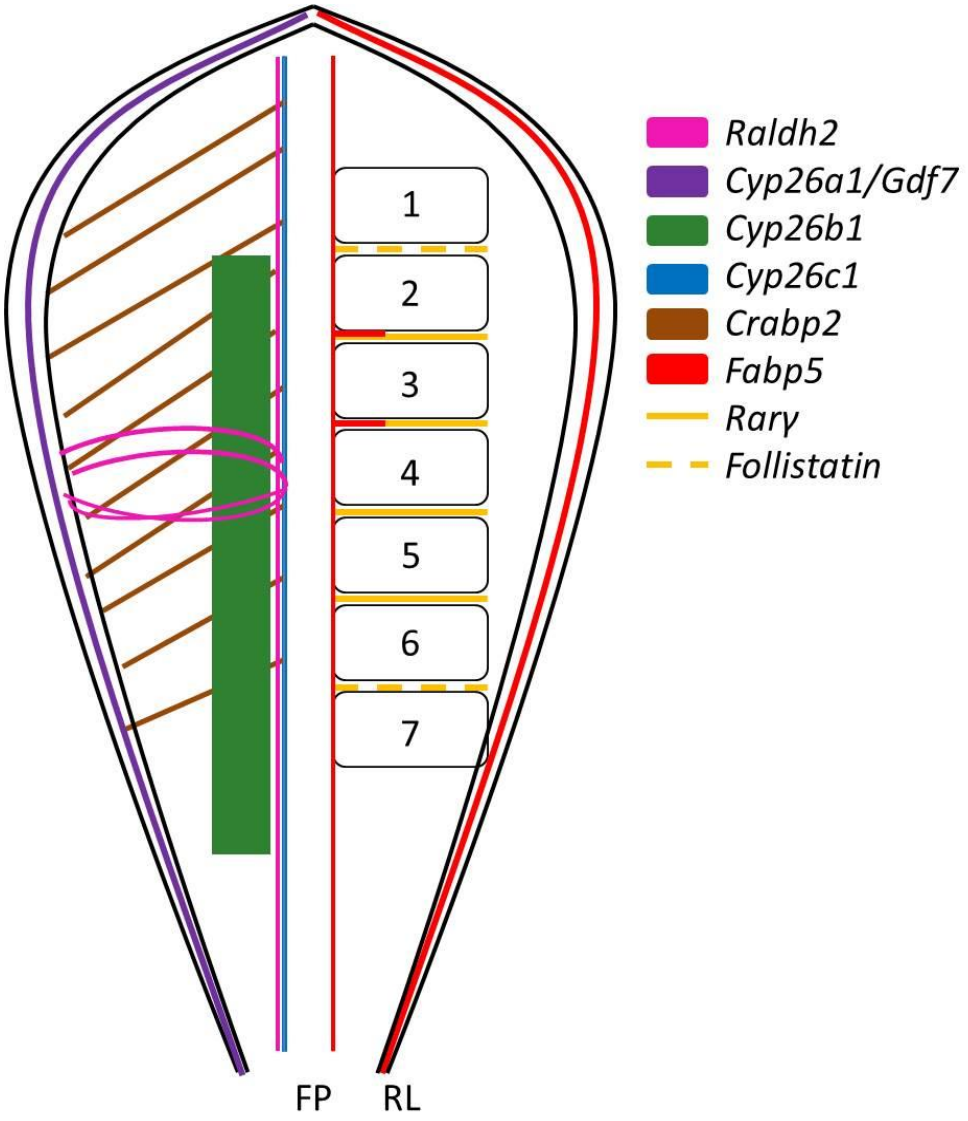

Figure 4.17: A schematic to show the expression of *Fabp5* and *Rarγ2* in the hindbrain compared to genes involved in retinoid metabolism and development of the hindbrain between E3.5-4.5.

Abbreviations: FP, floor plate; RL, rhombic lips. (Berggren et al., 1999; Reijntjes et al., 2005; Weisinger et al., 2008; Wilson et al., 2007). Curved lines of RALDH2 at rhombomere 4 are a representation of RALDH2 protein in rhombomeres 4 and 5 to the developing facial nerve.

Interestingly, *Fabp5* expression is complementary to that of *Crabp1* indicating that ATRA may be activating different pathways in these regions (Means and Gudas, 1997; Ruberte et al., 1991; Wilson et al., 2007). *Cyp26a1* is reported to be expressed in the rhombic lips while *Cyp26b1* and *Cyp26c1* are expressed in stripes adjacent to the floor plate (Wilson et al., 2007). Together, this indicates that there are low, carefully controlled levels of ATRA in *Fabp5* expressing regions of the hindbrain. Interestingly, RALDH2 is observed in a similar location to *Fabp5* at HH18. RALDH2 levels correlate with motor neurons in two stripes surrounding the floor plate at the level of the VII/VIIIth cranial nerve (Berggren et al., 1999). Lower levels of RALDH2 can also be seen in projections to the ganglion which appear to follow rhombomere boundaries in a similar, but more extensive manner than *Fabp5* (curved lines of RALDH2 in figure 4.17). This suggests that these regions may be RALDH2 positive neural projections and that ATRA and *Fabp5* may be involved in path-finding but this would need further investigation at HH20. It is also noted that *Raldh2* is expressed in the roof plate, adjacent to the *Fabp5* positive domain (Berggren et al., 1999; Wilson et al., 2007) which, when considered with the expression of the *Cyp26a1* in this region, may suggest a low level, paracrine ATRA signal is important for the development of nerves in this region.

Other genes are expressed in a similar pattern to *Fabp5* in the hindbrain: *Islet1* (Caton et al., 2000; Chambers et al., 2007), *Sulfatase 1* (*Sulf1*; (Garcia-Lopez et al., 2009)), *Paired-like homeobox 2b* (*Phox2b*) (Pattyn et al., 1997), *Wnt3a* (Narita et al., 2007), *ring finger protein 146* (RNF146; (GEISHA, March 2013), *signal sequence trap clone 273* (*SST273*; (Gejima et al., 2006)) *plexina1* and *plexina3* (Schwarz et al., 2008). It has been proposed that both *Islet1* and *SST273* are expressed in motor neurons (Chambers et al., 2007; GEISHA, March 2013; Gejima et al., 2006; Schwarz et al., 2008). This indicates that *Fabp5* may also be expressed in regions of differentiating motor neurons at the hindbrain floor plate. Spinal motor neurons are known to extend their axons away from the floor plate (Niederlander and Lumsden, 1996) as, in a similar fashion to BCCs; the floor plate repels motor neurons to ensure correct extension (Barnes et al., 2010; Chang et al., 1992). Consistent with the idea that *Fabp5* marks developing motor neurons, inactivation of *Phoxb2* causes atrophy of the cranial sensory ganglia, agenesis of the parasympathetic nervous system and impaired motor neuron development (Pattyn et al., 1997; Samad et al., 2004). It could be proposed that these phenotypes may also result from inactivation of *Fabp5*, a potential focus for future work. Interestingly, *RNF146* and *SST273* are seen to be

expressed in two stripes over the midbrain and forebrain (GEISHA, March 2013; Gejima et al., 2006) indicating that these genes may be part of a common pathway with FABP5/PPARβ and may be retinoid responsive. *Fabp5* may also overlap with *plexina1* and *plexina3* given their expression in murine hindbrains at E10.5 (Schwarz et al., 2008). Plexins are known to be involved in axon guidance pathways with semaforins and neuropilin. Of the genes overlapping with *Fabp5*, only *plexina3* was shown to be important for the development of motor neurons in cranial nerve VII (Schwarz et al., 2008). The expression of *Fabp5* is consistent with a role for FABP5: PPARβ and ATRA in the differentiation of motor neurons and their correct path-finding.

As mentioned previously, *Fabp5* is also expressed in the dorsal rhombic lips (figure 4.15A). This expression domain is also seen flanking the roof plate in other areas of the embryo: at the most rostral sections of the dorsal telencephalon and diencephalon, midbrain and flanking the midline of the spinal neural tube (figure 4.15A-C and 4.14E). The developing ventricles are found between the developing telencephalic vesicles, dorsal diencephalon and hindbrain and are specialised regions of the roof plate important in providing nutrients to the developing embryonic brain (Broom et al., 2012). The fact that *Fabp5* is expressed adjacent to the most rostral parts of the forebrain ventricles indicates a role specifically in the development of that section. The roof plate differentiates to form the choroid plexus in the hindbrain while the rhombic lips and adjacent neuroepithelium differentiate down the neuronal lineage. The hindbrain roof plate has been demonstrated to be a developmental compartment and a bi-directional organiser of neural and choroid plexus development. It has been demonstrated that this boundary directs development via the Delta-Notch pathway and is important for the production of dorsal *atonal homologue 1* positive neural crest derivatives in the adjacent rhombic lip. *cHairy2* and *Gdf7* are involved in the maintenance of the boundary at the dorsal rhombic lip (Broom et al., 2012). The expression of *Fabp5* in the dorsal rhombic lips supports the hypothesis that FABP5 is involved in boundary maintenance during embryonic development. The roof plate is also a region of proliferation and as such FABP5 may play a role in maintaining the proliferation boundary of this region (Broom et al., 2012). However, the fact that the roof plate itself has not been observed to express *Fabp5* at HH20 indicates that FABP5 may not play a role in proliferation of this structure. It has also been observed in this study that the roof plate expresses *Rarβ2* at HH20 (figure 4.12B). This implies that retinoid signalling may be

occurring in this region and that the interplay between the RARβ2 and PPARβ pathways may be crucial for correct development of the hindbrain at this developmental stage.

Interestingly, as well as marking the developing ventricles, the expression domains in the forebrain also flank the developing pineal gland and end of the developing forebrain (ANR). The ANR between the developing telencephalic vesicles expresses *Fgf8* at HH20 in a horseshoe shape (Crossley et al., 2001; Fuchs et al., 2010; Goodnough et al., 2007; Halilagic et al., 2007). This domain of *Fgf8* and *Fabp5* expression is complementary to *Bmp4* expression in the roof plate (Crossley et al., 2001). *Fgf8* at the ANR is expanded anteriorly and dorsally in the VAD quail at HH20 which was documented to affect forebrain splitting and frontonasal patterning (Halilagic et al., 2007). However, *Fgf8* expression was lost completely when embryos were treated with ATRA signalling antagonists at HH10 (Schneider et al., 2001). The expression of *Fabp5* in the ANR may indicate that this transduction pathway facilitates an antagonistic relationship in the forebrain as observed between ATRA and FGF8 in the development of neurons secreting gonadotrophin releasing hormone-1in this region (Sabado et al., 2012) and the limb (Mercader et al., 2000). However, *Fgf8* is also known to be expressed in the FEZ at HH20 (Hu et al., 2003) while *Fabp5* is never expressed in that region. Altogether, this indicates a specific role for FABP5/PPARβ in the correct development of the ANR, third ventricle and brain compartmentalisation.

The stripes seen in the midbrain and spinal cord regions are not connected to ventricular development. It could be proposed that the expression of *Fabp5* in these areas is again to delineate a boundary with the roof plate and are clearly worthy of further investigation. It can be seen that *Fabp5* is expressed in the developing motor column along the spinal cord which may overlap with: *Islet1* (GEISHA, March 2013), *SST273* (Gejima et al., 2006) and *CRABP2* (Maden et al., 1989). This suggests that FABP5: PPAR and CRABP2/RAR signalling are involved in the development of spinal cord motor neurons. Further characterisation of the ratio of these proteins in the developing neurons may generate a responding signature in each subtype. Further investigation in the sectioning of *Fabp5* hybridised embryos would be necessary to determine their location at the spinal cord floor plate. Altogether it can be concluded that FABP5/PPARβ signalling may be involved in the correct development of motor neurons, sensory neurons, boundary maintenance and correct brain development at HH20 of chick embryonic development.

Fabp5 is also seen to be expressed in the entire intersomitic cleft but this expression domain becomes progressively ventralised caudal to the wing bud (figure 4.15E). The intersomitic cleft delineates a boundary between developing somites, the lack of which causes severe effects (Evrard et al., 1998). Considering the work by Schug et al (2007) FABP5 could be maintaining cells at the intersomitic cleft by causing a proliferative, non-differentiating response to ATRA during development. However, this would require further investigation as would the ventralisation of *Fabp5* expression caudal to the wing bud. Little work has been carried out on the maintenance of the intersomitic boundary during embryonic development. Most research has concentrated on genes involved in the formation of the intersomitic boundary and patterning during somitogenesis e.g. *ephrinB2* (Watanabe et al., 2009), *lunatic fringe* (*lfng*) (Evrard et al., 1998), *Integrin α5* (Chong and Jiang, 2005), *misty somites* (*Mys*), *notch1*, *deltaD* and *Tbx24* (Kotani and Kawakami, 2008). Early research suggests that the cells of the intersomitic boundary express *tenascin* and may differentiate into tendons (meeting abstract-(Adds et al., 2009)) which could implicate FABP5/PPARβ signalling in tendon development. *Lfng* has been shown to be involved in intersomitic cleft formation and correct somite patterning. It is expressed during somitogenesis (Evrard et al., 1998) and then at HH20 in the intersomitic clefts and dorsal boundary (GEISHA, March 2013). *Mys* has been investigated in zebrafish using morpholinos to lower expression. This reduced the epithelialisation of somites and the intersomitic boundary was not maintained (Kotani and Kawakami, 2008). The expression pattern of *Mys* has not been characterised in chick or at later stages but it would be interesting to determine its location relative to *Fabp5* and whether manipulation of *Fabp5* in zebrafish generates a similar phenotype. As *Lfng* and *tenascin* expression overlaps with *Fabp5* expression it could be proposed that FABP5 is part of a signalling cascade with these genes to control somite patterning and tendon development.

FABP5/PPARβ and CRABP2/RAR as modulators of proliferation and differentiation in the developing chick limb.

The expression of *Fabp5* in the chick wing and hindlimb at HH20 does not correspond to the expression of any one gene during limb development. This region of the developing wing overlaps with the PZ, a region of undifferentiated and proliferating cells in the mesenchyme which are crucial for limb outgrowth and patterning (Summerbell, 1974).

Control of PD outgrowth and patterning is thought to be via the antagonistic relationship between FGF8 and ATRA signalling from the distal and proximal wing bud respectively (Mercader et al., 2000; Mic et al., 2004). Recent research has suggested that endogenous ATRA from *Raldh2* or *Rdh10* is not involved in PD patterning of the murine forelimb as *Meis1/2* expression is unaffected in these mutants (Cunningham et al., 2013). However, excess ATRA is known to induce markers of proximal regions such as *Meis2* (Mercader et al., 2000; Yashiro et al., 2004) while the ATRA negative distal region remains proliferative and undifferentiated due to FGF8 secreted from the AER (Niswander et al., 1994). The distal region is preserved in a low ATRA state due to the action of CYP26B1 in the distal mesenchyme and CYP26A1 in the AER (Reijntjes et al., 2005; Yashiro et al., 2004). The *Fabp5* expressing cells in the wing appear to correspond to the posterior part of the distal zone expressing *Cyp26b1* and the PZ. Considering the high levels of proliferation and ATRA reported in this region (Summerbell et al., 1973; Thaller and Eichele, 1987), it could be proposed that FABP5: PPARβ retinoid transduction may maintain proliferation in this region.

High FABP5:CRABP2 ratio has been shown to induce proliferation in retinoid treated cancer cell lines (Schug et al., 2007; Schug et al., 2008). Studies have also shown that *CRABP2* is found in an anterior to posterior gradient with *CRABP2* levels highest in the anterior wing bud (Maden et al., 1989; Ruberte et al., 1991). Conversely, this is the opposite to the gradient of ATRA levels reported previously (Thaller and Eichele, 1987). Interestingly the levels of CRABP2 and FABP5 in the developing wing would therefore generate a gradient of high CRABP2:FABP5 to high FABP5:CRABP2 from anterior to posterior. This would suggest that excess levels of ATRA present in the wing bud could result in a proliferative response in the *Fabp5* expressing region while it would induce apoptosis or differentiation in the regions of high CRABP2:FABP5 ratio. This is consistent with observations made by Galdones et al (2008): excess retinoid application increases RARE driven *β-galactosidase* staining in the proximal limb and the necrotic areas (Galdones and Hales, 2008), all of which are *Fabp5* negative in chick. Therefore, tightly controlled levels of ATRA are needed for the correct balance between proliferation and differentiation during wing development. This hypothesis also provides an elegant mechanism behind the differential effect of ATRA in the anterior vs. posterior limb (Martinez-Ceballos and Burdsal, 2001) as well as the inability of ATRA to alter limb development when placed in the posterior regions (Tickle et al., 1985). Further work to

validate this theory would be to investigate the expression of *Fabp5* after treatment with ATRA and whether manipulation of the levels of CRABP2:FABP5 can recapitulate digit duplication or other phenotypes associated with ATRA excess.

FABP5/PPARβ may also be implicated in PD limb patterning. *Rarγ* and *Cyp26b1* have been shown to have overlapping expression domains in distal limbs and therefore may be involved in retinoid teratogenesis. The abnormal ATRA concentrations generated due to *Cyp26b1* knock out caused two separable effects in the developing limb: apoptosis and altered PD patterning as well as delayed chondrogenesis. *Cyp26b1*/*Rarγ* double knockout mice exhibit partially rescued limbs (Pennimpede et al., 2010b). This implies that the teratogenic effects of ATRA occur via RARγ. However, the phenotypes of these knockout mice do not conform to this hypothesis as in *Cyp26b1*/*Rarγ* double knockout mice the zeugopod is still malformed implying that another receptor is involved in teratogenesis. It could be proposed that RARβ2 causes the aberrant PD patterning due to its distribution, induction by ATRA and downstream effects of inducing *Meis2* ((Mercader et al., 2000; Smith et al., 1995) and figure 4.9).

However, it could also be due to either RARα or FABP5/PPARβδ. Considering that *Rarα* has been documented to be ubiquitously expressed in the developing forelimb (Dolle, 2009) and no studies have so far investigated *Rarα* expression in chick limb, it is unlikely to be the mechanism behind the alteration in the PD axis. The cells of the *Fabp5* expression domain in the distal wing partially overlap with the *Cyp26b1* expression domain (Pennimpede et al., 2010b; Reijntjes et al., 2003) and these cells would give rise to the ulna, elbow and associated tissue (Sato et al., 2007; Vargesson et al., 1997) which further supports the hypothesis that FABP5/PPARβ retinoid transduction may be involved in PD patterning. CRABP2 levels have been documented to be elevated at the distal limb tip adjacent to the AER (Maden et al., 1988) which would overlap with a small portion of the *Fabp5* expressing domain. This could result in high CRABP: FABP5 in the distal wing tip and high FABP5:CRABP2 in the area which will give rise to the zeugopod. It has been shown that ATRA induces *Crabp2* expression in mouse and human (Astrom et al., 1994) which would alter the FABP5:CRABP2 ratio causing abnormal patterning in the *Cyp26b1*/*Rarγ* knockout mouse.

The proposals suggested here for FABP5/PPARβ mediated retinoid transduction during limb development also suggest a role for FABP5 in digit duplication and other limb phenotypes generated with ATRA excess (see chapter 6). The differential expression of *Fabp5* in the limb and facial processes could provide a mechanism for the differences between the EC19 and EC23 as mentioned previously. Different affinities for CRABP2 and FABP5 may also explain the differences in digit duplications seen with EC23 and ATRA if ATRA and EC23 exhibit different affinities for FABP5 and CRABP2. This would be consistent with previous research that retinoids do not need to bind CRABP2 with high affinity to generate digit duplications (Maden et al., 1991) although it increases their potency if they do bind CRABP2 (Keeble and Maden, 1984). This would lead to alteration of target genes depending on the level of affinity. If these retinoids bound to PPARβ with high affinity, it would be expected that PPAR responsive genes would be altered after 24hrs in the limb bud. This does not appear to be the case (chapter 5) although consideration of recent microarray analysis of PPARβδ targets (Adhikary et al., 2011) would need further investigation. Alternatively, this response could occur over a shorter time period and that by 24hrs at this dosage of retinoid the transcriptional responses are similar between EC23 and ATRA. Further research could include investigation of FABP5 affinity of synthetic retinoids to corroborate this hypothesis.

Overall, it can be concluded that *Fabp5* and *Pparβ* exhibit interesting expression patterns at HH20 of chick embryonic development. *Pparβ* is expressed ubiquitously except the roof plate of the hindbrain and the midbrain. Therefore, *Fabp5* expression indicates areas of active PPARβ signalling. Interestingly, these appear to correlate with regions of low ATRA levels or which are sensitive to altered ATRA levels: the distal limb and rhombic lips or surrounding the floor plate. They also correlate with regions of proliferation, such as the wing bud progress zone and the trigeminal BCCs, consistent with *in vitro* analysis of the role of FABP5/PPARβδ mediated retinoid signalling (Schug et al., 2007). FABP5 may also be involved in boundary maintenance in the developing nervous system and somites as well as the correct development of motor neurons, sensory neurons and the brain. That FABP5 is worthy of further study is most evident from the implications it could have for the understanding of embryonic limb development, Hirschsprung's Disease and neural development.

Conclusions:

From the data presented here it can be concluded that EC23 is potentially resistant to metabolism while EC19 is not. It has recently been shown that ATRA can be metabolised to 16-*hydroxy*-RA by the CYP26 enzymes. All sites known to be substrates for CYP26 mediated metabolism are blocked in EC23 and EC19 bar the carbon equivalent to carbon 16 (red circle; figure 1.5; (Henderson, 2011; Topletz et al., 2012)). EC19 is metabolised to a lesser extent than ATRA, which is consistent with potential metabolism at the site equivalent to carbon 16 as the only site at which oxidation can occur and a differential binding of retinoids dependent on the terminal carboxylic acid. EC23 appears to be less metabolised than EC19 and may be due to a combination of only one site available for CYP26 action as well as the different position of the carboxylic acid group which may affect CYP26 binding. The decreased metabolism of EC23 can contribute to the potency and effects seen with EC23 as it will activate RARs over a longer period than ATRA in a similar manner to TTNPB (Pignatello et al., 1999, 2002). The metabolism of EC19 cannot be solely responsible for the great difference in phenotypes generated from EC19 treatment when compared to EC23 and ATRA as higher concentrations of EC19 do not generate the same phenotypes (Budge, 2010) indicating that its receptor specificity is important. Considering the location of the receptors investigated here: EC23 is likely to be a pan-agonist including FABP5, while EC19 is likely to be an agonist for RARβ1 and is unlikely to bind FABP5. The investigation into the receptor expression patterns has generated novel expression domains for *Rarβ1, Rarβ2* and *Rarγ2* as well as characterising the expression of *Pparβ* and *Fabp5* at HH20 of chick embryonic development.

Chapter 5) Investigation into the genetic targets of retinoids: a comparison of the naturally occurring ATRA and a novel synthetic retinoid EC23 which is photostable and potentially resistant to metabolism.

Introduction.

Given the large body of research into the effect of ATRA on development and also on limb development, some retinoid responsive genes have been elucidated. Many of these have been documented as a result of application with a bead soaked in ATRA and using whole mount *in situ* hybridisation: *Shh* (Riddle et al., 1993), *Hand2 (Fernandez-Teran et al., 2000)*, *Hoxb8* (Stratford et al., 1997), *Hoxd11-13* (Izpisua-Belmonte et al., 1991), *hoxc6* (Oliver et al., 1990), *Meis2* (Mercader et al., 2000) and *Emx2* (Prols et al., 2004). A review of this work and other studies in other species is summarised in a review by Balmer and Blomhoff (2002) and indicates that there is likely to be 532 retinoid genetic targets. These targets were proposed by the analysis of 1191 published articles and were graded according to their regulation and the evidence described (Balmer and Blomhoff, 2002).

These methods were useful in the study of retinoids and their action during development but complete determination of retinoid responsive genes and their mechanisms of action can only be achieved by expression profiling. Such analysis has been carried out previously using *in vitro* methods and investigating different cell types: neural crest (Williams et al., 2004), LPM (Waxman et al., 2008), limb (Ali-Khan and Hales, 2006) or chondrogenic micromass cultures (James et al., 2005). Expression profiling of retinoid genetic targets has also been investigated in whole rat embryos at somite stages 2-4 cultured in rat serum containing ATRA for 4hrs (Luijten et al., 2010).

Ali-Khan and Hales (2006) investigated retinoid targets after culturing dissected E12 limb buds with retinol acetate dissolved in ethanol at 2 different concentrations for 3hrs. This study used medium designed to promote bone growth without serum. This indicated that the early response was to up-regulate gene expression and particularly genes involved in teratogenesis. They identified four genes as master regulators of the teratogenic response: *Hes1*, *Eya2*, *Id3* and *Snai1* (Ali-Khan and Hales, 2006). However, cultured limbs develop differently to *in vivo* embryonic development due to the presence of serum, lack of blood supply and non-localised exposure to materials or signalling proteins. It has also been shown that the correct development of the heart may be dependent on signalling from the limb (Waxman et al., 2008) and the reverse could be true. As mentioned, Ali-Khan and Hales (2006) investigated the effects of retinol rather than ATRA which is the primary bioactive retinoid (Niederreither et al., 1999). This implies that the genetic targets found

by Ali-Khan and Hales (2006) are genes whose expression is modified in response to retinoids rather than solely to ATRA.

Many differentiation processes occur during limb development to form a functioning limb and which involve a change in gene expression. Transcription factors specific to developmental processes are altered. Each stage of chondrogenesis is marked by the expression of specific markers: *sox9* and *scleraxis* are expressed in early condensations (Lorda-Diez et al., 2011) and subsequent cartilage development is associated with the up-regulation of *collagen type II* and *collagen type IX* (Hall and Miyake, 2000). *Pax1* has been implicated as an early marker of scapula cartilage development (Huang et al., 2000) chapter 3). Many genes have been associated with joint formation: *Gdf5*, *Wnt14* and *autotaxin* (*enpp2*) ((Bachner et al., 1999; Francis-West et al., 1999; Loganathan et al., 2005; Storm and Kingsley, 1996); see chapter 3). Muscle and tendon development also occur in a regulated manner during limb development under the control of various transcription factors. *Myogenic differentiation 1* (*MyoD1*) is implicated in the control of myogenic differentiation as are: *Pax3*, *myogenic factor 5* (*Myf5*), *myogenin*, *Hoxa11* and *Hoxa13* (Kablar et al., 1997; Weintraub et al., 1991; Yamamoto et al., 1998). Interesting, *scleraxis* has been documented as a marker of cartilage condensations but is also a key marker of tendon development (Cserjesi et al., 1995; Schweitzer et al., 2001). *Tgfβ2*, *Fgf8* and *Fgf18* have been implicated as growth factors controlling tendon development (Edom-Vovard and Duprez, 2004; Pryce et al., 2009). Other proteins such as *tenomodulin* and *teneurin-2* are also involved (Lorda-Diez et al., 2009; Tucker et al., 2001b).

Chapter 3 described the phenotypes generated with ATRA and two synthetic photostable retinoids, EC23 and EC19, in detail which are summarised here. Despite the similarity in structure of EC23 and EC19, EC19 caused no effect on the limb when applied to the anterior wing bud. EC23 and ATRA both affected limb development but EC23 is two orders of magnitude more potent than ATRA. EC23 and ATRA both affect the entire PD axis of the wing causing: reductions to scapula blade development; alterations to cartilage element size of the humerus, radius and ulna; fusions at the elbow joint and digit duplications. EC23 and ATRA differ in the frequency of these effects with ATRA generating them more frequently. They also differ in that they generate different types of digit duplications: ATRA can generate the full mirror image duplication whereas EC23 tends to duplicate multiple extra digits of the most anterior identity. Chapter 4 indicated that ATRA and EC23 are also differentially metabolised in that EC23 is certainly more

resistant to metabolism by the CYP26 enzymes than ATRA if not, completely resistant. Recent work by Topletz et al (Topletz et al., 2012) suggests that if metabolism at any of the known sites is possible, it may still be metabolised at the carbon in the equivalent position to C16 in ATRA. The differences in digit duplications produced by ATRA and EC23 and their metabolism prompted further investigation by determining their genetic targets.

Considering the limitations of the previous literature, this chapter aims to investigate retinoid and ATRA genetic targets *in vivo* and will be the first *in vivo* analysis of ATRA targets, although this subject is also being addressed by Towers and Tickle (unpublished). Given the interesting phenotypes reported in chapter 3, this study investigates the changes in gene expression after treatment with EC23 and ATRA for 24hrs by application of a retinoid soaked bead. It has been documented that expression of *Hoxb8* (Stratford et al., 1997), *Hand2* (Fernandez-Teran et al., 2000) and *Shh* (Riddle et al., 1993) can be up-regulated in the anterior wing by 24hrs, which are key markers of digit duplication and therefore the mechanism of action of EC23 may be elucidated at this time-point. By 24hrs after retinoid treatment the treated wings have reached HH23 which coincides with early events of cartilage condensation and muscle development. It is hoped that this study will highlight *in vivo* retinoid and ATRA genetic targets, particularly with reference to the mechanisms behind phenotypes described and the differences in retinoids assayed. It will also allow an insight into the effects of ATRA metabolites in the chick wing bud using the synthetic retinoid EC23 which is potentially resistant to metabolism.

Methods:

The methods used to investigate the alteration of gene expression after retinoid treatments are mainly addressed in chapter 2. Briefly, ATRA, EC23 or DMSO was applied to the anterior wing bud at HH20 as described in chapter 2 and shown in figure 5.1. The chick embryos were then re-incubated for 24hrs at which point the anterior treated wing was dissected off for RNA isolation and subsequent microarray analysis of gene expression. 16 anterior wing buds were collected per treatment to provide sufficient RNA for analysis and to decrease variation in the datasets. Three replicates were collected per treatment. RNA was then isolated and its integrity was visualised by agarose gel electrophoresis before the RNA was sent away for microarray analysis and then again using the Agilent Bioanalyser before and during analysis (see chapter 2 for more details).

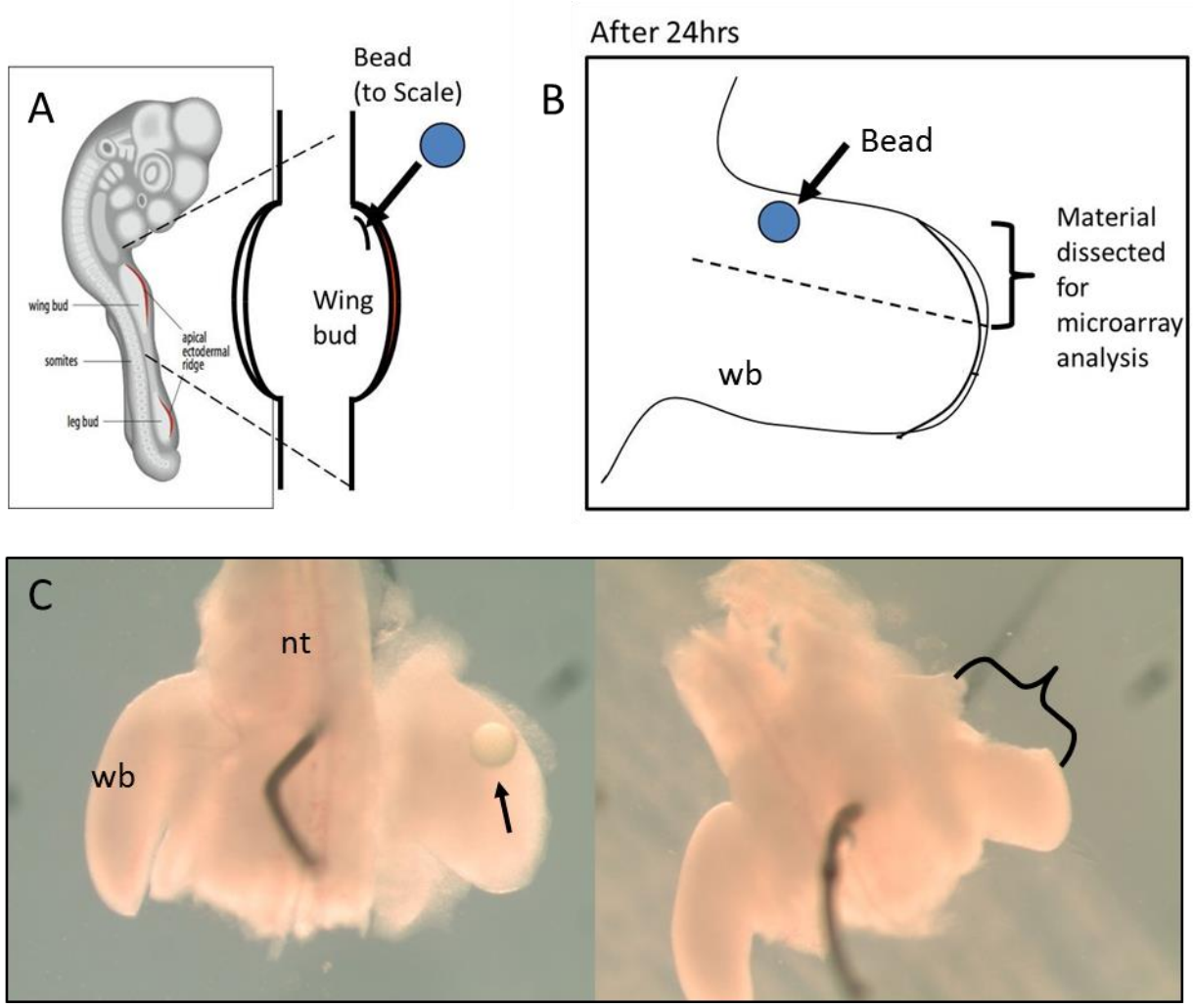

Figure 5.1: The Method for treatment and isolation of RNA for microarray analysis.
A) shows the method for *in ovo* microsurgery used in previous chapters to treat HH20 chick embryos with retinoid or DMSO. B) shows a diagram of a chick wing bud 24hrs after treatment. Dashed line indicates dissections made: anterior third was taken for microarray analysis. C) shows the dorsal view of an embryo after 24hrs treatment before and after dissection for microarray analysis. The wings were pinned to agar for dissection. The arrow in the left picture indicates the bead. This was removed before dissecting the anterior portion of the wing bud. The picture on the right shows the same wings after dissection: brackets indicate the material dissected off for microarray analysis. Abbreviations: nt, neural tube; wb, wing bud.

Figure 5.2A shows the gel containing the pools sent to Newcastle and figure 5.2B shows the gel containing the pools for Roslin. As can be seen the RNA pools are of good quality with little degradation and rRNA in the correct proportion. This analysis was corroborated by electropherograms produced at either Newcastle (figure 5.3) or Roslin (figure 5.4) from analysis on the Agilent Bioanalyser. These traces show no degradation of the rRNA species and that there are no smaller RNA products present. As a result electropherograms 5.4C and 5.4D were designated with a RNA integrity value (RIN) of 10. Considering this is the highest value and that all other electropherograms are of similar standard, this indicates that the RNA produced was of high quality and could reliably be used for microarray analysis (Schroeder et al., 2006).

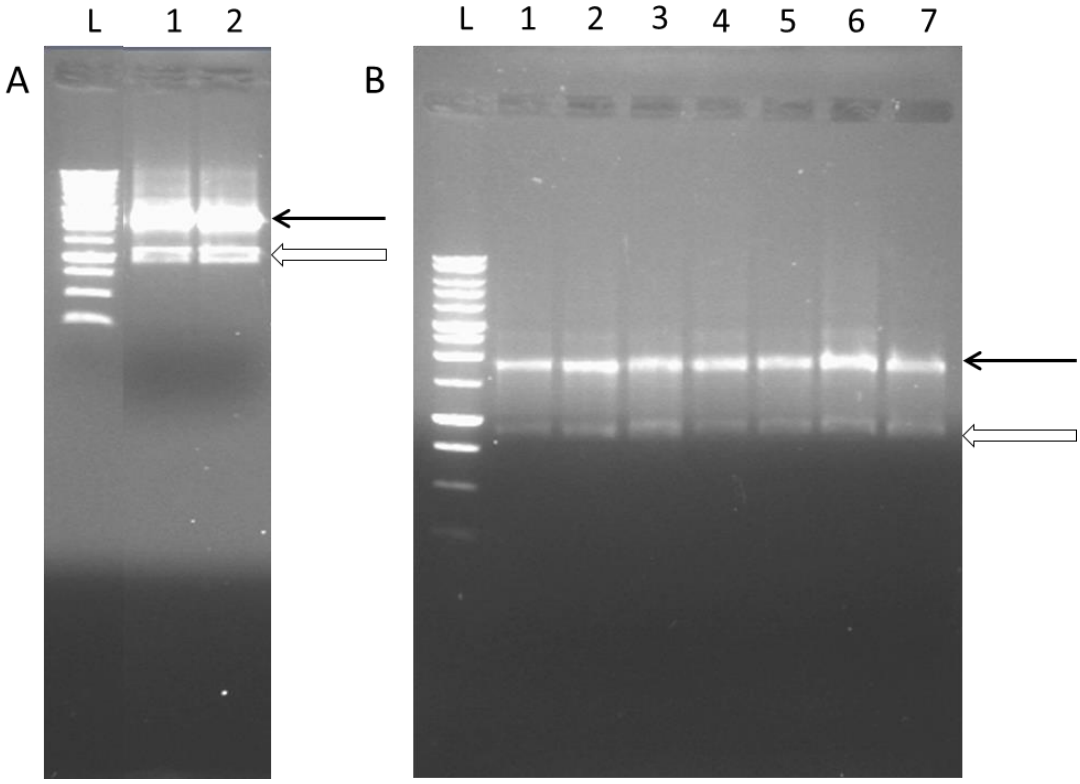

Figure 5.2: Analysing the integrity of isolated RNA by agarose gel electrophoresis.
A) shows the analysis of RNA sent to Centre for Life, Newcastle. Lanes: 1 RNA from anterior wing buds treated with DMSO (pool 1), 2 RNA from anterior wing buds treated with 0.01mg/ml EC23 (pool 1). B) shows the analysis of RNA sent to the Roslin Institute in Edinburgh for microarray analysis. Lanes: 1-3 are RNA samples from anterior wing buds treated with 1mg/ml ATRA (pools 1-3), lanes 4 and 5 are RNA samples from anterior wing buds treated with 0.01mg/ml EC23 (pools 2 and 3) and lanes 6 and 7 show RNA samples from anterior wing buds treated with DMSO (pools 2 and 3). 200ng was run per sample on a 1% agarose: TBE gel at 200V for 10mins. L is ladder. Black arrows indicate the position of 28S rRNA and white arrows indicate the position of 18S rRNA.

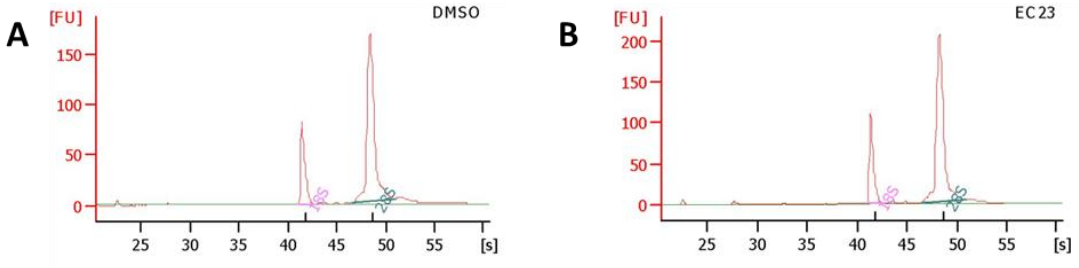

Figure 5.3: Analysis of RNA isolated for microarray analysis using the Agilent Bioanalyser at Centre for Life, Newcastle.

Electropherograms are of RNA isolated from DMSO (A) or EC23 (B) treated anterior wing buds used for microarray analysis.

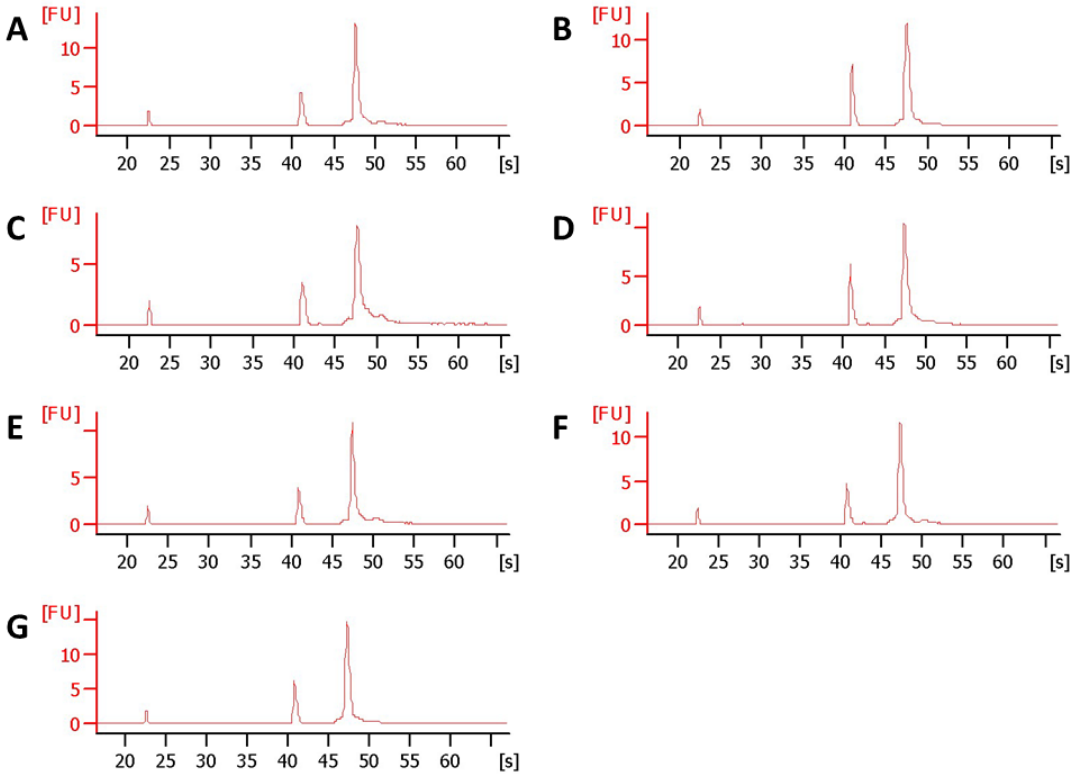

Figure 5.4: Analysis of RNA isolated for microarray analysis using the Agilent Bioanalyser at The Roslin Institute, Edinburgh.

A and B) are RNA from DMSO treated anterior wings, pools 2 and 3. C and D) are electropherograms of RNA from anterior wings treated with 0.01mg/ml EC23, pools 2 and 3. E-G) are electropherograms of RNA from anterior wings treated with 1mg/ml ATRA, pools 1-3. C and D) were designated RIN values of 10.

Analysis of Gene Expression:

Images of the stained chips were imported into GeneSpring GX11.5 (Agilent Technologies, Inc.) for analysis. The data was normalised using GeneChip-Robust Multiarray Averaging (GC-RMA) normalisation algorithm. This normalisation is optimal as it considers the ratio of signal hybridised to perfect match vs. mismatch probe sets and therefore generates more accurate data and is robust to outliers. The data was plotted as box and whisker plots as an indication of variation between arrays. As can be seen from figure 5.5 the two microarrays hybridised at Newcastle University were different and there was significant variation between those carried out at Newcastle and those carried out in Edinburgh for the same treatments. This may have been due to the use of a different amount of RNA as starting material, operator or batch of arrays which have been documented as sources of variation in microarray analysis (Chen et al., 2011a; Johnson et al., 2007; Walker et al., 2008).

In order to include the microarray data generated in Newcastle, batch correction was necessary. This was carried out using empirical Bayes statistical tests in the R programme (Johnson et al., 2007). The corrected values were then re-imported into GeneSpring GX11.5 for further analysis. As can be seen from figure 5.6, this resulted in data with comparable means and standard deviations which allowed further analysis. The data was then filtered so that only genes which were expressed above the lowest 20% of values in at least one condition (and all three replicates) were used for analysis. This filter removed around 8000 transcripts. These genes were then clustered using both hierarchical clustering and K-means clustering to investigate treatment similarity (figure 5.7). Genes were then filtered using >2 fold change with respect to DMSO ($p < 0.05$) as a threshold for biological significance. Statistical significance of these changes was calculated using a T-Test with p-values corrected for multiple tests.

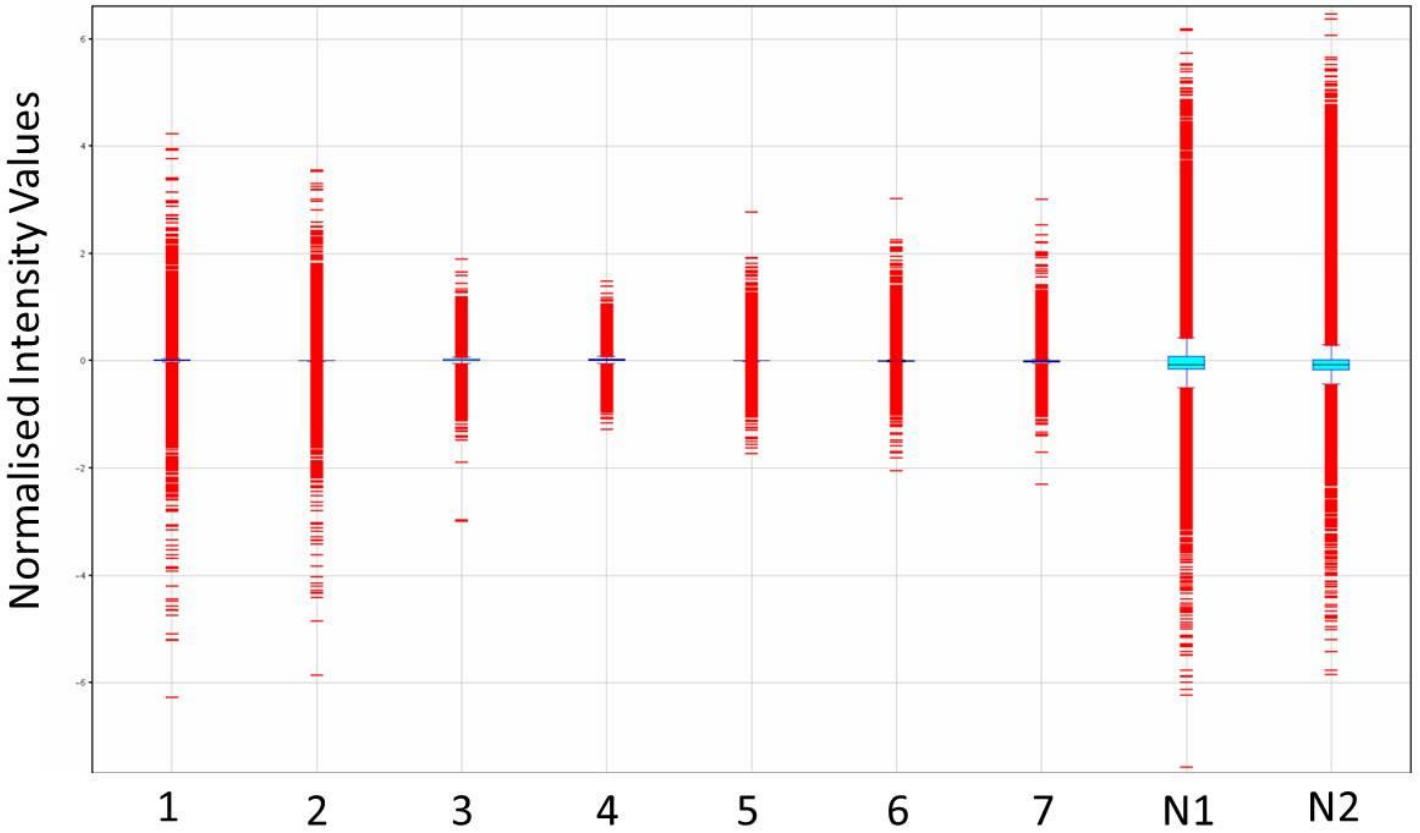

Figure 5.5: Box and whisker plots of normalised intensity values for all data generated by microarray analysis.

.CEL files were imported into GeneSpring 11.5 for analysis. Data was normalised and control probes were removed before box and whisker plot analysis. 1 and 2) show data from chips hybridised with RNA from anterior wing buds treated with DMSO carried out at the Roslin Institute. 3 and 4) show data from chips hybridised with RNA from anterior wing buds treated with 0.01mg/ml EC23 carried out at the Roslin Institute. 5-7) show data from chips hybridised with RNA from anterior wing buds treated with 1mg/ml ATRA, carried out at the Roslin Institute. N1 and N2) show data from chips hybridised with RNA from anterior wing buds treated with DMSO and 0.01mg/ml EC23 respectively but carried out at Centre for Life, Newcastle.

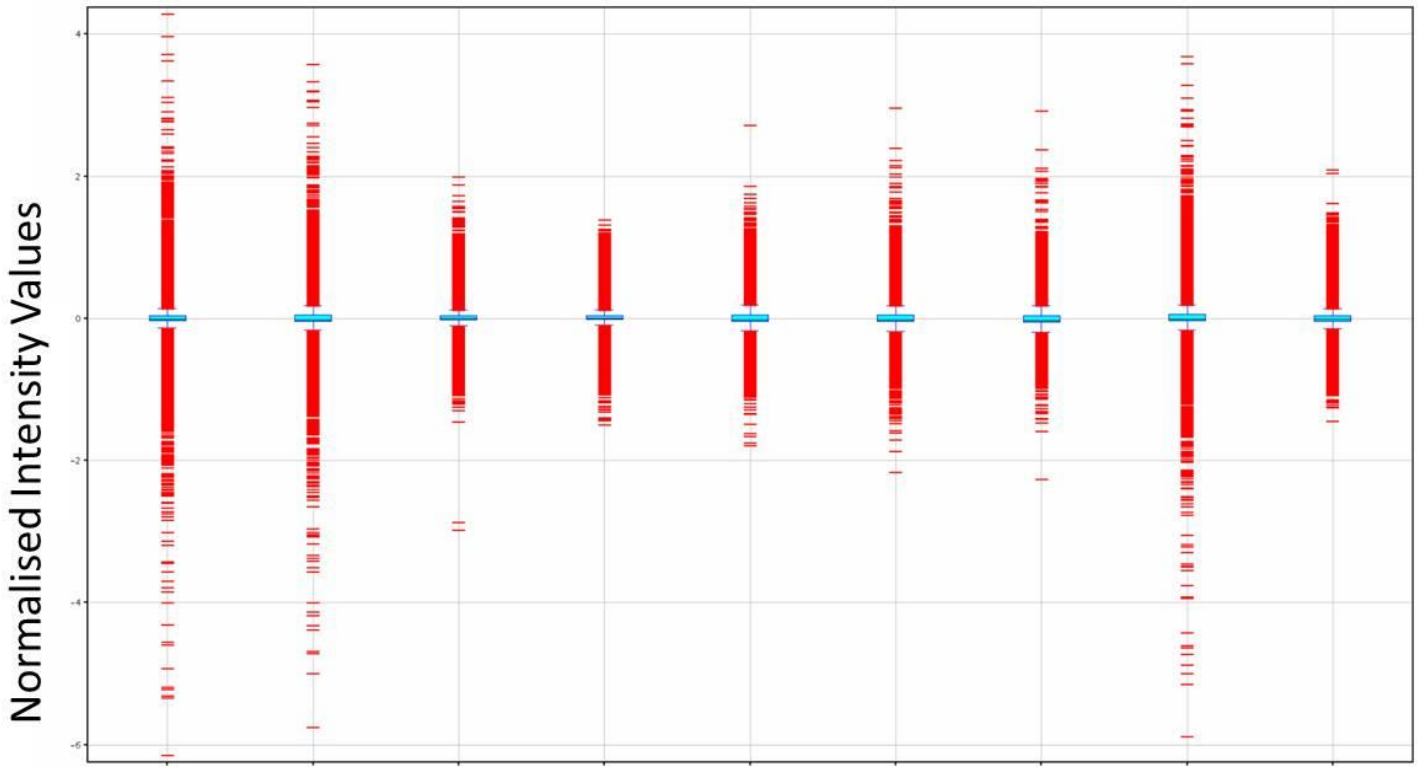

Figure 5.6: Box and whisker plots of normalised intensity values for all data generated by microarray analysis after batch correction.

Batch correction was carried out in R programme and then re-imported into GeneSpring 11.5 for analysis. 1 and 2) show data from chips hybridised with RNA from anterior wing buds treated with DMSO carried out at the Roslin Institute. 3 and 4) show data from chips hybridised with RNA from anterior wing buds treated with 0.01mg/ml EC23 carried out at the Roslin Institute. 5-7) show data from chips hybridised with RNA from anterior wing buds treated with 1mg/ml ATRA, carried out at the Roslin Institute. N1 and N2) show data from chips hybridised with RNA from anterior wing buds treated with DMSO and 0.01mg/ml EC23 respectively but carried out at Centre for Life, Newcastle.

Results:

EC23 and ATRA alter distinct groups of genes.

ATRA is known to generate digit duplications (chapter 3;(Tickle et al., 1982)) while DMSO causes no effect on digit development. It was shown in chapter 3 that EC23 was able to mimic the effect of ATRA on limb development and effects were observed on the entire PD axis of the wing in response to both retinoids. Considering these phenotypes, it would be expected that DMSO treated wings had a different genetic profile to retinoid treated wings.

It can be observed from the box and whisker plots that the treatments fall into three groups on the variance in their gene expression profile: DMSO exhibits greater variance to ATRA which is greater than EC23 (figure 5.6). This can also be seen after the results from two distinct cluster analyses. Hierarchical and K-means clustering were used to analyse the similarities between retinoid and DMSO treatments. These are two distinct clustering algorithms which cluster data together without a priori knowledge or reference to function and biological significance. Data clustered together by these algorithms has the sole property of being more similar to the cluster in which it is located than to other clusters of data. These are useful techniques to determine similarity between treatment groups or a group of genes which are similarly regulated within datasets. Hierarchical and K-means clustering are two different types: supervised and unsupervised respectively. Hierarchical clustering determines distance between two data-points and links the two as a cluster, it then re-calculates distance between the cluster and other data-points until all clusters are linked. K-means clustering, however, clusters data randomly based on the desired number of clusters (k) and then re-clusters data until the profiles in each cluster are as similar as possible. Two distinct clustering methods were used to investigate the validity of the data generated and verify that the main cause of variation was the difference in treatment (Shannon et al., 2003; Stekel, 2003).

Hierarchical and K-means clustering indicate that DMSO and retinoid treated genetic targets are distinct (figure 5.4). This is true even when *k* is changed from 2 to 3 (figure 5.7B-C). It can also be seen when k=4 although the clustering seen was visually less accurate (figure 5.7D). Despite the similarities in phenotypes observed with both retinoids

the clustering analysis indicates that the expression profiles of the two retinoids are also distinct however, they are more similar to each other than to DMSO (figure 5.7A and 5.7B). These differences may provide insights into targets of ATRA metabolites *in vivo* or be the mechanism behind the differences in digit duplication demonstrated previously (chapter 3). Cluster analysis also validates the method used for isolating RNA as the pools within treatments are more similar to each other than to the other pools. Given that the expression profiles can be sorted in such a robust way by three different methods, this validates the methodology used and allows us to consider the data in detail in the following sections to understand the biological significance of the variation between the treatment groups.

The box and whisker plots in figure 5.6 indicate that there is a large change in expression profile in response to retinoid. There is a noticeably smaller range in expression values in the retinoid treated pools compared with the DMSO treated pools (Figure 5.6 compare lanes 2-7 and N2 with 1, 2, N1). This is consistent with the idea that EC23 and ATRA are altering gene expression more than DMSO and that DMSO appears to allow more diversity in gene expression. This suggests that the action of retinoids is to inhibit correct transcription during embryonic development or to maintain the cells in a different transcriptional state to DMSO treatment. There is also a smaller range of expression values in EC23 treated compared to ATRA treated pools (figure 5.6). Consistent with this it can also be seen that gene expression in response to ATRA is often more extreme than EC23 in terms of fold change (tables later). It appears that EC23 generates a more severe retinoid response than ATRA which is an intermediate between EC23 and DMSO. This may be due to the more efficient metabolism of ATRA compared to EC23 (chapter 4) allowing limb development to recover from the teratogenic threat.

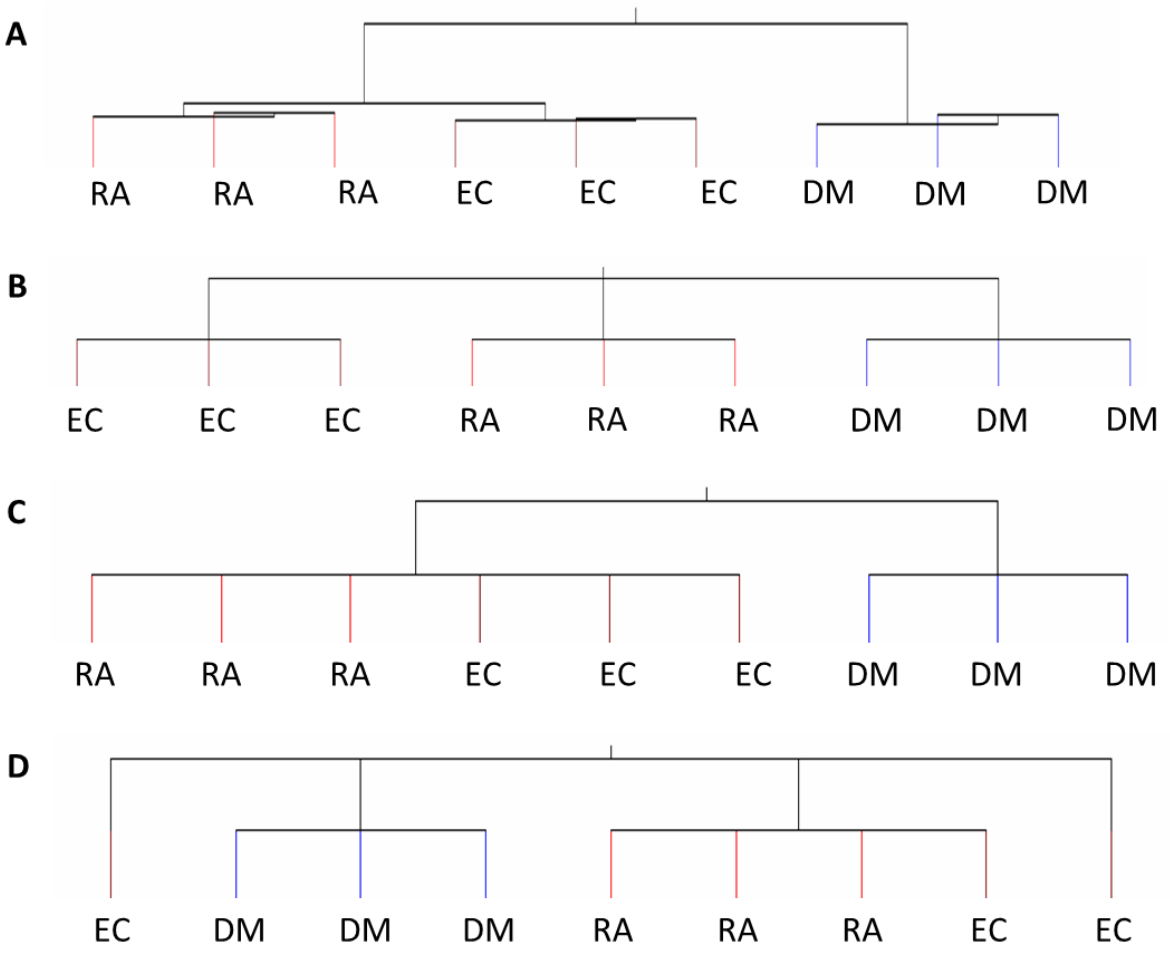

Figure 5.7: Cluster analysis of all data from all microarray chips after batch correction.

A) show hierarchical clustering of all data in GeneSpring after batch correction. B-D) show K-means clustering of all data with B) k=3, C) k=2 and D) k=4. Abbreviations: DM, DMSO treated anterior wing buds; EC, 0.01mg/ml EC23 treated anterior wing buds; RA, 1mg/ml ATRA treated anterior wing buds.

Both EC23 and ATRA cause transcriptional repression and activation.

Previous research on retinoid genetic targets has indicated that they cause their effects by activating transcription (Ali-Khan and Hales, 2006; Astrom et al., 1990). Consistent with this there is evidence that unliganded RARs are important for some developmental processes as they repress retinoid responsive genetic responses (Damm et al., 1993; Koide et al., 2001). However, a study by Luijten et al (2010) has indicated that retinoids can both up and down-regulate gene expression during embryonic development. Therefore, the regulation of genetic targets after retinoid treatment is of interest.

It can be seen from the volcano plots (figure 5.8) and table 5.1 that EC23 and ATRA have caused statistically significant up-regulation and down-regulation of genetic targets. 214 transcripts significantly up-regulated by more than 2-fold in ATRA treated wing buds compared to 150 transcripts in EC23 treated wing buds. Interestingly, 221 transcripts were significantly down-regulated in the ATRA treated limb buds compared to 158 in the EC23 treated wing buds (table 5.1). Fewer genes are significantly altered in response to EC23 treatment than in response to ATRA (compare figure 5.8A and 5.8B, and table 5.1). This is consistent with the decreased range of expression values in response to EC23 compared to ATRA from box-whisker plots (figure 5.6 compare lanes 5-7 with 3, 4, N2).

Table 5.1: A comparison of the number of genes significantly altered in response to 1mg/ml ATRA or 0.01mg/ml EC23 with respect to DMSO in the anterior wing bud.

Treatment	Up-regulated			Down-regulated		
	Common	Specific	**Total**	Common	Specific	**Total**
ATRA	130	84	**214**	127	94	**221**
EC23	130	20	**150**	127	31	**158**

Common genes are those which are up or down regulated in response to both EC23 and ATRA. Specific genes are those which show significant change in expression in response to only ATRA or EC23 by microarray analysis.

When comparing the ATRA and EC23 targets produced (with respect to DMSO), it can be seen that there are some transcripts present in response to both retinoids (common targets) and some are specific to one retinoid (specific). These genes may provide novel insights into the role of the metabolites *in vivo*. Considering that EC23 is more resistant to metabolism and regulates fewer "specific" genes the difference between genes altered in response to ATRA than EC23 may be due to the difference in metabolism (see chapter 4). However, they could also be due to differences between structure and isomerisation (see

chapter 1). Interestingly, a comparison was made between the expression profiles of ATRA and EC23 treated RNA only generated 5 transcripts significantly up-regulated and 6 transcripts significantly down-regulated in ATRA with respect to EC23 (based on fold change >1.5, $p<0.05$; see table 5.2). This suggests that the difference between ATRA and EC23 is of magnitude of response rather than absolute changes in gene expression profile.

Table 5.2: The genes altered significantly in response to ATRA with respect to those altered in response to EC23.

Gene Title	Gene Symbol	Fold change
---	---	+3.3
chromosome 6 open reading frame 32	*C6orf32*	+2.7
Periostin, osteoblast specific factor	*Postn*	+2.5
heme oxygenase (decycling) 1	*Hmox1*	+2.0
ALX homeobox 1	*Alx1*	+2.0
---	---	-1.6
---	---	-1.7
RNA binding motif protein 24	*Rbm24*	-1.7
LIM homeobox 9	*Lhx9*	-1.8
Hypothetical protein LOC771883	*LOC771883*	-1.9

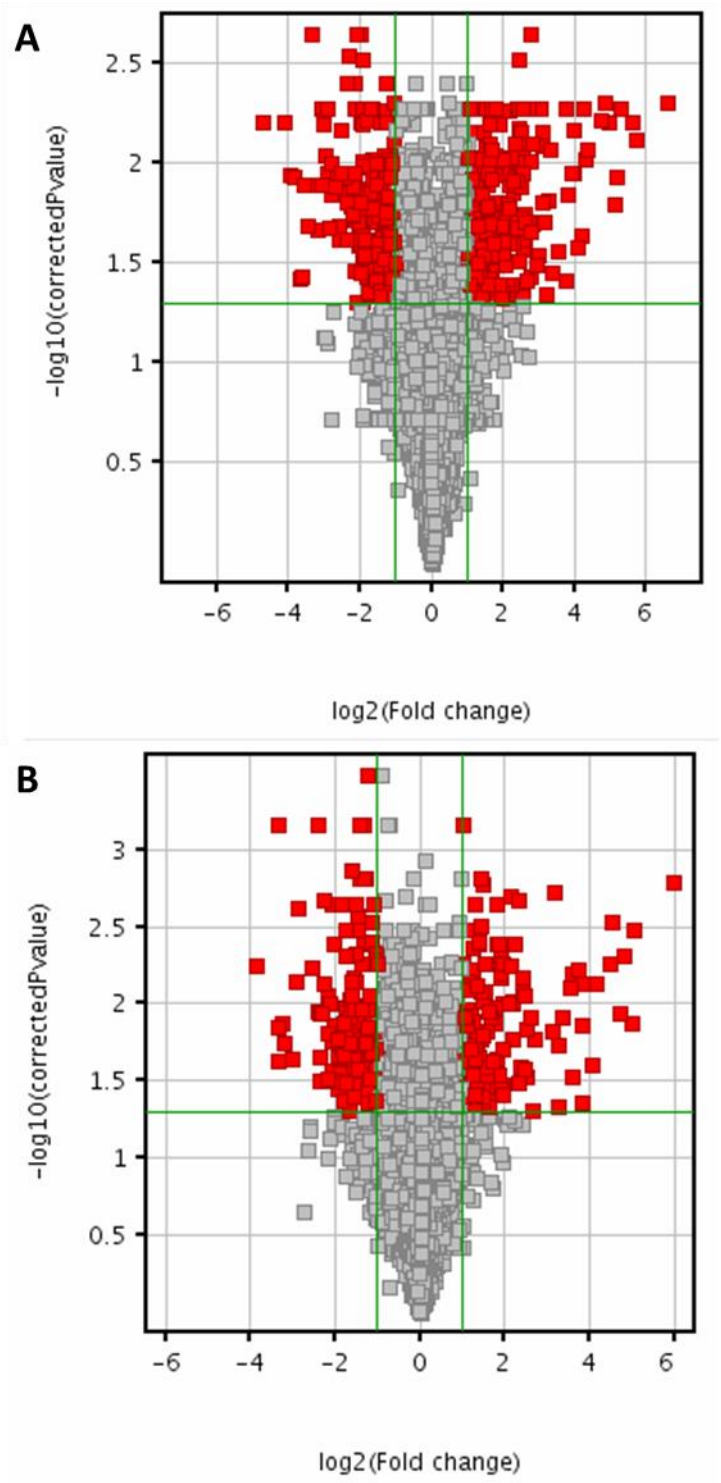

Figure 5.8: Filtering of data to determine significantly altered genes in response to EC23 and ATRA using volcano plots.

Gene expression is plotted as log2 (fold change) vs. the log 10p-value. The horizontal green lines indicate the threshold above which genes are significantly altered. The vertical green lines indicate the genes which are altered by 2 fold or more either up (right) or down (left). Statistical significance was calculated using a t-test and corrected for multiple tests. Fold change was calculated with respect to DMSO treatment. Genes which have been significantly altered 2 fold are indicated in red. A) shows genes significantly altered by 1mg/ml ATRA. B) shows genes significantly altered by 0.01mg/ml EC23.

Functional Classification:

The genes yielded after filtering for >2fold change ($p<0.05$) were subjected to annotation analysis using the Database for Annotation Visualisation and Integrated Discovery (DAVID). The genes were clustered using the Functional Annotation Clustering Tool (Huang da et al., 2009). This analysed the genes presented to determine the known biological processes associated with them and whether they were enriched in the dataset. It then clustered the annotation terms on similarity and provided an enrichment score highlighting those processes which are most altered in the genes up or down-regulated in response to both retinoids. Considering that the datasets used to investigate functional analysis are retinoid as compared to DMSO, it indicates that these processes are altered in retinoid treatment to a greater extent than DMSO treated wings.

Table 5.3: Functional Classification of genes up-regulated in response to ATRA and EC23 using DAVID.

ATRA		EC23	
Function	**Enrichment**	**Function**	**Enrichment**
Embryonic Skeletal Development	3.45	TFs in embryonic development	3.72
Transcription factors	2.78	Carbohydrate binding proteins	1.56
Epithelial cell proliferation	1.75	Cation binding	1.15
Cation binding proteins	1.53	+ve regulators of transcription	1.10
Transcriptional regulators	1.46	ECM and Adhesion	1.10
Oxidative metabolism	1.45		
Kidney/limb embryonic development	1.43		
+ve regulators of transcription	1.25		
Cytoskeleton	1.24		
Cell and Neural development	1.08		

Abbreviations: ATRA, all-trans retinoic acid; ECM, extracellular matrix; TFs, transcription factors; +ve, positive.

The top 10 most enriched clusters for ATRA and EC23 treatments are shown in table 5.3 (up-regulated genes) and table 5.4 (down-regulated genes). Due to the difference in the number of genes analysed the enrichment scores are not comparable between the two datasets however, conclusions can be drawn from their relative positions. Interestingly

only 5 functions were clustered in the EC23 up-regulated genes compared to 10 in the ATRA treated dataset (table 5.3). This is consistent with an up-regulation of disparate targets in response to the more potent EC23 and appears to be less coordinated than ATRA. ATRA could be interpreted as a more regulated change in gene expression as table 3 shows the coordinated up-regulation of many transcription pathways.

It is particularly notable that ATRA up-regulates skeletal, neural and embryonic development and proliferation while EC23 down-regulates these functions (compare tables 5.3 and 5.4). The up-regulation of these functional groups in ATRA but not EC23 targets is consistent with the idea that these retinoids may be showing different stages of the retinoid response or that they alter different processes to achieve digit duplication and the phenotypes seen in chapter 3. The comparison of EC23 and ATRA genetic targets yielded very few significantly different targets (table 5.2) indicating that, for the most part, where a gene showed significant change in one treatment it was significantly altered in the other treatment although the magnitude of the response was different. Considering this, it can be proposed that the expression profiles of the limb 24hrs after EC23 or ATRA exhibit different stages of the retinoid response rather than altering different processes. Considering the great enrichment of transcription factors in the EC23 up-regulated dataset while there are other functional classifications present in ATRA target genes, the retinoid response may be to up-regulate transcription factors (EC23) which then coordinate up-regulation of other pathways (ATRA).

The clusters enriched in the ATRA up-regulated genes suggest that ATRA is affecting skeletal development, although not limb development (see table 5.3 and below), and increasing cell proliferation. The enrichment of genes involved in epithelial proliferation is consistent with previous research which suggests that ATRA must increase AER length in order to generate new digits and full digit duplications (Tickle et al., 1989). The fact that EC23 does not cause an increase in epithelial proliferation is consistent with the phenotypes seen where it can only induce additional digit 1s and that limb development is blocked. The idea that genes involved in skeletal development are being up-regulated suggests that ATRA is re-patterning the anterior-posterior axis to allow skeletal development (the earliest sign of limb differentiation) to take place and also that it is recovering from the initial inhibition of development.

Interestingly, there is also a cluster of genes involved in oxidative metabolism, including the *Cyp26* enzymes, in the up-regulated ATRA genes suggesting that these wings are

metabolically active to try and neutralise excess ATRA. This is consistent with the ability of ATRA to up-regulate *Cyp26* in the anterior wing bud as seen previously (Martinez-Ceballos and Burdsal, 2001). This also indicates that ATRA treated wing buds are more likely to contain oxidative derivatives of ATRA than EC23, especially as this cluster is not enriched in EC23 up-regulated targets. This is consistent with data suggesting that EC23 is resistant to metabolism at most known sites by the CYP26 enzymes (see chapters 1 and 4). This provides further evidence that ATRA is metabolised more than EC23 in the developing wing bud and that the additional functional classes in ATRA may reflect that ATRA metabolites are needed for these pathways, which are this not available with EC23.

Table 5.4: Functional Classification of the genes down-regulated in response to ATRA and EC23 using DAVID.

ATRA		EC23	
Function	**Enrichment**	**Function**	**Enrichment**
Limb Development	3.57	ECM	3.34
ECM	3.12	Embryonic development	3.00
Embryonic development	2.88	Skeletal Development	2.90
Blood vessel development	2.57	Adhesion	2.56
Urogenital development	2.54	Patterning	2.40
Growth factors	2.33	Lung development	2.15
Neural Development	2.16	Neural Development	1.92
Muscle Development Inc. adhesion	2.10	+ve regulators of proliferation	1.83
Patterning genes	2.07	Ear Development	1.74
Muscle development	2.04	Urogenital Development.	1.67

Abbreviations: ATRA, all-trans retinoic acid; ECM, extracellular matrix; inc, including; +ve, positive.

Table 5.4 shows the functional classification of the down-regulated genes in response to ATRA and EC23. Interestingly similar numbers of clusters are formed in response to both retinoids suggesting that both retinoids coordinate the down-regulation of many processes unlike the differential coordination of up-regulated genes. A hypothesis for the differences between the coordination of the retinoid targets may be that the primary response to retinoid is to down-regulate genes including those involved in limb development (see table 5.4) and in fact stall limb development. Once the retinoid is metabolised retinoid treated wings can undergo re-specification or continuation of normal limb development

(enrichment of skeletal development genes in ATRA up-regulated dataset; table 5.4). Considering the differences in metabolism of EC23 and ATRA, this may account for the differences in coordination of genes: EC23 treated wing buds are inhibiting limb development at 24hrs while ATRA treated wings begin to recover. It could also be proposed that EC23 and ATRA have different abilities to activate the RARs while their ability to repress transcription is similar. This may be the case as the similar retinoid, TTNPB, has decreased affinity for and activation of the RARs (Pignatello et al., 1997). However, these differences in activation could also be due to the oxidation products of ATRA which are decreased or absent with EC23. Therefore, it is not possible to comment on receptor activation at the present time.

When the anterior limb was harvested, embryos were estimated to be at HH23 from the size of the contralateral wing. At this point in normal, untreated limb development muscle differentiation is starting to occur within the limb as well as significant chondrogenesis and vascular remodelling (Duprez, 2002; Vargesson, 2003). Muscle precursors are known to enter the limb between HH15-18 but then are rearranged into the dorsal and ventral muscle masses between HH21-23 (Murray and Wilson, 1997) which express *myod1* (Weintraub et al., 1991). Nerves are held at the brachial plexus at this time-point until HH25 (Araujo et al., 1998; Landmesser and Morris, 1975). Considering that table 5.4 shows an enrichment of genes involved in limb development in the ATRA down-regulated dataset it is perhaps unsurprising that these processes are also enriched in the down-regulated genes. This provides further evidence that the ATRA treated wings are stalled in their development. Cartilage development occurs before subsequent muscle development and innervation (Al-Ghaith and Lewis, 1982; Duprez, 2002; Searls et al., 1972). The up-regulation of genes involved in skeletal development in the ATRA treated wing and down-regulation of muscle development indicates that the ATRA treated wing is at an earlier developmental stage than the DMSO treated wing e.g. the limb is being re-specified. This is supported by the fact that genes involved in patterning are enriched in the down-regulated dataset (table 5.4). In response to EC23, a number of these processes are also seen in the clusters from the down-regulated gene sets but blood vessel development is far less enriched and there is no cluster of genes involved in muscle development or containing growth factors. This lack of genes involved in muscle development in the EC23 treated wing bud when considered with the down-regulation of genes involved in skeletal development may indicate that EC23 is stalling limb development further than ATRA. However, it could also

indicate that EC23 does not affect or cause duplication of muscle development and may represent an area for further study.

Overall this functional clustering suggests that there is little difference between the function of ATRA and EC23 down-regulated targets as many of the clusters are present in response to both retinoids with differences in their enrichment score. However, their up-regulated targets appear to be functionally different. The analysis indicates that EC23 up-regulates many unrelated genes but down-regulates skeletal and neural development in a coordinated manner. ATRA, however, up and down-regulates genes in a coordinated fashion causing, mainly, a down-regulation of differentiation. The fact that ATRA up-regulates genes which cluster under "oxidative metabolism" while EC23 does not is more evidence that EC23 is metabolised less and that ATRA treated wing buds may contain oxidative derivatives of ATRA while EC23 treated wing buds will not.

Consideration of the genetic targets.

The discussion of the genes in the following sections focuses on a selection of genes from those altered in response to either EC23 or ATRA treatment. The selection of these genes was influenced by the level of change to their expression, the current knowledge on their expression patterns, known roles in the limb bud system and phenotypes which their manipulation have produced in previous literature which could aid the understanding of EC23 and ATRA in the current study. Given this selection process, it must be noted that many genes were not investigated but which may also play a role in the development of the phenotypes generated by EC23 and ATRA as they have not been documented previously or are un-annotated transcripts. This is a shortcoming of the present analysis but the current analysis is intended as a baseline from which further investigation and experiments can be generated to enhance our understanding of the effect of retinoids in limb development.

Both EC23 and ATRA induce a common response.

As previously indicated from table 5.1 and the cluster analysis (figure 5.7), ATRA and EC23 induce a common retinoid response. Among these are genes which are known to be retinoid responsive as well as genes which may contribute to the phenotypes observed in

chapter 3. The following sections address the individual genes in more detail to try and elucidate key markers or regulators of limb and digit development.

Retinoid responsive genes

It can be seen that a number of genes known to be up-regulated by retinoid treatment were present after treatment with both ATRA and EC23 (see table 5.5) one of which is the most up-regulated gene in response to both retinoids (*Cyp26a1*). These include genes which are known to encode proteins involved in retinoid metabolism or signalling: *Cyp26* (Reijntjes et al., 2005), *dehydrogenase/reductase member 3* (*dhrs3;* (Feng et al., 2010)), *Rarβ* (Rowe et al., 1991), *retinol binding protein* (*rbp5*), *stimulated by retinoic acid 6 homologue* (*stra6*) (Bouillet et al., 1995) and *cyp1b1* (Chambers et al., 2007; Choudhary et al., 2007). Interestingly, both retinoids up-regulate a receptor through which retinoids can modulate gene expression: *Rarβ1* and *Rarβ2/4* (Nagpal et al., 1992). *Rarβ2* is known to be retinoid responsive and expressed at the proximal limb (Mendelsohn et al., 1994a; Nagpal et al., 1992; Smith et al., 1995). Of particular interest is the up-regulation of *Cyp1b1* by both retinoids consistent with previous research. This has previously been documented to convert retinol to retinoic acid (Chambers et al., 2007; Choudhary et al., 2007). *Rbp5* and *Stra6* are thought to be involved in retinoid transport (Blomhoff and Blomhoff, 2006) indicating that this is affected at high concentrations of retinoid.

Table 5.5: The response of genes involved in retinoid metabolism and signalling after ATRA or EC23 treatment.

Gene	Gene Title	ATRA	EC23
Cyp26A1	Cytochrome P450, family 26, subfamily A, polypeptide 1	+98.14	+63.94
Cyp26B1	Cytochrome P450, family 26, subfamily B, polypeptide 1	+6.80	+4.98
Cyp26C1	Cytochrome P450, family 26, subfamily C, polypeptide 1	+6.65	+5.54
Rbp5	Retinol Binding Protein 5 (Cellular)	+4.54	+3.54
Stra6	stimulated by retinoic acid gene 6 homolog (mouse)	+4.40	+2.77
Dhrs3	dehydrogenase/reductase (SDR family) member 3	+28.44	+22.85
Cyp1b1	cytochrome P450, family 1, subfamily B, polypeptide 1	+2.90	+2.42
Rarβ	retinoic acid receptor, beta	+5.85	+4.58
Rarβ1	retinoic acid receptor, beta	+5.19	+4.70
Rarβ2/4	retinoic acid receptor, beta	+15.33	+11.67

+ denotes up-regulation.

It can be seen that other genes altered by both retinoids have been previously implicated as being retinoid responsive (see tables below). Those from the up-regulated list are: *Pbx1* (Qin et al., 2004), *Meis2* (Mercader et al., 2000), *Hoxa4* (Packer et al., 1998), *Hoxb3* (Leroy and De Robertis, 1992), *Hoxb4* (Folberg et al., 1999), *Hoxb5* (Conlon and Rossant, 1992), *Periostin* (Lindner et al., 2005) and *Wnt11* (Uysal-Onganer and Kypta, 2012). Those from the down-regulated genes are: *Lect1/chondromodulin* (Azizan et al., 2000), *collagen type 7* (LOC416696)(Chen et al., 1997), *Gnot1 homeodomain protein* (*Gnot*) (Knezevic et al., 1995) and *Snail homologue 2 (Drosophila)* (*Slug/Snai2*) (Buxton et al., 1997).

It can be concluded that genes known to be involved in the retinoid metabolism and signalling pathways are up-regulated as are genes known to be responsive to ATRA. The functional clustering observed previously showed that targets of both retinoids are enriched in genes involved in oxidative metabolism or cation binding which include cytochrome oxidases and glutathione transferases. This functional clustering as well as the fact that *Cyp26a1* is the most up-regulated gene in response to both retinoids, indicate that a major part of the retinoid response is to metabolise excess levels so that limb development can continue.

Changes to axis patterning

Many of the genes known to be retinoid responsive (above) are also implicated in limb axis patterning. It has been documented from studies on Axolotl (Maden, 1983) and on the chick wing bud (Mercader et al., 2000), that retinoids can affect the PD axis and cause proximalisation of limb bud cells. The changes to digit development resulting from retinoid treatment are a manifestation of changes to AP axis patterning possibly via the induction of an ectopic ZPA (Wanek et al., 1991). The genetic mechanisms behind this are thought to involve an increase in *Hoxb8* expression (Stratford et al., 1997) followed by increased *Hand2* (Fernandez-Teran et al., 2000) and *Shh* expression (Riddle et al., 1993). Therefore, the genetic targets were interrogated for these markers as well as to their expression patterns during normal limb development.

Table 5.6 shows the effect of ATRA and EC23 on genes involved in axis patterning. As shown, *Hoxb8* is up-regulated by retinoid treatment consistent with previous literature

(Stratford et al., 1997) and with the phenotypes generated in chapter 3. This has been suggested to position the ZPA early in limb development prior to *Hand2* and *Shh* expression and possibly before limb initiation (Fernandez-Teran et al., 2000; Lu et al., 1997; Stratford et al., 1997). The fact that this is reminiscent of very early time points of wing development suggests that retinoids may stall limb development causing the anterior wing to exhibit properties shown by the posterior wing before initiation. Previous research has suggested that *Hand2* expression is up-regulated by 20hrs and *Shh* by 24hrs ATRA treatment (Fernandez-Teran et al., 2000; Riddle et al., 1993), however, in this microarray analysis both *Hand2* and *Shh* are absent in response to either retinoid. Altogether, this indicates that the retinoid treated wings are at earlier stages of development compared to DMSO treated wings and retinoid treatments of previous studies.

Hox genes have been documented to control axis patterning in many areas of the developing embryo. Their roles have been studied extensively and *hoxa9-13* and *hoxd9-13* are expressed in the developing limb bud in very distinct spatio-temporal patterns (Izpisua-Belmonte et al., 1991; Yokouchi et al., 1991b). They have been shown to be ectopically induced in the anterior wing bud during the process of digit duplication in response to retinoid (Izpisua-Belmonte et al., 1992). Interestingly the expression of neither the *5'hoxa* nor *hoxd* genes is altered in response to both ATRA and EC23 (but see later) as would be expected with axis re-specification and subsequent digit duplication. Considering that Izpisúa-Belmonte et al (1991) began to see *Hoxd13* expression in the anterior wing after 48hrs of 1mg/ml ATRA treatment, this may indicate that digit duplication is at a very early time point. However, other members of the *Hox* family are altered after retinoid treatment (table 5.6).

Table 5.6: The response of genes involved in axis patterning or anteriorly restricted genes after ATRA or EC23 treatment.

Gene Title	Gene Symbol	ATRA	EC23
Homeobox a4	*Hoxa4*	+5.43	+2.67
Homeobox b3	*Hoxb3*	+18.0	+11.8
Homeobox b4	*Hoxb4*	+19.7	+14.2
Homeobox b5	*Hoxb5*	+13.4	+9.6
Homeobox b8	*Hoxb8*	+34.6	+14.3
Distal-less Homeobox 5	*Dlx5*	-4.5	-2.8
Distal-less Homeobox 6	*Dlx6*	-7.8	-4.5
Goosecoid Homeobox	*Gsc*	+3.2	+2.4
Secreted phosphoprotein 1/Osteopontin / Bone Sialoprotein	*Spp1*	-3.2	-2.1
Lim homeobox 9	*Lhx9*	-3.9	-2.7
Chondromodulin	*Lect1*	-3.4	-2.8
Gnot1 Homeodomain Protein	*Gnot1*	-15.6	-5.1
Differential screening-selected gene Aberrant in Neuroblastoma	*DAN*	-4.5	-3.6
Platelet-derived Growth Factor C.	*Pdgf-c*	-2.9	-2.2
Snail Homolog 2 (Drosophila)	*Snai2/Slug*	-2.2	-2.2

+ denotes up-regulation; - denotes down-regulation.

Consistent with posteriorisation to the anterior wing bud as shown by increased *Hoxb8* expression, *Lhx9* and *Dlx5* expression are down-regulated. Expression of *Lhx9* (Nohno et al., 1997) and *Dlx5* (Ferrari et al., 1995) are restricted to the anterior wing bud at HH23 and therefore down-regulation of these genes is highly significant. Table 5.6 also shows other genes normally expressed in the anterior wing which are down-regulated by both retinoids: *Lect1/chondromodulin* (Shukunami et al., 1999), *Gnot* (Ranson et al., 1995), *Goosecoid homeobox* (*Gsc*) (Heanue et al., 1997), *differential screening-selected gene aberrant in neuroblastoma* (*NO3/DAN*) (Gerlach-Bank et al., 2002; Ogita et al., 2001), *platelet derived growth factor-c* (*Pdgf-c*) (Ding et al., 2000) and *Slug/Snai2* (Buxton et al., 1997). This suggests that re-specification of anterior-posterior axis is occurring in retinoid treated wing buds consistent with the phenotypes generated (chapter 3) and previous literature. The fact that more anterior genes are down-regulated than the number of posterior genes up-regulated (*Hoxb8* alone) is consistent with the hypothesis that retinoid treated wing buds are at early stages of digit duplication.

Consistent with the role of retinoids in proximalisation of limb bud cells (Mercader et al., 1999) many genes restricted along the PD axis are altered accordingly. Table 5.7 shows

genes known to be expressed in proximal limbs which are up-regulated in response to both retinoids: *Emx2* (Prols et al., 2004), *Meis2* (Mercader et al., 2000), *Pbx1* (Capellini et al., 2006), *Pleiotropin* (Mittapalli et al., 2009), *Gsc* (Gaunt et al., 1993; Heanue et al., 1997), *Alx1* (Beverdam and Meijlink, 2001; GEISHA), *Cyp1b1* (Chambers et al., 2007), *receptor tyrosine kinase-like orphan receptor 1* (*Ror1*) and *Slit homologue 1 (Drosophila)* (*Slit1;* (Vargesson et al., 2001)). Some of these genes have been implicated or necessary for scapula development and may provide the mechanism for the truncated scapulae seen with these retinoids (see chapter 3 and discussion). The up-regulation of these genes suggests that retinoid treated wings are becoming more proximalised ((Mercader et al., 2000); figures 5.9-11).

Table 5.7: The response of genes with proximal-distal restriction to ATRA or EC23 treatment.

Gene Title	Gene Symbol	ATRA	EC23
Empty Spiracles Homeobox 2	*Emx2*	+4.2	+3.0
Meis homeobox 2	*Meis2*	+2.8	+2.5
Pre-B-cell leukaemia homeobox 1	*Pbx1*	+3.6	+3.0
Pleiotropin	*Ptn*	+2.9	+2.1
Goosecoid Homeobox	*Gsc*	+3.2	+2.4
Aristaless Homeobox 1	*Alx1*	+4.0	+2.0
Slit Homolog 1	*Slit1*	+4.1	+3.4
Receptor tyrosine kinase-like orphan receptor 1	*Ror1*	+3.1	+2.7
Gnot1 Homeodomain Protein	*Gnot*	-15.6	-5.1
Sal-like 1	*Sall1*	-4.9	-3.1
Snail homolog 2 (Drosophila)	*Snai2/Slug*	-2.2	-2.2

+ denotes up-regulation; - denotes down-regulation.

Concurrent with an up-regulation in genes in the proximal region of the limb, there is also a down-regulation of genes usually restricted to the distal limb (see table 5.7). These include: *Gnot* (Ranson et al., 1995), *Sal-like 1* (*Sall1*) (Capdevila et al., 1999) and *Slug/Snai2* (Buxton et al., 1997). Fewer distally restricted genes are significantly altered than proximal genes (3 distally restricted against 7 proximally restricted). This may reflect the fact that ATRA directly regulates proximal genes but indirectly regulates distal genes via FGF8, SHH and CYP26B1 (Probst et al., 2011). Overall, this data is consistent with previous literature than retinoid treatment causes proximalisation of cells (Mercader et al., 2000) and that the retinoids affect the entire PD axis of the limb (chapter 3).

Overall this data indicates that the retinoid response is to up-regulate genes associated with proximal and posterior patterning of the limb while down-regulating genes associated with anterior and distal limb development which is consistent with the phenotypes seen in chapter 3. This is consistent with the functional analyses carried out previously indicating that genes involved in patterning are enriched in both ATRA and EC23 down-regulated target genes providing further support that development is being stalled. The absence of these from the up-regulated data set indicates that these genes have not yet been documented in axis patterning or that other functional attributes are present at a far more enriched level.

EC23 and ATRA have similar effects on proximal relocation of cells.

ATRA and EC23 have been shown to up-regulate proximally restricted genes and down-regulate distally restricted genes. It is known that ATRA causes proximal relocation of cells around the bead (Mercader et al., 2000) which is probably due to a change in adhesive properties (Tamura et al., 1997; Wada, 2011). It has also been well documented that ATRA soaked beads are found in more proximal positions than untreated beads (Mercader et al., 2000). The following section explores whether this occurs with the stable retinoid EC23 compared to naturally occurring ATRA, particularly given the alteration of proximally restricted genes. Unlike previous applications of retinoid in the present study, HH23 chick wing buds were treated with EC23 or ATRA soaked beads dipped in 1mM DiI. These were re-incubated for 48hrs (Mercader et al., 2000) and then fixed in 4% PFA. DiI was used to track cells which had come into contact with substances loaded onto the bead. The labelled cells were used to investigate the effect of retinoid on cell distribution within the limb bud.

Representative images showing how measurement of labelled cell area and distance from the AER was carried out is shown in figure 5.10. Area of cells was calculated using un-flattened limbs and the ellipse tool to capture 95% of labelled cells in ImageJ. Un-flattened limbs were used to determine area of labelled cells as flattening displaced cells in an AP direction. The distance that labelled cells had relocated was estimated using the line tool in ImageJ. This was drawn from the most distal part of the ellipse surrounding the cells to the closest part of the AER as this was deemed the most reproducible method. This was carried out on flattened limbs as the expansion of the limb in the PD axis upon flattening was less than in the AP axis and therefore would provide a more accurate measurement.

It can be seen that EC23 and ATRA affected both the PD and AP location of labelled cells. Figure 5.9 shows representative composites of phase and fluorescent images of limbs after DMSO, ATRA or EC23 treatment in un-flattened limbs. It can be seen that labelled cells in the presence of DMSO are widely spread around the bead in both AP and PD axes. In response to retinoid the dispersal of the labelled cells along either axis appears to be less as shown by the decrease in average area of cell dispersal (figure 5.11A) but this is not statistically significant. It is evident from flattened limbs that cells exposed to retinoid are

found further from the distal tip of the wing after 48hrs treatment (figures 5.10 and 5.11B). This indicates that ATRA and EC23 cause significant proximal relocation of cells. It also appears that EC23 causes cells to be relocated further than ATRA treatment but this is not statistically significant (figure 5.11B). Therefore EC23 mimics the effect of ATRA on cell relocation in the wing bud consistent with previous literature (Mercader et al., 2000) and is consistent with the alteration of genes seen earlier (table 5.7).

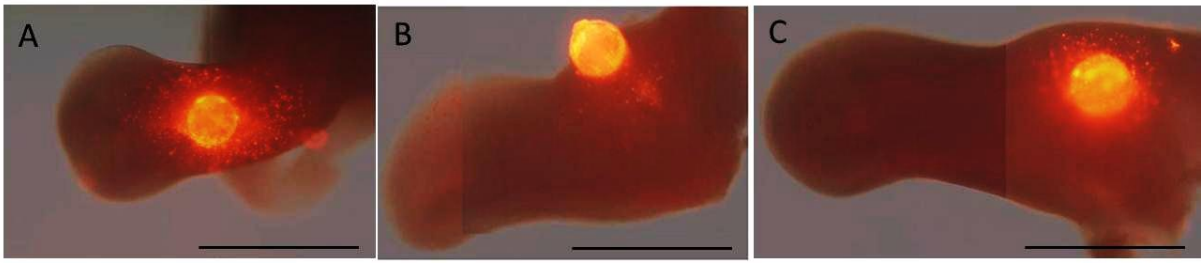

Figure 5.9: The dispersion of cells around beads soaked in DMSO or retinoid on un-flattened limbs. HH23 wings were treated with DMSO or retinoid by a bead implanted into the most distal AER. The bead was dipped in DiI before implantation to allow treated cells to be visualised. A-C) are merged montages of images taken in phase contrast and fluorescence. A) indicates the spread of cells after DMSO treatment. B) shows cell dispersal after 1mg/ml ATRA treatment. C) shows cell dispersal after 0.01mg/ml EC23 treatment. Areas of labelled cells were calculated using the ellipse tool in ImageJ as shown in figure 5.10. Scale bars are 1mm and n=6.

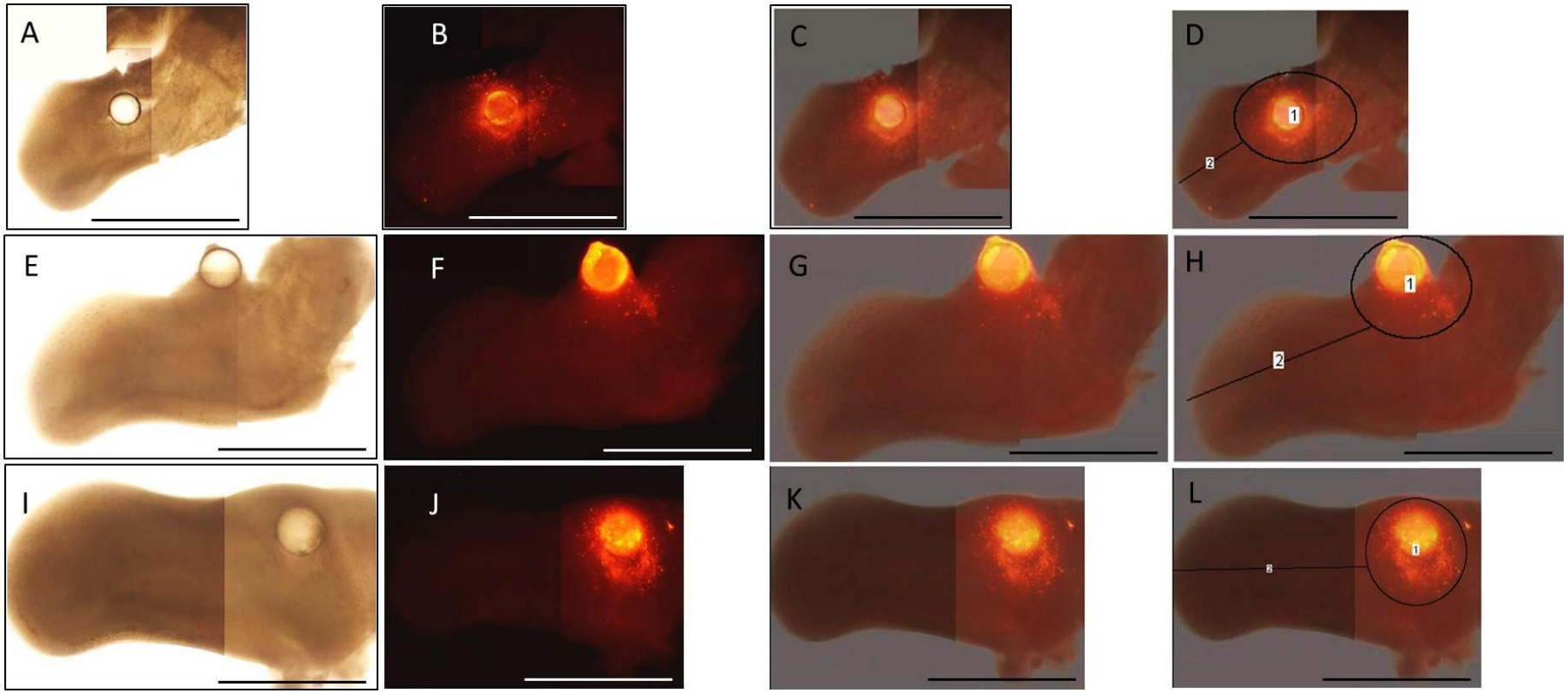

Figure 5.10: The extent of migration of retinoid treated cells compared to DMSO.

HH23 wings were treated with DMSO, ATRA or EC23 placed in a disto-central slit and allowed to develop for 48hrs before fixing and visualisation. Beads were labelled with DiI before implanting so that cells in the immediate vicinity of the bead are labelled. A-D) were treated with DMSO. E-H) were treated with 1mg/ml ATRA. I-L) were treated with 0.01mg/ml EC23. A, E and I) are imaged under phase contrast. B, F and J) are fluorescent images of the same wing. C, G and K) are merged images of the previous two. D, H and L are merged images showing representative measurements taken on the same wing bud using Image J. 1 is the ellipse (area of labelled cell dispersal) and 2 is a measure of relative proximal-distal location of labelled cells. Scale bars are 1mm and n=6.

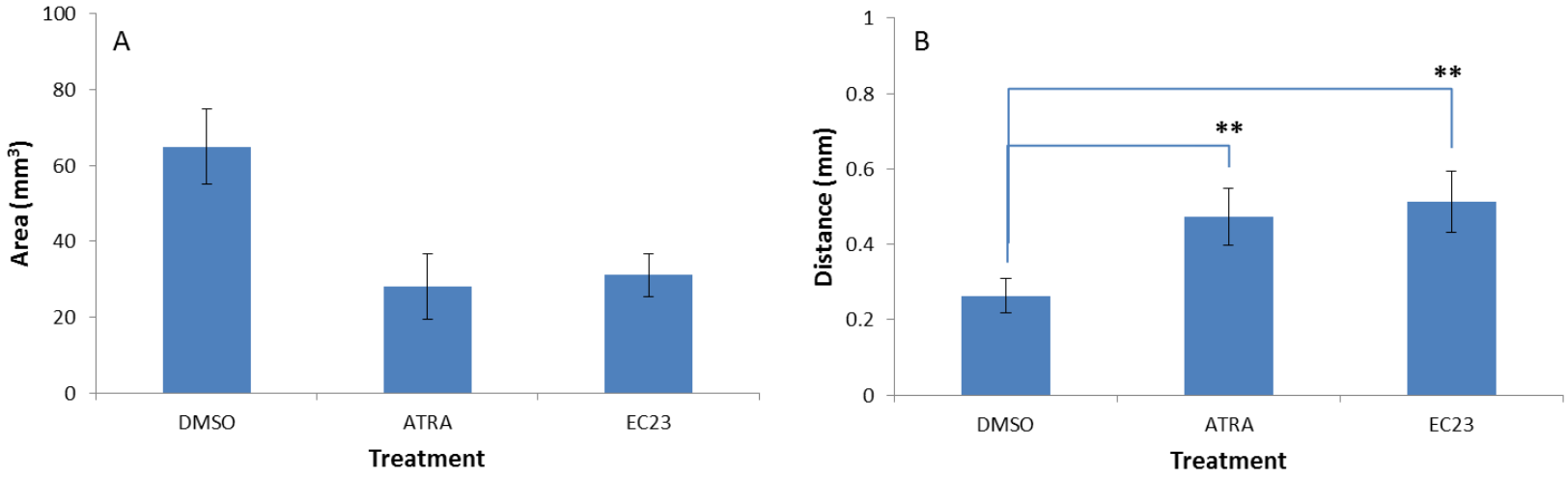

Figure 5.11: The extent of proximalisation of retinoid treated cells.

Chick wings were treated with DMSO or retinoid at HH23 by implanting the bead at the AER. DiI was used to label cells treated by the bead. Embryos were then harvested after 48hrs and cell migration investigated by measuring area and distance migrated of labelled cells (see figure 5.10). A) shows the extent of cell dispersion around the bead in the anterior-posterior axis by measuring the area of an ellipse drawn around 95% of labelled cells on un-flattened wings. B) shows the shortest distance of cell migration to proximal limb after treatment with retinoid and compared to DMSO. This was measured after limbs had been flat mounted onto a slide (see figure 5.10). Significance was tested using an unpaired t-test. * $p<0.05$, ** $p<0.01$, *** $p<0.001$. N=6 per treatment.

The effect of retinoid on Shh expression.

Considering that both ATRA and EC23 generate digit duplications, it may be proposed that these retinoids would induce expression of genes associated with ectopic ZPA formation. It has been shown that excess ATRA can induce *Shh* expression in the anterior wing bud at low levels at 24hrs (Riddle et al., 1993) and that preaxial polydactyly can be associated with an ectopic anterior ZPA (Qu et al., 1997; Wanek et al., 1991). The factors involved in the positioning or induction of the ZPA are thought to be *Hand2* (Charite et al., 2000; Fernandez-Teran et al., 2000), *Alx4* (Takahashi et al., 1998), *Gli3* (te Welscher et al., 2002) and *Hoxb8* (Stratford et al., 1997). Therefore it seemed likely that the generated digit duplication may correlate with a change in expression level of one of these genes after 24hrs retinoid treatment.

As mentioned earlier, neither retinoid altered expression of *Shh* or *Hand2*. There was also no alteration in *Gli3* or *Alx4* expression. As previously mentioned, the up-regulation of *Hoxb8* indicates that the anterior wing bud may be in the early stages of digit duplication. The expression of *Shh* after 24hrs retinoid treatment was then validated by whole mount *in situ* hybridisation. Figure 5.9 shows that after 24hr treatment with either ATRA or EC23 no ectopic *Shh* domain is observed as expected from microarray analysis of the anterior wing bud after retinoid treatment. This is not consistent with the study by Riddle et al (1993) which documented low *Shh* levels in the anterior wing bud after 24hrs of retinoid. Considering that it had been documented that ATRA could induce *Shh* expression between 24-30hrs of treatment (Stratford et al., 1999) and that levels were increased at 36hrs (Riddle et al., 1993), *Shh* expression in the anterior wing bud was also investigated after 30hrs retinoid treatment. As seen in figure 5.10, ATRA was able to induce *Shh* expression in the anterior wing bud at a similar frequency to the number of severe digit duplications observed (n=2 /6, compare to table 3.2). However, EC23 was never observed to induce *Shh* expression in the anterior wing (n=11). The absence of *Shh* expression after 30hrs EC23 treatment vs. 30hrs ATRA treatment suggests that digit duplication or limb development is inhibited in EC23 treated wings vs. ATRA treated wings. This inhibition of limb development may preclude the production of more posterior digit duplication. It was also observed that the endogenous posterior *Shh* domain was often reduced in treated wing buds after 30hrs compared to the contralateral limb bud (figure 5.10) but not after 24hrs (figure 5.9). This suggests that these quantities of retinoid inhibit normal limb development as well as cause digit duplication.

The inhibition of limb development suggested by these observations is consistent with the functional analyses carried out previously using DAVID as ATRA down-regulated genes are enriched for genes involved in limb development. However, the same cannot be said for EC23 target genes. Instead, EC23 down-regulates processes involved in limb development while ATRA down-regulates genes in limb development but up-regulates genes in skeletal development. These functional analyses, when considered alongside the analysis of *Shh* expression, indicate that ATRA treated wing buds recover from excess retinoids quicker than EC23 treated wing buds and begin to re-specify the AP axis.

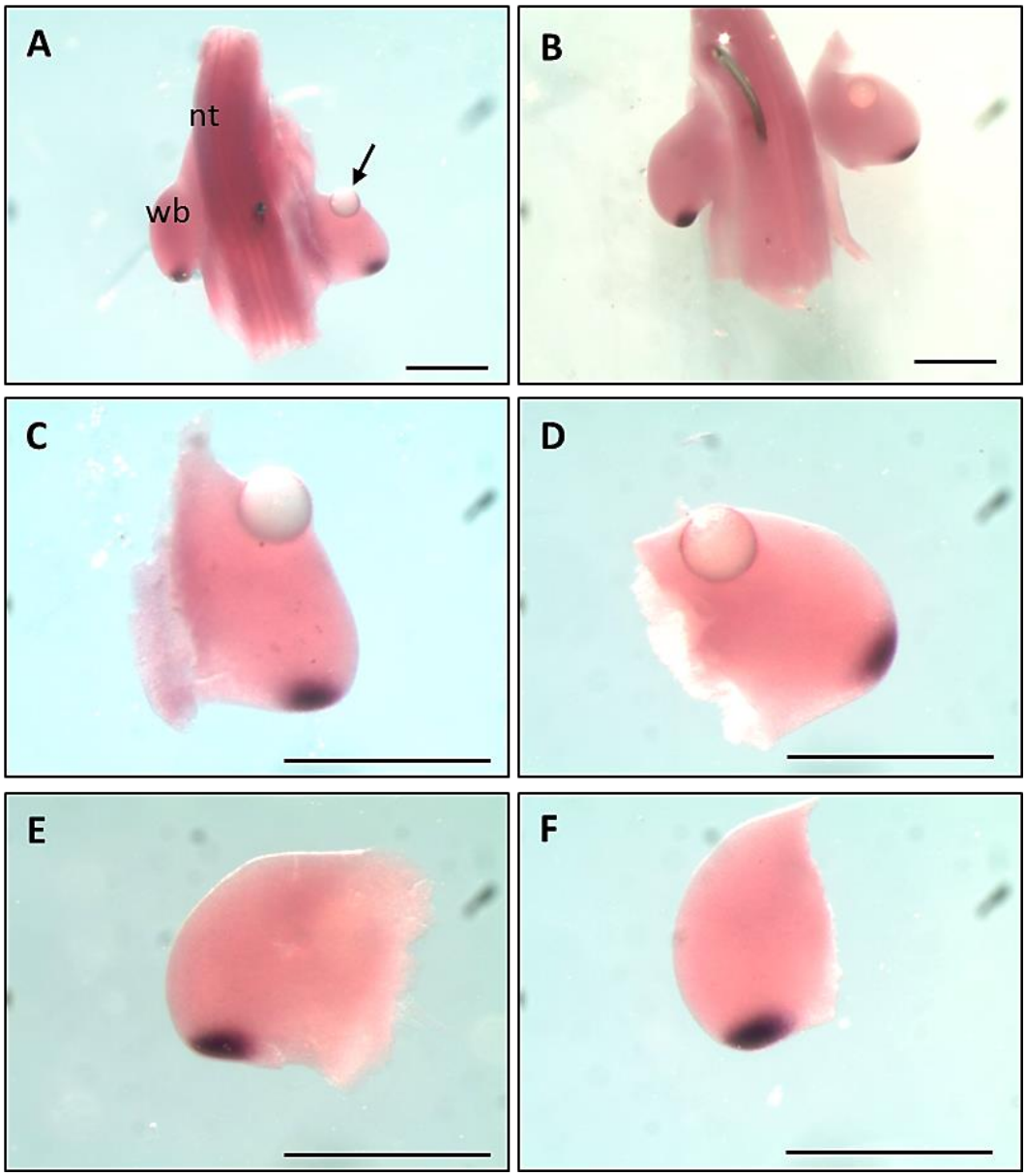

Figure 5.12: The expression of *Shh* after 24hrs treatment with 1mg/ml ATRA or 0.01mg/ml EC23.

A, C and E) represent *Shh* expression after treatment with 1mg/ml ATRA after 24hrs. B, D and F) represent *Shh* expression after treatment with 0.01mg/ml EC23 for 24hrs. A and B) are dorsal views of embryos pinned to agar; operated wing is right and anterior top. C-F) are dorsal views of wing buds dissected: C and D are retinoid treated and E and F are the contralateral wing buds to those depicted in C and D. The arrow in A indicates the bead. Abbreviations: nt, neural tube; wb, wing bud. Scale bars are 1mm.

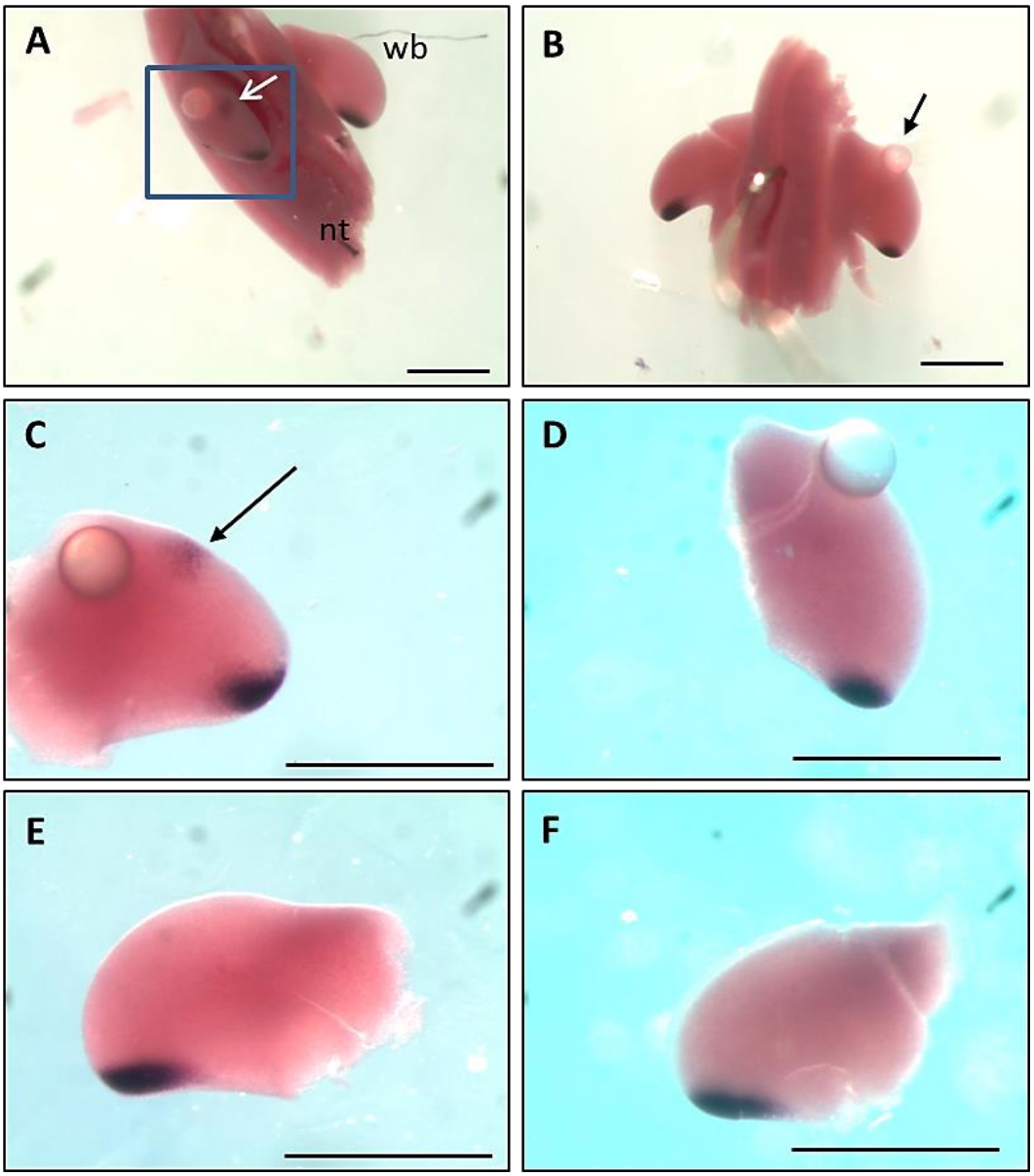

Figure 5.13: The expression of *Shh* after 30hrs treatment with 1mg/ml ATRA or 0.01mg/ml EC23. A, C and E) represent *Shh* expression after treatment with 1mg/ml ATRA after 30hrs. B, D and F) represent *Shh* expression after treatment with 0.01mg/ml EC23 for 30hrs. A is a right lateral right view of the torso. The box in A) indicates the operated wing and highlights ectopic expression of *Shh* (white arrow). B) is dorsal view of embryo pinned to agar; operated wing is right and anterior top. C-F) are dorsal views of wing buds dissected: C and D are retinoid treated and E and F are the contralateral wing buds to those depicted in C and D. The arrow in C) highlights ectopic *Shh* expression in response to 30hrs treatment with 1mg/ml ATRA. Abbreviations: nt, neural tube; wb, wing bud. Scale bars are 1mm.

Retinoids inhibit limb outgrowth:

It has been seen that high concentrations of retinoids can cause inhibition of limb outgrowth leading to limb truncations (see chapter 3(Tickle et al., 1985)). Considering that endogenous *Shh* expression appears to be decreased and that only early indicators of digit duplication are altered, it may be proposed that genes involved in the control of limb outgrowth are likewise inhibited in response to retinoids.

Interestingly, table 5.8 shows a number of genes linked to limb outgrowth are down-regulated in retinoid treated anterior wing buds. *Tbx5* is essential for limb development and correct forelimb identity but also for correct outgrowth of the anterior limb bud (Rallis et al., 2003). *Lhx9* is an anterior marker during chick limb development (Nohno et al., 1997) but during mouse limb development has been implicated in regulating limb outgrowth (Tzchori et al., 2009). *Short stature homeobox* (*Shox*; table 5.10) has also been implicated in limb outgrowth as it is known to cause shortened limbs when mutated (Sabherwal et al., 2007). The down-regulation of these genes is consistent with the idea that retinoids are inhibiting some pathways controlling limb outgrowth and further supporting the idea that limb development is stalled by both retinoids.

Table 5.8: The response of genes involved in limb outgrowth to 1mg/ml ATRA or 0.01mg/ml EC23.

Gene title	Gene Symbol	ATRA	EC23
T-box 5	*Tbx5*	-3.5	-2.8
Lim homeobox 9	*Lhx9*	-5.1	-2.9
Fibroblast growth factor 1	*Fgf1*	-6.0	-3.8
Fibroblast growth factor 13	*Fgf13*	-2.1	-2.0
Fibroblast growth factor 18	*Fgf18*	-4.4	-2.3
Transforming growth factor β2	*Tgfβ2*	-5.5	-3.1

- denotes down-regulation.

Growth Factors

Correct limb development has been shown to be partly under the control of *Shh* in the ZPA. Limb development is also controlled by two other signalling centres: the AER and the dorsal ectoderm (Niswander et al., 1994; Parr and McMahon, 1995). The AER controls growth in the PD axis via the secretion of the following proteins: FGF2, FGF4, FGF8, FGF9 and FGF17 although FGF8 alone is sufficient to sustain outgrowth (Mariani

et al., 2008). Interestingly, other FGFs (*fgf2, fgf10, fgf12* and *fgf13*) are expressed in the mesenchyme of the limb and they may have other roles e.g. *fgf10* is involved in limb initiation and AER maintenance (Ohuchi et al., 1997; Zakany et al., 2007). BMP, TGFβ and WNT signalling are also known to influence limb size and differentiation (Brunet et al., 1998; Choocheep et al., 2010; Loganathan et al., 2005; Macias et al., 1997; Spagnoli et al., 2007). Considering that these signalling pathways are interrelated, particularly the FGF-SHH signalling loop, and that the endogenous level of *Shh* expression was reduced in retinoid treated wing buds, the retinoid genetic targets were interrogated for changes to the expression of these genes.

As shown in table 5.8, the expression of some *Fgf* genes has been down-regulated after retinoid treatment. Oddly the FGFs which are altered in response to both retinoids are not those traditionally linked to AER function: *Fgf2*, *Fgf4*, *Fgf8*, *Fgf9* and *Fgf17*. The fact that these *Fgfs* are not significantly altered indicates that EC23 and ATRA are not shortening the limb or generating digit duplications by disrupting AER-FGFs despite the fact that genetic targets of both are enriched for genes involved in epithelial proliferation (see later), therefore disruption to the AER could occur via another mechanism. However, retinoids may inhibit outgrowth as those *Fgfs* altered may have hitherto unappreciated roles in communication or outgrowth. *Fgf13* (Munoz-Sanjuan et al., 1999) and *Fgf18* (Ohbayashi et al., 2002) have been linked to limb cartilage development and their down-regulation is consistent with dysregulation of chondrogenesis. Interestingly *Fgf18* is also expressed in the anterior-distal wing bud mesenchyme (GEISHA, March 2013) and therefore may further support a suppression of distal identity as discussed previously.

Tgfβ2 is also down-regulated after 24hrs retinoid treatment. *Tgfβ2* has been implicated in the control of chondrogenesis (Miura and Shiota, 2000) and its down-regulation at 24hrs is consistent with inhibition of humerus development, which is occurring at this time (Searls et al., 1972). This inhibition of cartilage development is also consistent with the functional analysis of EC23 regulated genes but not those of ATRA down-regulated genes. This indicates that other genes may be altered in response to ATRA causing the function of skeletal development to be enriched in ATRA targets (see later for ATRA specific genes). *Tgfβ2* has also been implicated in the control of limb outgrowth (Lorda-Diez et al., 2010) and tendon development (Edom-Vovard and Duprez, 2004) indicating that EC23 and ATRA may be causing effects on aspects of limb development other than solely affecting cartilage development. This is consistent with the functional classifications seen previously

although neither outgrowth or tendon development are present in the functions clustered. This may indicate that only few genes involved in limb outgrowth and tendon development are altered in response to retinoid.

ECM

Growth factor signalling is also known to be affected by the composition of the ECM. FGFs, TGFβ and BMP signalling are some of the pathways affected by ECM composition (Johnson and Newfeld, 2002; Thisse and Thisse, 2005). The presence of heparan sulphate proteoglycans (HSPGs) in the ECM is required for some interactions e.g. FGF1-FGFR2 (Thisse and Thisse, 2005). There are known to be many changes to the ECM during limb bud development most of which have been studied in the context of chondrogenesis. One of the major changes is the dynamic expression of collagen: *Collagen type I* is produced early while *collagen type II* and *X* indicate early and later cartilage development (Behonick and Werb, 2003). *Collagen type IX* is also coexpressed with *collagen type II* in the early stages of cartilage condensation. Many cell surface proteoglycans contain the carbohydrate β-D-Gal-Nac-D-Gal as it is up-regulated in chondrogenesis (Hall and Miyake, 1995). Investigation of ECM markers and modifiers in the retinoid genetic targets are therefore of interest to determine the effect of retinoids on limb development.

Table 5.9: The response of genes involved in ECM composition and cell adhesion to ATRA or EC23 treatment.

Gene Title	Gene Symbol	ATRA	EC23
N-cadherin	*Cdh2*	-2.1	-2.0
Collagen, type XIV, alpha1	*Col14α1*	+3.0	+2.4
Collagen, type IX, alpha3	*Col9α3*	-5.1	-5.4
CD44 molecule (Indian blood group)	*Cd44*	-4.0	-2.6
CD200 molecule	*Cd200*	+3.7	+2.2
UDP-N-acetyl-alpha-D-galactosamine:polypeptide N-acetylgalactosaminyltransferase 6 (GalNAc-T6)	*Galnt6*	+7.1	+5.8
UDP-N-acetyl-alpha-D-galactosamine:polypeptide N-acetylgalactosaminyltransferase 9 (GalNAc-T9)	*Galnt9*	-3.9	-4.1
Cadherin 17 (LI)	*Cdh17*	+5.7	+6.0
ADAM metallopeptidase with thrombospondin type 1 motif, 17	*Adamts17*	+2.3	+2.9
Matrillin 4	*Matn4*	-10.4	-10.2

+ denotes up-regulation; - denotes down-regulation.

As can be seen from table 5.9, *N-cadherin* (*cdh2*) is down-regulated by retinoid. N-cadherin has been shown to be essential for cell aggregation during cartilage condensation (Oberlender and Tuan, 1994a) as well as later stages of chondrogenesis (Delise and Tuan, 2002). This indicates that the early events of chondrogenesis are inhibited in response to retinoid. As *N-cadherin* is a target of TGFβ2 (Miura and Shiota, 2000), other genes in this pathway may also be down-regulated. Interestingly, there is a concurrent up-regulation of *cadherin 17* in response to retinoid. *Cadherin17* has not been linked to limb development although it has been implicated in the correct development of the pronephric ducts in zebrafish (Horsfield et al., 2002). This supports the idea that there is a great change in the ECM of the developing limb after retinoid treatment.

Unexpectedly there is no change in *collagen type II* which is an early marker of cartilage differentiation (Hall and Miyake, 1995). However, retinoids cause increased *col14α1* which is thought to bind to a member of the CD44 family (Ehnis et al., 1996). *Cd44* (Indian) is seen to be down-regulated in response to retinoid indicating that this member is unlikely to be the *col14* receptor. As previously mentioned *collagen type IX* is involved in later steps of cartilage differentiation (Hall and Miyake, 1995) therefore the down-regulation of *col9α3* indicates that chondrogenesis is delayed. *Galnt9* is also down-

regulated which is involved in O-linked glycosylation (Ten Hagen et al., 2001). There are known to be many sites for O-glycosylation in ECM proteins e.g. *collagen I* and HSPG (Gould et al., 1992), this therefore further implicated retinoids in modulating the ECM. Interestingly there is also a down-regulation of *matrilin4* expression in response to retinoid. This gene is a cartilage matrix protein and is known to be connected to scapula development (Feenstra et al., 2012). The down-regulation of these genes suggests that the changes to ECM are not consistent with cartilage development and support the idea that retinoids are inhibiting limb development by the inhibition of chondrogenesis.

Retinoids inhibit developmental processes occurring in the developing wing.

As previously mentioned many processes occur simultaneously during limb development to ensure the correct number and positioning of cartilage, tendons, muscle and nerves for correct limb function. It has been shown previously that muscle as well as cartilage is duplicated after ATRA application to the anterior wing bud (Yamamoto et al., 1998). Although the effect of these retinoids on other aspects of limb development has not been the subject of this study, EC23 and ATRA may alter the expression of genes involved in these processes as well as those involved in cartilage development.

Table 5.10: The response of genes known to be involved in differentiation of cartilage, muscle, tendon, nerve and vascular development to ATRA and EC23.

Gene Title	Gene Symbol	ATRA	EC23
Cartilage Development			
Periostin, osteoblast specific factor.	*Postn/Osf2*	+8.3	+3.1
wingless-type MMTV integration site family, member 11	*Wnt11*	+6.1	+3.8
Chondromodulin/Leukocyte Cell Derived Chemotaxin 1.	*Lect1*	-3.4	-2.8
Cytokine like 1	*Cytl1*	-8.7	-4.4
EGF-containing fibulin-like extracellular matrix protein 1/ Fibulin-3	*Efemp1*	-17.5	-14.4
Fibulin-5	*Fbln5*	-2.7	-2.4
Sperm Adhesion Molecule1 (PH-20 hyaluronidase)	*Spam1*	-2.8	-2.3
Short stature homeobox	*Shox*	-3.3	-2.9
Thrombospondin 4	*Thbs4*	-2.5	-2.5
Tendon Development			
Collagen, type XIV, alpha 1 (undulin)	*Col14α1*	+3.0	+2.4
odz, odd Oz/ten-m homolog 2 (Drosophila)/teneurin-2	*Odz2*	+6.2	+3.7
Pleiotropin	*Ptn*	+2.9	+2.1
Slit homologue 1	*Slit1*	+4.1	+3.4
Muscle Development			
Mesenchyme Homeobox 2	*Meox2*	-6.0	-3.4
Ectonucleotide pyrophosphatase/phosphodiesterase 2/Autotaxin	*Enpp2*	-3.9	-2.9
Brain Derived Neurotrophic Factor.	*Bdnf*	-2.3	-2.1
Vascular Development			
hairy/enhancer-of-split related with YRPW motif 1	*Hey1*	-2.2	-2.4

+ denotes up-regulation; - denotes down-regulation.

Many genes implicated in these processes have been altered by retinoid treatment (see table 5.10). Both retinoids have up-regulated some genes or their receptors implicated in cartilage development: *Periostin* (Zhu et al., 2008b), *slit1* (Vargesson et al., 2001), and *wnt11* (Uysal-Onganer and Kypta, 2012). *Periostin* has been seen to be expressed in mouse chondrocytes at a later stage than studied here (Zhu et al., 2008b) and this may indicate an earlier role for this gene in chick wing development. However, EC23 and ATRA have down-regulated more genes linked to cartilage development consistent with the idea that cartilage development is inhibited: *lect1* (Shukunami et al., 1999), *cytokine-like 1* (*Cytl1*) (Kim et al., 2007), *EGF-containing fibulin-like extracellular matrix protein 1* (*efemp1*)

(Wakabayashi et al., 2010), *Sperm Adhesion Molecule1 (PH-20 hyaluronidase)* (*Spam1*) (Bastow et al., 2008), *n-cadherin* (Oberlender and Tuan, 1994a), *Shox2* (Yu et al., 2007) and *thrombospondin 4* (Tucker et al., 1995).

Genes involved in tendon development are also altered in response to both retinoids. Retinoids up-regulate *Col14α1*, *pleiotropin* and *Odz2* (see table 5.10) which have been implicated in tendon development later (Edom-Vovard and Duprez, 2004; Mittapalli et al., 2009; Tucker et al., 2001b). As mentioned previously, there is down-regulation of *Tgfβ2* and *Fgf18* both of which are implicated in tendon development (Edom-Vovard and Duprez, 2004). Overall, the changes in expression after retinoid treatment are consistent with dysregulation of tendon development but given that *Tgfβ2* is thought to be an important regulator, these are consistent with an inhibition of tendon development.

Both retinoids also appear to down-regulate genes known to be involved in muscle development: *Fgf1* (Itoh et al., 1996) and *mesenchyme homeobox 2* (*Meox2*) (Mankoo et al., 1999). *Slit1* has also been linked to myogenesis (Vargesson et al., 2001) and nerve development indicating that retinoids affect all aspects of limb development. Similarly, retinoids also down-regulate *enpp2* and *Bdnf* which have been linked to muscle and limb nervous development (Fotopoulou et al., 2010; Tucker et al., 2001a). Interestingly both retinoids also alter genes which have been connected to the control of vascular development: *hairy/enhancer-of-split related with YRPW motif 1* (*Hey1*) (Fischer et al., 2004) or its inhibition: *Lect1* (Shukunami et al., 2005).

Overall, these observations suggest that these developmental processes are being inhibited in response to retinoid, consistent with the functional analyses described previously.

Genes showing differential regulation by the two retinoids tested.

As shown in table 5.1 some genes appear to be altered to a greater extent after treatment with only one of the retinoids. Selected genes which are only seen to exhibit 2 fold change significantly in response to ATRA are shown in table 5.11. It can be seen that only ATRA induces the following genes expressed in the proximal wing: *Lix1 homologue (chicken)* (*Lix1*) (Swindell et al., 2001) and down-regulates genes expressed in the distal or posterior wing: *Gastrulation brain homeobox 2* (*Gbx2*) (Niss and Leutz, 1998), *Msx1* (Zhang et al., 1997), *Lhx2* (Lu et al., 2000), *Sall1* (Farrell and Munsterberg, 2000), *tumour necrosis*

factor receptor superfamily, member 19 (*Tnfrsf19*) (Pispa et al., 2003) and *hoxa13* (Yamamoto et al., 1998) as well as altering those mentioned previously. 5' hox genes have been implicated in limb axis patterning (Boulet and Capecchi, 2004; Small and Potter, 1993) and, consistent with the change in PD axis patterning discussed previously, ATRA down-regulates *Hoxa11* and *Hoxa13*. These genes are thought to pattern the zeugopod and autopod limb segments respectively and support the idea that ATRA causes proximalisation of the limb bud cells.

Table 5.11: A selection of genes specifically altered in response to ATRA but not EC23 after microarray analysis and which may affect limb development.

Gene Name	Gene Symbol	ATRA FC
Axis patterning and retinoid responsive		
Dual specificity phosphatase 5	*Dusp5*	+2.8
Lix1 homologue (chicken)	*Lix1*	+10.3
Gastrulation brain homeobox 2	*Gbx2*	-2.4
Msh homeobox 1	*Msx1*	-2.1
LIM homeobox 2	*Lhx2*	-2.6
Sal-like 1 (Drosophila)	*Sall1*	-3.0
tumour necrosis factor receptor superfamily, member 19	*Tnfrsf19*	-2.3
Homeobox a11	*Hoxa11*	-2.8
Homeobox a13	*Hoxa13*	-13.0
Cartilage Development		
Collagen type VI α3	*Col6α3*	+2.6
Dispatched homologue 1	*Disp1*	-2.7
Doublecortex	*Dcx*	+2.8
ecotropic viral integration site 1	*Evi1*	-2.6
FRAS1 related extracellular matrix 1	*Frem1*	-4.7
Noggin	*Nog*	+5.9
Paired box 9	*Pax9*	-4.1
Sulfatase 1	*Sulf1*	-2.1
Syndecan 3	*Sdc3*	+2.7
Tendon Development		
Scleraxis	*Scx*	-2.3
Nervous Development		
Activated leukocyte cell adhesion molecule	*Alcam*	-3.4
Muscle Development		
calcium channel, voltage-dependent, gamma subunit 4	*Cacng4*	-2.3
Delta-like 1 (Drosophila)	*Dll1*	-2.3
Myogenic differentiation 1	*MyoD1*	-9.2
Vascular Development		
Angiopoeitin 2	*Angpt2*	-3.6

+ denotes up-regulation; - denotes down-regulation.

Interestingly, both *hoxa11* and *hoxa13* have been implicated in cartilage and muscle patterning, indicating as before, that developmental processes are delayed in the retinoid response. This is further supported by the down-regulation of other genes which may be involved in the control of cartilage development: *Dispatched homologue 1* (*Disp1;* (Tsiairis and McMahon, 2008)), *Dual specificity phosphatase 5* (*Dusp5*; (Bobick and Kulyk, 2008)), *Pax9* (LeClair et al., 1999) and *Sulfatase 1* (*Sulf1*; (Zhao et al., 2006)); tendon development: *scleraxis* (*Scx*; (Schweitzer et al., 2001)); nerve development: *Activated leukocyte cell adhesion molecule* (*Alcam*; (Weiner et al., 2004)) and *Gbx2* (Bouillet et al., 1995; Byrd and Meyers, 2005); muscle development: *calcium channel, voltage-dependent, gamma subunit 4* (*cacng4*; (Kious et al., 2002)), *Delta-like 1* (*Dll1*; (Rios et al., 2011)) and *MyoD* (Delfini et al., 2000; Kablar et al., 1997); and vascular development: *Angiopoeitin 2* (*Angpt2*; (Kim et al., 2006)). The down-regulation of *Lhx2*, mentioned previously as a distal wing marker, also has a role in limb outgrowth (Rodriguez-Esteban et al., 1998) suggesting that normal limb outgrowth is impaired in response to retinoid. The up-regulation of *Dusp5*, which is thought to maintain stem cell potency (Chen et al., 2011b), is consistent with this hypothesis.

However, it can be seen that there is an up-regulation in some early markers of cartilage development in response to ATRA: *syndecan 3* (*sdc3*), *noggin* and *col6α3* (Brunet et al., 1998; Hall and Miyake, 2000; Quarto et al., 1993). These have been shown to be early markers of condensation and chondrogenesis which would indicate that ATRA treated wing buds are overcoming the developmental delay.

Table 5.12: A selection of the genes specifically altered in response to EC23 but not ATRA and which may play a role in limb development.

Gene Name	Gene Symbol	EC23 FC
Retinoid metabolism		
Retinaldehyde dehydrogenase 2	*Raldh2*	-4.1
Growth factors		
Fibroblast growth factor 9	*Fgf9*	-2.83
Fibroblast growth factor 16	*Fgf16*	-3.2
Cartilage development		
Bone morphogenetic protein receptor, type IB	*Bmpr1b*	-2.6
R-spondin 3 homolog (Xenopus laevis)	*Rspo3*	-2.1
Nervous development		
Leucine rich repeat and Ig domain containing 1	*Lingo1*	-2.2
Similar to KIAA0315 /// plexin B2	*Plexinb2*	-2.0
Muscle development		
Annexin A1	*Anxa1*	-2.0
bHLH transcription factor beta3	*Beta3*	-3.4
Hepatocyte growth factor	*Hgf*	+2.3

+ denotes up-regulation; - denotes down-regulation.

It is interesting that far fewer genes are significantly altered in response to EC23 alone than to ATRA alone (compare tables 5.11 and 5.12). This is likely to be due to the fact that EC23 cannot isomerise in response to light and is metabolised to a lesser extent. Table 5.12 shows a selection of the genes which are altered in response to EC23 alone. It can be seen that EC23 down-regulates *Raldh2*, the most important retinoic acid synthesising enzyme during limb development (Niederreither et al., 1999). This provides further evidence that the limb bud cells are less able to metabolise EC23 compared to ATRA (see chapter 4). In addition to the *Fgfs* described previously (*Fgf1*, *Fgf13* and *Fgf18*), EC23 down-regulates two further *Fgfs*. *Fgf9* has been documented to be expressed in the AER and is involved in the development of the stylopod (Hung et al., 2007) as well as *Fgf16*

whose role in limb development is unknown, although it does play a role in limb initiation in Zebrafish (Nomura et al., 2006). This is consistent with the previous finding that EC23 down-regulated target genes are enriched in positive regulators of epithelial proliferation.

Bmpr1b (Karamboulas et al., 2010; Pizette and Niswander, 1999) and *Rspondin2* (Aoki et al., 2008) have been implicated in cartilage development supporting the idea that cartilage differentiation is impaired. Other developmental processes are also down-regulated in response to EC23: nervous development (outside of the limb): *Lingo1* (Okafuji and Tanaka, 2005) and *PlexinB2* (Perala et al., 2010); and muscle development: *AnnexinA1* (Bizzarro et al., 2010) and *bHLH transcription factor beta3* (*Beta3*) (Peyton et al., 1996). Conversely there is an up-regulation of *hepatocyte growth factor* (*Hgf*) expression which is known to be involved in the early stages of myoblast migration (Ohuchi and Noji, 1999) indicating that the effects of EC23 on muscle development need further characterisation. From its expression pattern in the chick wing, *Hgf* has also been implicated in limb outgrowth (Heymann et al., 1996).

Therefore it can be seen that the response to both EC23 and ATRA is to inhibit limb development. Due to the differences in metabolism and isomerisation of these compounds, it appears that ATRA treated pools can overcome this delay earlier than EC23 treated pools and begin cartilage differentiation. It can also be seen that ATRA alters the expression of more genes with PD restrictions. This supports the evidence that limb re-specification is occurring and that it is occurring earlier than in EC23 treated wings.

Validation by qPCR.

To confirm microarray analysis by another technique, validation was carried out using real time quantitative PCR on selected genes. The genes validated were: *Raldh2*, *Cyp26A1*, *Emx2*, *Meis2*, *Hoxb8*, *Hoxa13*, *Lhx9*, *n-cadherin*, *Hgf* and *Col6α3*. Their regulation after microarray analysis and the reason for analysis is shown in the table 5.13 below.

Table 5.13: The targets chosen for validation with qPCR.

Gene	Regulation	Biological Reason
Raldh2	↓ EC23 only	Retinoid metabolism (Niederreither et al., 1999)
Cyp26a1	↑ Most in both	ATRA target and retinoid metabolism (White et al., 1997)
Meis2	↑ in both	Proximal marker (Mercader et al., 2000)
Emx2	↑ in both	Proximal and scapula marker (Prols et al., 2004).
Hoxa13	↓ in ATRA	Distal Marker (Yamamoto et al., 1998)
Hoxb8	↑ in both	Patterns posterior wing and retinoid responsive (Stratford et al., 1997)
Lhx9	↓ in both	Anterior marker (Nohno et al., 1997)
N-Cadherin	↓ in both	Early condensation marker (Oberlender and Tuan, 1994b)
Hgf	↑ in EC23	Limb skeletal muscle migration (Mic and Duester, 2003)
Col6a3	↑ in ATRA	Early chondrogenesis (Quarto et al., 1993)
Gapdh	-	Housekeeping

↑ denotes up-regulation; ↓ denotes down-regulation.

qPCR targets were chosen such that each mode of regulation could be validated as shown in table 5.13. Figure 5.11 shows the expression of *glyceraldehyde-3-phosphate dehydrogenase* (*Gapdh*), used in the present study as a housekeeping gene to which gene expression was normalised, remains constant in all pools of RNA treated with retinoid or DMSO. The first DMSO treated pool is an exception to this and the expression of all genes assayed by qPCR are altered in this pool. This has caused the alteration in gene expression between DMSO and retinoid treated pools to be statistically insignificant for the following genes e.g. *Raldh2, Hoxa13* and *Cdh2*. Due to this, it is recommended that this data and the conclusions herein are considered preliminary until another pool of RNA can be analysed.

However, it can be seen from figures 5.12 and 5.13 that qPCR validates the microarray analysis as the genes analysed follow the trends seen in the microarray analysis. That said, qPCR does indicate that some genes thought to be specific to one retinoid is also seen to be significantly altered in response to the other retinoid e.g. *Col6α3, Hgf* and *Hoxa13* (figure 5.13C). This could be due to the fact that the qPCR method is significantly more sensitive than microarray analysis. However, it should be noted that the "specific" genes tested are altered further in the RNA from treatment with the "specific" retinoid. This is consistent with the comparison of microarray chips hybridised to RNA from ATRA and EC23 treated wing buds which yielded very few significantly altered genes (table 5.3) even when the fold change was lowered to >1.5fold. Therefore, it is likely that both retinoids alter the

same targets but the magnitude of their response differs and may be the cause of the differences in phenotypes seen. This has wider implications in that, given that EC23 is more resistant to CYP26 mediated metabolism, this indicates that the metabolites are unlikely to be altering gene expression in the anterior wing bud as there is in fact little qualitative difference between the two retinoids.

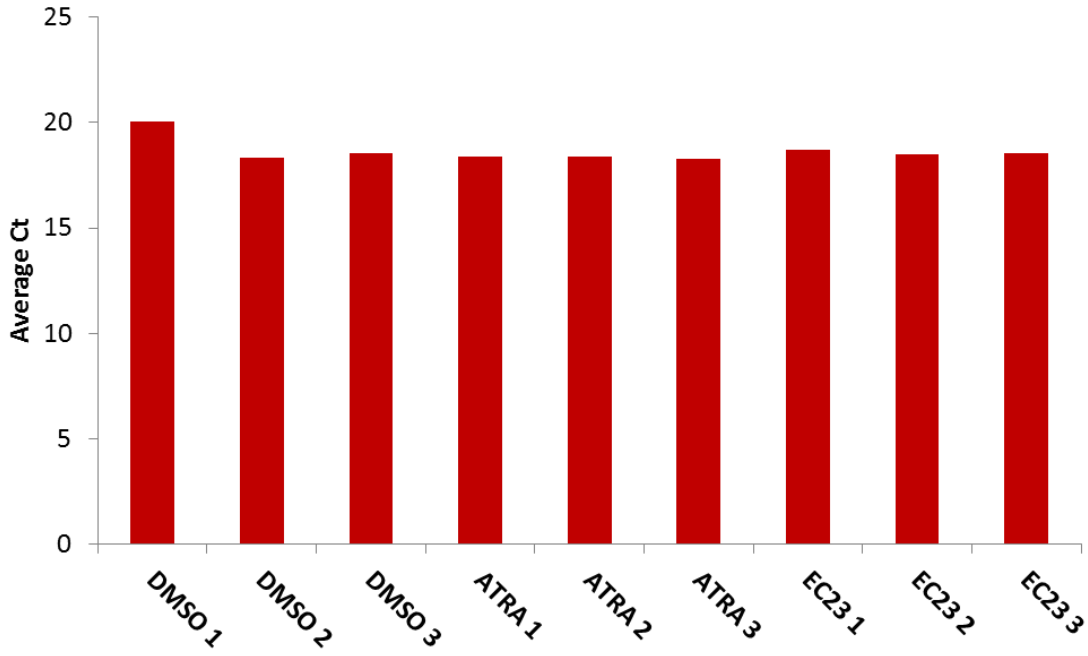

Figure 5.14: The Expression of *Gapdh* in response to all treatments.
Numbers refer to the replicate of RNA. Average CT is the number of cycles taken for the gene to be expressed.

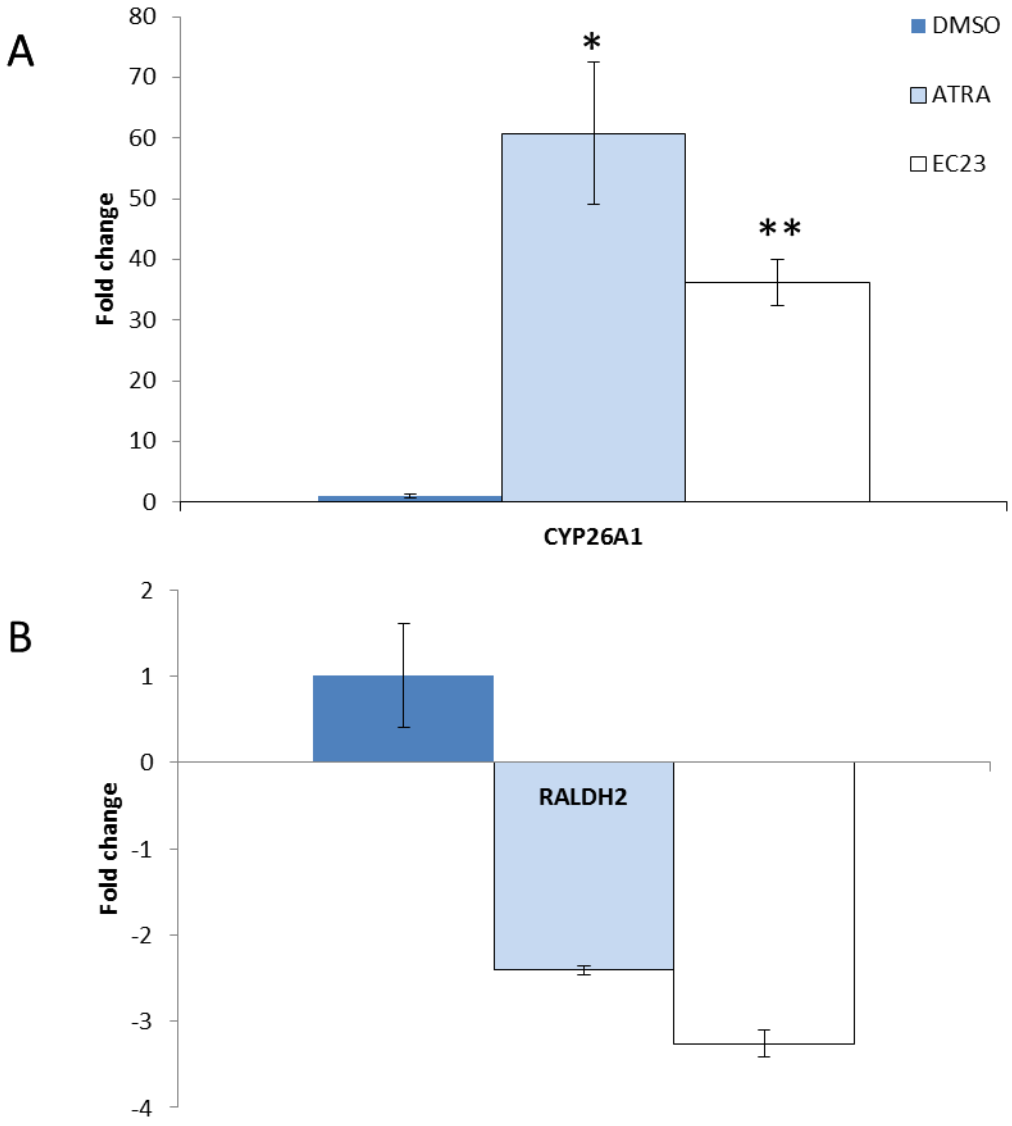

Figure 5.15: qPCR validation of the genes involved in retinoid metabolism after ATRA or EC23 treatment.

A) shows the expression of *CYP26A1* by qPCR. B) shows the expression of *Raldh2* by qPCR. Fold change is with respect to DMSO treated wing buds. RNA used was from the same pool as the RNA used for the original microarray analysis. N=3, error bars ± standard deviation. Statistical significance was tested using unpaired students t-test. * $p<0.05$, ** $p<0.01$, *** $p<0.001$.

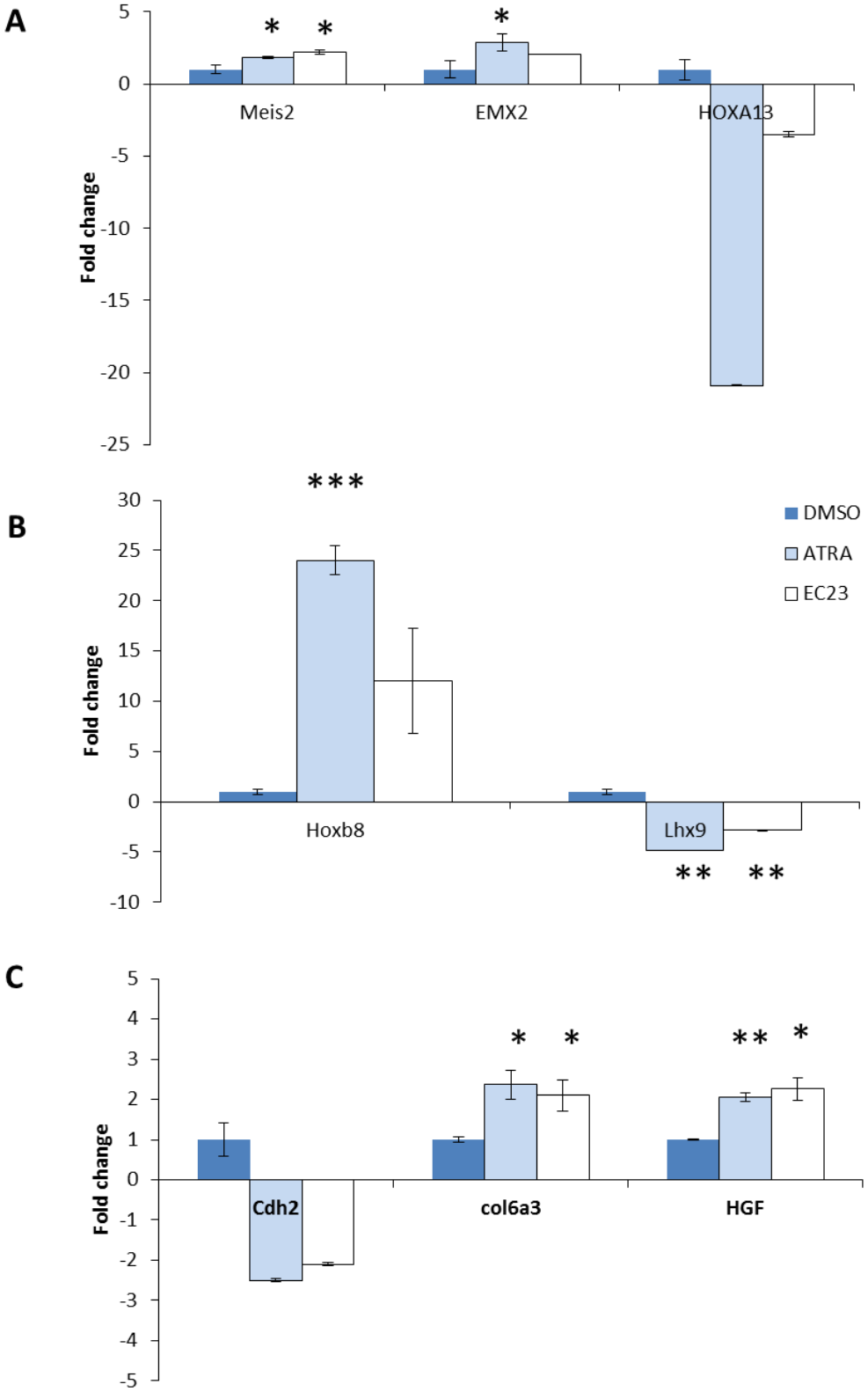

Figure 5.16: qPCR validation of genes involved in wing bud axis patterning or differentiation after retinoid treatment.

A) shows validation of genes known to be involved in PD axis patterning. B) shows validation of genes involved in AP axis patterning. C) shows validation of genes involved in differentiation processes. Fold change is with respect to DMSO treated wing buds. RNA used was from the same RNA pool as that used for the original microarray analysis. N=3, error bars ± standard deviation. Statistical significance was tested using unpaired students t-test. * $p<0.05$, ** $p<0.01$, *** $p<0.001$. For abbreviations see table 5.13.

Discussion:

The results outlined in this chapter have investigated the genetic response of the anterior wing bud to 24hrs treatment with ATRA or EC23. It has been seen that EC23 and ATRA alter similar genetic targets and that any differences between these retinoids are likely to be due to magnitude of retinoid response and differences in their metabolism: ATRA consistently alters genetic targets to a greater extent than EC23 treated wings. This is notable when the mean fold change of the 30 most up-regulated common genes is compared: 21.82 in ATRA treated wings versus 14.62 in EC23 treated wings. Similarly, comparison between the 30 most down-regulated genes shows the mean down-regulation as -8.68 in ATRA and -5.66 in EC23. This is also supported by the low number of significantly altered genes after comparison between EC23 treated and ATRA treated wing bud RNA pools (table 5.2). It has also been seen that both retinoids appear to alter genes involved in axis patterning but only *Hoxb8* associated with early digit duplication (tables 5.6 and 5.7). Of particular significance is that the retinoid targets indicate that at these quantities and concentrations of EC23 and ATRA, retinoids inhibit limb development (tables 5.8-10). This is particularly evident from the inhibition of endogenous *Shh* expression in the posterior of the retinoid treated wing (figure 5.10). Interestingly, from the genetic targets and the up-regulation of *Shh* expression after 30hrs in ATRA but not EC23 treated wing buds, it appears that ATRA treated wing buds overcome this developmental inhibition earlier than EC23 treated wing buds (figure 5.10, tables 5.11 and 5.12). This may be due to their differences in metabolism and may provide a mechanism for the differences in digit duplications seen. The target genes and their implications are discussed in the following sections.

Functional classification and clustering.

The clustering of microarray data and functional classification of the genes indicate that EC23 and ATRA treatments initiate a similar response. This is due to the fact that despite its dissimilar structure EC23 behaves as a retinoid. Considering the structure of EC23, this observation further supports evidence that the trimethylcyclohexenyl ring and carboxylic acid groups are significant for RAR binding and retinoid signalling (Barnard et al., 2009). The fact that ATRA treated wing buds overcome their developmental delay earlier than EC23 treated wing buds (tables 5.3 and 5.4; discussed later) may be due to the differences

in metabolism of these compounds. EC23 is metabolised to a lesser extent than ATRA (chapter 4) and therefore may directly affect retinoid responsive genes for a longer period as the ATRA analogue is still present. This would be consistent with evidence that the related retinoid, TTNPB, activates *β2RARE* driven *luciferase* for a longer time period than ATRA (Pignatello et al., 1999), and implies that metabolism of the excess retinoid is an important part of the retinoid response.

On the other hand, controversial evidence has been produced on the effects of the retinoid metabolites (Niederreither et al., 2002a; Pijnappel et al., 1993; Reijntjes et al., 2005). 4-*oxo*-retinoic acid and 4-*hydroxy* retinoic acid are produced by the CYP26 enzymes and are two of the primary metabolites of ATRA. Genetic studies in mouse infer that the CYP26 enzymes function to eliminate excess retinoid from the developing embryo and maintain appropriate ATRA levels (Niederreither et al., 2002a; Topletz et al., 2012; White et al., 1997). However, 4-*oxo*-RA has been documented to cause effects of its own (Pijnappel et al., 1993) and in fact to rescue VAD (Reijntjes et al., 2005). Therefore, in the ATRA treated pools there may be other retinoid derivatives responsible for the genetic response. Perhaps, it is more likely that the CYP26 metabolism products are having the biggest effect on the ATRA genetic targets. The resistance of metabolism observed with EC23 would cause the dynamic turn-over of retinoid to be inhibited which may be necessary for differentiation processes. This is supported by the fact that ATRA alters the expression of more genes than EC23 and that the genes altered have a wide range of interacting functions as shown in the DAVID functional classifications. This would be expected from a greater range of retinoids in the ATRA treated wing buds. However, analysis of EC23 and ATRA treated wing bud RNA treated microarray chips indicate that there is little significant difference between EC23 and ATRA. This suggests that in fact the metabolites have little effect in the developing wing at this time and therefore may implicate stalling as the reason for the apparent differences.

Likewise the fact that EC23 is also photostable may generate a different set of genetic targets. ATRA undergoes isomerisation to 9-*cis* RA and 13-*cis* RA in response to light (Christie et al., 2008; Thaller et al., 1993). These compounds have been shown to be present in developing organisms but have been associated with pathological ATRA excess (Horton and Maden, 1995) and are thought to have little significance at physiological concentrations. It has been proposed that 9-*cis* RA can activate RXR and therefore may affect: retinoid, vitamin D and PPAR receptor pathways as these can all dimerise with

RXR (Germain et al., 2006). Whether there are genetic targets of the retinoid isomers is unknown, but they may still have indirect effects in that they will reduce the concentration of active ATRA in the ATRA treated wing buds. Interestingly ATRA has also been proposed to activate PPARβδ/RXR heterodimers (Shaw et al., 2003) which will be discussed in chapter 6. During these experiments, ATRA was shielded from light during the operation procedure and eggs were incubated in the dark. Under these conditions it has been documented that ATRA is stable whereas upon exposure to light for 3 days 63% of the ATRA is degraded (Christie et al., 2008). Therefore, these isomers may cause less of an effect but it is possible that ATRA is converted to these isomers by *in vivo* enzymes as has been documented in rat embryos (Chen and Juchau, 1998).

Response of genes involved in retinoid metabolism and signalling.

Retinoids are shown to alter genes involved in retinoid metabolism and signalling (table 5.5). Consistent with the idea that excess retinoid causes malformation to the developing wing, the *Cyp26* genes are some of the most up-regulated. This response supports the idea that the limb is trying to eliminate excess retinoid by conversion to oxidative derivatives as suggested by Niederreither et al (2002). Manipulations of *Cyp26b1* have also generated similar phenotypes to those observed in chapter 3 and will be discussed later. Also highly up-regulated are other genes known to be retinoid responsive and involved in the retinoid signalling pathway e.g. *dhrs3* and *Rarβ2*. *Dhrs3* has been shown to inhibit retinoid production by a negative feedback mechanism on the conversion of retinol to retinal (Feng et al., 2010). This combined with the up-regulation of *Cyp26* is consistent with the hypothesis that the limb is regulating retinoid levels tightly in the developing wing bud and eliminating the excess. *Rarβ* has been proposed to be the receptor which modulates retinoic acid teratogenesis in the branchial arches (Matt et al., 2003). Given the expression domain of *Rarβ2* (chapter 4; (Smith et al., 1995)) and the fact that retinoid induced reorganisation of the AER occurs via the mesenchyme (Tickle et al., 1989), activation of RARβ in the limb could occur in the present study and explain the absence of other *Rar* subtypes in the datasets. Interestingly *Cyp1b1* is also up-regulated in response to both retinoids. *Cyp1b1* has been shown to convert retinol to ATRA without the intermediate oxidation step (Chambers et al., 2007). This could indicate a dysregulation of retinoid metabolism or that *Cyp1b1* is capable of converting ATRA back into retinol to maintain correct retinoid levels in the developing limb.

The significant down-regulation of *Raldh2* in EC23 but not ATRA treated wing buds is also of interest. *Raldh2* is thought to be the most important ATRA synthesising enzyme during embryonic development as its knock out demonstrates that it is essential for the early stages of embryonic development (Niederreither et al., 1999). The other retinaldehyde dehydrogenases are very restricted during development (Mic et al., 2000) but, more particularly for this study, have not been linked to limb development and are also not altered here. *Raldh2*, however, is known to be expressed at the proximal wing bud (Swindell et al., 1999) and knock out of *Raldh2* causes severe limb malformations in mouse (Mic et al., 2004; Niederreither et al., 2002b). Knockout of both *Raldh2* and *Cyp26a1* in mouse partially rescues the phenotypes seen with *Raldh2* single knockout mice (Niederreither et al., 2002a) indicating that correct ATRA levels rather than oxidative derivatives are important for embryonic development. Similar to *Dhrs3* up-regulation, down-regulation of *Raldh2* indicates a further decrease in the level of retinoid production to regulate the levels of ATRA present. This further decrease in retinoid production in EC23 treated wings is consistent with the idea that EC23 is potentially resistant to metabolism. It could be hypothesised that as EC23 is not metabolised, retinoid levels are increased and the CYP26 enzymes are overcome. This could cause the secondary effects of decreasing retinoid synthesis via *Dhrs3a* and *Raldh2* in EC23 treated wing buds. As the CYP26 enzymes can metabolise ATRA the ATRA treated wing bud does not decrease retinoid production to the same extent.

Retinoid responsive genes in the anterior wing may be common to other organ systems and the general teratogenic response.

The microarray data presented here is the first analysis of retinoid responsive genes *in vivo* using the chick wing bud as a model system. Other studies of retinoid responsive genes have mainly used *in vitro* models (Ali-Khan and Hales, 2006; Qin et al., 2002; Williams et al., 2004). Ali-khan and Hales (2006) have presented data on mouse limb retinoid responsive genes after 3hrs cultured in response to retinol. There are some similarities in the retinoid responsive genes in that both retinoid responses involve the up-regulation of *Wnt11* and *Ror1*. However, their analysis did not yield any genes significantly down-regulated by vitamin A whereas from the current analysis it can be seen that more genes are down-regulated than are up-regulated by retinoid.

Some genes up-regulated after 3hrs culture were down-regulated after 24hrs treatment here: *Snai2*, *Hey1* and *Msx1* (Ali-Khan and Hales, 2006). This is most likely due to the fact that Ali-Khan and Hales analysed direct retinoid targets by investigating gene expression after 3hrs, particularly given that microarray analysis after 6hrs retinoid treatment showed 21 genes to be down-regulated (Qin et al., 2002). This suggests that many genes altered in the present study may be indirect targets of the two retinoids. The differences between these two arrays may indicate the differences between retinoid compounds used, exposure time, species and treatment method. Interestingly and despite these differences, both the present study and that of Ali-Khan and Hales (2006) have concluded that the retinoid response is impaired differentiation as a result of teratogenesis. This is consistent with the phenotypes that they have seen in that untreated cultured limbs generate three limb segments with recognisable radius, ulna, wrist elements and digits, whereas ATRA treated limbs are shorter and develop two elements with few recognisable elements (Ali-Khan and Hales, 2003). Analysis of these arrays indicates *Msx1* (Bensoussan-Trigano et al., 2011), *Pbx*, *Meis* and *insulin like growth factor* (*Igf*; (Qin et al., 2002)) as interesting avenues for further research as they have been linked to cartilage element shortening and phocomelia possibly due to impaired differentiation. This is comparable to present study where *Pbx1*, *Meis2* and *Msx1* are altered (tables 5.7 and 5.11) and can be linked to the phenotypes produced in the wing bud (later and chapter 6).

531 genes have been suggested to be concrete or potential retinoid genetic targets through the analysis of 1191 published papers depending on the evidence presented (Balmer and Blomhoff, 2002). They split the retinoid responsive genes according to regulation where group 3 were shown to be directly regulated, group 0 were implied to be retinoid regulated or indirectly regulated and groups 1 and 2 showed intermediate evidence. The genes shown in table 5.14 are those from this review (Balmer and Blomhoff, 2002) which have been seen to be retinoid responsive after 24hrs in the present study although they may not have been mentioned in the results section. Only 23 of the 531 genes were seen in the present work and often exhibit a different regulation to that suggested by Balmer and Blomhoff (2002).

Table 5.14: A list of the genes determined to be retinoid responsive in both the present study and those suggested by Balmer and Blomhoff in 2002.

Group 3		**Group 2**		**Group 1**		**Group 0**	
Present study	***Reg. BB***	***Present study***	***Reg. BB***	***Present study***	***Reg. BB***	***Present study***	***Reg. BB***
Egr1; up	Up	*Protocadherin15*; up (E)	*Cdh15;* up	*AR*; dn	Vrs	*Col4α5*; dn (A)	up *Col4α1*
Hoxa4; up	Up	*Cyp26*; up	Up	*CA2*; up (A)	Up	*Enpp2;* dn	Up
Hoxb4; up	Up	*Gbx2*; dn (A)	Up	*Cd44*; dn	Vrs	*Fgf1* ; dn	Up
Rarβ; up	Up	*Gnrh*; dn	Up	*Cdh2*; dn	Vrs	*Gsc*; up	Dn
Rbp5; up	Up *Rbp1*	*Gpx3*; up	*Gpx2*; up	*Fgf9*; dn (E)	Up	*Hgf* ; up (E)	Dn
		Gstz1/A3; up (A)	*Gstp1*; vrs	*Jun*; up (A)	Up		
		Laminin A2; dn *LaminG3*; up	*Laminin B1*; up	*Msx1*; dn (A)	Vrs		
		Meis2; up	Up	*Pth1r*; dn	Vrs		
				Slug; dn	Dn		
				Tcf1; dn	Up		
				Tgfβ2; dn	Up		

Abbreviations: Reg. BB, regulation in Balmer and Blomhoff (2002); A, ATRA; Ar, androgen receptor; CA2, carbonic anhydrase 2; dn, down; E, EC23; Egr1, early growth response 1; Gnrh, gonadotrophin releasing hormone; Gpx, glutathione peroxidase; Gstz, glutathione s-transferase zeta; Pth1r, parathyroid hormone receptor 1; Tcf1, transcription factor 1, hepatic; vrs, various.

However, Balmer and Blomhoff (2002) were not specific to any tissue but tried to list any retinoid responsive genes at the time. They also were not specific to any species and for many of the genes listed; there is no known validated sequence in chicken. Interestingly only 21% of the genes seen to be retinoid responsive in this study and suggested by Balmer and Blomhoff (2002) are known to be directly regulated. This is consistent with the idea that many of the targets seen in the present study are indirect targets of ATRA and EC23 as mentioned with respect to down-regulated genes.

A recent study has been conducted to investigate conserved genes responsive to retinoic acid using analysis of promoter regions for DR5 RAREs within 10kBp from transcription start sites. Only 6 RAREs are conserved between all jawed vertebrates one of which is *Meis1*. They found that 138 genes have RAREs conserved between mouse and human and the following were also altered in the present study: *enpp2*, *Hey1*, *Hoxb3*, *Meis2*, *Rarβ* and *Ror1*. They note that other genes e.g. *Gbx2* and *Cyp26b1*, both of which are retinoid

responsive here, are not present in their dataset as they used 10kBp from the start and highly conserved genes as their criteria (Lalevee et al., 2011).

Interestingly, despite species differences, some of the genes presented in this study as retinoid responsive have also been shown to be retinoid responsive in the mouse (Ali-Khan and Hales, 2006), Zebrafish (Feng et al., 2010) and the rat (Luijten et al., 2010) as shown in table 5.15. Feng et al (2009) treated zebrafish embryos with ATRA and an antagonist to elucidate retinoid targets. The following genes were up-regulated in response to ATRA in both this study and that of Feng et al (2009): *Hoxa4*, *Dhrs3*, *Cyp26a1*, *Wnt11*, *Meis2* and *Hoxb5*. Retinoid decreased the expression of *Raldh2* and *Lrrn6* in both studies. Interestingly, unlike Ali-Khan and Hales (2006), the study by Feng et al (2009) was not specific to the limb bud but investigated the whole embryo response and treatment was for 5hrs. Recently, Luijten et al (2010) used whole rat embryo culture to investigate the teratogenic effects of ATRA. Many genes found altered after retinoid treatment for 24hrs are also in the dataset from Luijten et al after 4hrs of retinoid treatment: *Cyp26A1*, *Dhrs3*, *Dlx5*, *Dusp5*, *Enpp2*, *ecotropic viral integration site 1* (*Evi1*), *fgf18*, *Gbx2*, *Hey1*, *Hoxa5*, *Meis2*, *neural precursor cell expressed, developmentally down-regulated 9* (*Nedd9*), *Pax9* and *Rarβ*. As with the genes from Feng et al (2009) there are some similarities despite the fact that the species, treatment method and treatment times are different. The genes common to this study, Ali-Khan and Hales (2006), Feng et al (2009) and Luijten et al (2010) may therefore form genes of a more "general retinoid response". Table 5.15 shows the genes seen in this study and those others with those in bold as seen in the present study and 2 or more others. These genes may form part of the general ATRA response: *Cyp26*, *Meis2* and *Dhrs3* as the studies exhibiting these used ATRA as the treatment. Those others may form a more general retinoid response and may, on further study, be particular to one tissue.

Table 5.15 : Genes determined to be retinoid responsive in the present study and their comparison with others.

Study	Retinoid responsive genes
Balmer and Blomhoff (2002)	*Egr1*, ***Hoxa4***, *Hoxb4*, ***Rarβ***, ***Cyp26***, ***Gbx2***, ***Meis2***, *AR, Ca2, Cd44, Cdh2, Fgf9, Jun, Msx1, Pth1r, Slug, Tcf1, Tgfβ2,* ***Enpp2***, *Fgf1*, *Gsc* and *Hgf.*
Ali-Khan and Hales (2006)	*Hoxa11*, *Ror1*, *Snai2*, *Hey1*, *Jun* and ***Wnt11***.
Feng et al (2009)	***Hoxa4***, ***Dhrs3***, ***Cyp26a1***, ***Wnt11***, ***Meis2***, *Hoxb5*, *Raldh2* and *Lrrn6*
Luijten et al (2010)	***Cyp26A1***, ***Dhrs3***, *Dlx5*, *Dusp5*, ***Enpp2***, *Evi1*, *Fgf18*, ***Gbx2***, *Hey1*, *Hoxa5*, ***Meis2***, *Nedd9*, *Pax9* and ***Rarβ***

Genes in bold are genes present in 2 or more studies.

It could also be proposed that these genes may form a more general "teratogen response" activated in the embryo to ensure that normal development is continued as soon as possible. Huang and Hales (Huang and Hales, 2009) investigated the genetic response to cyclophosphamide in mouse limbs cultured for 3hrs. They proposed that there was a general teratogenic response based on the following genes with those in bold appearing altered in the present study: *hypoxia inducible factor 1α* (*hif1α*), *necdin* (*ndn*), ***hes1***, *myogenin* (*myog*), ***egr1***, *E2F transcription factor 1* (*e2f1*), ***bmpr1b***, *phosphoprotein enriched in astrocytes 15* (*pea15*), *Harvey rat sarcoma virus oncogene 1* (*hras1*), *Mad homologue 1* (*smad1*), *V-abl Abelson murine leukaemia oncogene 1* (*abl1*) and *transcription terminator factor 1* (*ttf1*); and that it was hypoxia related. Again, despite the difference in species and compound investigated some genes or their homologues are common to both Huang and Hales (2009) and the present study: *Hey1* and *Egr1*. *Hey1* is a notch target gene and has been implicated in embryonic vascular differentiation from its knockout mouse which is suggested to be due to impaired differentiation (Fischer et al., 2004). *Egr1* has been implicated in zebrafish oculogenesis due to the phenotype produced by mopholino knock down which manifests as impaired differentiation (Hu et al., 2006). The presence of these genes in the present study suggests that the response to teratogen is to impair differentiation and is consistent with the hypothesis that retinoids stall wing development. *Bmpr1b*, which is only responsive to EC23 in the present study, suggests that dysregulated BMP signalling may have formed an earlier part of the ATRA response (Ali-Khan and Hales, 2006) and may control the teratogenic response. These genes would be an interesting avenue for further research into teratogen as well as retinoid response.

Stalling.

As mentioned in the results section, it can be seen that application of both retinoids to the anterior wing bud causes an inhibition of differentiation usually occurring at this stage (tables 5.4, 5.8, 5.9 and 5.10). This suggests that the development of the anterior wing bud at this stage of the retinoid response is stalled when compared to the DMSO treated wing bud. The phenotypes presented in chapter 3 after treatment with either retinoid included a decrease in limb outgrowth as evidenced by the shortening of cartilage elements and supported by the genetic targets seen in this chapter (table 5.8). The decrease to endogenous *Shh* expression observed after 30hrs retinoid treatment (figure 5.10) further supports the idea that the response to retinoid is to stall limb development and outgrowth. *Shh* is known to indirectly regulate limb size by maintaining a positive feedback loop with FGFs in the AER (Niswander et al., 1994) and knock-down of *Disp1*, required for long-range SHH signalling, in mice causes shortening of the long bones (Tsiairis and McMahon, 2008). Limb outgrowth is stopped when this signalling loop cannot be maintained due to the expansion of non-*Shh* expressing cells previously belonging to the ZPA (Scherz et al., 2004). As there is a decrease in *Shh* expression here, it would follow that there would be a concomitant decrease in FGF4 signalling in the posterior forelimb bud. However, given that the current analysis investigated the retinoid genetic targets of the anterior wing bud, alteration to *Fgf4* expression would not be expected in the tissues analysed.

Previously, SHH was thought to specify digit identity along the anterior-posterior axis. It is still thought that SHH concentration is important for posterior digit identity (Harfe et al., 2004; Towers et al., 2008; Zhu et al., 2008a) but that SHH is also important for maintaining proliferation in the anterior wing for anterior digit specification (Towers et al., 2008). Paradoxically a decrease in posterior SHH here results in normal digit 123 development and often duplication of at least the most anterior digit. This could be due to the fact that whilst endogenous *Shh* is decreased in response to retinoid, after the limb has recovered *Shh* may be maintained for the same length of time to allow normal limb development in a similar manner to its expression after application of an inhibitor of proliferation (Towers et al., 2008).

Consistent with a down-regulation of endogenous *Shh* and inhibition of limb outgrowth many genes which are down-regulated after retinoid treatment are involved in regulating limb outgrowth (table 5.8). *Tbx5* has been implicated in determination of forelimb identity

and scapula development but it is also linked to limb outgrowth (Rallis et al., 2003), particularly of the anterior limb in which SHH-dependent proliferation is also proposed to be important (Towers et al., 2008). *Lhx9* has also been implicated in limb outgrowth due to its knockout mouse phenotypes (Rallis et al., 2003; Tzchori et al., 2009). Increased levels of *Tgfβ2* have been shown to inhibit mesodermal proliferation (Lorda-Diez et al., 2010) and therefore, similar to *Msx1*, the retinoid treated wing buds may be attempting to normalise development by increasing proliferation. Developmental stalling and the implications for the phenotypes observed in chapter 3 are further discussed in chapter 6.

Cartilage development.

One of the crucial points in limb development is the development of cartilage. The cartilage is the first tissue to differentiate in the limb and cartilage condensations are the first morphological sign of differentiation. The cartilage is then thought to act as a template for the other tissues: tendon, muscle and nerve (Duprez, 2002). As previously mentioned some of the earliest markers of cartilage condensation are: *Noggin*, *Syndecan3*, *Bmpr1b*, *n-cadherin* and *Tgfβ2*. These genes are all altered in response to one or both of the retinoids here. During condensation *collagen type II* is switched on with *collagen type IX* (Hall and Miyake, 1995) concurrent with significant alteration to the ECM. Interestingly, *collagen type IX* is down-regulated in response to both retinoids.

Tgfβ2 is needed to allow the process of chondrogenesis to occur in the condensations and acts upstream of *n-cadherin* (Miura and Shiota, 2000) which has been shown to be necessary for the production of cartilage condensations. Consistent with this *Tgfβ2* and *n-cadherin* are down-regulated in response to both retinoids. This suggests that cartilage condensation is inhibited in response to both retinoids. Low levels of *Dlx5* and *Dlx6* (as seen after both retinoids) can inhibit cartilage development (Hsu et al., 2006; Robledo et al., 2002). *Pax9* is also known to be involved in cartilage development (LeClair et al., 1999) and is down-regulated in this array consistent with inhibition of cartilage development. *Thrombospondin4* and *Dcx* are known to be involved in cartilage development and their expression increases and decreases during differentiation respectively (James et al., 2005). However, in this microarray analysis the expression of these genes is reversed and *Dcx* is only altered in response to ATRA. *Fgf18* has been shown to be down-regulated in response to both retinoids. FGF18 has been implicated in the regulation of chondrogenic differentiation (Ohbayashi et al., 2002), particularly in the

mouse cranial structure (Hajihosseini and Heath, 2002) where it is shown that deficiency of *Fgf18* causes delayed development of cartilage and bone (Ohbayashi et al., 2002). The alteration of these genes is consistent with the data presented in chapter 4 which suggests that both retinoids inhibit cartilage development.

Analysis of the ATRA or EC23 specific genes suggests that ATRA treated wing buds are recovering from the inhibition of wing development initiated as a retinoid response which is consistent with the observation that there is an enrichment of genes involved in embryonic skeletal and limb development in response to ATRA but not EC23 (tables 5.3 and 5.11). EC23 appears to inhibit limb outgrowth to a greater extent than ATRA as it down-regulates *Fgf9*, a growth factor secreted from the AER and which is involved in outgrowth. This is consistent with the functional classification of down-regulated retinoid treated genes (table 5.4). Similarly, *Lhx2* (down-regulated in ATRA table 5.11) has been shown to control limb outgrowth in both mouse (Tzchori et al., 2009) and chick (Nohno et al., 1997) and therefore indicates limb outgrowth is still inhibited. ATRA treated anterior wing buds, however, appear to be recovering from inhibition of limb outgrowth. It has been shown that defects seen in *Shh* knockout mice can be partially rescued by decreasing *Msx1* expression and hence apoptosis (Lallemand et al., 2009). *Msx1* with *Msx2* has been shown to control anterior limb apoptosis (Lallemand et al., 2005) and therefore down-regulation of *Msx1* in the anterior wing in response to ATRA is consistent with an attempt to preserve normal limb development. It has also been implicated in the control of digit identity (Bensoussan-Trigano et al., 2011; Lallemand et al., 2005).

Cd44 and *Syndecan3* have been implicated in the control of cartilage condensation boundaries (Behonick and Werb, 2003; Hall and Miyake, 1995). While *Cd44* is down-regulated in response to both retinoids suggesting inhibition of cartilage development, *Syndecan 3* is up-regulated in response to ATRA. There is also an up-regulation of *col6α3* after ATRA treatment which has been implicated in the earliest stages of cartilage development (Quarto et al., 1993). Similarly, *Bmpr1b* and *noggin* are both known to be expressed in cartilage condensations (Capdevila and Johnson, 1998; Kawakami et al., 1996; Pizette and Niswander, 2000; Zhu et al., 2008a). As shown they are differentially regulated after retinoid application: *Bmpr1b* is down-regulated after EC23 treatment while *noggin* is up regulated after ATRA treatment (tables 5.11 and 5.12). It has been shown that knock out or production of dominant negative *BMPR1B* causes decreased or absent cartilage condensations (Ashique et al., 2002; Karamboulas et al., 2010). The down-

regulation of *Bmpr1b* in response to EC23 is further evidence that cartilage differentiation is being inhibited. The up-regulation of *noggin* in response to ATRA, however, is evidence that ATRA treated wing buds are overcoming the inhibition to limb development and initiating the early stages of condensation consistent with the enrichment of embryonic skeletal development in ATRA up-regulated genes during functional clustering. Both retinoid treatments indicate that BMP signalling is altered as part of the response. Both retinoid treatments also indicate that limb outgrowth and cartilage differentiation is inhibited but that ATRA treated wing buds are overcoming this delay in development.

Tendon and muscle development:

Although early stages of limb development are centred on cartilage condensation, other processes are also occurring such as early differentiation of muscle and tendon progenitors. Similar to cartilage markers, these are also altered in response to retinoid indicating that limb development is inhibited. *Fgf18* has been shown to be expressed later in distal tendons and *Tgfβ2* has been implicated as a regulator of tendon development as it modulates the expression of *col12* and *col14* (Edom-Vovard and Duprez, 2004), all of which are altered after retinoid treatment (tables 5.8 and 5.10). It has also been suggested that *Tgfβ2* is needed to maintain the survival of tendon progenitor cells during limb development (Pryce et al., 2009). *Tgfβ2* has also been suggested to act upstream of the tendon marker *scleraxis* when applied to micromass cultures (Lorda-Diez et al., 2009; Pryce et al., 2009), also down-regulated in response to ATRA. These alterations indicate that tendon development may be inhibited in response to retinoid but more so in response to ATRA.

With respect to muscle development, these retinoids differentially regulate many factors involved in differentiation (tables 5.11 and 5.12). Of particular interest, *Wnt11* is up-regulated in response to both ATRA and EC23. *Wnt11* has been implicated in the patterning of muscle during limb development, particularly the regulations of fast vs. slow myocytes produced (Anakwe et al., 2003) which suggests that muscle patterning is occurring in retinoid treated wings but perhaps at an aberrant developmental stage. However, *Hgf* was shown to be up-regulated in response to EC23 alone. *Hgf* is known to be expressed ubiquitously in the limb until HH22 when it is expressed in anterior and posterior stripes and then is distally restricted by HH23 (Heymann et al., 1996). During limb development it has been implicated in regulating the migration of muscle progenitors

to the developing limb (Ohuchi and Noji, 1999) and if injected causes a down-regulation of *MyoD1* and muscle differentiation, maintaining cells in an undifferentiated state (Scaal et al., 1999). Increased *Hgf* expression in the anterior wing may therefore indicate that limb development has been inhibited and that the cells are in a less differentiated state with respect to muscle development. The differential effect on *Hgf* expression between EC23 and ATRA is consistent with the functional clustering whereby ATRA decreases muscle development while there is no evidence for enrichment for this function with EC23. Increased *Hgf* expression is also consistent with a study by Mic and Duester (2003) which showed that *Raldh2* knockout mice altered the position of *Hgf* expression in the limb to an anterior-proximal domain (Mic and Duester, 2003). EC23 treated wings are similar in that they have reduced *Raldh2* expression and an increase in *Hgf* in the anterior wing which is consistent with the change in position of myogenesis in the previous study (Mic and Duester, 2003). It can be noted that ATRA inhibits muscle differentiation according to functional clustering and due to the down-regulation of *MyoD1* (tables 5.4 and 5.11). Given that increased *Hgf* down-regulates *MyoD1* (Scaal et al., 1999) and the differential regulation of *Hgf* and *MyoD1* by these retinoids, this is consistent with the idea that EC23 treated wing buds are more inhibited than ATRA treated wing buds causing cells to be maintained in a less differentiated state (tables 5.11 and 5.12). Therefore it can be concluded that both muscle and tendon development may be inhibited by both retinoids as well as cartilage development.

Retinoids alter limb AP patterning.

Patterning of the AP axis has been proposed to be due to the ZPA and SHH. ATRA has been shown to indirectly induce *Shh* in the anterior wing bud prior to digit duplication (Riddle et al., 1993). This *Shh* domain is thought to act as an ectopic ZPA and lead to the mirror image duplication of digits as documented (Wanek et al., 1991). This is formed following the ectopic expression of the following in the anterior mesoderm: *Hoxb8* (4hrs; (Stratford et al., 1997)), *Hand2* (20hrs; (Fernandez-Teran et al., 2000)) and *Shh* (24hrs; (Riddle et al., 1993)). As EC23 and ATRA have been shown to generate digit duplications, it would be expected that these genes were altered after 24hrs. The data presented here shows that, of these factors, only *Hoxb8* is expressed in the anterior wing 24hrs after retinoid treatment. Given the previously determined sequence of genes up-regulated to produce an ectopic ZPA, the up-regulation of only *Hoxb8* expression in retinoid treated anterior wing buds suggests the limb is in the early stages of re-specifying the AP axis**.** The

lack of these later markers of digit duplication, along with a down-regulation of differentiation markers, indicates that the quantity of retinoid applied may have stalled limb development compared to previous studies.

However, this change in *Hoxb8* expression cannot explain the differences in the types of digit duplications observed in chapter 3 (although it may be implicated-see chapter 6) as it is altered in response to both EC23 and ATRA. However, it can be seen from this study that ATRA and EC23 have a differential effect on *Shh* expression in the anterior wing: ATRA up-regulates *Shh* after 30hrs while EC23 is never seen to up-regulate it at this time point. This up-regulation of *Shh* in response to 30hrs ATRA treatment is later than observed by Riddle et al (1993) who document induction of *Shh* after 24hrs treatment. This delay in *Shh* up-regulation may be due to differences in retinoid application: Riddle et al (1993) used AG1-X2 beads to apply 1mg/ml ATRA to the anterior wing bud but as they imitated Tickle et al (1985), it is likely that they used beads of smaller diameter to the present study. It is likely that the delay to *Shh* up-regulation is due to inhibition of limb development as suggested by the down-regulation of many differentiation processes which should occur at HH23 seen from the microarray analysis. This may also provide a mechanism behind the different duplications seen with EC23 and ATRA and is discussed further in chapter 6.

There are alterations to other genes consistent with an alteration of AP axis patterning after 24hrs retinoid treatment. At the point of microarray analysis (HH23) *Lhx9* is an anterior marker (Nohno et al., 1997) and its down-regulation is consistent with a change to the AP axis (table 5.8). It may also suggest a delay to anterior digit development if *Lhx9* is induced at a later time-point in retinoid treated embryos (Wang et al., 2011), which could be an avenue for further study. Another transcription factor is also involved in limb AP polarity: *Msx1* the expression of which has been described as downstream of Gli3R in the anterior limb (Lallemand et al., 2009). Therefore, its down-regulation here (table 5.11) may also suggest that there is a change in the post-translational state of GLI3 in the anterior wing bud in response to ATRA. This would be consistent with a change in AP patterning given that high levels of GLI3A are seen in the posterior limb prior to ZPA formation (te Welscher et al., 2002).

Retinoid treatment at the high concentrations and quantities studied here, therefore, causes re-specification of the AP axis at a delayed time point compared to other studies. The

retinoid potentially resistant to metabolism alters the AP axis less, consistent with the phenotypes seen in chapter 3.

Retinoids alter limb PD patterning and cause proximalisation of limb bud cells.

The data presented in chapter 3 indicated that the entire PD axis was affected by both retinoids: reduction to the scapula, shortening and thickening of the stylopod and zeugopod, and digit duplication in the autopod. The effect on the entire PD axis of the wing may be due to retinoid effect on a process such as chondrogenesis which occurs at different time points along the PD axis (see later). However, ATRA is known to cause the up-regulation of some genes expressed proximally (table 5.7; (Mercader et al., 2000; Prols et al., 2004)) indicating that retinoids cause a change to PD patterning also consistent with these phenotypes. Many of these are involved in scapula development and these proximally restricted genes are discussed in the chapter 6. Concurrent with up-regulation of proximally restricted genes, the expression of some distally expressed genes is down-regulated, although this is more pronounced in ATRA treated wing buds (tables 5.7 and 5.11). Consistent with these alterations both EC23 and ATRA can cause proximal relocation of wing bud cells (figures 5.7 and 5.8).

ATRA treated wing buds exhibit down-regulation of *Hoxa11*, *Hoxa13*, *Lhx2* and *Msx1* amongst others which may also play an important role in the ATRA phenotypes (table 5.11). *Hoxa11* and *Hoxa13* are known to be markers of zeugopod and autopod development respectively (Rosello-Diez et al., 2011). Their down-regulation is consistent with a greater re-specification of the PD axis in response to ATRA than EC23. The down-regulation in response to ATRA but not EC23 is consistent with the differences in metabolism between these retinoids as qPCR indicates that EC23 also down-regulates *Hoxa13* but to a lesser extent (figure 5.13A). *Lhx2* has been shown to be a distal limb marker and to control limb outgrowth in both mouse (Tzchori et al., 2009) and chick (Nohno et al., 1997). *Msx1* is expressed in the distal limb adjacent to the AER (Lu et al., 2000; Zhang et al., 1997)). Therefore, ATRA down-regulates markers of distal wing development consistent with a proximalisation of limb bud cells suggested previously (figure 5.8 ;(Mercader et al., 2000; Yashiro et al., 2004)).

Mercader et al (2000) have also shown that ATRA and distally produced FGFs have an antagonistic relationship during limb development (Mercader et al., 2000). The FGFs

thought to be essential for AER function have not been altered in the present study but interestingly *Fgf9* is down-regulated in response to EC23 treatment. *Fgf9* is also known to be expressed in the AER and around chondrogenic condensations suggesting involvement in proximal cartilage development (Hung et al., 2007). This indicates that the AER function may be more compromised in response to EC23 than ATRA which is consistent with the DAVID functional classification: ATRA up-regulated genes involved in epithelial proliferation whereas EC23 down-regulated them (tables 5.3 and 5.4). Considering the increased number of distally expressed genes down-regulated in response to ATRA compared to EC23, this is consistent with a greater change in PD patterning in response to ATRA. This is also consistent with the hypothesis that limb development is further inhibited in response to EC23 than ATRA.

A consequence of the up-regulation of these proximally restricted genes is that ATRA and EC23 have been shown to affect limb bud cell affinity here (figures 5.7 and 5.8) and by Mercader et al (2000). ATRA causes the proximal relocation of chick limb bud cells which is mimicked by EC23. Although differential effects are seen on digit development between these retinoids, their effect on proximal relocation is the same consistent with the similarities in their effects on proximal limb development: both can cause scapula malformations and shortening of more proximal cartilage elements.

Previous investigation into retinoid alteration of PD identity has suggested the alteration of adhesive properties. When mixed limb bud cells are known to sort into their PD, AP regions in a stage dependent manner (Ide et al., 1994). This can be altered by ATRA: treatment of older distal mesenchyme causes mixing with younger proximal mesenchyme and also contributes to more proximal structures (Tamura et al., 1997). This suggests that ATRA endows cells with proximal adhesive properties which, from this study, also appears to be true of EC23 and is consistent with the similarities in their genetic targets. There has been extensive research into the control of adhesion in the developing limb, particularly as this may be a mechanism for maintaining positional identity and also is crucial for the first step of cartilage development. It has been suggested that *n-cadherin* is expressed throughout the limb bud but then becomes enriched in the distal region (Oberlender and Tuan, 1994b; Yajima et al., 1999) and its levels throughout the limb correlate with the number of cartilage elements formed from that part. *N-cadherin* is also known to be expressed in the cartilage condensations under the control of *Tgfβ2* and, if inhibited, will cause delayed and malformation of cartilage development (Miura and

Shiota, 2000; Yajima et al., 1999). Considering that ATRA has been shown to down-regulate *n-cadherin* previously (Yajima et al., 1999) and in the present study, as well as the phenotypes generated with both of these retinoids, altered *n-cadherin* may provide a mechanism behind this cellular proximal relocation particularly as *Tgfβ2* is also down-regulated here (figures 5.7 and 5.8, tables 5.7 and 5.8).

Limb development is also tightly controlled by the *Hox* transcription factors which exhibit restricted expression during limb development and which have also been implicated in the control of limb bud cell adhesion. *Hoxa13* is expressed in the distal limb bud and is known to be important for autopod development as well as muscle development. *Hoxa13* positive cells sort out from *hoxa13* negative cells (Yokouchi et al., 1995) while misexpression in the zeugopod causes distal transformation and the formation of many, short elements rather than the zeugopodal elements (Yajima et al., 2002; Yokouchi et al., 1995). It also alters the expression of adhesion molecules such as *Eph receptor A4* (*epha4*) and *epha7* (Stadler et al., 2001) which have been implicated in proximal positional identity, boundary formation, motor neuron, tendon and muscle differentiation during limb development (Araujo et al., 1998; D'Souza and Patel, 1999; Flenniken et al., 1996; Iwamasa et al., 1999; Patel et al., 1996). Interestingly, retinoids have also been shown to affect *Eph* and *Ephrin* expression e.g. *ephb2* (Bouillet et al., 1995) which may also play a role in altering limb bud cell identity, however, none of these are present in the retinoid target genes presented here. This is consistent with the idea that, due to the high quantities of retinoid applied, limb development is inhibited. Another hox gene *Meis2* is a retinoid target but is expressed in the proximal mesenchyme of the developing limb bud (Mercader et al., 1999; Mercader et al., 2000). Its overexpression causes proximal relocation of distal cells while its knock down blocks ATRA mediated proximalisation (Mercader et al., 2005). Altogether this indicates that ATRA and EC23 are likely to be altering limb bud cell identity via the suppression of distal FGF, subsequent up-regulation of *Meis2* and the down-regulation of *n-cadherin* and *Tgfb2*. The down-regulation of *Hoxa13* in response to ATRA alone (table 5.11) is consistent with ATRA treated wing buds being at a later developmental stage than those treated with EC23.

Conclusions:

The results presented in this chapter have further characterised the response to retinoid in the developing limb. The novel findings have indicated that the synthetic retinoid EC23 alters genes in the anterior wing bud in a similar manner to ATRA but differs in the magnitude of the response. Both retinoids appear to inhibit wing development and differentiation which may possibly be due to the metabolism of excess retinoid. This is particularly likely given that EC23 treated wing buds appear to be further inhibited than ATRA treated wing buds. This may lead to the types of digit duplications observed in chapter 3 as EC23 may be unable to induce an ectopic ZPA within sufficient time to allow severe duplications observed with ATRA. However, it could also be unable to induce *Shh* in the anterior wing bud at all and therefore only allow formation of additional digit 1s as this digit is thought to be *Shh*-independent (see chapter 6). EC23 also appears to mimic the effect of ATRA in the proximalisation of limb bud cells and alteration of cell affinity. Interestingly, many of the genes altered in response to ATRA and EC23 have also been implicated in scapula development, elbow development or regulation of cartilage size in the developing limb and therefore are avenues worthy of further work (see chapter 6).

Chapter 6) Further discussion, concluding remarks and recommendations for future work.

Summary of findings:

The present study has investigated the activity of two novel synthetic retinoids which are resistant to photoisomerisation, EC23 and EC19. Application of EC23 and EC19 to anterior chick wing buds has indicated that, despite their similar structures, EC23 and EC19 demonstrate differential potencies and effects *in vivo*. EC23 was seen to mimic the effects of ATRA: reducing cartilage element and scapula blade length, elbow fusions and generating digit duplications, while EC19 had no affect at the quantities tested. Interestingly, EC23 was able to generate a digit duplication not observed with ATRA: duplication of multiple additional digit 1s. EC19 and EC23 both inhibited upper beak outgrowth in a similar manner to ATRA but the effects of EC19 were milder compared to either ATRA or EC23. It was shown that EC23 and ATRA cause down-regulation of *Pax1* expression, known to be involved in the development of the scapula which may contribute to the mechanism behind this phenotype. The different potencies and effects seen with EC23 versus EC19 were shown to be partly due to differences in their metabolism: EC19 appears to be metabolised by the CYP26 enzymes, although to a lesser extent than ATRA, while EC23 is more resistant to metabolism. Similarly, they may differ in the activation of isoforms of the RARs: EC23 is likely to be a pan-agonist while EC19 could be specific to RARβ1 on the basis of receptor distribution. Interestingly, EC23 may also activate the FABP5/PPARβδ pathway for retinoid signalling as these are expressed in the limb but not the developing facial processes, it is concluded that EC19 is unlikely to bind them and FABP5/PPARβδ binding may provide another mechanism for their differential effects. EC23 was subsequently investigated further to determine the effects of the metabolites and isomers on gene expression in chick limb development after 24hrs retinoid treatment. EC23 and ATRA alter similar genetic targets but differ in the magnitude of their effects. Further analysis of these targets indicates that high concentrations and quantities of retinoids inhibit limb development and differentiation until the excess retinoid is metabolised to suitable levels. EC23 was not seen to induce *Shh* expression in the anterior wing bud unlike ATRA and may provide a mechanism to explain the different duplications observed with these two retinoids. This chapter discusses the major implications of this work and directions for further study.

Differential effects seen with two retinoids of similar structure: EC19 and EC23.

The present study has further characterised the effects of the novel, photostable, synthetic retinoids EC23 and EC19 *in vivo*. Using the chick wing bud as a model system as previously for the investigation of retinoids (Eichele et al., 1985; Summerbell, 1983; Tickle et al., 1982), I report their effects *in vivo* when applied at high quantities. Consistent with previous investigation by my research group (Budge, 2010; Christie et al., 2008), it is noted that EC23 is more toxic and more potent than EC19 and generates effects comparable to ATRA, while EC19 causes no effect on the limb and milder effects on the developing upper beak (chapter 3). These differences in potencies between EC23 and ATRA compared to EC19 are unlikely to be due to metabolism given that EC19 and ATRA are seen to be metabolised by the CYP26 enzymes (chapter 4) and therefore is more likely to be due to their structural differences (discussed further in chapter 4).

The structural difference between EC23 and EC19 is solely the position of the carboxylic acid group. In EC23 its position indicates that EC23 is similar to ATRA while the position in EC19 is reminiscent of 13CRA. As mentioned throughout this work, 13CRA is teratogenic but its effects are mainly thought to be due to its inter-conversion to ATRA given that its affinity for retinoic acid binding proteins is low (Chen and Juchau, 1998; Keeble and Maden, 1984; Klaassen et al., 2001; Maden and Summerbell, 1986; Ruhl et al., 2001). Considering that EC19 is metabolised and has a similar structure to 13CRA, this compound could be of use in determining the effects of 13CRA alone. This compound and its comparison to EC23 also suggest that the position of the terminal carboxylic acid group is of importance for retinoid function *in vivo* and metabolism.

These differential effects may also be due to differences in binding to retinoic acid binding proteins and activation of the receptors. The present study has investigated the localisation of *Rarβ1*, *Rarβ2*, *Rarγ2*, *Pparβ* and *Fabp5* in an attempt to determine if any of these receptors can be ruled out in terms of activation by EC23 and EC19 (chapter 4). Considering that EC23 and EC19 are structurally similar to the RAR pan-agonist TTNPB (see figure 1.5) it would be hypothesized that, likewise, EC23 and EC19 were pan-agonists of the RARs which has in fact been shown for EC23 (Gambone et al., 2002). However, as EC23 affects the both the wing and facial processes while EC19 does not, it is likely that EC23 is a pan-agonist of the RARs and PPARβδ pathways while EC19 is unlikely to bind

as efficiently to FABP5, RARγ or RARβ2 as EC23 given that these are expressed in the limb bud mesoderm and, in fact, *Fabp5* is specific to the limb (chapter 4). On the basis of localisation, activation of RARβ1 by EC19 cannot be ruled out.

Metabolites and isomers are not the main cause of retinoid effects *in vivo*.

The study of retinoids in development has been hindered by the fact that, although ATRA is known to be the most important biologically active retinoid (Kistler, 1987; Niederreither et al., 1999), its isomers and oxidative metabolites are also bioactive and may therefore play a role in embryonic development (Pijnappel et al., 1993; Reijntjes et al., 2005; Thaller et al., 1993). The current understanding from genetic studies is that ATRA metabolites are a product of metabolism and have no role in embryonic development, rather that the levels of ATRA must be tightly controlled (Niederreither et al., 2002a). EC23 and ATRA generate similar phenotypes (chapter 3) and alter similar genes but differ in the magnitude of their response (chapter 5) despite the fact that EC23 is resistant to CYP26-mediated metabolism (chapter 4). Therefore, the results of the current study are consistent with Niederreither et al (2002) indicating that oxidative derivatives of ATRA are not necessary for development. Similarly, EC23 is resistant to photo-isomerisation and therefore indicates that 9CRA and 13CRA are not necessary for limb development and is consistent with previous research indicating that these are only present after application of high concentrations of ATRA (Horton and Maden, 1995). Considering that the structure of EC19 is reminiscent of 13CRA but the effects of EC19 are milder than EC23, this provides further evidence that the retinoid response is not due to the isomer 13CRA. EC23 is therefore a useful experimental tool for investigating the effects of ATRA without hindrance of its oxidative derivatives or isomers.

The retinoid response is to stall limb bud development until the teratogen is metabolised.

The present study has further characterised the molecular and cellular response to retinoids in the developing wing bud and relates them to the phenotypes observed. It has been seen that the response to retinoid is to inhibit differentiation observed in the down-regulation of *Pax1* (chapter 3). An inhibition of chondrogenesis, tendon and muscle development has also been observed in response to both retinoids by the decreased cartilage production

after treatment of micromass cultures (chapters 4) as well as the down-regulation of many differentiation markers including: *col9*, *scleraxis*, *Tgfβ2* and *MyoD* (chapter 5). Considering the role documented for TGFβ2 in the limb (Lorda-Diez et al., 2010; Lorda-Diez et al., 2009; Miura and Shiota, 2000; Pryce et al., 2009; Spagnoli et al., 2007) and the phenotypes after manipulation, TGFβ2 is likely to be important for limb development, in conjunction with BMPs (discussed later), and a key molecule altered after application of either EC23 or ATRA. This inhibition of development indicates that the retinoid treated wings are stalled with respect to DMSO treated wings and is consistent with previous research by Ali-Khan and Hales (2006). They showed that retinol acetate altered cell adhesion consistent with inhibition of chondrogenesis and up-regulated *Id3*, *Hes1* and *Snai1* which are markers of undifferentiated states (Ali-Khan and Hales, 2006).

Developmental stalling by retinoids has also been suggested by Maden et al (1983) after application to amputated limbs of axolotl. He noted that there is a concentration dependent inhibition of regeneration post retinoid treatment: regeneration should occur within 18 days but by day 15 after retinoid no regeneration has occurred. A decrease in proliferation was noted and it was suggested that, similar to the chick wing, no development occurs while exposed to retinoid although subsequent differentiation in axolotl occurred as normal (Maden, 1983). The differential effects of ATRA and EC23 may be due to the differential stalling seen after their application: EC23 treated wing buds are stalled to a greater extent than ATRA treated anterior wing buds. This differential stalling of the retinoid treated anterior wing buds may provide a mechanism for digit duplication (discussed later) and aberrant chondrogenesis or elbow fusion.

This stalling of development as a retinoid response appears to be due to persistence of excess retinoid given that up-regulation of *Cyp26* and other genes involved in metabolism is a common feature of other microarray analysis after excess retinoid (chapter 5; (Ali-Khan and Hales, 2006; Feng et al., 2010; Luijten et al., 2010)). The differential metabolism of EC23 and ATRA therefore is consistent with the differential stalling exhibited by EC23 and ATRA treated anterior wing buds mentioned previously. This is also consistent with a recent study by Miletich et al (2011). They show that insufficient BMP levels during a critical juncture of tooth development causes a 24hr developmental delay during which time the correct BMP threshold is achieved. At this point development can proceed and subsequently the delay is rectified such that correct development of the tooth is observed (Miletich et al., 2011).

A similar effect may be seen in the present study but instead of insufficient levels there are teratogenic levels of ATRA which need to be rectified before correct development of the wing can be re-initiated and the delay amended. In chapter 5, I have suggested that inhibition of endogenous, posterior *Shh* may contribute to this developmental stalling. Inhibition of proliferation in the limb has been shown to lead to a transient down-regulation of *Shh* expression which subsequently recovers and is maintained for the correct length of time (Towers et al., 2008). Given that many retinoid treated wing buds continue to develop with a normal digit pattern, this may be the mechanism behind it, as well as the fact that stalled limb buds also recover to produce a limb with three segments. Further work is necessary to show that stalling of the limb bud occurs after retinoid treatment but comparison of this and other systems where developmental stalling is apparent may allow us to improve our knowledge of the correct regulation of development. Interestingly, I have carried out a preliminary comparison of the present study and an investigation of the teratogen cyclophosphamide and it appears that a common response is alteration of BMP signalling (Huang and Hales, 2009). This is also seen as an early response to retinoid in the developing limb (Ali-Khan and Hales, 2006) as well as implicated in malformations of dermomyotome-derived portions of the scapula (Wang et al., 2005) and may prove to be the mechanism behind teratogen response and correct timing of organogenesis.

Mechanisms behind retinoid induced elbow fusions and alteration of cartilage element size.

It was noted in chapter 3 that EC23 and ATRA caused the following effects: digit duplication, shortening of zeugopodal cartilage elements, elbow fusions and scapula malformations. EC23 and ATRA generated distinct types of digit duplication and the mechanisms behind these are discussed in a later section of this chapter. The genes linked to the scapula are also discussed at a later point. These effects on the more proximal elements are consistent with the ability of both EC23 and ATRA to cause the proximal relocation of treated limb bud cells, altered cell: cell adhesion and their ability to inhibit chondrogenesis (chapter 4 and 5; (Mercader et al., 2000; Summerbell, 1983)). Some of the genes seen to be altered by the retinoids and which are implicated in the production of digit duplication, zeugopodal cartilage element shortening and elbow fusions will be discussed in this section in order of decreasing similarity with the phenotypes observed in chapter 3.

Some of the most up-regulated genes in response to both ATRA and EC23 are the *Cyp26* enzymes. Humans with *Cyp26b1* mutations have exhibited shortened proximal cartilage elements and elbow fusions are also seen in mouse knock outs (Laue et al., 2011; Yashiro et al., 2004). This indicates that retinoids are involved in the regulation of chondrogenesis, differentiation of the interzone and limb size. Another study of *Cyp26b1* knockout mice has indicated that the cells were maintained in a prechondrogenic state: expressing higher levels of pre-chondrogenic markers *versican* and *tenascin C* and lower levels of alcian blue staining than wild type after 6 days of culture (Dranse et al., 2011). This is thought to be the mechanism behind shorter limb development observed in these mutants as cartilage differentiation was inhibited. Although these studies have investigated *Cyp26* knock out, they also are likely to involve retinoid excess and therefore are pertinent to the present study. The excess concentration of retinoid applied here may have overcome the CYP26 enzymes resulting in phenotypes similar to *Cyp26* deficiency: shorter limb elements and joint fusions. The mechanism proposed for the phenotypes seen with *Cyp26b1* knockout mice and similar phenotypes seen here is also consistent with the inhibition of cartilage development seen with EC23 and ATRA (chapter 4 and 5). The more severe phenotypes seen with EC23 compared to ATRA are also consistent with the fact that EC23 is resistant to CYP26-mediated metabolism (chapter 4) as retinoid levels would be correspondingly higher and further inhibit chondrogenesis.

Msx1/Msx2 knockout mice exhibit either shortening or absence of the radius concurrent with preaxial polydactyly (Bensoussan-Trigano et al., 2011) similar to phenotypes observed with ATRA in chapter 3. It can be concluded that down-regulation of *Msx1* may be an important contributor to the phenotypes generated with ATRA (table 5.12) and it may be altered to a lesser extent after 24hrs in response to EC23. *Fgf13* has been implicated in limb development as overexpression causes radial shortening and ectopic digit 1 development (Munoz-Sanjuan et al., 1999). *Fgf13* down-regulation in response to both retinoids (table 5.9) is not consistent with the phenotypes seen in chapter 3 but overexpression was performed at a later stage than retinoid treatment here leaving open the possibility that *Fgf13* overexpression after retinoid treatment may occur at a different stage.

Interestingly ectopic expression of the proximally expressed *Meis1* or *Meis2* appears to produce normal stylopod element size whilst the zeugopod and autopod (*Meis2* only) are

affected leading to: shortened ulna, bending of the radius and development of digits 1 and 3 or just digit 2 (Capdevila et al., 1999; Mercader et al., 1999). *Meis2* up-regulation here (table 5.8), amongst other dysregulated proximally expressed genes, may contribute to the phenotypes presented in chapter 3 where changes to cartilage element size or scapula malformation are documented.

A number of other genes have been manipulated in previous studies which have resulted in similar shortening of limb cartilage elements and elbow fusions indicating that they may contribute to the effects of ATRA and EC23. *Tgfβ2* is down-regulated in response to both retinoids (table 5.9) and has been previously mentioned with respect to the control of cartilage and tendon differentiation in the limb bud and *n-cadherin* expression (Lorda-Diez et al., 2009; Miura and Shiota, 2000) consistent with retinoid inhibition of chondrogenesis (chapter 4). *Tgfβ2* knockout mice have a malformed olecranon process (elbow) as well as shortening of the radius and ulna (Sanford et al., 1997) similar to *Rarα/γ* knockout mice (Lohnes et al., 1994). Considering the similarity of these phenotypes with those seen in chapter 3, *Tgfβ2* may be one of the major contributors to the phenotypes generated.

Concurrent with a decreased *Tgfβ2*, *Noggin* is up-regulated in response to ATRA (table 5.12) indicating that BMP dysregulation may be important for the retinoid response. Up-regulation of *Noggin* in response to ATRA after 24hrs may be consistent with the shortening of the scapula blade and head agenesis as NOGGIN injection to the dermomyotome at HH20 has caused this phenotype (Wang et al., 2005). Given that excess expression of *Noggin* after onset of chondrogenesis causes excess cartilage production (Pizette and Niswander, 2000), *Noggin* up-regulation after 24hrs in the anterior wing could cause the excessive production of cartilage in response to retinoid e.g. elbow fusions. This is not consistent with *Noggin* knockout mice which have thicker cartilage elements and a malformed olecranon (Brunet et al., 1998) similar to the phenotypes seen in response to EC23 and ATRA. Also, *Noggin* expression is up-regulated rather than down-regulation in response to ATRA and is not significantly altered in response to EC23 despite the phenotypes seen in response to both retinoids in chapter 3. This is contradictory and may suggest that BMP signalling is increased on retinoid treatment and that *Noggin* up-regulation is an indirect effect which would be consistent with up-regulation of *Bmp4* and *Bmp7* observed after 3hrs retinol treatment (Ali-Khan and Hales, 2006). Application of BMP2 and BMP7 to the anterior wing has shown to affect radius and ulna development

similar to those phenotypes seen in chapter 3 (Macias et al., 1997). The up-regulation of *Noggin* in response to ATRA may therefore be due to a dysregulation of BMP signalling to attenuate the phenotypes produced. Considering that *Noggin* is not significantly altered in response to EC23, this may lead to the more severe cartilage thickenings and joint fusions seen in chapter 3 as BMP dysregulation is unchecked and *Noggin* cannot be modulated if the retinoid persists.

Other transcription factors are also linked with alteration of cartilage element size and elbow fusions and are altered by ATRA and EC23. The shortened elements seen in response to ATRA and EC23 may be partly due to decreased expression of *Lhx9* and *Lhx2* (ATRA only) as *Lhx2*/*Lhx9* knockout mice exhibit shortened limbs particularly affecting the zeugopod and digits (Tzchori et al., 2009). Whole mount *in situ* hybridisation and microarray analysis of the developing digits has also suggested that *Lhx9* is a marker for digit 1 identity in the chick wing bud at later stages (Wang et al., 2011). This is not consistent with the down-regulation of *Lhx9* expression in response to both retinoids (table 5.9) considering that EC23 and ATRA generate at least one additional digit 1 but its expression over time during the retinoid response may be interesting to investigate. *Shox* is seen to be down-regulated by retinoid treatment (table 5.10) mutations of which have been linked to short stature, Leri Weill syndrome, Langer syndrome and Turner's syndrome in humans (Sabherwal et al., 2007). *Shox* has also been shown to control stylopod development in mouse (Yu et al., 2007). Therefore dysregulation of this transcription factor concurrent with altered *Meis2* expression and proximal relocation of limb bud cells may contribute to the shortened and thickened humerus observed in chapter 3. *Pbx1* is implicated in the control of correct cartilage element size when concurrent with decreased *Pbx2* (Capellini et al., 2006). Up-regulation of *Pbx1* after retinoid treatment indicates that dysregulation of this gene with respect to others expressed in similar domains may contribute to the shortening of limb cartilage elements.

Interestingly, a number of markers have been documented for joint development: *Cd44*, *Enpp2* and *Sulf1* (Ohuchi et al., 2007; Sohaskey et al., 2008) which are down-regulated in response to both retinoids (table 5.10). This is consistent with a dysregulation of joint development which may lead to the elbow fusions and limb shortening seen in chapter 3. Interestingly overexpression of *Hoxa13* (down-regulated in response to ATRA; table 5.12) has also affected expression of *Enpp2* (autotaxin) and *Shox* (chapter 5) (Zakany and

Duboule, 2007) which suggests inhibition of normal limb development and dysregulation of these genes may lead to joint fusions.

Mechanisms behind retinoid induced scapula malformation.

It was also observed in chapter 3 that application of either ATRA or EC23 could cause malformation of the scapula, mainly blade reduction and the absence of scapula head development. Retinoids have been shown previously to affect shoulder girdle development in that they can duplicate the coracoid (Oliver et al., 1990) and that *Rarα/γ* knockout mice have malformed scapulae (Lohnes et al., 1994). However, excess retinoid has not been documented to truncate the scapula in previous literature and this may be due to the high concentration and quantity of retinoid released into the chick wing in this study. The truncation of the scapula blade has, however, been documented with retinoid signalling antagonists (Prols et al., 2004) however this cannot be consistent with the present study. Genes altered after retinoid treatment which may be linked to the scapula malformations are discussed in the following section.

Excess ATRA leads to an up-regulation of *Meis1* which is a marker of the proximal limb (Mercader et al., 1999; Mercader et al., 2000). Ectopic expression of *Meis1* or *Meis2* (up-regulated after retinoid treatment-chapter 5) causes loss of distal structures (Capdevila et al., 1999; Mercader et al., 1999) while knockout mice have not yet been described. *Emx2* has been shown to be retinoid responsive. Knockout mice exhibit the dramatic phenotype of complete scapula agenesis and an absence of the scapula condensation suggesting that *Emx2* is needed to make the entire scapula condensation (Pellegrini et al., 2001; Prols et al., 2004). Concurrent with scapula agenesis in *Emx2* knockout mice, there is also an expansion of *Pax1* expression (Pellegrini et al., 2001) suggesting that an antagonism between these two factors is important for correct pectoral girdle development. The opposite case can be observed upon retinoid application in this study: *Emx2* expression in up-regulated (chapter 5) but at 48hrs there is a decrease in *Pax1* expression (chapter 3).

Interestingly, overexpression of *Emx2* does not influence scapula formation but instead induces an ectopic digit in the anterior limb (Prols et al., 2004) indicating a role in digit development and that it may contribute to malformations of the scapula and digit duplications (chapter 3) from its up-regulation in response to retinoid (chapter 5). Similar

to *Emx2*, the proximally expressed *Pbx1* and *Alx1* have also been implicated in scapula development (Capellini et al., 2010; Selleri et al., 2001). *Pbx1* and *Pbx2* are proposed to interact and regulate gene expression (Capellini et al., 2006); however, only *Pbx1* is altered in response to EC23 and ATRA. This, combined with evidence that *Pbx1* and *Meis1* can interact to regulate gene expression in mouse (Mercader et al., 2009) indicates that aberrant expression of transcription factors involved in scapula development may lead to the malformations observed in chapter 3. The up-regulation of these genes involved in proximal development is also of interest as despite their up-regulation, correct development of the proximal limb does not result. This may support the idea that the stalling of limb development is too severe after retinoid treatment to allow correct proximal development. The up-regulation of these genes in response to both retinoids indicates that they may play a similar role in the correct development of the chick scapula as previously documented for mouse.

Retinoid effect on differentiation as a mechanism behind the effects on the PD axis.

As mentioned, previous studies have not shown that anteriorly applied ATRA can affect the more proximal elements in the zeugopod, stylopod or limb girdle unless at high concentrations or earlier stages of development (Oliver et al., 1990; Summerbell, 1983). This may be due to the fact that these elements are specified earlier in development (Sato et al., 2007; Vargesson et al., 1997) and therefore this indicates that the retinoid effect on these elements is mainly due to aberrant control or inhibition of cartilage development, both of which can be seen from the effects on limb bud cell micromass cultures and microarray targets (chapters 4 and 5). It can also be noted that inhibition of chondrogenesis can also be proposed as a mechanism behind the shortening of cartilage elements discussed in the previous section. NOGGIN injection into the dermomyotome between HH20-22 generated similar phenotypes on the scapula as seen in the present study (Wang et al., 2005). *Noggin* expression is up-regulated in response to ATRA while *Bmpr1b* is down-regulated in response to EC23 indicating that BMP signalling is dysregulated in response to both retinoids. This has been linked to the control of cartilage element size previously and, similar to inhibition of chondrogenesis, could provide a mechanism for the effects of retinoid on all elements proximal to the autopod.

Therefore, this aberrant control of genes involved in cartilage development and proximally expressed genes may contribute to the shortening or widening of cartilage elements as well as the elbow fusions, digit duplications and scapula truncations observed with both retinoids.

Mechanisms behind the different digit duplications observed with EC23 and ATRA.

As mentioned earlier, I have shown that both ATRA and EC23 can duplicate digits and cause alteration to AP pattering in the developing wing (chapters 3 and 5). Despite the fact that EC23 mimics ATRA in other aspects of limb development, it generates a different type of digit duplication when applied at the present concentration and quantity. Unlike ATRA, it causes digit duplication of multiple additional digit 1s (chapter 3). This has been documented previously with applications of low concentrations of SHH (Yang et al., 1997) but not with retinoid. The mechanism behind this differential effect on digit duplication is unclear but in the following sections I put forward some proposals for future testing.

Both retinoids are seen to up-regulate *Hoxb8* but they differ in the magnitude of change: *Hoxb8* is up-regulated to a greater extent in ATRA than EC23 treated wing buds (chapter 5). This could then cause a different response in the anterior wing bud: ATRA may generate an ectopic ZPA as described (Riddle et al., 1993; Wanek et al., 1991) and implied from up-regulation of *Shh* after 30hrs treatment (figure 5.14), while EC23 may cause digit duplication independent of an ectopic ZPA as it was never seen to up-regulate *Shh* expression in the anterior wing bud (figure 5.14). This leads to two possible conclusions which are not mutually exclusive: either that limb development is delayed to such an extent that any ectopic *Shh* is induced far later after EC23 treatment and therefore can only duplicate the most anterior digits or that EC23 generates digit duplications independently of *Shh*.

Length of SHH exposure, SHH concentration and SHH dependent proliferation are thought to determine AP patterning of the developing digits (Harfe et al., 2004; Towers et al., 2008; Zhu et al., 2008a). ZPA grafting has shown that the window for digit duplication is up to HH25 after which grafting is ineffective (Summerbell, 1974); however retinoids cannot induce digit duplications after HH22 (Summerbell, 1983). Therefore, if digit duplication is stalled by the high concentrations of EC23, there would not be a large

window of time available to allow induction of sufficiently high levels of *Shh* for the correct exposure time in the anterior wing to generate mirror image digit duplication. The SHH induced may only allow the duplication of the most anterior digit as its levels could be much reduced similar to previous experiments (Yang et al., 1997) and lower than ATRA treated wings. On the other hand, it has been suggested that the development of digit 1 is *Shh* independent in mice (Chiang et al., 2001). This being the case, the duplication of additional digits of digit 1 identity may be due to the fact that EC23 does not induce *Shh* in the anterior wing. This may still be true if EC23 were to induce very low levels of *shh* anteriorly as these may increase SHH-dependent proliferation but not be above the threshold needed to specify digit 2 and 3 identity.

Considering that EC23 can generate mirror image digit duplications at lower quantities and concentrations, presumably via *Shh* induction, I favour the hypothesis that EC23 treated wing buds are stalled to such an extent that any *Shh* induction in the anterior wing occurs too late for the specification of more posterior digits. Additional digits of the most anterior identity are duplicated as retinoid induced proliferation still occurs, possibly involving FABP5 (discussed below). Further work will be necessary to verify the different effects of EC23 and ATRA on *Shh* and proliferation in the anterior wing bud.

Effects of retinoids in the limb and model for the involvement of FABP5.

SHH dependent proliferation has been shown to be important for the development of digits 1 and 2 in chick (Towers et al., 2008; Towers et al., 2011). Given the necessity for SHH to specify more posterior digits (Harfe et al., 2004; Riddle et al., 1993; Towers et al., 2008; Yang et al., 1997), it could be argued that the application of such high quantities of EC23 and subsequent stalling of wing development has led to an uncoupling of proliferation and digit specification in the wing bud. Increased proliferation as a result of excess retinoid application still occurs with high levels of retinoid, presumably via re-organisation of the AER (Tickle et al., 1989) and possibly via FABP5 (see later), as up to three additional digits form (chapter 3). However, the fact that only the most anterior identity is specified with EC23 suggests that SHH signalling and proliferation are uncoupled consistent with the absence of *Shh* expression in the anterior wing after 24 or 30hrs (chapter 5). This is consistent with previous models of limb development which implicate proliferation, SHH concentration and exposure time to SHH as important for digit development (Ahn and

Joyner, 2004; Harfe et al., 2004; Towers et al., 2008; Zhu et al., 2008a). It is also consistent with previous studies indicating that SHH is important for specification of digit identity (Davey et al., 2006; Towers et al., 2008).

ATRA has been shown to promote both proliferation and differentiation in cancer cell lines, decreasing their use as chemotherapeutic agents, although the mechanism behind this is unclear. CRABP2 channels ATRA to the nucleus to bind and activate RARs (Budhu and Noy, 2002; Dong et al., 1999). Shaw et al showed previously that PPARβδ can also be activated by ATRA (Shaw et al., 2003) and subsequent research showed that FABP5 could translocate ATRA to the nucleus and activate PPARβδ in HaCaT cells (Schug et al., 2007). The FABP5/PPARβδ pathway has been implicated in the promotion of proliferation versus apoptosis or differentiation in response to ATRA by manipulation of the FABP5:CRABP2 ratio in cancer cell lines (Schug et al., 2007). Cells derived from a mammary carcinoma containing high levels of CRABP2 (MCF-7) and which usually undergo apoptosis in response to ATRA, were promoted to proliferate if the ratio of FABP5:CRABP2 was increased. Manipulation of the levels to decrease this ratio increased differentiation and apoptosis via the CRABP2/RAR pathway in cells derived from a tumour which normally contained high levels of FABP5. Therefore, differential activation of the PPAR pathway versus the RAR pathway has been proposed to cause the contradictory effects of ATRA in cancer treatment (Schug et al., 2007; Schug et al., 2008). Interestingly, recent research has implicated the differential activation of RAR and PPARβδ receptors by ATRA at different stages of neurogenesis as well as high levels of FABP5 in the brain, providing evidence that FABP5/PPARβδ signalling may play a role *in vivo* (Yu et al., 2012).

Fabp5 has been observed to exhibit a highly restricted expression pattern in the developing chick embryo at HH20. Interestingly *Fabp5* is restricted to the posterior wing bud overlapping the PZ and absent from the ZPA (chapter 4 and figure 6.1A). Considering that the PZ is an area of high proliferation in the developing wing bud, FABP5 function *in vivo* may be to promote proliferation upon binding ATRA and subsequent activation of PPARβδ as suggested *in vitro* (Schug et al., 2007). Concurrent with this, there are two different CRABPs in chick: CRABP1 and CRABP2. The expression pattern of these transcripts has not been investigated but the distribution of these proteins has been documented. CRABP1 has been seen to be located in an anterior high, posterior low gradient in the developing chick wing (Maden et al., 1988; Maden and Summerbell, 1986). CRABP2 is also documented in the chick wing bud, highest at the distal tip overlapping

with the PZ at HH23. In this region levels are higher in the posterior and middle of the wing bud (Miyagawa-Tomita et al., 1992).

Given the expression of *Fabp5* and the distribution of CRABP protein, areas of the PZ may have a different FABP5:CRABP2 ratio. If the relationship described *in vitro* also exists in the limb bud this may provide a mechanism for retinoid control of proliferation in the distal wing bud. Mic et al have shown that retinoid signalling occurs throughout the limb bud at a similar stage in mouse using a RARE driven *β-galactosidase* reporter construct but that a proximal-high distal-low gradient is still apparent (Mic et al., 2004). Differential FABP5/CRABP2 activation may aid the separation of proliferative and non-proliferative response to ATRA in the PZ and posterior limb. Consistent with this, previous studies have indicated that CRABP2 enhances ATRA binding to RAR (Dong et al., 1999) and is most important when ATRA levels are limited (Budhu and Noy, 2002), similar to the situation at the distal wing bud. ATRA has also been documented to play a role in the correct development of the AER in mouse *Raldh2* knockouts (Mic et al., 2004), which could be CRABP2 mediated given its location. Similarly CRABP/RAR signalling may also be involved in the reorganisation of the AER given that there is an area of high CRABP1 and CRABP2 at the distal wing tip in the PZ until HH24 of chick limb development (Maden et al., 1988; Maden et al., 1989; Tickle et al., 1989). Therefore, if ATRA and EC23 can also bind or up-regulate FABP5 and activate PPARβδ *in vivo*, activation of this pathway may cause increased proliferation in the PZ, after expansion of the AER, allowing an increase in the digit progenitor pool and digit condensations produced.

The effect of EC23 and ATRA on proliferation via differential activation of RAR/PPARβδ pathways and *Shh* expression could determine the number and identity of the digits formed (summarised in figure 6.1). Activation of FABP5/PPARβδ by proximally produced ATRA could promote proliferation of the progenitor pool in the posterior distal wing bud and simultaneously control differentiation, apoptosis and wing bud shape at the anterior PZ (CRABP2/RAR; figure 6.1A-B). Up to a certain threshold of excess retinoid, these pathways would be unified leading to mirror image duplications. Excess retinoid would activate both pathways in the distal wing causing increased proliferation and *Shh* induction in the anterior wing, after the wing has recovered from retinoid-induced developmental stalling, although the mechanism behind this recovery is unclear (figure 6.1C).

However, elevation of retinoid levels over this threshold could lead to additional digit 1s or generate 323 duplications and truncated wings. EC23 can cause more severe stalling of

wing development in the present study (chapter 5) and could cause duplication of only the most anterior digit if it enhanced proliferation via FABP5:PPARβδ but *Shh* expression was not induced in the anterior wing within the time window for digit specification (HH25; figure 6.1D). Continued development of the increased progenitor pool in the absence of *Shh* or induction of low levels could give rise to additional digits of the most anterior identity as seen previously (Yang et al., 1997). This is consistent with the *talpid3* mutant where digit identity is not specified as a member of the *Shh* signalling pathway is not functional (Davey et al., 2006).

High concentrations of retinoids can also cause more severe digit duplications such as 323 as well as truncations of the autopod (chapter 3; (Tickle et al., 1985)). Vastly elevated retinoid levels, or wings which cannot cope with EC23, may cause an over-activation of CRABP2: RAR pathway throughout the entire PZ for a prolonged period. This could lead to an increased CRABP2/RAR activation and subsequent apoptosis in the PZ leading to truncations. This elevated level of ATRA may also cause over-activation of FABP5/PPARβδ pathway but, as this is solely present in the posterior wing bud, it may be insufficient to prevent the CRABP2/RAR induced apoptosis across the entire progress zone. In some cases *Shh* may still be induced in the anterior limb causing the 323 digit duplication if any autopodal cells survive via FABP5/PPARβδ over-activation (figure 6.1E). This theory for FABP5 in limb development fits with other research that retinoids do not need to bind CRABP2 with high affinity to generate digit duplications (Maden et al., 1991). That it increases their potency if they do bind CRABP2 (Keeble and Maden, 1984) may be due to an effect on re-specification of cells in the PZ.

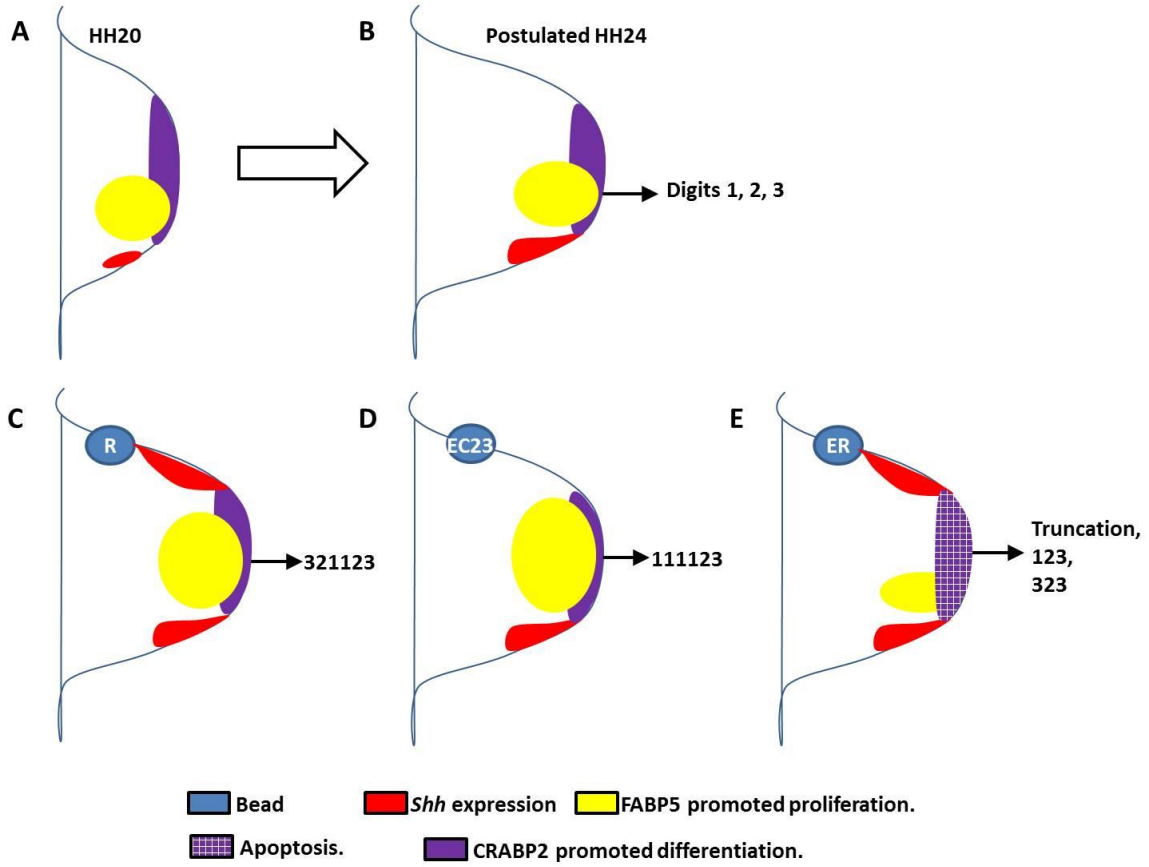

Figure 6.1: A model for digit duplication with respect to CRABP2 and FABP5.
A) indicates the current knowledge of FABP5 and proposed CRABP2 localisation at HH20. B-E) are hypotheses for the involvement of these retinoid binding proteins in digit development in untreated embryos and retinoid excess at HH24. A) and B) postulate that differential activation of CRABP2 and FABP5 in the wing by endogenous ATRA controls differentiation and proliferation in the production of digits. C-E) show hypotheses for the effects seen with retinoid (R; C), EC23 (D) and excess retinoid (ER; E). Abbreviations: ATRA, all trans retinoic acid; CRABP2, cellular retinoic acid binding protein 2; FABP5, fatty acid binding protein 5; *Shh*, sonic hedgehog.

This hypothesis requires further investigation as does the expression of *Crabp1*, *Crabp2*, *Pparβ* and *Fabp5* during subsequent wing development and the affinities of EC23 and ATRA for FABP5 as compared to CRABP2. The affinity for ATRA to FABP5 and CRABP2 have been investigated in COS-7 cells using similar procedures to be 57nM (Schug et al., 2007) and 0.13nM (Dong et al., 1999) respectively, reflecting the role of CRABP2 at low levels of retinoid (Budhu and Noy, 2002). This could indicate that FABP5 is not important for normal limb development given that retinoid levels in the distal wing are thought to be lower although signalling occurs throughout the limb bud at a similar stage to HH20 (Mic et al., 2004; Yashiro et al., 2004) and that *Fabp5* null mice are not documented to exhibit a limb phenotype (Yu et al., 2012). However, it may still be consistent with a role of FABP5 in excess levels of retinoid as at higher levels its activation

may become more prominent compared to that of CRABP2 and cause enhanced proliferation.

Interestingly, there is no evidence from the microarray analysis of retinoid treated anterior wings that there is an increase in either *Fabp5* or *Crabp2* expression (chapter 5) despite the fact that ATRA can induce *Crabp2* expression and both retinoids can increase levels of CRABP2 in TERA2.cl.SP12 cells (Astrom et al., 1994; Balmer and Blomhoff, 2002; Maltman et al., 2009). This does not rule out increased activation of these proteins and alteration to the expression of these proteins may have occurred previously which would not be observed after microarray analysis. Were this to be the case, targets of PPARβδ would be expected; particularly in the datasets from EC23 treated anterior wing buds from the model described (figure 6.1D). The targets of PPARβδ have been elusive as this receptor has been relatively uncharacterised compared to the other PPARs. It has been shown to repress the action of the other PPARs (Shi et al., 2002) and also to repress many genes, only a subset of which are de-repressed by microarray analysis after treatment with a PPARβδ agonist (Adhikary et al., 2011). This study (Adhikary et al., 2011) and its comparison with the microarray analysis of retinoid targets presented here may suggest the activation of this pathway in the developing chick limb. However, considering this study used a human prostate cell line (Adhikary et al., 2011) the PPARβδ targets in the chick wing may be distinct to those *in vitro* and this requires investigation, as do the effects of PPARβδ agonists *in vivo*.

Retinoids and FGFs.

It has been documented previously that retinoids and FGFs have an antagonistic relationship in the developing limb bud (Mercader et al., 2000). This has previously been linked to PD patterning but recent research has suggested that ATRA synthesis is not necessary for PD patterning i.e. *Meis1/2* expression in mouse as they are not altered in *Rdh10* or *Raldh2* null mice (Cunningham et al., 2013). Given the phenotypes seen with excess ATRA and the spread of *Meis1/2* expression (Mercader et al., 2000; Yashiro et al., 2004), the antagonistic relationship is still evident in the limb and may affect PD patterning indirectly via FGF8 suppression. Consistent with this, analysis of retinoid responsive genes in the anterior wing bud indicates that at least three FGFs (*fgf1*, *fgf13* and *fgf18*) are down-

regulated and *Meis2* is up-regulated by both EC23 and ATRA (chapter 5). EC23 also down-regulates *Fgf9* and *Fgf16* (chapter 5). Alongside the support for this antagonistic relationship this down-regulation of *Fgf* also implies that limb outgrowth is inhibited and may provide a mechanism behind the phenotypes seen on the humerus (chapter 3; (Hung et al., 2007)). The antagonistic relationship between FGF8 and ATRA has been implicated for murine forelimb initiation and observations suggest that this is dependent of the levels of FGF in the secondary heart field (Cunningham et al., 2013; Zhao et al., 2009). This implies that FGF-ATRA antagonism is used in other areas of development. Among these other areas is the forebrain. It has been shown that ATRA inhibits the development of GNRH-1 neurons whilst FGF8 promotes it (Sabado et al., 2012). Similarly, the expression of *Fgf8* at the ANR has an antagonistic relationship with ATRA (Halilagic et al., 2007) which may be due to signalling via the FABP5/PPARβδ pathway given that the expression domain of *Fabp5* is similar to that of *Fgf8* (chapter 4). This indicates that the results seen from the microarray analysis of retinoid targets and the expression of *Fabp5* may have wider implications for other regions during embryonic development.

Future work.

Considering the novel findings and implications for limb development described in this work, there are a number of avenues available for future investigation. One of the major findings is that high quantities of retinoid can stall development but which can be corrected depending on the metabolism of the retinoid. This requires further work to prove that cartilage development in ATRA and EC23 treated wings are stalled compared to DMSO treatment. It also appears that non-metabolisable retinoid (EC23) can cause stalling of wing development to a greater extent and appears to uncouple proliferation and SHH signalling. The effect of EC23 on SHH signalling in the anterior wing bud at later time points is a vital experiment needed to confirm the mechanisms behind the novel duplications of additional digits with anterior identity. EC23 could also be used for future study of the development of digit 1 in chick and whether, like mouse (Chiang et al., 2001), it is *Shh* independent. As mentioned in chapter 5 and the present chapter, the comparison of this work and other studies of retinoid or teratogenic effects may improve our understanding of the mechanisms involved in ensuring that correct development occurs within the correct time-frame. BMP dysregulation has been implicated in this and other

aspects of the phenotypes observed in this study and therefore they would be an interesting avenue for further study at earlier time points including the master regulator TGFβ2.

In this work, I have proposed a model to explain the phenotypes generated with excess retinoid via the potential binding of the retinoic acid binding proteins CRABP2 and FABP5. However, these proposals assume that FABP5 plays the same role *in vivo* as has been previously described *in vitro* (Schug et al., 2007; Shaw et al., 2003). An important area for future work is to investigate the expression of *Fabp5* after retinoid treatment and whether manipulation of *Fabp5* levels affects digit duplication or limb development. Linked to the hypothesis of FABP5 involvement in limb development, another area of future work is to investigate the binding of EC23 and EC19 to RARs, CRABP2, FABP5 and PPARβδ as well as further characterisation of all *Rars*, *Pparβ* and *Fabp5* expression during chick development. Similarly, given the interesting expression of *Fabp5* in other areas of the developing embryo, it would be of interest to manipulate the levels of *Fabp5* to confirm its role in the development and border control of the developing nervous system.

Another major finding here is that excess retinoids can cause malformation of the scapula. As discussed earlier, the microarray analysis of EC23 or ATRA genetic targets have implicated many genes linked to mouse scapula development and which need further characterisation in chick. However, other proximally restricted genes may provide further avenues for investigation into the control of scapula development, one of which is seen to be altered in response to both EC23 and ATRA (*Gsc*; chapter 5). *Gsc* is perhaps, one of the more interesting prospects for the regulation of scapula and joint development in chick. It has been shown to be expressed in the chick limb from HH20 onwards in an anterior-ventral-proximal domain (Heanue et al., 1997). This domain is similar to the later domain of *Pax1* expression, a known marker of scapula development (Huang et al., 2000; LeClair et al., 1999). In mouse and chicken, it is then described to be expressed surrounding the developing cartilage and the shoulder, elbow and wrist joints (Gaunt et al., 1993; Heanue et al., 1997). The mouse knock out does not exhibit a limb phenotype (Yamada et al., 1995) and the phenotype exhibited by *Gsc* misexpression in chick is of a change to the angle and length of limb outgrowth as well as elbow fusions (Heanue et al., 1997). This implicates *Gsc* up-regulation in this microarray (chapter 5) as one of the mechanisms behind elbow fusion and cartilage element length concurrent with *Cyp26* and other genes such as *enpp2*. While the misexpression of *Gsc* alone may not have generated a scapula

phenotype, it is possible that its up-regulation after retinoid treatment in conjunction with other genes involved in scapula development (*Alx1, Pbx1* and *Emx2*; chapter 5) and down-regulation of *Pax1* expression, it may have contributed to the phenotypes observed previously (chapter 3).

Blimp1 is not seen to be altered in response to retinoid in the present study however; *Blimp1* knockout in Zebrafish causes shortening or absence of the scapulocoracoid in a similar frequency to the present study (Lee et al, 2006) and may therefore be of interest. Interestingly a study of the genetic targets of *LIM homeobox transcription factor 1, beta* (*Lmx1b*) in mouse has striking similarity to the present data. *Lmx1b* is induced by *Wnt7a* in the dorsal ectoderm and controls the production of dorsal fate. WNT7A signalling is also thought to interact with the ZPA and AER in correct limb development (Capdevila and Belmonte, 2001) which fits with observations that limb development is inhibited here alongside similar phenotypes. *Lmx1b* knockout mice exhibit scapula hypoplasia amongst other malformations and mutation to this gene in humans causes Nail-Patella syndrome, indicating a role in joint development (Feenstra et al., 2012). Feenstra et al (2012) generated a list of 23 genes which were altered in *Lmx1b* knockout mice over 2 days of limb development (Feenstra et al., 2012). Many of these genes are implicated in the development of the scapula as it is a dorsal limb structure. Interestingly, 10 of the 23 genes are also seen to be altered in response to retinoid in the present work. There are also 4 genes altered in response to retinoid also altered in *Lmx1b* knockout mouse limbs at E11.5 in another study (Krawchuk and Kania, 2008). Considering that the number of similar genes is high and that two of the phenotypes seen with retinoids are also seen in *Lmx1b* knockout mice, it is likely that *Lmx1b* may play an earlier role in the retinoid response and is an interesting avenue for further research for both scapula and elbow development.

Whilst *Hoxb8* has been implicated in digit duplication, it is also of interest to note that *Hoxb8* has been linked to scapula development and is up-regulated in response to both retinoids (chapter 5; (Charite et al., 1994). It has been considered an important factor in the production of the ZPA (normal or ectopic) but interestingly, overexpression under the *βRARE* promoter caused malformation of the scapula as well as digit duplication and reduced zeugopod length in mouse. Malformation was shown to be thinning of the scapula as well as abnormalities of the acromion concurrent with malformation of the olecranon. Interestingly, they also noted that under these conditions, there was a delay in development

between anterior and posterior halves of the limb with respect to patterning (Charite et al., 1994), similar to that described with retinoid (chapter 5; (Ali-Khan and Hales, 2006). This may indicate that *Hoxb8* is an important regulator of limb development, may contribute to the developmental delay seen with both retinoids tested here and is worthy of future work.

Concluding remarks:

Altogether, it can be seen that EC23 and EC19 appear to be analogues of ATRA and 13CRA and therefore can be useful tools to study their effects *in vivo*. As EC23 is resistant to CYP26 induced metabolism but causes the same effects *in vivo* as ATRA, it can be concluded that the oxidative metabolites of ATRA do not play a role in development. The differential effect of EC23 on digit development and differentiation compared to ATRA indicates that high levels of retinoid can stall wing development. That ATRA treated wings overcome the developmental stalling quicker than EC23 treated wings indicates that metabolism is a vital part of the early retinoid response. This may allow investigation into teratogenic targets and mechanisms by which the developmental schedule is maintained with respect to other organs. The effects of EC23 also indicate that proliferation and *Shh* induction have been uncoupled in the anterior wing leading to duplication of multiple digit 1s and are consistent with the current understanding of digit development. Given the expression of *Fabp5* in the developing embryo, it may be involved in the control of proliferation in the developing wing, amongst other interesting areas, and provides a mechanism by which EC23 and ATRA may cause the effects seen.

Appendices.

Appendix 1: The 30 most up-regulated genes in response to 1mg/ml ATRA.

Gene Symbol	Gene Title	FC	Corrected p-value
CYP26A1	cytochrome P450, family 26, subfamily A, polypeptide 1	98.14	0.0050
CMBL	carboxymethylenebutenolidase homolog (Pseudomonas)	52.29	0.0076
---	---	47.95	0.0061
NEFM	neurofilament, medium polypeptide 150kDa	38.37	0.0053
---	---	35.34	0.0117
HOXB8	homeobox B8	34.56	0.0159
NEFM	neurofilament, medium polypeptide 150kDa	31.26	0.0061
DHRS3	dehydrogenase/reductase (SDR family) member 3	28.44	0.0050
---	---	26.96	0.0061
PDE1A	Phosphodiesterase 1A, calmodulin-dependent	20.64	0.0085
HOXB4	homeobox B4	19.66	0.0095
---	---	18.83	0.0053
HOXB3	homeobox B3	18.00	0.0227
SIAH3	seven in absentia homolog 3 (Drosophila)	16.94	0.0266
NEFL	neurofilament, light polypeptide 68kDa	15.84	0.0112
RARB	retinoic acid receptor, beta	15.33	0.0068
PGM5	phosphoglucomutase 5	14.98	0.0111
---	---	14.08	0.0143
TFPI2	tissue factor pathway inhibitor 2	13.40	0.0053
HOXB5	homeobox B5	13.37	0.0389
LOC422895	hypothetical gene supported by CR390900	11.50	0.0272
LIX1	Lix1 homolog (chicken)	10.25	0.0353
LYG2	lysozyme G-like 2	9.84	0.0085
LOC423474	hypothetical LOC423474	9.46	0.0153
GATA5	GATA binding protein 5	9.25	0.0454
PAMR1	peptidase domain containing associated with muscle regeneration 1	8.91	0.0196
---	---	8.56	0.0157
GPM6A	glycoprotein M6A	8.45	0.0070
---	---	8.37	0.0081
POSTN	periostin, osteoblast specific factor	8.258	0.00001

Abbreviations: FC, fold change with respect to DMSO; ---, unknown. Significance was calculated using a t-test and the p-value was corrected for multiple tests.

Appendix 2: The 30 most down-regulated genes in response to 1mg/ml ATRA.

Gene Symbol	Gene Title	FC	Corrected p-value
CPA6	carboxypeptidase A6	-26.71	0.00001
EFEMP1	EGF-containing fibulin-like extracellular matrix protein 1	-17.51	0.00001
GNOT1	Gnot1 homeodomain protein	-15.57	0.00007
MSTN	myostatin	-14.54	0.00008
HOXA13	homeobox A13	-13.04	0.00093
TMEM215	Transmembrane protein 215	-12.51	0.00091
C6orf142	chromosome 6 open reading frame 142	-12.18	0.00010
FGF13	fibroblast growth factor 13	-11.24	0.00030
MATN4	matrilin 4	-10.43	0.00000
MNX1	motor neuron and pancreas homeobox 1	-10.41	0.00010
MYOD1	myogenic differentiation 1	-9.16	0.00032
CYTL1	cytokine-like 1	-8.68	0.00000
DNER	delta/notch-like EGF repeat containing	-8.52	0.00010
---	---	-8.35	0.00001
RELN	reelin	-8.08	0.00001
DLX6	distal-less homeobox 6	-7.79	0.00003
---	---	-7.70	0.00000
---	---	-7.56	0.00007
---	---	-7.39	0.00031
RLBP1	retinaldehyde binding protein 1	-7.11	0.00012
---	---	-6.93	0.00005
---	---	-6.61	0.00010
MAB21L2	mab-21-like 2 (C. elegans)	-6.61	0.00008
CA8	carbonic anhydrase VIII	-6.23	0.00006
STK17A	serine/threonine kinase 17a	-6.10	0.00038
FGF1	fibroblast growth factor 1 (acidic)	-6.01	0.00029
MEOX2	mesenchyme homeobox 2	-5.89	0.00002
LMO3	LIM domain only 3 (rhombotin-like 2)	-5.81	0.00006
GNRH1	gonadotropin-releasing hormone 1 (luteinizing-releasing	-5.73	0.00006
TGFB2	transforming growth factor, beta 2	-5.46	0.00008

Abbreviations: FC, fold change with respect to DMSO; ---, unknown. Significance was calculated using a t-test and the p-value was corrected for multiple tests.

Appendix 3: The 30 most up-regulated genes in response to 0.01mg/ml EC23.

Gene Symbol	Gene Title	FC	Corrected p-value
CYP26A1	cytochrome P450, family 26, subfamily A, polypeptide 1	63.94	0.00160
---	---	33.13	0.00329
CMBL	carboxymethylenebutenolidase homolog (Pseudomonas)	31.99	0.01325
NEFM	neurofilament, medium polypeptide 150kDa	27.90	0.00482
---	---	26.12	0.01130
DHRS3	dehydrogenase/reductase (SDR family) member 3	22.85	0.00295
NEFM	neurofilament, medium polypeptide 150kDa	22.29	0.00547
---	---	17.93	0.00741
SIAH3	seven in absentia homolog 3 (Drosophila)	16.46	0.02467
HOXB8	homeobox B8	14.34	0.04387
PDE1A	Phosphodiesterase 1A, calmodulin-dependent	14.31	0.00733
HOXB4	homeobox B4	14.24	0.01352
LYG2	lysozyme G-like 2	13.16	0.00603
---	---	11.92	0.00635
HOXB3	homeobox B3	11.83	0.02976
RARB	retinoic acid receptor, beta	11.67	0.00785
NEFL	neurofilament, light polypeptide 68kDa	10.05	0.01216
HOXB5	homeobox B5	9.62	0.04581
PGM5	phosphoglucomutase 5	9.51	0.01832
TFPI2	tissue factor pathway inhibitor 2	9.11	0.00184
---	---	8.75	0.01507
LOC423474	hypothetical LOC423474	6.50	0.01704
---	---	6.23	0.04876
CDH17	cadherin 17, LI cadherin (liver-intestine)	5.98	0.01216
GALNT6	UDP-N-acetyl-alpha-D-galactosamine:polypeptide N-acetylgalactosaminyltransferase 6 (GalNAc-T6)	5.77	0.02976
AADACL4	arylacetamide deacetylase-like 4	5.66	0.01437
CYP26C1	cytochrome P450, family 26, subfamily C, polypeptide 1	5.54	0.00870
---	---	5.43	0.02589
FER1L3	fer-1-like 3, myoferlin (C. elegans)	5.28	0.00676
---	---	5.27	0.00786

Abbreviations: FC, fold change with respect to DMSO; ---, unknown. Significance was calculated using a t-test and the p-value was corrected for multiple tests.

Appendix 4: The 30 most down-regulated genes in response to 0.01mg/ml EC23.

Gene Symbol	Gene Title	FC	Corrected p-value
EFEMP1	EGF-containing fibulin-like extracellular matrix protein 1	-14.43	0.00565
CPA6	carboxypeptidase A6	-10.30	0.01398
MATN4	matrilin 4	-10.20	0.00068
C6orf142	chromosome 6 open reading frame 142	-10.17	0.02317
COL9A1	collagen, type IX, alpha 1	-9.56	0.01337
MNX1	motor neuron and pancreas homeobox 1	-9.22	0.01777
MSTN	myostatin	-8.17	0.02236
RELN	reelin	-7.63	0.00717
---	---	-7.27	0.00233
RLBP1	retinaldehyde binding protein 1	-5.84	0.00576
COL9A3	collagen, type IX, alpha 3	-5.39	0.01097
---	---	-5.37	0.00068
---	---	-5.10	0.02178
GNOT1	Gnot1 homeodomain protein	-5.10	0.03134
COLEC12	collectin sub-family member 12	-5.08	0.01144
GNRH1	gonadotropin-releasing hormone 1 (luteinizing-releasing hormone)	-5.05	0.01134
LMO3	LIM domain only 3 (rhombotin-like 2)	-4.84	0.00212
---	---	-4.83	0.00729
ITGBL1	integrin, beta-like 1 (with EGF-like repeat domains)	-4.51	0.03033
---	---	-4.50	0.01556
DLX6	distal-less homeobox 6	-4.49	0.00870
CYTL1	cytokine-like 1	-4.42	0.00991
MASP1	mannan-binding lectin serine peptidase 1 (C4/C2 activating component of Ra-reactive factor)	-4.30	0.00221
FAM19A1	Family with sequence similarity 19 (chemokine (C-C motif)-like), member A1	-4.29	0.01709
STK17A	serine/threonine kinase 17a	-4.26	0.02687
ALDH1A2	aldehyde dehydrogenase 1 family, member A2	-4.13	0.01373
GALNT9	UDP-N-acetyl-alpha-D-galactosamine:polypeptide N-acetylgalactosaminyltransferase 9 (GalNAc-T9)	-4.07	0.00409
CBLN2	cerebellin 2	-3.98	0.03132
DNER	delta/notch-like EGF repeat containing	-3.91	0.01704
LOC408038	beta-keratin	-3.87	0.03484

Abbreviations: FC, fold change with respect to DMSO; ---, unknown. Significance was calculated using a t-test and the p-value was corrected for multiple tests.

References

Abbott, B.D., 2009. Review of the expression of peroxisome proliferator-activated receptors alpha (PPAR alpha), beta (PPAR beta), and gamma (PPAR gamma) in rodent and human development. Reprod Toxicol 27, 246-257.

Abe, M., Maeda, T., Wakisaka, S., 2008. Retinoic acid affects craniofacial patterning by changing Fgf8 expression in the pharyngeal ectoderm. Dev Growth Differ 50, 717-729.

Abu-Abed, S., Dolle, P., Metzger, D., Beckett, B., Chambon, P., Petkovich, M., 2001. The retinoic acid-metabolizing enzyme, CYP26A1, is essential for normal hindbrain patterning, vertebral identity, and development of posterior structures. Gene Dev 15, 226-240.

Abu-Hijleh, G., Padmanabhan, R., 1997. Retinoic acid-induced abnormal development of hindlimb joints in the mouse. European journal of morphology 35, 327-336.

Acloque, H., Wilkinson, D., Nieto, M.A., 1996. In situ hybridization analysis of chick embryos in whole mount and tissue sections.

Acloque, H., Wilkinson, D.G., Nieto, M.A., 2008. In situ hybridization analysis of chick embryos in whole-mount and tissue sections. Methods in cell biology 87, 169-185.

Adds, P.J., Brown, N.A., Ataliotis, P., Evans, D.J.R., 2009. Proceedings of the Anatomical Society of Great Britain and Ireland. J. Anat. 215.

Adhikary, T., Kaddatz, K., Finkernagel, F., Schonbauer, A., Meissner, W., Scharfe, M., Jarek, M., Blocker, H., Muller-Brusselbach, S., Muller, R., 2011. Genomewide analyses define different modes of transcriptional regulation by peroxisome proliferator-activated receptor-beta/delta (PPARbeta/delta). Plos One 6, e16344.

Ahn, S., Joyner, A.L., 2004. Dynamic changes in the response of cells to positive hedgehog signaling during mouse limb patterning. Cell 118, 505-516.

Al-Ghaith, L.K., Lewis, J.H., 1982. Pioneer growth cones in virgin mesenchyme: an electron-microscope study in the developing chick wing. J Embryol Exp Morphol 68, 149-160.

Ali-Khan, S.E., Hales, B.F., 2003. Caspase-3 mediates retinoid-induced apoptosis in the organogenesis-stage mouse limb. Birth defects research. Part A, Clinical and molecular teratology 67, 848-860.

Ali-Khan, S.E., Hales, B.F., 2006. Novel retinoid targets in the mouse limb during organogenesis. Toxicol Sci 94, 139-152.

Altman, J., Bayer, S.A., 1984. The development of the rat spinal cord. Advances in anatomy, embryology, and cell biology 85, 1-164.

Alvares, L.E., Winterbottom, F.L., Jorge, E.C., Rodrigues Sobreira, D., Xavier-Neto, J., Schubert, F.R., Dietrich, S., 2009. Chicken dapper genes are versatile markers for mesodermal tissues, embryonic muscle stem cells, neural crest cells, and neurogenic placodes. Dev Dyn 238, 1166-1178.

Anakwe, K., Robson, L., Hadley, J., Buxton, P., Church, V., Allen, S., Hartmann, C., Harfe, B., Nohno, T., Brown, A.M., Evans, D.J., Francis-West, P., 2003. Wnt signalling regulates myogenic differentiation in the developing avian wing. Development 130, 3503-3514.

Anderson, G.L., Funk, A.B., Hanson, E.S., Hill, J.L., Smith, M.A., 2001. Alternative methods for assessing chondrogenesis in micromass culture. Toxicol Method 11, 89-105.

Aoki, M., Kiyonari, H., Nakamura, H., Okamoto, H., 2008. R-spondin2 expression in the apical ectodermal ridge is essential for outgrowth and patterning in mouse limb development. Dev Growth Differ 50, 85-95.

Aquino, J.B., Hjerling-Leffler, J., Koltzenburg, M., Edlund, T., Villar, M.J., Ernfors, P., 2006. In vitro and in vivo differentiation of boundary cap neural crest stem cells into mature Schwann cells. Exp Neurol 198, 438-449.

Araujo, M., Piedra, M.E., Herrera, M.T., Ros, M.A., Nieto, M.A., 1998. The expression and regulation of chick EphA7 suggests roles in limb patterning and innervation. Development 125, 4195-4204.

Ashique, A.M., Fu, K., Richman, J.M., 2002. Signalling via type IA and type IB bone morphogenetic protein receptors (BMPR) regulates intramembranous bone formation, chondrogenesis and feather formation in the chicken embryo. The International journal of developmental biology 46, 243-253.

Astrom, A., Pettersson, U., Chambon, P., Voorhees, J.J., 1994. Retinoic acid induction of human cellular retinoic acid-binding protein-II gene transcription is mediated by retinoic acid receptor-retinoid X receptor heterodimers bound to one far upstream retinoic acid-responsive element with 5-base pair spacing. J Biol Chem 269, 22334-22339.

Astrom, A., Pettersson, U., Krust, A., Chambon, P., Voorhees, J.J., 1990. Retinoic acid and synthetic analogs differentially activate retinoic acid receptor dependent transcription. Biochem Biophys Res Commun 173, 339-345.

Azizan, A., Gaw, J.U., Govindraj, P., Tapp, H., Neame, P.J., 2000. Chondromodulin I and pleiotrophin gene expression in bovine cartilage and epiphysis. Matrix Biol 19, 521-531.

Bachner, D., Ahrens, M., Betat, N., Schroder, D., Gross, G., 1999. Developmental expression analysis of murine autotaxin (ATX). Mech Dev 84, 121-125.

Bain, D.L., Heneghan, A.F., Connaghan-Jones, K.D., Miura, M.T., 2007. Nuclear receptor structure: Implications for function. Annu Rev Physiol 69, 201-220.

Balmer, J.E., Blomhoff, R., 2002. Gene expression regulation by retinoic acid. J Lipid Res 43, 1773-1808.

Barnard, J.H., Collings, J.C., Whiting, A., Przyborski, S.A., Marder, T.B., 2009. Synthetic retinoids: structure-activity relationships. Chemistry 15, 11430-11442.

Barnes, G.L., Hsu, C.W., Mariani, B.D., Tuan, R.S., 1996. Chicken Pax-1 gene: Structure and expression during embryonic somite development. Differentiation 61, 13-23.

Barnes, S.H., Price, S.R., Wentzel, C., Guthrie, S.C., 2010. Cadherin-7 and cadherin-6B differentially regulate the growth, branching and guidance of cranial motor axons. Development 137, 805-814.

Barua, A.B., Sidell, N., 2004. Retinoyl beta-glucuronide: a biologically active interesting retinoid. J Nutr 134, 286S-289S.

Bastida, M.F., Sheth, R., Ros, M.A., 2009. A BMP-Shh negative-feedback loop restricts Shh expression during limb development. Development 136, 3779-3789.

Bastien, J., Rochette-Egly, C., 2004. Nuclear retinoid receptors and the transcription of retinoid-target genes. Gene 328, 1-16.

Bastow, E.R., Byers, S., Golub, S.B., Clarkin, C.E., Pitsillides, A.A., Fosang, A.J., 2008. Hyaluronan synthesis and degradation in cartilage and bone. Cell Mol Life Sci 65, 395-413.

Behonick, D.J., Werb, Z., 2003. A bit of give and take: the relationship between the extracellular matrix and the developing chondrocyte. Mech Dev 120, 1327-1336.

Benko, S., Love, J.D., Beladi, M., Schwabe, J.W., Nagy, L., 2003. Molecular determinants of the balance between co-repressor and co-activator recruitment to the retinoic acid receptor. J Biol Chem 278, 43797-43806.

Bensoussan-Trigano, V., Lallemand, Y., Saint Cloment, C., Robert, B., 2011. Msx1 and Msx2 in limb mesenchyme modulate digit number and identity. Dev Dyn 240, 1190-1202.

Berggren, K., McCaffery, P., Drager, U., Forehand, C.J., 1999. Differential distribution of retinoic acid synthesis in the chicken embryo as determined by immunolocalization of the retinoic acid synthetic enzyme, RALDH-2. Dev Biol 210, 288-304.

Beverdam, A., Meijlink, F., 2001. Expression patterns of group-I aristaless-related genes during craniofacial and limb development. Mech Dev 107, 163-167.

Bizzarro, V., Fontanella, B., Franceschelli, S., Pirozzi, M., Christian, H., Parente, L., Petrella, A., 2010. Role of Annexin A1 in mouse myoblast cell differentiation. J Cell Physiol 224, 757-765.

Blentic, A., Gale, E., Maden, M., 2003. Retinoic acid signalling centres in the avian embryo identified by sites of expression of synthesising and catabolising enzymes. Dev Dyn 227, 114-127.

Blomhoff, R., Blomhoff, H.K., 2006. Overview of retinoid metabolism and function. J Neurobiol 66, 606-630.

Bobick, B.E., Kulyk, W.M., 2008. Regulation of cartilage formation and maturation by mitogen-activated protein kinase signaling. Birth defects research. Part C, Embryo today : reviews 84, 131-154.

Bouillet, P., Oulad-Abdelghani, M., Vicaire, S., Garnier, J.M., Schuhbaur, B., Dolle, P., Chambon, P., 1995. Efficient cloning of cDNAs of retinoic acid-responsive genes in P19 embryonal carcinoma cells and characterization of a novel mouse gene, Stra1 (mouse LERK-2/Eplg2). Dev Biol 170, 420-433.

Boulet, A.M., Capecchi, M.R., 2004. Multiple roles of Hoxa11 and Hoxd11 in the formation of the mammalian forelimb zeugopod. Development 131, 299-309.

Braissant, O., Wahli, W., 1998. Differential expression of peroxisome proliferator-activated receptor-alpha, -beta, and -gamma during rat embryonic development. Endocrinology 139, 2748-2754.

Bravo-Ambrosio, A., Kaprielian, Z., 2011. Crossing the border: molecular control of motor axon exit. International journal of molecular sciences 12, 8539-8561.

Bron, R., Vermeren, M., Kokot, N., Andrews, W., Little, G.E., Mitchell, K.J., Cohen, J., 2007. Boundary cap cells constrain spinal motor neuron somal migration at motor exit points by a semaphorin-plexin mechanism. Neural Dev 2, 21.

Broom, E.R., Gilthorpe, J.D., Butts, T., Campo-Paysaa, F., Wingate, R.J., 2012. The roof plate boundary is a bi-directional organiser of dorsal neural tube and choroid plexus development. Development 139, 4261-4270.

Brown, J.M., Robertson, K.E., Wedden, S.E., Tickle, C., 1997. Alterations in Msx 1 and Msx 2 expression correlate with inhibition of outgrowth of chick facial primordia induced by retinoic acid. Anat Embryol (Berl) 195, 203-207.

Brown, N.A., Wiger, R., 1992. Comparison of Rat and Chick Limb Bud Micromass Cultures for Developmental Toxicity Screening. Toxicol in Vitro 6, 101-107.

Bruneau, S., Mourrain, P., Rosa, F.M., 1997. Expression of contact, a new zebrafish DVR member, marks mesenchymal cell lineages in the developing pectoral fins and head and is regulated by retinoic acid. Mech Dev 65, 163-173.

Brunet, L.J., McMahon, J.A., McMahon, A.P., Harland, R.M., 1998. Noggin, cartilage morphogenesis, and joint formation in the mammalian skeleton. Science 280, 1455-1457.

Budge, J.J.R., 2010. The Biological Effects of Novel Synthetic Retinoids, Durham theses, Durham University. Available at Durham E-Theses Online: http://etheses.dur.ac.uk/781/.

Budhu, A.S., Noy, N., 2002. Direct channeling of retinoic acid between cellular retinoic acid-binding protein II and retinoic acid receptor sensitizes mammary carcinoma cells to retinoic acid-induced growth arrest. Mol Cell Biol 22, 2632-2641.

Burke, A.C., Feduccia, A., 1997. Developmental Patterns and the Identification of Homologies in the avian hand. Science 278.

Buxton, P.G., Kostakopoulou, K., Brickell, P., Thorogood, P., Ferretti, P., 1997. Expression of the transcription factor slug correlates with growth of the limb bud and is regulated by FGF-4 and retinoic acid. The International journal of developmental biology 41, 559-568.

Byrd, N.A., Meyers, E.N., 2005. Loss of Gbx2 results in neural crest cell patterning and pharyngeal arch artery defects in the mouse embryo. Dev Biol 284, 233-245.

Caldwell, R.B., Kierzek, A.M., Arakawa, H., Bezzubov, Y., Zaim, J., Fiedler, P., Kutter, S., Blagodatski, A., Kostovska, D., Koter, M., Plachy, J., Carninci, P., Hayashizaki, Y., Buerstedde, J.M., 2005. Full-length cDNAs from chicken bursal lymphocytes to facilitate gene function analysis. Genome biology 6, R6.

Capdevila, J., Belmonte, J.C.I., 2001. Patterning mechanisms controlling vertebrate limb development. Annu Rev Cell Dev Bi 17, 87-132.

Capdevila, J., Johnson, R.L., 1998. Endogenous and ectopic expression of noggin suggests a conserved mechanism for regulation of BMP function during limb and somite patterning. Dev Biol 197, 205-217.

Capdevila, J., Tsukui, T., Rodriquez Esteban, C., Zappavigna, V., Izpisua Belmonte, J.C., 1999. Control of vertebrate limb outgrowth by the proximal factor Meis2 and distal antagonism of BMPs by Gremlin. Mol Cell 4, 839-849.

Capehart, A.A., 2010. Proteolytic cleavage of versican during limb joint development. Anat Rec (Hoboken) 293, 208-214.

Capellini, T.D., Di Giacomo, G., Salsi, V., Brendolan, A., Ferretti, E., Srivastava, D., Zappavigna, V., Selleri, L., 2006. Pbx1/Pbx2 requirement for distal limb patterning is mediated by the hierarchical control of Hox gene spatial distribution and Shh expression. Development 133, 2263-2273.

Capellini, T.D., Vaccari, G., Ferretti, E., Fantini, S., He, M., Pellegrini, M., Quintana, L., Di Giacomo, G., Sharpe, J., Selleri, L., Zappavigna, V., 2010. Scapula development is governed by genetic interactions of Pbx1 with its family members and with Emx2 via their cooperative control of Alx1. Development 137, 2559-2569.

Cash, D.E., Bock, C.B., Schughart, K., Linney, E., Underhill, T.M., 1997. Retinoic acid receptor alpha function in vertebrate limb skeletogenesis: A modulator of chondrogenesis. J Cell Biol 136, 445-457.

Caton, A., Hacker, A., Naeem, A., Livet, J., Maina, F., Bladt, F., Klein, R., Birchmeier, C., Guthrie, S., 2000. The branchial arches and HGF are growth-promoting and chemoattractant for cranial motor axons. Development 127, 1751-1766.

Chambers, D., Wilson, L., Maden, M., Lumsden, A., 2007. RALDH-independent generation of retinoic acid during vertebrate embryogenesis by CYP1B1. Development 134, 1369-1383.

Chang, S., Fan, J., Nayak, J., 1992. Pathfinding by cranial nerve VII (facial) motorneurons in the chick hindbrain. Development 114, 815-823.

Charite, J., de Graaff, W., Shen, S., Deschamps, J., 1994. Ectopic expression of Hoxb-8 causes duplication of the ZPA in the forelimb and homeotic transformation of axial structures. Cell 78, 589-601.

Charite, J., McFadden, D.G., Olson, E.N., 2000. The bHLH transcription factor dHAND controls Sonic hedgehog expression and establishment of the zone of polarizing activity during limb development. Development 127, 2461-2470.

Chen, C., Grennan, K., Badner, J., Zhang, D., Gershon, E., Jin, L., Liu, C., 2011a. Removing batch effects in analysis of expression microarray data: an evaluation of six batch adjustment methods. Plos One 6, e17238.

Chen, H., Juchau, M.R., 1998. Biotransformation of 13-cis- and 9-cis-retinoic acid to all-trans-retinoic acid in rat conceptal homogenates. Evidence for catalysis by a conceptal isomerase. Drug Metab Dispos 26, 222-228.

Chen, M., Goyal, S., Cai, X., O'Toole, E.A., Woodley, D.T., 1997. Modulation of type VII collagen (anchoring fibril) expression by retinoids in human skin cells. Biochim Biophys Acta 1351, 333-340.

Chen, Q., Zhou, Y., Zhao, X., Zhang, M., 2011b. Effect of dual-specificity protein phosphatase 5 on pluripotency maintenance and differentiation of mouse embryonic stem cells. J Cell Biochem 112, 3185-3193.

Chevallier, A., 1977. Origine des ceintures scapulaires et pelviennes chez l'embryon d'oiseau. . J. Embryol. exp. Morph., 42, 275-292.

Chiang, C., Litingtung, Y., Harris, M.P., Simandl, B.K., Li, Y., Beachy, P.A., Fallon, J.F., 2001. Manifestation of the limb prepattern: limb development in the absence of sonic hedgehog function. Dev Biol 236, 421-435.

Cho, S.H., Oh, C.D., Kim, S.J., Kim, I.C., Chun, J.S., 2003. Retinoic acid inhibits chondrogenesis of mesenchymal cells by sustaining expression of N-cadherin and its associated proteins. J Cell Biochem 89, 837-847.

Chong, S.W., Jiang, Y.J., 2005. Off limits--integrins holding boundaries in somitogenesis. Trends Cell Biol 15, 453-457.

Choocheep, K., Hatano, S., Takagi, H., Watanabe, H., Kimata, K., Kongtawelert, P., Watanabe, H., 2010. Versican facilitates chondrocyte differentiation and regulates joint morphogenesis. J Biol Chem 285, 21114-21125.

Choudhary, D., Jansson, I., Rezaul, K., Han, D.K., Sarfarazi, M., Schenkman, J.B., 2007. Cyp1b1 protein in the mouse eye during development: an immunohistochemical study. Drug Metab Dispos 35, 987-994.

Christie, V.B., Barnard, J.H., Batsanov, A.S., Bridgens, C.E., Cartmell, E.B., Collings, J.C., Maltman, D.J., Redfern, C.P.E., Marder, T.B., Przyborski, S., Whiting, A., 2008. Synthesis and evaluation of synthetic retinoid derivatives as inducers of stem cell differentiation. Org Biomol Chem 6, 3497-3507.

Cioffi, M., Searls, R.L., Hilfer, S.R., 1980. Sulfated Proteoglycan Accumulation during Development of the Embryonic Chick Limb Bud Studied by Electron-Microscopic Autoradiography. J Embryol Exp Morph 55, 195-209.

Collins, C.A., Watt, F.M., 2008. Dynamic regulation of retinoic acid-binding proteins in developing, adult and neoplastic skin reveals roles for beta-catenin and Notch signalling. Dev Biol 324, 55-67.

Conlon, R.A., Rossant, J., 1992. Exogenous retinoic acid rapidly induces anterior ectopic expression of murine Hox-2 genes in vivo. Development 116, 357-368.

Correia, K.M., Conlon, R.A., 2001. Whole-mount in situ hybridization to mouse embryos. Methods 23, 335-338.

Cortina-Ramirez, G.E., Chimal-Monroy, J., 2007. Differential effects of vascular endothelial growth factor on joint formation during limb development. Ann N Y Acad Sci 1116, 134-140.

Coulpier, F., Le Crom, S., Maro, G.S., Manent, J., Giovannini, M., Maciorowski, Z., Fischer, A., Gessler, M., Charnay, P., Topilko, P., 2009. Novel features of boundary cap cells revealed by the analysis of newly identified molecular markers. Glia 57, 1450-1457.

Crossley, P.H., Martinez, S., Ohkubo, Y., Rubenstein, J.L., 2001. Coordinate expression of Fgf8, Otx2, Bmp4, and Shh in the rostral prosencephalon during development of the telencephalic and optic vesicles. Neuroscience 108, 183-206.

Crotwell, P.L., Mabee, P.M., 2007. Gene expression patterns underlying proximal-distal skeletal segmentation in late-stage zebrafish, Danio rerio. Dev Dyn 236, 3111-3128.

Cserjesi, P., Brown, D., Ligon, K.L., Lyons, G.E., Copeland, N.G., Gilbert, D.J., Jenkins, N.A., Olson, E.N., 1995. Scleraxis: a basic helix-loop-helix protein that prefigures skeletal formation during mouse embryogenesis. Development 121, 1099-1110.

Cui, J., Michaille, J.J., Jiang, W., Zile, M.H., 2003. Retinoid receptors and vitamin A deficiency: differential patterns of transcription during early avian development and the rapid induction of RARs by retinoic acid. Dev Biol 260, 496-511.

Cunningham, T.J., Zhao, X., Sandell, L.L., Evans, S.M., Trainor, P.A., Duester, G., 2013. Antagonism between Retinoic Acid and Fibroblast Growth Factor Signaling during Limb Development. Cell reports.

d'Amico-Martel, A., Noden, D.M., 1980. An autoradiographic analysis of the development of the chick trigeminal ganglion. J Embryol Exp Morphol 55, 167-182.

D'Souza, D., Patel, K., 1999. Involvement of long- and short-range signalling during early tendon development. Anat Embryol (Berl) 200, 367-375.

Damm, K., Heyman, R.A., Umesono, K., Evans, R.M., 1993. Functional Inhibition of Retinoic Acid Response by Dominant Negative Retinoic Acid Receptor Mutants. P Natl Acad Sci USA 90, 2989-2993.

Davey, M.G., Paton, I.R., Yin, Y., Schmidt, M., Bangs, F.K., Morrice, D.R., Smith, T.G., Buxton, P., Stamataki, D., Tanaka, M., Munsterberg, A.E., Briscoe, J., Tickle, C., Burt, D.W., 2006. The chicken talpid3 gene encodes a novel protein essential for Hedgehog signaling. Genes Dev 20, 1365-1377.

Dawd, D.S., Hinchliffe, J.R., 1971. Cell death in the "opaque patch" in the central mesenchyme of the developing chick limb: a cytological, cytochemical and electron microscopic analysis. J Embryol Exp Morphol 26, 401-424.

Dawson, M.I., Hobbs, P.D., Derdzinski, K.A., Chao, W.R., Frenking, G., Loew, G.H., Jetten, A.M., Napoli, J.L., Williams, J.B., Sani, B.P., et al., 1989. Effect of structural modifications in the C7-C11 region of the retinoid skeleton on biological activity in a series of aromatic retinoids. J Med Chem 32, 1504-1517.

de The, H., Vivanco-Ruiz, M.M., Tiollais, P., Stunnenberg, H., Dejean, A., 1990. Identification of a retinoic acid responsive element in the retinoic acid receptor beta gene. Nature 343, 177-180.

Delfini, M.C., Hirsinger, E., Pourquie, O., Duprez, D., 2000. Delta 1-activated notch inhibits muscle differentiation without affecting Myf5 and Pax3 expression in chick limb myogenesis. Development 127, 5213-5224.

Delise, A.M., Tuan, R.S., 2002. Analysis of N-cadherin function in limb mesenchymal chondrogenesis in vitro. Dev Dyn 225, 195-204.

Dickman, E.D., Thaller, C., Smith, S.M., 1997. Temporally-regulated retinoic acid depletion produces specific neural crest, ocular and nervous system defects. Development 124, 3111-3121.

Ding, H., Wu, X., Kim, I., Tam, P.P., Koh, G.Y., Nagy, A., 2000. The mouse Pdgfc gene: dynamic expression in embryonic tissues during organogenesis. Mech Dev 96, 209-213.

Dolle, P., 2009. Developmental expression of retinoic acid receptors (RARs). Nucl Recept Signal 7, e006.

Dolle, P., Ruberte, E., Kastner, P., Petkovich, M., Stoner, C.M., Gudas, L.J., Chambon, P., 1989. Differential Expression of Genes Encoding Alpha,Beta and Gamma-Retinoic Acid Receptors and Crabp in the Developing Limbs of the Mouse. Nature 342, 702-705.

Dolle, P., Ruberte, E., Leroy, P., Morriss-Kay, G., Chambon, P., 1990. Retinoic acid receptors and cellular retinoid binding proteins. I. A systematic study of their differential pattern of transcription during mouse organogenesis. Development 110, 1133-1151.

Dong, D., Ruuska, S.E., Levinthal, D.J., Noy, N., 1999. Distinct roles for cellular retinoic acid-binding proteins I and II in regulating signaling by retinoic acid. J Biol Chem 274, 23695-23698.

Dranse, H.J., Sampaio, A.V., Petkovich, M., Underhill, T.M., 2011. Genetic deletion of Cyp26b1 negatively impacts limb skeletogenesis by inhibiting chondrogenesis. J Cell Sci 124, 2723-2734.

Drossopoulou, G., Lewis, K.E., Sanz-Ezquerro, J.J., Nikbakht, N., McMahon, A.P., Hofmann, C., Tickle, C., 2000. A model for anteroposterior patterning of the vertebrate limb based on sequential long- and short-range Shh signalling and Bmp signalling. Development 127, 1337-1348.

Duboc, V., Logan, M.P., 2011. Regulation of limb bud initiation and limb-type morphology. Dev Dyn 240, 1017-1027.

Duprez, D., 2002. Signals regulating muscle formation in the limb during embryonic development. The International journal of developmental biology 46, 915-925.

Durland, J.L., Sferlazzo, M., Logan, M., Burke, A.C., 2008. Visualizing the lateral somitic frontier in the Prx1Cre transgenic mouse. J. Anat. 212, 590-602.

Edom-Vovard, F., Duprez, D., 2004. Signals regulating tendon formation during chick embryonic development. Dev Dyn 229, 449-457.

Ehnis, T., Dieterich, W., Bauer, M., Lampe, B., Schuppan, D., 1996. A chondroitin/dermatan sulfate form of CD44 is a receptor for collagen XIV (undulin). Exp Cell Res 229, 388-397.

Eichele, G., Tickle, C., Alberts, B.M., 1984. Microcontrolled release of biologically active compounds in chick embryos: beads of 200-microns diameter for the local release of retinoids. Anal Biochem 142, 542-555.

Eichele, G., Tickle, C., Alberts, B.M., 1985. Studies on the mechanism of retinoid-induced pattern duplications in the early chick limb bud: temporal and spatial aspects. J Cell Biol 101, 1913-1920.

Elmazar, M.M., Reichert, U., Shroot, B., Nau, H., 1996. Pattern of retinoid-induced teratogenic effects: possible relationship with relative selectivity for nuclear retinoid receptors RAR alpha, RAR beta, and RAR gamma. Teratology 53, 158-167.

Evrard, Y.A., Lun, Y., Aulehla, A., Gan, L., Johnson, R.L., 1998. lunatic fringe is an essential mediator of somite segmentation and patterning. Nature 394, 377-381.

Farrell, E.R., Munsterberg, A.E., 2000. csal1 is controlled by a combination of FGF and Wnt signals in developing limb buds. Dev Biol 225, 447-458.

Feenstra, J.M., Kanaya, K., Pira, C.U., Hoffman, S.E., Eppey, R.J., Oberg, K.C., 2012. Detection of genes regulated by Lmx1b during limb dorsalization. Dev Growth Differ 54, 451-462.

Fell, H.B., Canti, R.G., 1934. Experiments on the Development in vitro of the Avian Knee-Joint. Proceedings of the Royal Society of London. Series B, Biological Sciences. 116, 316-351.

Feng, L., Hernandez, R.E., Waxman, J.S., Yelon, D., Moens, C.B., 2010. Dhrs3a regulates retinoic acid biosynthesis through a feedback inhibition mechanism. Dev Biol 338, 1-14.

Fernandez-Teran, M., Piedra, M.E., Kathiriya, I.S., Srivastava, D., Rodriguez-Rey, J.C., Ros, M.A., 2000. Role of dHAND in the anterior-posterior polarization of the limb bud: implications for the Sonic hedgehog pathway. Development 127, 2133-2142.

Ferrari, D., Kosher, R.A., 2006. Expression of Dlx5 and Dlx6 during specification of the elbow joint. The International journal of developmental biology 50, 709-713.

Ferrari, D., Sumoy, L., Gannon, J., Sun, H., Brown, A.M., Upholt, W.B., Kosher, R.A., 1995. The expression pattern of the Distal-less homeobox-containing gene Dlx-5 in the developing chick limb bud suggests its involvement in apical ectodermal ridge activity, pattern formation, and cartilage differentiation. Mech Dev 52, 257-264.

Fiorella, P.D., Napoli, J.L., 1991. Expression of cellular retinoic acid binding protein (CRABP) in Escherichia coli. Characterization and evidence that holo-CRABP is a substrate in retinoic acid metabolism. J Biol Chem 266, 16572-16579.

Fischer, A., Schumacher, N., Maier, M., Sendtner, M., Gessler, M., 2004. The Notch target genes Hey1 and Hey2 are required for embryonic vascular development. Genes Dev 18, 901-911.

Fisher, M.E., Clelland, A.K., Bain, A., Baldock, R.A., Murphy, P., Downie, H., Tickle, C., Davidson, D.R., Buckland, R.A., 2008. Integrating technologies for comparing 3D gene expression domains in the developing chick limb. Dev Biol 317, 13-23.

Flenniken, A.M., Gale, N.W., Yancopoulos, G.D., Wilkinson, D.G., 1996. Distinct and overlapping expression patterns of ligands for Eph-related receptor tyrosine kinases during mouse embryogenesis. Dev Biol 179, 382-401.

Folberg, A., Nagy Kovacs, E., Luo, J., Giguere, V., Featherstone, M.S., 1999. RARbeta mediates the response of Hoxd4 and Hoxb4 to exogenous retinoic acid. Dev Dyn 215, 96-107.

Fotopoulou, S., Oikonomou, N., Grigorieva, E., Nikitopoulou, I., Paparountas, T., Thanassopoulou, A., Zhao, Z., Xu, Y., Kontoyiannis, D.L., Remboutsika, E., Aidinis, V., 2010. ATX expression and LPA signalling are vital for the development of the nervous system. Dev Biol 339, 451-464.

Francis-West, P.H., Abdelfattah, A., Chen, P., Allen, C., Parish, J., Ladher, R., Allen, S., MacPherson, S., Luyten, F.P., Archer, C.W., 1999. Mechanisms of GDF-5 action during skeletal development. Development 126, 1305-1315.

Francis-West, P.H., Robertson, K.E., Ede, D.A., Rodriguez, C., Izpisua-Belmonte, J.C., Houston, B., Burt, D.W., Gribbin, C., Brickell, P.M., Tickle, C., 1995. Expression of genes encoding bone morphogenetic proteins and sonic hedgehog in talpid (ta3) limb buds: their relationships in the signalling cascade involved in limb patterning. Dev Dyn 203, 187-197.

Francis, P.H., Richardson, M.K., Brickell, P.M., Tickle, C., 1994. Bone morphogenetic proteins and a signalling pathway that controls patterning in the developing chick limb. Development 120, 209-218.

Frohman, M.A., Martin, G.R., 1989. Rapid Amplification of cDNA Ends Using Nested Primers. Technique- A journal of Methods in Cell and Molecular Biology 1, 165-170.

Frolik, C.A., Roberts, A.B., Tavela, T.E., Roller, P.P., Newton, D.L., Sporn, M.B., 1979. Isolation and identification of 4-hydroxy- and 4-oxoretinoic acid. In vitro metabolites of all-trans-retinoic acid in hamster trachea and liver. Biochemistry-Us 18, 2092-2097.

Fuchs, A., Inthal, A., Herrmann, D., Cheng, S., Nakatomi, M., Peters, H., Neubuser, A., 2010. Regulation of Tbx22 during facial and palatal development. Dev Dyn 239, 2860-2874.

Galdones, E., Hales, B.F., 2008. Retinoic acid receptor gamma-induced misregulation of chondrogenesis in the murine limb bud in vitro. Toxicol Sci 106, 223-232.

Gale, E., Prince, V., Lumsden, A., Clarke, J., Holder, N., Maden, M., 1996. Late effects of retinoic acid on neural crest and aspects of rhombomere. Development 122, 783-793.

Gambone, C.J., Hutcheson, J.M., Gabriel, J.L., Beard, R.L., Chandraratna, R.A., Soprano, K.J., Soprano, D.R., 2002. Unique property of some synthetic retinoids: activation of the aryl hydrocarbon receptor pathway. Mol Pharmacol 61, 334-342.

Garcia-Lopez, R., Soula, C., Martinez, S., 2009. Expression analysis of Sulf1 in the chick forebrain at early and late stages of development. Dev Dyn 238, 2418-2429.

Gaunt, S.J., Blum, M., De Robertis, E.M., 1993. Expression of the mouse goosecoid gene during mid-embryogenesis may mark mesenchymal cell lineages in the developing head, limbs and body wall. Development 117, 769-778.

GEISHA, March 2013. Data for this paper was retrieved from the GEISHA database, University of Arizona, Tucson, AZ 85724; World Wide Web URL: http://geisha.arizona.edu;.

Gejima, R., Okafuji, T., Tanaka, H., 2006. The LRR and Ig domain-containing membrane protein SST273 is expressed on motoneurons. Gene Expr Patterns 6, 235-240.

Gerlach-Bank, L.M., Ellis, A.D., Noonen, B., Barald, K.F., 2002. Cloning and expression analysis of the chick DAN gene, an antagonist of the BMP family of growth factors. Dev Dyn 224, 109-115.

Germain, P., Chambon, P., Eichele, G., Evans, R.M., Lazar, M.A., Leid, M., de Lera, A.R., Lotan, R., Mangelsdorf, D.J., Gronemeyer, H., 2006. International Union of Pharmacology. LXIII. Retinoid X receptors. Pharmacol Rev 58, 760-772.

Germain, P., Iyer, J., Zechel, C., Gronemeyer, H., 2001. Co-regulator recruitment and the mechanism of retinoic acid receptor synergy. Nature 415, 187-192.

Germain, P., Kammerer, S., Perez, E., Peluso-Iltis, C., Tortolani, D., Zusi, F.C., Starrett, J., Lapointe, P., Daris, J.P., Marinier, A., de Lera, A.R., Rochel, N., Gronemeyer, H., 2004. Rational design of RAR-selective ligands revealed by RAR beta crystal stucture. Embo Rep 5, 877-882.

Ghyselinck, N.B., Dupe, V., Dierich, A., Messaddeq, N., Garnier, J.M., Rochette-Egly, C., Chambon, P., Mark, M., 1997. Role of the retinoic acid receptor beta (RARbeta) during mouse development. The International journal of developmental biology 41, 425-447.

Golding, J.P., Cohen, J., 1997. Border controls at the mammalian spinal cord: late-surviving neural crest boundary cap cells at dorsal root entry sites may regulate sensory afferent ingrowth and entry zone morphogenesis. Molecular and cellular neurosciences 9, 381-396.

Gomaa, M.S., Yee, S.W., Milbourne, C.E., Barbera, M.C., Simons, C., Brancale, A., 2006. Homology model of human retinoic acid metabolising enzyme cytochrome P450 26A1 (CYP26A1): active site architecture and ligand binding. Journal of enzyme inhibition and medicinal chemistry 21, 361-369.

Goodnough, L.H., Brugmann, S.A., Hu, D., Helms, J.A., 2007. Stage-dependent craniofacial defects resulting from Sprouty2 overexpression. Dev Dyn 236, 1918-1928.

Gould, S.E., Upholt, W.B., Kosher, R.A., 1992. Syndecan 3: a member of the syndecan family of membrane-intercalated proteoglycans that is expressed in high amounts at the onset of chicken limb cartilage differentiation. Proc Natl Acad Sci U S A 89, 3271-3275.

Guthrie, S., 2007. Patterning and axon guidance of cranial motor neurons. Nature reviews. Neuroscience 8, 859-871.

Hajihosseini, M.K., Heath, J.K., 2002. Expression patterns of fibroblast growth factors-18 and -20 in mouse embryos is suggestive of novel roles in calvarial and limb development. Mech Dev 113, 79-83.

Halilagic, A., Ribes, V., Ghyselinck, N.B., Zile, M.H., Dolle, P., Studer, M., 2007. Retinoids control anterior and dorsal properties in the developing forebrain. Dev Biol 303, 362-375.

Hall, B.K., Miyake, T., 1995. Divide, accumulate, differentiate: cell condensation in skeletal development revisited. The International journal of developmental biology 39, 881-893.

Hall, B.K., Miyake, T., 2000. All for one and one for all: condensations and the initiation of skeletal development. Bioessays 22, 138-147.

Hamburger, V., Hamilton, H.L., 1951. A Series of Normal Stages in the Development of the Chick Embryo. J Morphol 88, 49-&.

Harfe, B.D., Scherz, P.J., Nissim, S., Tian, F., McMahon, A.P., Tabin, C.J., 2004. Evidence for an expansion-based temporal Shh gradient in specifying vertebrate digit identities. Cell 118, 517-528.

Hassell, J.R., Horigan, E.A., 1982. Chondrogenesis - a Model Developmental System for Measuring Teratogenic Potential of Compounds. Teratogen Carcin Mut 2, 325-331.

Heanue, T.A., Johnson, R.L., Izpisua-Belmonte, J.C., Stern, C.D., De Robertis, E.M., Tabin, C.J., 1997. Goosecoid misexpression alters the morphology and Hox gene expression of the developing chick limb bud. Mech Dev 69, 31-37.

Helms, J.A., Kim, C.H., Hu, D., Minkoff, R., Thaller, C., Eichele, G., 1997. Sonic hedgehog participates in craniofacial morphogenesis and is down-regulated by teratogenic doses of retinoic acid. Dev Biol 187, 25-35.

Henderson, A., Paul, 2011. Small Molecules for Controlling Stem Cell Differentiation,

Durham theses, Durham University. Available at Durham E-Theses Online: http://etheses.dur.ac.uk/3559/.

Heyman, R.A., Mangelsdorf, D.J., Dyck, J.A., Stein, R.B., Eichele, G., Evans, R.M., Thaller, C., 1992. 9-cis retinoic acid is a high affinity ligand for the retinoid X receptor. Cell 68, 397-406.

Heymann, S., Koudrova, M., Arnold, H., Koster, M., Braun, T., 1996. Regulation and function of SF/HGF during migration of limb muscle precursor cells in chicken. Dev Biol 180, 566-578.

Hihi, A.K., Michalik, L., Wahli, W., 2002. PPARs: transcriptional effectors of fatty acids and their derivatives. Cell Mol Life Sci 59, 790-798.

Hill, R.E., 2007. How to make a zone of polarizing activity: insights into limb development via the abnormality preaxial polydactyly. Dev Growth Differ 49, 439-448.

Hinchliffe, J.R.a.E., D. A., 1967. Limb development in the polydactylous talpid3 mutant of the fowl. J. Embryol. exp. Morph., 17, 10.

Hjerling-Leffler, J., Marmigere, F., Heglind, M., Cederberg, A., Koltzenburg, M., Enerback, S., Ernfors, P., 2005. The boundary cap: a source of neural crest stem cells that generate multiple sensory neuron subtypes. Development 132, 2623-2632.

Hofmann, C., Drossopoulou, G., McMahon, A., Balling, R., Tickle, C., 1998. Inhibitory action of BMPs on Pax1 expression and on shoulder girdle formation during limb development. Dev Dyn 213, 199-206.

Hojo, M., Takada, I., Kimura, W., Fukuda, K., Yasugi, S., 2006. Expression patterns of the chicken peroxisome proliferator-activated receptors (PPARs) during the development of the digestive organs. Gene Expr Patterns 6, 171-179.

Holder, N., 1977. An experimental investigation into the early development of the chick elbow joint. J Embryol Exp Morphol 39, 115-127.

Hoover, F., Glover, J.C., 1998. Regional pattern of retinoid X receptor-alpha gene expression in the central nervous system of the chicken embryo and its up-regulation by exposure to 9-cis retinoic acid. J Comp Neurol 398, 575-586.

Horsfield, J., Ramachandran, A., Reuter, K., LaVallie, E., Collins-Racie, L., Crosier, K., Crosier, P., 2002. Cadherin-17 is required to maintain pronephric duct integrity during zebrafish development. Mech Dev 115, 15-26.

Horton, C., Maden, M., 1995. Endogenous distribution of retinoids during normal development and teratogenesis in the mouse embryo. Dev Dyn 202, 312-323.

Hsu, S.H., Noamani, B., Abernethy, D.E., Zhu, H., Levi, G., Bendall, A.J., 2006. Dlx5- and Dlx6-mediated chondrogenesis: Differential domain requirements for a conserved function. Mech Dev 123, 819-830.

Hu, C.Y., Yang, C.H., Chen, W.Y., Huang, C.J., Huang, H.Y., Chen, M.S., Tsai, H.J., 2006. Egr1 gene knockdown affects embryonic ocular development in zebrafish. Molecular vision 12, 1250-1258.

Hu, D., Helms, J.A., 1999. The role of Sonic hedgehog in normal and abnormal craniofacial morphogenesis. Development 126, 4873-4884.

Hu, D., Marcucio, R.S., 2009. A SHH-responsive signaling center in the forebrain regulates craniofacial morphogenesis via the facial ectoderm. Development 136, 107-116.

Hu, D., Marcucio, R.S., Helms, J.A., 2003. A zone of frontonasal ectoderm regulates patterning and growth in the face. Development 130, 1749-1758.

Huang, C., Hales, B.F., 2009. Teratogen responsive signaling pathways in organogenesis stage mouse limbs. Reprod Toxicol 27, 103-110.

Huang da, W., Sherman, B.T., Lempicki, R.A., 2009. Systematic and integrative analysis of large gene lists using DAVID bioinformatics resources. Nat Protoc 4, 44-57.

Huang, R.J., Christ, B., Patel, K., 2006. Regulation of scapula development. Anat Embryol 211, S65-S71.

Huang, R.J., Zhi, Q.X., Patel, K., Wilting, J., Christ, B., 2000. Dual origin and segmental organisation of the avian scapula. Development 127, 3789-3794.

Hudson, K.S., Andrews, K., Early, J., Mjaatvedt, C.H., Capehart, A.A., 2010. Versican G1 domain and V3 isoform overexpression results in increased chondrogenesis in the developing chick limb in ovo. Anat Rec (Hoboken) 293, 1669-1678.

Hung, I.H., Yu, K., Lavine, K.J., Ornitz, D.M., 2007. FGF9 regulates early hypertrophic chondrocyte differentiation and skeletal vascularization in the developing stylopod. Dev Biol 307, 300-313.

Ide, H., Wada, N., Uchiyama, K., 1994. Sorting out of cells from different parts and stages of the chick limb bud. Dev Biol 162, 71-76.

Idres, N., Marill, J., Flexor, M.A., Chabot, G.G., 2002. Activation of retinoic acid receptor-dependent transcription by all-trans-retinoic acid metabolites and isomers. J Biol Chem 277, 31491-31498.

Itoh, N., Mima, T., Mikawa, T., 1996. Loss of fibroblast growth factor receptors is necessary for terminal differentiation of embryonic limb muscle. Development 122, 291-300.

Iulianella, A., Lohnes, D., 1997. Contribution of retinoic acid receptor gamma to retinoid-induced craniofacial and axial defects. Dev Dynam 209, 92-104.

Iwamasa, H., Ohta, K., Yamada, T., Ushijima, K., Terasaki, H., Tanaka, H., 1999. Expression of Eph receptor tyrosine kinases and their ligands in chick embryonic motor neurons and hindlimb muscles. Dev Growth Differ 41, 685-698.

Izpisua-Belmonte, J.C., Brown, J.M., Duboule, D., Tickle, C., 1992. Expression of Hox-4 genes in the chick wing links pattern formation to the epithelial-mesenchymal interactions that mediate growth. Embo J 11, 1451-1457.

Izpisua-Belmonte, J.C., Tickle, C., Dolle, P., Wolpert, L., Duboule, D., 1991. Expression of the homeobox Hox-4 genes and the specification of position in chick wing development. Nature 350, 585-589.

James, C.G., Appleton, C.T.G., Ulici, V., Underhill, T.M., Beier, F., 2005. Microarray analyses of gene expression during chondrocyte differentiation identifies novel regulators of hypertrophy. Mol Biol Cell 16, 5316-5333.

Jiang, H., Soprano, D.R., Li, S.W., Soprano, K.J., Penner, J.D., Gyda, M., Kochhar, D.M., 1995. MODULATION OF LIMB BUD CHONDROGENESIS BY RETINOIC ACID AND RETINOIC ACID RECEPTORS. Int. J. Dev. Biol. 39, 617-627.

Johnson, A.N., Newfeld, S.J., 2002. The TGF-beta family: signaling pathways, developmental roles, and tumor suppressor activities. TheScientificWorldJournal 2, 892-925.

Johnson, W.E., Li, C., Rabinovic, A., 2007. Adjusting batch effects in microarray expression data using empirical Bayes methods. Biostatistics 8, 118-127.

Kablar, B., Krastel, K., Ying, C., Asakura, A., Tapscott, S.J., Rudnicki, M.A., 1997. MyoD and Myf-5 differentially regulate the development of limb versus trunk skeletal muscle. Development 124, 4729-4738.

Kane, M.A., 2012. Analysis, occurrence, and function of 9-cis-retinoic acid. Biochim Biophys Acta 1821, 10-20.

Karamboulas, K., Dranse, H.J., Underhill, T.M., 2010. Regulation of BMP-dependent chondrogenesis in early limb mesenchyme by TGFbeta signals. J Cell Sci 123, 2068-2076.

Karlsson, M., Strid, A., Sirsjo, A., Eriksson, L., 2008. Homology Models and Molecular Modeling of Human Retinoic Acid Metabolizing Enzymes Cytochrome P45026A1 (CYP26A1) and P450 26B1 (CYP26B1). J. Chem. Theory Comput. 4, 1021-1027.

Kastner, P., Krust, A., Mendelsohn, C., Garnier, J.M., Zelent, A., Leroy, P., Staub, A., Chambon, P., 1990. Murine isoforms of retinoic acid receptor gamma with specific patterns of expression. Proc Natl Acad Sci U S A 87, 2700-2704.

Kastner, P., Mark, M., Ghyselinck, N., Krezel, W., Dupe, V., Grondona, J.M., Chambon, P., 1997. Genetic evidence that the retinoid signal is transduced by heterodimeric RXR/RAR functional units during mouse development. Development 124, 313-326.

Kawakami, Y., Ishikawa, T., Shimabara, M., Tanda, N., Enomoto-Iwamoto, M., Iwamoto, M., Kuwana, T., Ueki, A., Noji, S., Nohno, T., 1996. BMP signaling during bone pattern determination in the developing limb. Development 122, 3557-3566.

Keeble, S., Maden, M., 1984. The Relationship among Retinoid Structure, Affinity for Retinoic Acid-Binding Protein, and Ability to Respecify Pattern in the Regenerating Axolotl Limb. Dev Biol 132, 26-34.

Kim, J., Lo, L., Dormand, E., Anderson, D.J., 2003. SOX10 maintains multipotency and inhibits neuronal differentiation of neural crest stem cells. Neuron 38, 17-31.

Kim, J.S., Ryoo, Z.Y., Chun, J.S., 2007. Cytokine-like 1 (Cytl1) regulates the chondrogenesis of mesenchymal cells. J Biol Chem 282, 29359-29367.

Kim, K.L., Shin, I.S., Kim, J.M., Choi, J.H., Byun, J., Jeon, E.S., Suh, W., Kim, D.K., 2006. Interaction between Tie receptors modulates angiogenic activity of angiopoietin2 in endothelial progenitor cells. Cardiovascular research 72, 394-402.

Kious, B.M., Baker, C.V., Bronner-Fraser, M., Knecht, A.K., 2002. Identification and characterization of a calcium channel gamma subunit expressed in differentiating neurons and myoblasts. Dev Biol 243, 249-259.

Kistler, A., 1987. Limb Bud Cell-Cultures for Estimating the Teratogenic Potential of Compounds - Validation of the Test System with Retinoids. Arch Toxicol 60, 403-414.

Kistler, A., Mislin, M., Gehrig, A., 1985. Chondrogenesis of Limb-Bud Cells - Improved Culture Method and the Effect of the Potent Teratogen Retinoic Acid. Xenobiotica 15, 673-679.

Kitamoto, T., Momoi, M., Momoi, T., 1989. Expression of cellular retinoic acid binding protein II (chick-CRABP II) in the chick embryo. Biochem Biophys Res Commun 164, 531-536.

Klaassen, I., Brakenhoff, R.H., Smeets, S.J., Snow, G.B., Braakhuis, B.J., 2001. Metabolism and growth inhibition of four retinoids in head and neck squamous normal and malignant cells. Br J Cancer 85, 630-635.

Klaholz, B.P., Mitschler, A., Belema, M., Zusi, C., Moras, D., 2000. Enantiomer discrimination illustrated by high-resolution crystal structures of the human nuclear receptor hRARgamma. Proc Natl Acad Sci U S A 97, 6322-6327.

Kleywegt, G.J., Bergfors, T., Senn, H., Le Motte, P., Gsell, B., Shudo, K., Jones, T.A., 1994. Crystal structures of cellular retinoic acid binding proteins I and II in complex with all-trans-retinoic acid and a synthetic retinoid. Structure 2, 1241-1258.

Kliewer, S.A., Umesono, K., Noonan, D.J., Heyman, R.A., Evans, R.M., 1992. Convergence of 9-cis retinoic acid and peroxisome proliferator signalling pathways through heterodimer formation of their receptors. Nature 358, 771-774.

Knezevic, V., Ranson, M., Mackem, S., 1995. The organizer-associated chick homeobox gene, Gnot1, is expressed before gastrulation and regulated synergistically by activin and retinoic acid. Dev Biol 171, 458-470.

Kochhar, D.M., Penner, J.D., 1992. Analysis of High Dysmorphogenic Activity of Ro-13-6307, a Tetramethylated Tetralin Analog of Retinoic Acid. Teratology 45, 637-645.

Koide, T., Downes, M., Chandraratna, R.A.S., Blumberg, B., Umesono, K., 2001. Active repression of RAR signaling is required for head formation. Gene Dev 15, 2111-2121.

Kontges, G., Lumsden, A., 1996. Rhombencephalic neural crest segmentation is preserved throughout craniofacial ontogeny. Development 122, 3229-3242.

Kostetskii, I., Linask, K.K., Zile, M., 1996. Vitamin A deficiency and the expression of retinoic acid receptors during early cardiogenesis in quail embryo. Roux's Arch Dev Biol 205, 260-271.

Kotani, T., Kawakami, K., 2008. Misty somites, a maternal effect gene identified by transposon-mediated insertional mutagenesis in zebrafish that is essential for the somite boundary maintenance. Dev Biol 316, 383-396.

Krawchuk, D., Kania, A., 2008. Identification of genes controlled by LMX1B in the developing mouse limb bud. Dev Dyn 237, 1183-1192.

Krezel, W., Dupe, V., Mark, M., Dierich, A., Kastner, P., Chambon, P., 1996. RXR gamma null mice are apparently normal and compound RXR alpha +/-/RXR beta -/-/RXR gamma -/- mutant mice are viable. Proc Natl Acad Sci U S A 93, 9010-9014.

Kuijper, S., Beverdam, A., Kroon, C., Brouwer, A., Candille, S., Barsh, G., Meijlink, F., 2005. Genetics of shoulder girdle formation: roles of Tbx15 and aristaless-like genes. Development 132, 1601-1610.

Kurokawa, R., DiRenzo, J., Boehm, M., Sugarman, J., Gloss, B., Rosenfeld, M.G., Heyman, R.A., Glass, C.K., 1994. Regulation of retinoid signalling by receptor polarity and allosteric control of ligand binding. Nature 371, 528-531.

Lalevee, S., Anno, Y.N., Chatagnon, A., Samarut, E., Poch, O., Laudet, V., Benoit, G., Lecompte, O., Rochette-Egly, C., 2011. Genome-wide in silico identification of new conserved and functional retinoic acid receptor response elements (direct repeats separated by 5 bp). J Biol Chem 286, 33322-33334.

Lallemand, Y., Bensoussan, V., Cloment, C.S., Robert, B., 2009. Msx genes are important apoptosis effectors downstream of the Shh/Gli3 pathway in the limb. Dev Biol 331, 189-198.

Lallemand, Y., Nicola, M.A., Ramos, C., Bach, A., Cloment, C.S., Robert, B., 2005. Analysis of Msx1; Msx2 double mutants reveals multiple roles for Msx genes in limb development. Development 132, 3003-3014.

Lammer, E.J., Chen, D.T., Hoar, R.M., Agnish, N.D., Benke, P.J., Braun, J.T., Curry, C.J., Fernhoff, P.M., Grix, A.W., Jr., Lott, I.T., et al., 1985. Retinoic acid embryopathy. The New England journal of medicine 313, 837-841.

Lampron, C., Rochette-Egly, C., Gorry, P., Dolle, P., Mark, M., Lufkin, T., LeMeur, M., Chambon, P., 1995. Mice deficient in cellular retinoic acid binding protein II (CRABPII) or in both CRABPI and CRABPII are essentially normal. Development 121, 539-548.

Landmesser, L., Morris, D.G., 1975. The development of functional innervation in the hind limb of the chick embryo. The Journal of physiology 249, 301-326.

Laue, K., Pogoda, H.M., Daniel, P.B., van Haeringen, A., Alanay, Y., von Ameln, S., Rachwalski, M., Morgan, T., Gray, M.J., Breuning, M.H., Sawyer, G.M., Sutherland-Smith, A.J., Nikkels, P.G., Kubisch, C., Bloch, W., Wollnik, B., Hammerschmidt, M., Robertson, S.P., 2011. Craniosynostosis and multiple skeletal anomalies in humans and zebrafish result from a defect in the localized degradation of retinoic acid. Am J Hum Genet 89, 595-606.

Leboy, P.S., Vaias, L., Uschmann, B., Golub, E., Adams, S.L., Pacifici, M., 1989. Ascorbic-Acid Induces Alkaline-Phosphatase, Type-X Collagen, and Calcium Deposition in Cultured Chick Chondrocytes. J Biol Chem 264, 17281-17286.

LeClair, E.E., Bonfiglio, L., Tuan, R.S., 1999. Expression of the paired-box genes Pax-1 and Pax-9 in limb skeleton development. Dev Dynam 214, 101-115.

Lee, Y.M., Osumi-Yamashita, N., Ninomiya, Y., Moon, C.K., Eriksson, U., Eto, K., 1995. Retinoic acid stage-dependently alters the migration pattern and identity of hindbrain neural crest cells. Development 121, 825-837.

Lehmann, J.M., Zhang, X.K., Pfahl, M., 1992. RAR gamma 2 expression is regulated through a retinoic acid response element embedded in Sp1 sites. Mol Cell Biol 12, 2976-2985.

Leid, M., Kastner, P., Chambon, P., 1992a. Multiplicity Generates Diversity in the Retinoic Acid Signaling Pathways. Trends Biochem Sci 17, 427-433.

Leid, M., Kastner, P., Lyons, R., Nakshatri, H., Saunders, M., Zacharewski, T., Chen, J.Y., Staub, A., Garnier, J.M., Mader, S., et al., 1992b. Purification, cloning, and RXR identity of the HeLa cell factor with which RAR or TR heterodimerizes to bind target sequences efficiently. Cell 68, 377-395.

Leroy, P., De Robertis, E.M., 1992. Effects of lithium chloride and retinoic acid on the expression of genes from the Xenopus laevis Hox 2 complex. Dev Dyn 194, 21-32.

Leroy, P., Krust, A., Zelent, A., Mendelsohn, C., Garnier, J.M., Kastner, P., Dierich, A., Chambon, P., 1991. Multiple isoforms of the mouse retinoic acid receptor alpha are generated by alternative splicing and differential induction by retinoic acid. Embo J 10, 59-69.

Levin, A.A., Sturzenbecker, L.J., Kazmer, S., Bosakowski, T., Huselton, C., Allenby, G., Speck, J., Kratzeisen, C., Rosenberger, M., Lovey, A., et al., 1992. 9-cis retinoic acid stereoisomer binds and activates the nuclear receptor RXR alpha. Nature 355, 359-361.

Lewis, P.M., Dunn, M.P., McMahon, J.A., Logan, M., Martin, J.F., St-Jacques, B., McMahon, A.P., 2001. Cholesterol modification of sonic hedgehog is required for long-range signaling activity and effective modulation of signaling by Ptc1. Cell 105, 599-612.

Lindner, V., Wang, Q., Conley, B.A., Friesel, R.E., Vary, C.P., 2005. Vascular injury induces expression of periostin: implications for vascular cell differentiation and migration. Arteriosclerosis, thrombosis, and vascular biology 25, 77-83.

Loganathan, P.G., Nimmagadda, S., Huang, R., Scaal, M., Christ, B., 2005. Comparative analysis of the expression patterns of Wnts during chick limb development. Histochemistry and cell biology 123, 195-201.

Lohnes, D., Kastner, P., Dierich, A., Mark, M., LeMeur, M., Chambon, P., 1993. Function of retinoic acid receptor gamma in the mouse. Cell 73, 643-658.

Lohnes, D., Mark, M., Mendelsohn, C., Dolle, P., Dierich, A., Gorry, P., Gansmuller, A., Chambon, P., 1994. Function of the Retinoic Acid Receptors (Rars) during Development .1. Craniofacial and Skeletal Abnormalities in Rar Double Mutants. Development 120, 2723-2748.

Lorda-Diez, C.I., Montero, J.A., Diaz-Mendoza, M.J., Garcia-Porrero, J.A., Hurle, J.M., 2011. Defining the earliest transcriptional steps of chondrogenic progenitor specification during the formation of the digits in the embryonic limb. Plos One 6, e24546.

Lorda-Diez, C.I., Montero, J.A., Garcia-Porrero, J.A., Hurle, J.M., 2010. Tgfbeta2 and 3 are coexpressed with their extracellular regulator Ltbp1 in the early limb bud and modulate mesodermal outgrowth and BMP signaling in chicken embryos. Bmc Dev Biol 10, 69.

Lorda-Diez, C.I., Montero, J.A., Martinez-Cue, C., Garcia-Porrero, J.A., Hurle, J.M., 2009. Transforming growth factors beta coordinate cartilage and tendon differentiation in the developing limb mesenchyme. J Biol Chem 284, 29988-29996.

Loudig, O., Babichuk, C., White, J., Abu-Abed, S., Mueller, C., Petkovich, M., 2000. Cytochrome P450RAI(CYP26) promoter: a distinct composite retinoic acid response element underlies the complex regulation of retinoic acid metabolism. Mol Endocrinol 14, 1483-1497.

Loudig, O., Maclean, G.A., Dore, N.L., Luu, L., Petkovich, M., 2005. Transcriptional co-operativity between distant retinoic acid response elements in regulation of Cyp26A1 inducibility. Biochem J 392, 241-248.

Lu, C.H., Rincon-Limas, D.E., Botas, J., 2000. Conserved overlapping and reciprocal expression of msh/Msx1 and apterous/Lhx2 in Drosophila and mice. Mech Dev 99, 177-181.

Lu, H.C., Revelli, J.P., Goering, L., Thaller, C., Eichele, G., 1997. Retinoid signaling is required for the establishment of a ZPA and for the expression of Hoxb-8, a mediator of ZPA formation. Development 124, 1643-1651.

Luijten, M., van Beelen, V.A., Verhoef, A., Renkens, M.F., van Herwijnen, M.H., Westerman, A., van Schooten, F.J., Pennings, J.L., Piersma, A.H., 2010. Transcriptomics analysis of retinoic acid embryotoxicity in rat postimplantation whole embryo culture. Reprod Toxicol 30, 333-340.

Lund, B.W., Piu, F., Gauthier, N.K., Eeg, A., Currier, E., Sherbukhin, V., Brann, M.R., Hacksell, U., Olsson, R., 2005. Discovery of a potent, orally available, and isoform-selective retinoic acid beta2 receptor agonist. J Med Chem 48, 7517-7519.

Luo, J., Pasceri, P., Conlon, R.A., Rossant, J., Giguere, V., 1995. Mice lacking all isoforms of retinoic acid receptor beta develop normally and are susceptible to the teratogenic effects of retinoic acid. Mech Dev 53, 61-71.

Macias, D., Ganan, Y., Sampath, T.K., Piedra, M.E., Ros, M.A., Hurle, J.M., 1997. Role of BMP-2 and OP-1 (BMP-7) in programmed cell death and skeletogenesis during chick limb development. Development 124, 1109-1117.

MacLean, G., Abu-Abed, S., Dolle, P., Tahayato, A., Chambon, P., Petkovich, M., 2001. Cloning of a novel retinoic-acid metabolizing cytochrome P450, Cyp26B1, and comparative expression analysis with Cyp26A1 during early murine development. Mech Develop 107, 195-201.

Maclean, G., Dolle, P., Petkovich, M., 2009. Genetic disruption of CYP26B1 severely affects development of neural crest derived head structures, but does not compromise hindbrain patterning. Dev Dyn 238, 732-745.

Maden, M., 1983. The effect of vitamin A on the regenerating axolotl limb. J Embryol Exp Morphol 77, 273-295.

Maden, M., 1994. Distribution of cellular retinoic acid-binding proteins I and II in the chick embryo and their relationship to teratogenesis. Teratology 50, 294-301.

Maden, M., Ong, D.E., Summerbell, D., Chytil, F., 1988. Spatial distribution of cellular protein binding to retinoic acid in the chick limb bud. Nature 335, 733-735.

Maden, M., Ong, D.E., Summerbell, D., Chytil, F., Hirst, E.A., 1989. Cellular retinoic acid-binding protein and the role of retinoic acid in the development of the chick embryo. Dev Biol 135, 124-132.

Maden, M., Sonneveld, E., van der Saag, P.T., Gale, E., 1998. The distribution of endogenous retinoic acid in the chick embryo: implications for developmental mechanisms. Development 125, 4133-4144.

Maden, M., Summerbell, D., 1986. Retinoic acid-binding protein in the chick limb bud: identification at developmental stages and binding affinities of various retinoids. J Embryol Exp Morphol 97, 239-250.

Maden, M., Summerbell, D., Maignan, J., Darmon, M., Shroot, B., 1991. The respecification of limb pattern by new synthetic retinoids and their interaction with cellular retinoic acid-binding protein. Differentiation 47, 49-55.

Mahmood, R., Kiefer, P., Guthrie, S., Dickson, C., Mason, I., 1995. Multiple roles for FGF-3 during cranial neural development in the chicken. Development 121, 1399-1410.

Maltman, D.J., Christie, V.B., Collings, J.C., Barnard, J.H., Fenyk, S., Marder, T.B., Whiting, A., Przyborski, S.A., 2009. Proteomic profiling of the stem cell response to retinoic acid and synthetic retinoid analogues: identification of major retinoid-inducible proteins. Mol Biosyst 5, 458-471.

Mangelsdorf, D.J., Borgmeyer, U., Heyman, R.A., Zhou, J.Y., Ong, E.S., Oro, A.E., Kakizuka, A., Evans, R.M., 1992. Characterization of three RXR genes that mediate the action of 9-cis retinoic acid. Genes Dev 6, 329-344.

Mangelsdorf, D.J., Umesono, K., Kliewer, S.A., Borgmeyer, U., Ong, E.S., Evans, R.M., 1991. A Direct Repeat in the Cellular Retinol-Binding Protein Type-Ii Gene Confers Differential Regulation by Rxr and Rar. Cell 66, 555-561.

Mankoo, B.S., Collins, N.S., Ashby, P., Grigorieva, E., Pevny, L.H., Candia, A., Wright, C.V., Rigby, P.W., Pachnis, V., 1999. Mox2 is a component of the genetic hierarchy controlling limb muscle development. Nature 400, 69-73.

Mariani, F.V., Ahn, C.P., Martin, G.R., 2008. Genetic evidence that FGFs have an instructive role in limb proximal-distal patterning. Nature 453, 401-405.

Marill, J., Capron, C.C., Idres, N., Chabot, G.G., 2002. Human cytochrome P450s involved in the metabolism of 9-cis- and 13-cis-retinoic acids. Biochem Pharmacol 63, 933-943.

Marill, J., Cresteil, T., Lanotte, M., Chabot, G.G., 2000. Identification of human cytochrome P450s involved in the formation of all-trans-retinoic acid principal metabolites. Mol Pharmacol 58, 1341-1348.

Mark, M., Ghyselinck, N.B., Chambon, P., 2006. Function of retinoid nuclear receptors. Lessons from genetic and pharmacological dissections of the retinoic acid signaling pathway during mouse embryogenesis. Annu Rev Pharmacol 46, 451-480.

Marmigere, F., Ernfors, P., 2007. Specification and connectivity of neuronal subtypes in the sensory lineage. Nature reviews. Neuroscience 8, 114-127.

Maro, G.S., Vermeren, M., Voiculescu, O., Melton, L., Cohen, J., Charnay, P., Topilko, P., 2004. Neural crest boundary cap cells constitute a source of neuronal and glial cells of the PNS. Nat Neurosci 7, 930-938.

Martinez-Ceballos, E., Burdsal, C.A., 2001. Differential expression of chicken CYP26 in anterior versus posterior limb bud in response to retinoic acid. J Exp Zool 290, 136-147.

Matt, N., Ghyselinck, N.B., Wendling, O., Chambon, P., Mark, M., 2003. Retinoic acid-induced developmental defects are mediated by RARbeta/RXR heterodimers in the pharyngeal endoderm. Development 130, 2083-2093.

McGonnell, I.M., Clarke, J.D., Tickle, C., 1998. Fate map of the developing chick face: analysis of expansion of facial primordia and establishment of the primary palate. Dev Dyn 212, 102-118.

McNeill, E.M., Roos, K.P., Moechars, D., Clagett-Dame, M., 2010. Nav2 is necessary for cranial nerve development and blood pressure regulation. Neural Dev 5, 6.

McSorley, L.C., Daly, A.K., 2000. Identification of human cytochrome P450 isoforms that contribute to all-trans-retinoic acid 4-hydroxylation. Biochem Pharmacol 60, 517-526.

Means, A.L., Gudas, L.J., 1997. The CRABP I gene contains two separable, redundant regulatory regions active in neural tissues in transgenic mouse embryos. Dev Dyn 209, 59-69.

Mendelsohn, C., Larkin, S., Mark, M., Lemeur, M., Clifford, J., Zelent, A., Chambon, P., 1994a. Rar-Beta Isoforms - Distinct Transcriptional Control by Retinoic Acid and Specific Spatial Patterns of Promoter Activity during Mouse Embryonic-Development. Mech Develop 45, 227-241.

Mendelsohn, C., Lohnes, D., Decimo, D., Lufkin, T., Lemeur, M., Chambon, P., Mark, M., 1994b. Function of the Retinoic Acid Receptors (Rars) during Development .2. Multiple Abnormalities at Various Stages of Organogenesis in Rar Double Mutants. Development 120, 2749-2771.

Mendelsohn, C., Ruberte, E., Chambon, P., 1992. Retinoid Receptors in Vertebrate Limb Development. Dev Biol 152, 50-61.

Mendelsohn, C., Ruberte, E., LeMeur, M., Morriss-Kay, G., Chambon, P., 1991. Developmental analysis of the retinoic acid-inducible RAR-beta 2 promoter in transgenic animals. Development 113, 723-734.

Mercader, N., Leonardo, E., Azpiazu, N., Serrano, A., Morata, G., Martinez, C., Torres, M., 1999. Conserved regulation of proximodistal limb axis development by Meis1/Hth. Nature 402, 425-429.

Mercader, N., Leonardo, E., Piedra, M.E., Martinez-A, C., Ros, M.A., Torres, M., 2000. Opposing RA and FGF signals control proximodistal vertebrate limb development through regulation of Meis genes. Development 127, 3961-3970.

Mercader, N., Selleri, L., Criado, L.M., Pallares, P., Parras, C., Cleary, M.L., Torres, M., 2009. Ectopic Meis1 expression in the mouse limb bud alters P-D patterning in a Pbx1-independent manner. Int. J. Dev. Biol. 53, 1483-1494.

Mercader, N., Tanaka, E.M., Torres, M., 2005. Proximodistal identity during vertebrate limb regeneration is regulated by Meis homeodomain proteins. Development 132, 4131-4142.

Mic, F.A., Duester, G., 2003. Patterning of forelimb bud myogenic precursor cells requires retinoic acid signaling initiated by Raldh2. Dev Biol 264, 191-201.

Mic, F.A., Molotkov, A., Benbrook, D.M., Duester, G., 2003. Retinoid activation of retinoic acid receptor but not retinoid X receptor is sufficient to rescue lethal defect in retinoic acid synthesis. P Natl Acad Sci USA 100, 7135-7140.

Mic, F.A., Molotkov, A., Fan, X.H., Cuenca, A.E., Duester, G., 2000. RALDH3, a retinaldehyde dehydrogenase that generates retinoic acid, is expressed in the ventral retina, otic vesicle and olfactory pit during mouse development. Mech Develop 97, 227-230.

Mic, F.A., Sirbu, I.O., Duester, G., 2004. Retinoic acid synthesis controlled by Raldh2 is required early for limb bud initiation and then later as a proximodistal signal during apical ectodermal ridge formation. J Biol Chem 279, 26698-26706.

Michaille, J.J., Blanchet, S., Kanzler, B., Garnier, J.M., Dhouailly, D., 1994. Characterization of Cdnas Encoding the Chick Retinoic Acid Receptor Gamma-2 and Preferential Distribution of Retinoic Acid Receptor-Gamma Transcripts during Chick Skin Development. Dev Dynam 201, 334-343.

Michaille, J.J., Kanzler, B., Blanchet, S., Garnier, J.M., Dhouailly, D., 1995. Characterization of Cdnas Encoding 2 Chick Retinoic Acid Receptor-Alpha Isoforms and Distribution of Retinoic Acid Receptor-Alpha, Receptor-Beta and Receptor-Gamma Transcripts during Chick Skin Development. Int. J. Dev. Biol. 39, 587-596.

Michalik, L., Wahli, W., 1999. Peroxisome proliferator-activated receptors: three isotypes for a multitude of functions. Current opinion in biotechnology 10, 564-570.

Miletich, I., Yu, W.Y., Zhang, R., Yang, K., Caixeta de Andrade, S., Pereira, S.F., Ohazama, A., Mock, O.B., Buchner, G., Sealby, J., Webster, Z., Zhao, M., Bei, M., Sharpe, P.T., 2011. Developmental stalling and organ-autonomous regulation of morphogenesis. Proc Natl Acad Sci U S A 108, 19270-19275.

Miller, V.A., Rigas, J.R., Muindi, J.R., Tong, W.P., Venkatraman, E., Kris, M.G., Warrell, R.P., Jr., 1994. Modulation of all-trans retinoic acid pharmacokinetics by liarozole. Cancer chemotherapy and pharmacology 34, 522-526.

Mittapalli, V.R., Christ, B., Prols, F., Scaal, M., 2009. Pleiotrophin is expressed in avian somites and tendon anlagen. Histochemistry and cell biology 132, 413-422.

Miura, T., Shiota, K., 2000. TGFbeta2 acts as an "activator" molecule in reaction-diffusion model and is involved in cell sorting phenomenon in mouse limb micromass culture. Dev Dyn 217, 241-249.

Miyagawa-Tomita, S., Kitamoto, T., Momma, K., Takao, A., Momoi, T., 1992. Cellular retinoic acid binding protein type II was preferentially localized in medium and posterior parts of the progress zone of the chick limb bud. Biochem Biophys Res Commun 185, 217-223.

Mollard, R., Viville, S., Ward, S.J., Decimo, D., Chambon, P., Dolle, P., 2000. Tissue-specific expression of retinoic acid receptor isoform transcripts in the mouse embryo. Mech Develop 94, 223-232.

Morriss-Kay, G.M., Murphy, P., Hill, R.E., Davidson, D.R., 1991. Effects of retinoic acid excess on expression of Hox-2.9 and Krox-20 and on morphological segmentation in the hindbrain of mouse embryos. Embo J 10, 2985-2995.

Munoz-Sanjuan, I., Simandl, B.K., Fallon, J.F., Nathans, J., 1999. Expression of chicken fibroblast growth factor homologous factor (FHF)-1 and of differentially spliced isoforms of FHF-2 during development and involvement of FHF-2 in chicken limb development. Development 126, 409-421.

Murray, B., Wilson, D.J., 1997. Muscle patterning, differentiation and vascularisation in the chick wing bud. J Anat 190 (Pt 2), 261-273.

Nadin, L., Murray, M., 1999. Participation of CYP2C8 in retinoic acid 4-hydroxylation in human hepatic microsomes. Biochem Pharmacol 58, 1201-1208.

Nagpal, S., Zelent, A., Chambon, P., 1992. Rar-Beta-4, a Retinoic Acid Receptor Isoform Is Generated from Rar-Beta-2 by Alternative Splicing and Usage of a Cug Initiator Codon. P Natl Acad Sci USA 89, 2718-2722.

Nakanishi, S., Uyeki, E.M., 1985. Benzamide on Chondrocytic Differentiation in Chick Limb Bud Cell-Culture. J Embryol Exp Morph 85, 163-175.

Narita, T., Nishimatsu, S., Wada, N., Nohno, T., 2007. A Wnt3a variant participates in chick apical ectodermal ridge formation: distinct biological activities of Wnt3a splice variants in chick limb development. Dev Growth Differ 49, 493-501.

Niederlander, C., Lumsden, A., 1996. Late emigrating neural crest cells migrate specifically to the exit points of cranial branchiomotor nerves. Development 122, 2367-2374.

Niederreither, K., Abu-Abed, S., Schuhbaur, B., Petkovich, M., Chambon, P., Dolle, P., 2002a. Genetic evidence that oxidative derivatives of retinoic acid are not involved in retinoid signaling during mouse development. Nat Genet 31, 84-88.

Niederreither, K., McCaffery, P., Drager, U.C., Chambon, P., Dolle, P., 1997. Restricted expression and retinoic acid-induced downregulation of the retinaldehyde dehydrogenase type 2 (RALDH-2) gene during mouse development. Mech Dev 62, 67-78.

Niederreither, K., Subbarayan, V., Dolle, P., Chambon, P., 1999. Embryonic retinoic acid synthesis is essential for early mouse post-implantation development. Nat Genet 21, 444-448.

Niederreither, K., Vermot, J., Le Roux, I., Schuhbaur, B., Chambon, P., Dolle, P., 2003. The regional pattern of retinoic acid synthesis by RALDH2 is essential for the development of posterior pharyngeal arches and the enteric nervous system. Development 130, 2525-2534.

Niederreither, K., Vermot, J., Schuhbaur, B., Chambon, P., Dolle, P., 2000. Retinoic acid synthesis and hindbrain patterning in the mouse embryo. Development 127, 75-85.

Niederreither, K., Vermot, J., Schuhbaur, B., Chambon, P., Dolle, P., 2002b. Embryonic retinoic acid synthesis is required for forelimb growth and anteroposterior patterning in the mouse. Development 129, 3563-3574.

Niss, K., Leutz, A., 1998. Expression of the homeobox gene GBX2 during chicken development. Mech Dev 76, 151-155.

Niswander, L., 2008. Methods in avian embryology experimental and molecular manipulation of the embryonic chick limb. Method Cell Biol 87, 135-152.

Niswander, L., Jeffrey, S., Martin, G.R., Tickle, C., 1994. A Positive Feedback Loop Coordinates Growth and Patterning in the Vertebrate Limb. Nature 371, 609-612.

Niswander, L., Tickle, C., Vogel, A., Booth, I., Martin, G.R., 1993. Fgf-4 Replaces the Apical Ectodermal Ridge and Directs Outgrowth and Patterning of the Limb. Cell 75, 579-587.

Njar, V.C., Gediya, L., Purushottamachar, P., Chopra, P., Vasaitis, T.S., Khandelwal, A., Mehta, J., Huynh, C., Belosay, A., Patel, J., 2006. Retinoic acid metabolism blocking agents (RAMBAs) for treatment of cancer and dermatological diseases. Bioorg Med Chem 14, 4323-4340.

Nohno, T., Kawakami, Y., Wada, N., Ishikawa, T., Ohuchi, H., Noji, S., 1997. Differential expression of the two closely related LIM-class homeobox genes LH-2A and LH-2B during limb development. Biochem Biophys Res Commun 238, 506-511.

Nohno, T., Muto, K., Noji, S., Saito, T., Taniguchi, S., 1991. Isoforms of retinoic acid receptor beta expressed in the chicken embryo. Biochim Biophys Acta 1089, 273-275.

Noji, S., Nohno, T., Koyama, E., Muto, K., Ohyama, K., Aoki, Y., Tamura, K., Ohsugi, K., Ide, H., Taniguchi, S., et al., 1991. Retinoic acid induces polarizing activity but is unlikely to be a morphogen in the chick limb bud. Nature 350, 83-86.

Nomura, R., Kamei, E., Hotta, Y., Konishi, M., Miyake, A., Itoh, N., 2006. Fgf16 is essential for pectoral fin bud formation in zebrafish. Biochem Biophys Res Commun 347, 340-346.

Nowlan, N.C., Bourdon, C., Dumas, G., Tajbakhsh, S., Prendergast, P.J., Murphy, P., 2010. Developing bones are differentially affected by compromised skeletal muscle formation. Bone 46, 1275-1285.

Oberlender, S.A., Tuan, R.S., 1994a. Expression and functional involvement of N-cadherin in embryonic limb chondrogenesis. Development 120, 177-187.

Oberlender, S.A., Tuan, R.S., 1994b. Spatiotemporal profile of N-cadherin expression in the developing limb mesenchyme. Cell adhesion and communication 2, 521-537.

Ogita, J., Isogai, E., Sudo, H., Sakiyama, S., Nakagawara, A., Koseki, H., 2001. Expression of the Dan gene during chicken embryonic development. Mech Dev 109, 363-365.

Ogura, T., Alvarez, I.S., Vogel, A., Rodriguez, C., Evans, R.M., Izpisua Belmonte, J.C., 1996. Evidence that Shh cooperates with a retinoic acid inducible co-factor to establish ZPA-like activity. Development 122, 537-542.

Ohbayashi, N., Shibayama, M., Kurotaki, Y., Imanishi, M., Fujimori, T., Itoh, N., Takada, S., 2002. FGF18 is required for normal cell proliferation and differentiation during osteogenesis and chondrogenesis. Genes Dev 16, 870-879.

Ohuchi, H., Hayashibara, Y., Matsuda, H., Onoi, M., Mitsumori, M., Tanaka, M., Aoki, J., Arai, H., Noji, S., 2007. Diversified expression patterns of autotaxin, a gene for phospholipid-generating enzyme during mouse and chicken development. Dev Dyn 236, 1134-1143.

Ohuchi, H., Nakagawa, T., Yamamoto, A., Araga, A., Ohata, T., Ishimaru, Y., Yoshioka, H., Kuwana, T., Nohno, T., Yamasaki, M., Itoh, N., Noji, S., 1997. The mesenchymal factor, FGF10, initiates and maintains the outgrowth of the chick limb bud through interaction with FGF8, an apical ectodermal factor. Development 124, 2235-2244.

Ohuchi, H., Noji, S., 1999. Fibroblast-growth-factor-induced additional limbs in the study of initiation of limb formation, limb identity, myogenesis, and innervation. Cell Tissue Res 296, 45-56.

Okafuji, T., Tanaka, H., 2005. Expression pattern of LINGO-1 in the developing nervous system of the chick embryo. Gene Expr Patterns 6, 57-62.

Oliver, G., De Robertis, E.M., Wolpert, L., Tickle, C., 1990. Expression of a homeobox gene in the chick wing bud following application of retinoic acid and grafts of polarizing region tissue. Embo J 9, 3093-3099.

Ozpolat, B.D., Zapata, M., Daniel Fruge, J., Coote, J., Lee, J., Muneoka, K., Anderson, R., 2012. Regeneration of the elbow joint in the developing chick embryo recapitulates development. Dev Biol 372, 229-238.

Packer, A.I., Crotty, D.A., Elwell, V.A., Wolgemuth, D.J., 1998. Expression of the murine Hoxa4 gene requires both autoregulation and a conserved retinoic acid response element. Development 125, 1991-1998.

Parr, B.A., McMahon, A.P., 1995. Dorsalizing signal Wnt-7a required for normal polarity of D-V and A-P axes of mouse limb. Nature 374, 350-353.

Patel, K., Nittenberg, R., D'Souza, D., Irving, C., Burt, D., Wilkinson, D.G., Tickle, C., 1996. Expression and regulation of Cek-8, a cell to cell signalling receptor in developing chick limb buds. Development 122, 1147-1155.

Pattyn, A., Morin, X., Cremer, H., Goridis, C., Brunet, J.F., 1997. Expression and interactions of the two closely related homeobox genes Phox2a and Phox2b during neurogenesis. Development 124, 4065-4075.

Paulsen, D.F., Solursh, M., 1988. Microtiter Micromass Cultures of Limb-Bud Mesenchymal Cells. In Vitro Cell Dev B 24, 138-147.

Pellegrini, M., Pantano, S., Fumi, M.P., Lucchini, F., Forabosco, A., 2001. Agenesis of the scapula in Emx2 homozygous mutants. Dev Biol 232, 149-156.

Pennimpede, T., Cameron, D.A., MacLean, G.A., Li, H., Abu-Abed, S., Petkovich, M., 2010a. The role of CYP26 enzymes in defining appropriate retinoic acid exposure during embryogenesis. Birth defects research. Part A, Clinical and molecular teratology 88, 883-894.

Pennimpede, T., Cameron, D.A., MacLean, G.A., Petkovich, M., 2010b. Analysis of Cyp26b1/Rarg compound-null mice reveals two genetically separable effects of retinoic acid on limb outgrowth. Dev Biol 339, 179-186.

Perala, N., Peitsaro, N., Sundvik, M., Koivula, H., Sainio, K., Sariola, H., Panula, P., Immonen, T., 2010. Conservation, expression, and knockdown of zebrafish plxnb2a and plxnb2b. Dev Dyn 239, 2722-2734.

Persson, M., 1983. The role of movements in the development of sutural and diarthrodial joints tested by long-term paralysis of chick embryos. J Anat 137 (Pt 3), 591-599.

Peters, J.M., Lee, S.S., Li, W., Ward, J.M., Gavrilova, O., Everett, C., Reitman, M.L., Hudson, L.D., Gonzalez, F.J., 2000. Growth, adipose, brain, and skin alterations resulting from targeted disruption of the mouse peroxisome proliferator-activated receptor beta(delta). Mol Cell Biol 20, 5119-5128.

Peyton, M., Stellrecht, C.M., Naya, F.J., Huang, H.P., Samora, P.J., Tsai, M.J., 1996. BETA3, a novel helix-loop-helix protein, can act as a negative regulator of BETA2 and MyoD-responsive genes. Mol Cell Biol 16, 626-633.

Pignatello, M.A., Kauffman, F.C., Levin, A.A., 1997. Multiple factors contribute to the toxicity of the aromatic retinoid, TTNPB (Ro 13-7410): Binding affinities and disposition. Toxicol Appl Pharm 142, 319-327.

Pignatello, M.A., Kauffman, F.C., Levin, A.A., 1999. Multiple factors contribute to the toxicity of the aromatic retinoid TTNPB (Ro 13-7410): Interactions with the retinoic acid receptors. Toxicol Appl Pharm 159, 109-116.

Pignatello, M.A., Kauffman, F.C., Levin, A.A., 2002. Liarozole markedly increases all trans-retinoic acid toxicity in mouse limb bud cell cultures: A model to explain the potency of the aromatic retinoid (E)-4-[2-(5,6,7,8-tetrahydro-5,5,8,8-tetramethyl-2-naphthylenyl)-1-propenyl] benzoic acid. Toxicol Appl Pharm 178, 186-194.

Pijnappel, W.W., Hendriks, H.F., Folkers, G.E., van den Brink, C.E., Dekker, E.J., Edelenbosch, C., van der Saag, P.T., Durston, A.J., 1993. The retinoid ligand 4-oxo-retinoic acid is a highly active modulator of positional specification. Nature 366, 340-344.

Pispa, J., Mikkola, M.L., Mustonen, T., Thesleff, I., 2003. Ectodysplasin, Edar and TNFRSF19 are expressed in complementary and overlapping patterns during mouse embryogenesis. Gene Expr Patterns 3, 675-679.

Piu, F., Gauthier, N.K., Olsson, R., Currier, E.A., Lund, B.W., Croston, G.E., Hacksell, U., Brann, M.R., 2005. Identification of novel subtype selective RAR agonists. Biochem Pharmacol 71, 156-162.

Pizette, S., Niswander, L., 1999. BMPs negatively regulate structure and function of the limb apical ectodermal ridge. Development 126, 883-894.

Pizette, S., Niswander, L., 2000. BMPs are required at two steps of limb chondrogenesis: formation of prechondrogenic condensations and their differentiation into chondrocytes. Dev Biol 219, 237-249.

Power, S.C., Lancman, J., Smith, S.M., 1999. Retinoic acid is essential for Shh/Hoxd signaling during rat limb outgrowth but not for limb initiation. Dev Dyn 216, 469-480.

Powles, N., Marshall, H., Economou, A., Chiang, C., Murakami, A., Dickson, C., Krumlauf, R., Maconochie, M., 2004. Regulatory analysis of the mouse Fgf3 gene: control of embryonic expression patterns and dependence upon sonic hedgehog (Shh) signalling. Dev Dyn 230, 44-56.

Probst, S., Kraemer, C., Demougin, P., Sheth, R., Martin, G.R., Shiratori, H., Hamada, H., Iber, D., Zeller, R., Zuniga, A., 2011. SHH propagates distal limb bud development by enhancing CYP26B1-mediated retinoic acid clearance via AER-FGF signalling. Development 138, 1913-1923.

Prols, F., Ehehalt, F., Rodriguez-Niedenfuhr, M., He, L., Huang, R., Christ, B., 2004. The role of Emx2 during scapula formation. Dev Biol 275, 315-324.

Pryce, B.A., Watson, S.S., Murchison, N.D., Staverosky, J.A., Dunker, N., Schweitzer, R., 2009. Recruitment and maintenance of tendon progenitors by TGFbeta signaling are essential for tendon formation. Development 136, 1351-1361.

Qin, P., Cimildoro, R., Kochhar, D.M., Soprano, K.J., Soprano, D.R., 2002. PBX, MEIS, and IGF-I are potential mediators of retinoic acid-induced proximodistal limb reduction defects. Teratology 66, 224-234.

Qin, P., Haberbusch, J.M., Soprano, K.J., Soprano, D.R., 2004. Retinoic acid regulates the expression of PBX1, PBX2, and PBX3 in P19 cells both transcriptionally and post-translationally. J Cell Biochem 92, 147-163.

Qiu, X., Lim, C.H., Ho, S.H., Lee, K.H., Jiang, Y.J., 2009. Temporal Notch activation through Notch1a and Notch3 is required for maintaining zebrafish rhombomere boundaries. Development genes and evolution 219, 339-351.

Qu, S., Niswender, K.D., Ji, Q., van der Meer, R., Keeney, D., Magnuson, M.A., Wisdom, R., 1997. Polydactyly and ectopic ZPA formation in Alx-4 mutant mice. Development 124, 3999-4008.

Quarto, R., Dozin, B., Bonaldo, P., Cancedda, R., Colombatti, A., 1993. Type VI collagen expression is upregulated in the early events of chondrocyte differentiation. Development 117, 245-251.

Rallis, C., Bruneau, B.G., Del Buono, J., Seidman, C.E., Seidman, J.G., Nissim, S., Tabin, C.J., Logan, M.P., 2003. Tbx5 is required for forelimb bud formation and continued outgrowth. Development 130, 2741-2751.

Ranson, M., Tickle, C., Mahon, K.A., Mackem, S., 1995. Gnot1, a member of a new homeobox gene subfamily, is expressed in a dynamic, region-specific domain along the proximodistal axis of the developing limb. Mech Dev 51, 17-30.

Rastinejad, F., Wagner, T., Zhao, Q., Khorasanizadeh, S., 2000. Structure of the RXR-RAR DNA-binding complex on the retinoic acid response element DR1. Embo J 19, 1045-1054.

Reijntjes, S., Blentic, A., Gale, E., Maden, M., 2005. The control of morphogen signalling: regulation of the synthesis and catabolism of retinoic acid in the developing embryo. Dev Biol 285, 224-237.

Reijntjes, S., Gale, E., Maden, M., 2003. Expression of the retinoic acid catabolising enzyme CYP26B1 in the chick embryo and its regulation by retinoic acid. Gene Expr Patterns 3, 621-627.

Reijntjes, S., Gale, E., Maden, M., 2004. Generating gradients of retinoic acid in the chick embryo: Cyp26C1 expression and a comparative analysis of the Cyp26 enzymes. Dev Dyn 230, 509-517.

Reijntjes, S., Rodaway, A., Maden, M., 2007. The retinoic acid metabolising gene, CYP26B1, patterns the cartilaginous cranial neural crest in zebrafish. The International journal of developmental biology 51, 351-360.

Renaud, J.P., Rochel, N., Ruff, M., Vivat, V., Chambon, P., Gronemeyer, H., Moras, D., 1995. Crystal structure of the RAR-gamma ligand-binding domain bound to all-trans retinoic acid. Nature 378, 681-689.

Rhinn, M., Dolle, P., 2012. Retinoic acid signalling during development. Development 139, 843-858.

Ribes, V., Otto, D.M., Dickmann, L., Schmidt, K., Schuhbaur, B., Henderson, C., Blomhoff, R., Wolf, C.R., Tickle, C., Dolle, P., 2007. Rescue of cytochrome P450 oxidoreductase (Por) mouse mutants reveals functions in vasculogenesis, brain and limb patterning linked to retinoic acid homeostasis. Dev Biol 303, 66-81.

Riddle, R.D., Johnson, R.L., Laufer, E., Tabin, C., 1993. Sonic hedgehog mediates the polarizing activity of the ZPA. Cell 75, 1401-1416.

Rigas, J.R., Francis, P.A., Muindi, J.R., Kris, M.G., Huselton, C., DeGrazia, F., Orazem, J.P., Young, C.W., Warrell, R.P., Jr., 1993. Constitutive variability in the pharmacokinetics of the natural retinoid, all-trans-retinoic acid, and its modulation by ketoconazole. J Natl Cancer Inst 85, 1921-1926.

Riley, B.B., Chiang, M.Y., Storch, E.M., Heck, R., Buckles, G.R., Lekven, A.C., 2004. Rhombomere boundaries are Wnt signaling centers that regulate metameric patterning in the zebrafish hindbrain. Dev Dyn 231, 278-291.

Rios, A.C., Serralbo, O., Salgado, D., Marcelle, C., 2011. Neural crest regulates myogenesis through the transient activation of NOTCH. Nature 473, 532-535.

Rizgeliene, R., 1996. Skeleton pattern and joint formation in chorioallantoic grafts lacking the anterior or posterior necrotic zones. J Anat 189 (Pt 3), 601-608.

Roberts, A.B., Lamb, L.C., Sporn, M.B., 1980. Metabolism of all-trans-retinoic acid in hamster liver microsomes: oxidation of 4-hydroxy- to 4-keto-retinoic acid. Arch Biochem Biophys 199, 374-383.

Roberts, C., Ivins, S., Cook, A.C., Baldini, A., Scambler, P.J., 2006. Cyp26 genes a1, b1 and c1 are down-regulated in Tbx1 null mice and inhibition of Cyp26 enzyme function produces a phenocopy of DiGeorge Syndrome in the chick. Hum Mol Genet 15, 3394-3410.

Robledo, R.F., Rajan, L., Li, X., Lufkin, T., 2002. The Dlx5 and Dlx6 homeobox genes are essential for craniofacial, axial, and appendicular skeletal development. Genes Dev 16, 1089-1101.

Rochette-Egly, C., Germain, P., 2009. Dynamic and combinatorial control of gene expression by nuclear retinoic acid receptors (RARs). Nucl Recept Signal 7, e005.

Rodriguez-Esteban, C., Schwabe, J.W., Pena, J.D., Rincon-Limas, D.E., Magallon, J., Botas, J., Izpisua Belmonte, J.C., 1998. Lhx2, a vertebrate homologue of apterous, regulates vertebrate limb outgrowth. Development 125, 3925-3934.

Ros, M.A., Dahn, R.D., Fernandez-Teran, M., Rashka, K., Caruccio, N.C., Hasso, S.M., Bitgood, J.J., Lancman, J.J., Fallon, J.F., 2003. The chick oligozeugodactyly (ozd) mutant lacks sonic hedgehog function in the limb. Development 130, 527-537.

Rosello-Diez, A., Ros, M.A., Torres, M., 2011. Diffusible signals, not autonomous mechanisms, determine the main proximodistal limb subdivision. Science 332, 1086-1088.

Rowe, A., Brickell, P.M., 1995. Expression of the chicken retinoid X receptor-gamma gene in migrating cranial neural crest cells. Anat Embryol (Berl) 192, 1-8.

Rowe, A., Richman, J.M., Brickell, P.M., 1991. Retinoic Acid Treatment Alters the Distribution of Retinoic Acid Receptor-Beta Transcripts in the Embryonic Chick Face. Development 111, 1007-1016.

Rowe, A., Richman, J.M., Brickell, P.M., 1992. Development of the Spatial Pattern of Retinoic Acid Receptor-Beta Transcripts in Embryonic Chick Facial Primordia. Development 114, 805-813.

Ruberte, E., Dolle, P., Chambon, P., Morrisskay, G., 1991. Retinoic Acid Receptors and Cellular Retinoid Binding-Proteins .2. Their Differential Pattern of Transcription during Early Morphogenesis in Mouse Embryos. Development 111, 45-60.

Ruberte, E., Dolle, P., Krust, A., Zelent, A., Morriss-Kay, G., Chambon, P., 1990a. Specific spatial and temporal distribution of retinoic acid receptor gamma transcripts during mouse embryogenesis. Development 108, 213-222.

Ruberte, E., Dolle, P., Krust, A., Zelent, A., Morrisskay, G., Chambon, P., 1990b. Specific Spatial and Temporal Distribution of Retinoic Acid Receptor-Gamma Transcripts during Mouse Embryogenesis. Development 108, 213-222.

Ruhl, R., Plum, C., Elmazar, M.M., Nau, H., 2001. Embryonic subcellular distribution of 13-cis- and all-trans-retinoic acid indicates differential cytosolic/nuclear localization. Toxicol Sci 63, 82-89.

Sabado, V., Barraud, P., Baker, C.V., Streit, A., 2012. Specification of GnRH-1 neurons by antagonistic FGF and retinoic acid signaling. Dev Biol 362, 254-262.

Sabherwal, N., Bangs, F., Roth, R., Weiss, B., Jantz, K., Tiecke, E., Hinkel, G.K., Spaich, C., Hauffa, B.P., van der Kamp, H., Kapeller, J., Tickle, C., Rappold, G., 2007. Long-range conserved non-coding SHOX sequences regulate expression in developing chicken limb and are associated with short stature phenotypes in human patients. Hum Mol Genet 16, 210-222.

Samad, O.A., Geisen, M.J., Caronia, G., Varlet, I., Zappavigna, V., Ericson, J., Goridis, C., Rijli, F.M., 2004. Integration of anteroposterior and dorsoventral regulation of Phox2b transcription in cranial motoneuron progenitors by homeodomain proteins. Development 131, 4071-4083.

Sandell, L.L., Sanderson, B.W., Moiseyev, G., Johnson, T., Mushegian, A., Young, K., Rey, J.P., Ma, J.X., Staehling-Hampton, K., Trainor, P.A., 2007. RDH10 is essential for synthesis of embryonic retinoic acid and is required for limb, craniofacial, and organ development. Gene Dev 21, 1113-1124.

Sanford, L.P., Ormsby, I., Gittenberger-de Groot, A.C., Sariola, H., Friedman, R., Boivin, G.P., Cardell, E.L., Doetschman, T., 1997. TGFbeta2 knockout mice have multiple developmental defects that are non-overlapping with other TGFbeta knockout phenotypes. Development 124, 2659-2670.

Sanz-Ezquerro, J.J., Tickle, C., 2000. Autoregulation of Shh expression and Shh induction of cell death suggest a mechanism for modulating polarising activity during chick limb development. Development 127, 4811-4823.

Sato, K., Koizumi, Y., Takahashi, M., Kuroiwa, A., Tamura, K., 2007. Specification of cell fate along the proximal-distal axis in the developing chick limb bud. Development 134, 1397-1406.

Scaal, M., Bonafede, A., Dathe, V., Sachs, M., Cann, G., Christ, B., Brand-Saberi, B., 1999. SF/HGF is a mediator between limb patterning and muscle development. Development 126, 4885-4893.

Scherz, P.J., Harfe, B.D., McMahon, A.P., Tabin, C.J., 2004. The limb bud Shh-Fgf feedback loop is terminated by expansion of former ZPA cells. Science 305, 396-399.

Schmidt, K., Hughes, C., Chudek, J.A., Goodyear, S.R., Aspden, R.M., Talbot, R., Gundersen, T.E., Blomhoff, R., Henderson, C., Wolf, C.R., Tickle, C., 2009. Cholesterol metabolism: the main pathway acting downstream of cytochrome P450 oxidoreductase in skeletal development of the limb. Mol Cell Biol 29, 2716-2729.

Schmuth, M., Haqq, C.M., Cairns, W.J., Holder, J.C., Dorsam, S., Chang, S., Lau, P., Fowler, A.J., Chuang, G., Moser, A.H., Brown, B.E., Man, M.Q., Uchida, Y., Schoonjans, K., Auwerx, J., Chambon, R., Willson, T.M., Elias, P.M., Feingold, K.R., 2004. Peroxisome proliferator-activated receptor (PPAR)-beta/delta stimulates differentiation and lipid accumulation in keratinocytes. J. Invest. Dermatol. 122, 971-983.

Schneider-Maunoury, S., Topilko, P., Seitandou, T., Levi, G., Cohen-Tannoudji, M., Pournin, S., Babinet, C., Charnay, P., 1993. Disruption of Krox-20 results in alteration of rhombomeres 3 and 5 in the developing hindbrain. Cell 75, 1199-1214.

Schneider, R.A., Hu, D., Rubenstein, J.L., Maden, M., Helms, J.A., 2001. Local retinoid signaling coordinates forebrain and facial morphogenesis by maintaining FGF8 and SHH. Development 128, 2755-2767.

Schofield, J.N., Rowe, A., Brickell, P.M., 1992. Position-Dependence of Retinoic Acid Receptor-Beta Gene-Expression in the Chick Limb Bud. Dev Biol 152, 344-353.

Schroeder, A., Mueller, O., Stocker, S., Salowsky, R., Leiber, M., Gassmann, M., Lightfoot, S., Menzel, W., Granzow, M., Ragg, T., 2006. The RIN: an RNA integrity number for assigning integrity values to RNA measurements. Bmc Mol Biol 7, 3.

Schug, T.T., Berry, D.C., Shaw, N.S., Travis, S.N., Noy, N., 2007. Opposing effects of retinoic acid on cell growth result from alternate activation of two different nuclear receptors. Cell 129, 723-733.

Schug, T.T., Berry, D.C., Toshkov, I.A., Cheng, L., Nikitin, A.Y., Noy, N., 2008. Overcoming retinoic acid-resistance of mammary carcinomas by diverting retinoic acid from PPAR beta/delta to RAR. P Natl Acad Sci USA 105, 7546-7551.

Schwarz, Q., Waimey, K.E., Golding, M., Takamatsu, H., Kumanogoh, A., Fujisawa, H., Cheng, H.J., Ruhrberg, C., 2008. Plexin A3 and plexin A4 convey semaphorin signals during facial nerve development. Dev Biol 324, 1-9.

Schweitzer, R., Chyung, J.H., Murtaugh, L.C., Brent, A.E., Rosen, V., Olson, E.N., Lassar, A., Tabin, C.J., 2001. Analysis of the tendon cell fate using Scleraxis, a specific marker for tendons and ligaments. Development 128, 3855-3866.

Scott, W.J., Jr., Walter, R., Tzimas, G., Sass, J.O., Nau, H., Collins, M.D., 1994. Endogenous status of retinoids and their cytosolic binding proteins in limb buds of chick vs mouse embryos. Dev Biol 165, 397-409.

Searls, R.L., Hilfer, S.R., Mirow, S.M., 1972. Ultrastructural Study of Early Chondrogenesis in Chick Wing Bud. Dev Biol 28, 123-&.

Sela-Donenfeld, D., Kayam, G., Wilkinson, D.G., 2009. Boundary cells regulate a switch in the expression of FGF3 in hindbrain rhombomeres. Bmc Dev Biol 9, 16.

Seleiro, E., Rowe, A., Brickell, P., 1995. The chicken retinoid-X-receptor-alpha (RXRa) gene and its expression in the developing limb. Roux's Arch Dev Biol 204, 244-249.

Selleri, L., Depew, M.J., Jacobs, Y., Chanda, S.K., Tsang, K.Y., Cheah, K.S.E., Rubenstein, J.L.R., O'Gorman, S., Cleary, M.L., 2001. Requirement for Pbx1 in skeletal patterning and programming chondrocyte proliferation and differentiation. Development 128, 3543-3557.

Sessler, R.J., Noy, N., 2005. A ligand-activated nuclear localization signal in cellular retinoic acid binding protein-II. Mol Cell 18, 343-353.

Shannon, W., Culverhouse, R., Duncan, J., 2003. Analyzing microarray data using cluster analysis. Pharmacogenomics 4, 41-52.

Shaw, N., Elholm, M., Noy, N., 2003. Retinoic acid is a high affinity selective ligand for the peroxisome proliferator-activated receptor beta/delta. J Biol Chem 278, 41589-41592.

Shearman, R.M., Tulenko, F.J., Burke, A.C., 2011. 3D reconstructions of quail-chick chimeras provide a new fate map of the avian scapula. Dev Biol 355, 1-11.

Shepard, J.B., Gliga, D.A., Morrow, A.P., Hoffman, S., Capehart, A.A., 2008. Versican knock-down compromises chondrogenesis in the embryonic chick limb. Anat Rec (Hoboken) 291, 19-27.

Shepard, J.B., Krug, H.A., LaFoon, B.A., Hoffman, S., Capehart, A.A., 2007. Versican expression during synovial joint morphogenesis. International journal of biological sciences 3, 380-384.

Shi, Y., Hon, M., Evans, R.M., 2002. The peroxisome proliferator-activated receptor delta, an integrator of transcriptional repression and nuclear receptor signaling. Proc Natl Acad Sci U S A 99, 2613-2618.

Shigetani, Y., Howard, S., Guidato, S., Furushima, K., Abe, T., Itasaki, N., 2008. Wise promotes coalescence of cells of neural crest and placode origins in the trigeminal region during head development. Dev Biol 319, 346-358.

Shimshoni, J.A., Roberts, A.G., Scian, M., Topletz, A.R., Blankert, S.A., Halpert, J.R., Nelson, W.L., Isoherranen, N., 2012. Stereoselective formation and metabolism of 4-hydroxy-retinoic Acid enantiomers by cytochrome p450 enzymes. J Biol Chem 287, 42223-42232.

Shukunami, C., Oshima, Y., Hiraki, Y., 2005. Chondromodulin-I and tenomodulin: a new class of tissue-specific angiogenesis inhibitors found in hypovascular connective tissues. Biochem Biophys Res Commun 333, 299-307.

Shukunami, C., Yamamoto, S., Tanabe, T., Hiraki, Y., 1999. Generation of multiple transcripts from the chicken chondromodulin-I gene and their expression during embryonic development. FEBS Lett 456, 165-170.

Singley, C.T., Solursh, M., 1981. The spatial distribution of hyaluronic acid and mesenchymal condensation in the embryonic chick wing. Dev Biol 84, 102-120.

Small, K.M., Potter, S.S., 1993. Homeotic transformations and limb defects in Hox A11 mutant mice. Genes Dev 7, 2318-2328.

Smith, S.M., 1994. Retinoic acid receptor isoform beta 2 is an early marker for alimentary tract and central nervous system positional specification in the chicken. Dev Dyn 200, 14-25.

Smith, S.M., Eichele, G., 1991. Temporal and Regional Differences in the Expression Pattern of Distinct Retinoic Acid Receptor-Beta Transcripts in the Chick-Embryo. Development 111, 245-252.

Smith, S.M., Kirstein, I.J., Wang, Z.S., Fallon, J.F., Kelley, J., Bradshawrouse, J., 1995. Differential Expression of Retinoic Acid Receptor-Beta Isoforms during Chick Limb Ontogeny. Dev Dynam 202, 54-66.

Sohaskey, M.L., Yu, J., Diaz, M.A., Plaas, A.H., Harland, R.M., 2008. JAWS coordinates chondrogenesis and synovial joint positioning. Development 135, 2215-2220.

Song, Y., Hui, J.N., Fu, K.K., Richman, J.M., 2004. Control of retinoic acid synthesis and FGF expression in the nasal pit is required to pattern the craniofacial skeleton. Dev Biol 276, 313-329.

Sonneveld, E., van den Brink, C.E., van der Leede, B.J., Maden, M., van der Saag, P.T., 1999. Embryonal carcinoma cell lines stably transfected with mRARbeta2-lacZ: sensitive system for measuring levels of active retinoids. Exp Cell Res 250, 284-297.

Spagnoli, A., O'Rear, L., Chandler, R.L., Granero-Molto, F., Mortlock, D.P., Gorska, A.E., Weis, J.A., Longobardi, L., Chytil, A., Shimer, K., Moses, H.L., 2007. TGF-beta signaling is essential for joint morphogenesis. J Cell Biol 177, 1105-1117.

Srivastava, D., Cserjesi, P., Olson, E.N., 1995. A subclass of bHLH proteins required for cardiac morphogenesis. Science 270, 1995-1999.

Stadler, H.S., Higgins, K.M., Capecchi, M.R., 2001. Loss of Eph-receptor expression correlates with loss of cell adhesion and chondrogenic capacity in Hoxa13 mutant limbs. Development 128, 4177-4188.

Stekel, D.J., 2003. Microarray Bioinformatics. Cambridge University Press, New York.

Storm, E.E., Kingsley, D.M., 1996. Joint patterning defects caused by single and double mutations in members of the bone morphogenetic protein (BMP) family. Development 122, 3969-3979.

Storm, E.E., Kingsley, D.M., 1999. GDF5 coordinates bone and joint formation during digit development. Dev Biol 209, 11-27.

Stratford, T., Horton, C., Maden, M., 1996. Retinoic acid is required for the initiation of outgrowth in the chick limb bud. Curr. Biol. 6, 1124-1133.

Stratford, T., Logan, C., Zile, M., Maden, M., 1999. Abnormal anteroposterior and dorsoventral patterning of the limb bud in the absence of retinoids. Mech Dev 81, 115-125.

Stratford, T.H., Kostakopoulou, K., Maden, M., 1997. Hoxb-8 has a role in establishing early anterior-posterior polarity in chick forelimb but not hindlimb. Development 124, 4225-4234.

Sucov, H.M., IzpisuaBelmonte, J.C., Ganan, Y., Evans, R.M., 1995. Mouse embryos lacking RXR alpha are resistant to retinoic-acid-induced limb defects. Development 121, 3997-4003.

Summerbell, D., 1974. Interaction between the proximo-distal and antero-posterior co-ordinates of positional value during the specification of positional information in the early development of the chick limb-bud. J Embryol Exp Morphol 32, 227-237.

Summerbell, D., 1976. A descriptive study of the rate of elongation and differentiation of the skeleton of the developing chick wing. J Embryol Exp Morphol 35, 241-260.

Summerbell, D., 1983. The effect of local application of retinoic acid to the anterior margin of the developing chick limb. J Embryol Exp Morphol 78, 269-289.

Summerbell, D., Lewis, J.H., Wolpert, L., 1973. Positional information in chick limb morphogenesis. Nature 244, 492-496.

Sussman, F., de Lera, A.R., 2005. Ligand recognition by RAR and RXR receptors: binding and selectivity. J Med Chem 48, 6212-6219.

Swindell, E.C., Moeller, C., Thaller, C., Eichele, G., 2001. Cloning and expression analysis of chicken Lix1, a founding member of a novel gene family. Mech Dev 109, 405-408.

Swindell, E.C., Thaller, C., Sockanathan, S., Petkovich, M., Jessell, T.M., Eichele, G., 1999. Complementary domains of retinoic acid production and degradation in the early chick embryo. Dev Biol 216, 282-296.

Tachibana, K., Kobayashi, Y., Tanaka, T., Tagami, M., Sugiyama, A., Katayama, T., Ueda, C., Yamasaki, D., Ishimoto, K., Sumitomo, M., Uchiyama, Y., Kohro, T., Sakai, J., Hamakubo, T., Kodama, T., Doi, T., 2005. Gene expression profiling of potential peroxisome proliferator-activated receptor (PPAR) target genes in human hepatoblastoma cell lines inducibly expressing different PPAR isoforms. Nuclear receptor 3, 3.

Taimi, M., Helvig, C., Wisniewski, J., Ramshaw, H., White, J., Amad, M., Korczak, B., Petkovich, M., 2004. A novel human cytochrome P450, CYP26C1, involved in metabolism of 9-cis and all-trans isomers of retinoic acid. J Biol Chem 279, 77-85.

Takada, I., Yu, R.T., Xu, H.E., Lambert, M.H., Montana, V.G., Kliewer, S.A., Evans, R.M., Umesono, K., 2000. Alteration of a single amino acid in peroxisome proliferator-activated receptor-alpha (PPAR alpha) generates a PPAR delta phenotype. Mol Endocrinol 14, 733-740.

Takahashi, M., Tamura, K., Buscher, D., Masuya, H., Yonei-Tamura, S., Matsumoto, K., Naitoh-Matsuo, M., Takeuchi, J., Ogura, K., Shiroishi, T., Ogura, T., Belmonte, J.C.I., 1998. The role of Alx-4 in the establishment of anteroposterior polarity during vertebrate limb development. Development 125, 4417-4425.

Tamarin, A., Crawley, A., Lee, J., Tickle, C., 1984. Analysis of upper beak defects in chicken embryos following with retinoic acid. J Embryol Exp Morphol 84, 105-123.

Tamura, K., Yokouchi, Y., Kuroiwa, A., Ide, H., 1997. Retinoic acid changes the proximodistal developmental competence and affinity of distal cells in the developing chick limb bud. Dev Biol 188, 224-234.

Tan, N.S., Icre, G., Montagner, A., Bordier-ten-Heggeler, B., Wahli, W., Michalik, L., 2007. The nuclear hormone receptor peroxisome proliferator-activated receptor beta/delta potentiates cell chemotactism, polarization, and migration. Mol Cell Biol 27, 7161-7175.

Tan, N.S., Michalik, L., Desvergne, B., Wahli, W., 2005. Multiple expression control mechanisms of peroxisome proliferator-activated receptors and their target genes. The Journal of steroid biochemistry and molecular biology 93, 99-105.

Tan, N.S., Shaw, N.S., Vinckenbosch, N., Liu, P., Yasmin, R., Desvergne, B., Wahli, W., Noy, N., 2002. Selective cooperation between fatty acid binding proteins and peroxisome proliferator-activated receptors in regulating transcription. Mol Cell Biol 22, 5114-5127.

te Welscher, P., Fernandez-Teran, M., Ros, M.A., Zeller, R., 2002. Mutual genetic antagonism involving GLI3 and dHAND prepatterns the vertebrate limb bud mesenchyme prior to SHH signaling. Genes Dev 16, 421-426.

Ten Hagen, K.G., Bedi, G.S., Tetaert, D., Kingsley, P.D., Hagen, F.K., Balys, M.M., Beres, T.M., Degand, P., Tabak, L.A., 2001. Cloning and characterization of a ninth member of the UDP-GalNAc:polypeptide N-acetylgalactosaminyltransferase family, ppGaNTase-T9. J Biol Chem 276, 17395-17404.

Thaller, C., Eichele, G., 1987. Identification and spatial distribution of retinoids in the developing chick limb bud. Nature 327, 625-628.

Thaller, C., Hofmann, C., Eichele, G., 1993. 9-cis-retinoic acid, a potent inducer of digit pattern duplications in the chick wing bud. Development 118, 957-965.

Thatcher, J.E., Isoherranen, N., 2009. The role of CYP26 enzymes in retinoic acid clearance. Expert opinion on drug metabolism & toxicology 5, 875-886.

Theodorakis, K., Kyriakopoulou, K., Wassef, M., Karagogeos, D., 2002. Novel sites of expression of the bHLH gene NSCL1 in the developing nervous system. Mech Dev 119 Suppl 1, S103-106.

Thisse, B., Thisse, C., 2005. Functions and regulations of fibroblast growth factor signaling during embryonic development. Dev Biol 287, 390-402.

Thorogood, P.V., Hinchliffe, J.R., 1975. Analysis of Condensation Process during Chondrogenesis in Embryonic Chick Hind Limb. J Embryol Exp Morph 33, 581-606.

Tickle, C., 1981. The number of polarizing region cells required to specify additional digits in the developing chick wing. Nature 289, 295-298.

Tickle, C., Alberts, B., Wolpert, L., Lee, J., 1982. Local application of retinoic acid to the limb bond mimics the action of the polarizing region. Nature 296, 564-566.

Tickle, C., Crawley, A., 1988. The effects of local application of retinoids to different positions along the proximo-distal axis of embryonic chick wings. Roux's Arch Dev Biol 197, 27-36.

Tickle, C., Crawley, A., Farrar, J., 1989. Retinoic acid application to chick wing buds leads to a dose-dependent reorganization of the apical ectodermal ridge that is mediated by the mesenchyme. Development 106, 691-705.

Tickle, C., Lee, J., Eichele, G., 1985. A quantitative analysis of the effect of all-trans-retinoic acid on the pattern of chick wing development. Dev Biol 109, 82-95.

Timmons, P.M., Wallin, J., Rigby, P.W., Balling, R., 1994. Expression and function of Pax 1 during development of the pectoral girdle. Development 120, 2773-2785.

Topletz, A.R., Thatcher, J.E., Zelter, A., Lutz, J.D., Tay, S., Nelson, W.L., Isoherranen, N., 2012. Comparison of the function and expression of CYP26A1 and CYP26B1, the two retinoic acid hydroxylases. Biochem Pharmacol 83, 149-163.

Towers, M., Mahood, R., Yin, Y., Tickle, C., 2008. Integration of growth and specification in chick wing digit-patterning. Nature 452, 882-886.

Towers, M., Signolet, J., Sherman, A., Sang, H., Tickle, C., 2011. Insights into bird wing evolution and digit specification from polarizing region fate maps. Nature communications 2, 426.

Tsiairis, C.D., McMahon, A.P., 2008. Disp1 regulates growth of mammalian long bones through the control of Ihh distribution. Dev Biol 317, 480-485.

Tucker, K.L., Meyer, M., Barde, Y.A., 2001a. Neurotrophins are required for nerve growth during development. Nat Neurosci 4, 29-37.

Tucker, R.P., Adams, J.C., Lawler, J., 1995. Thrombospondin-4 is expressed by early osteogenic tissues in the chick embryo. Dev Dyn 203, 477-490.

Tucker, R.P., Chiquet-Ehrismann, R., Chevron, M.P., Martin, D., Hall, R.J., Rubin, B.P., 2001b. Teneurin-2 is expressed in tissues that regulate limb and somite pattern formation and is induced in vitro and in situ by FGF8. Dev Dyn 220, 27-39.

Tzchori, I., Day, T.F., Carolan, P.J., Zhao, Y., Wassif, C.A., Li, L., Lewandoski, M., Gorivodsky, M., Love, P.E., Porter, F.D., Westphal, H., Yang, Y., 2009. LIM homeobox transcription factors integrate signaling events that control three-dimensional limb patterning and growth. Development 136, 1375-1385.

Urbach, J., Rando, R.R., 1994. Isomerization of all-trans-retinoic acid to 9-cis-retinoic acid. Biochem J 299 (Pt 2), 459-465.

Uysal-Onganer, P., Kypta, R.M., 2012. Wnt11 in 2011 - the regulation and function of a non-canonical Wnt. Acta physiologica 204, 52-64.

Valasek, P., Theis, S., Krejci, E., Grim, M., Maina, F., Shwartz, Y., Otto, A., Huang, R.J., Patel, K., 2010. Somitic origin of the medial border of the mammalian scapula and its homology to the avian scapula blade. J. Anat. 216, 482-488.

Vargesson, N., 2003. Vascularization of the developing chick limb bud: role of the TGFbeta signalling pathway. J Anat 202, 93-103.

Vargesson, N., Clarke, J.D., Vincent, K., Coles, C., Wolpert, L., Tickle, C., 1997. Cell fate in the chick limb bud and relationship to gene expression. Development 124, 1909-1918.

Vargesson, N., Luria, V., Messina, I., Erskine, L., Laufer, E., 2001. Expression patterns of Slit and Robo family members during vertebrate limb development. Mech Dev 106, 175-180.

Venepally, P., Reddy, L.G., Sani, B.P., 1996. Analysis of the effects of CRABP I expression on the RA-induced transcription mediated by retinoid receptors. Biochemistry-Us 35, 9974-9982.

Vermeren, M., Maro, G.S., Bron, R., McGonnell, I.M., Charnay, P., Topilko, P., Cohen, J., 2003. Integrity of developing spinal motor columns is regulated by neural crest derivatives at motor exit points. Neuron 37, 403-415.

Voiculescu, O., Taillebourg, E., Pujades, C., Kress, C., Buart, S., Charnay, P., Schneider-Maunoury, S., 2001. Hindbrain patterning: Krox20 couples segmentation and specification of regional identity. Development 128, 4967-4978.

Wada, N., 2011. Spatiotemporal changes in cell adhesiveness during vertebrate limb morphogenesis. Dev Dyn 240, 969-978.

Wagner, M., Thaller, C., Jessell, T., Eichele, G., 1990. Polarizing activity and retinoid synthesis in the floor plate of the neural tube. Nature 345, 819-822.

Wakabayashi, T., Matsumine, A., Nakazora, S., Hasegawa, M., Iino, T., Ota, H., Sonoda, H., Sudo, A., Uchida, A., 2010. Fibulin-3 negatively regulates chondrocyte differentiation. Biochem Biophys Res Commun 391, 1116-1121.

Walker, W.L., Liao, I.H., Gilbert, D.L., Wong, B., Pollard, K.S., McCulloch, C.E., Lit, L., Sharp, F.R., 2008. Empirical Bayes accomodation of batch-effects in microarray data using identical replicate reference samples: application to RNA expression profiling of blood from Duchenne muscular dystrophy patients. BMC genomics 9, 494.

Wanek, N., Gardiner, D.M., Muneoka, K., Bryant, S.V., 1991. Conversion by retinoic acid of anterior cells into ZPA cells in the chick wing bud. Nature 350, 81-83.

Wang, B.G., He, L.W., Ehehalt, F., Geetha-Loganathan, P., Nimmagadda, S., Christ, B., Scaal, M., Huang, R.J., 2005. The formation of the avian scapula blade takes place in the hypaxial domain of the somites and requires somatopleure-derived BMP signals. Dev Biol 287, 11-18.

Wang, X., Penzes, P., Napoli, J.L., 1996. Cloning of a cDNA encoding an aldehyde dehydrogenase and its expression in Escherichia coli. Recognition of retinal as substrate. J Biol Chem 271, 16288-16293.

Wang, Z., Young, R.L., Xue, H., Wagner, G.P., 2011. Transcriptomic analysis of avian digits reveals conserved and derived digit identities in birds. Nature 477, 583-586.

Watanabe, T., Sato, Y., Saito, D., Tadokoro, R., Takahashi, Y., 2009. EphrinB2 coordinates the formation of a morphological boundary and cell epithelialization during somite segmentation. Proc Natl Acad Sci U S A 106, 7467-7472.

Watari-Goshima, N., Chisaka, O., 2011. Chicken HOXA3 gene: its expression pattern and role in branchial nerve precursor cell migration. International journal of biological sciences 7, 87-101.

Waxman, J.S., Keegan, B.R., Roberts, R.W., Poss, K.D., Yelon, D., 2008. Hoxb5b acts downstream of retinoic acid signaling in the forelimb field to restrict heart field potential in zebrafish. Dev Cell 15, 923-934.

Wedden, S.E., 1987. Epithelial Mesenchymal Interactions in the Development of Chick Facial Primordia and the Target of Retinoid Action. Development 99, 341-351.

Weiner, J.A., Koo, S.J., Nicolas, S., Fraboulet, S., Pfaff, S.L., Pourquie, O., Sanes, J.R., 2004. Axon fasciculation defects and retinal dysplasias in mice lacking the immunoglobulin superfamily adhesion molecule BEN/ALCAM/SC1. Molecular and cellular neurosciences 27, 59-69.

Weintraub, H., Davis, R., Tapscott, S., Thayer, M., Krause, M., Benezra, R., Blackwell, T.K., Turner, D., Rupp, R., Hollenberg, S., et al., 1991. The myoD gene family: nodal point during specification of the muscle cell lineage. Science 251, 761-766.

Weisinger, K., Wilkinson, D.G., Sela-Donenfeld, D., 2008. Inhibition of BMPs by follistatin is required for FGF3 expression and segmental patterning of the hindbrain. Dev Biol 324, 213-225.

Weston, A.D., Rosen, V., Chandraratna, R.A., Underhill, T.M., 2000. Regulation of skeletal progenitor differentiation by the BMP and retinoid signaling pathways. J Cell Biol 148, 679-690.

White, J.A., Beckett-Jones, B., Guo, Y.D., Dilworth, F.J., Bonasoro, J., Jones, G., Petkovich, M., 1997. cDNA cloning of human retinoic acid-metabolizing enzyme (hP450RAI) identifies a novel family of cytochromes P450. J Biol Chem 272, 18538-18541.

White, J.A., Guo, Y.D., Baetz, K., Beckett-Jones, B., Bonasoro, J., Hsu, K.E., Dilworth, F.J., Jones, G., Petkovich, M., 1996. Identification of the retinoic acid-inducible all-trans-retinoic acid 4-hydroxylase. J Biol Chem 271, 29922-29927.

White, J.A., Ramshaw, H., Taimi, M., Stangle, W., Zhang, A., Everingham, S., Creighton, S., Tam, S.P., Jones, G., Petkovich, M., 2000. Identification of the human cytochrome P450, P450RAI-2, which is predominantly expressed in the adult cerebellum and is responsible for all-trans-retinoic acid metabolism. Proc Natl Acad Sci U S A 97, 6403-6408.

Wilkinson, D., 1992. Whole mount in situ hybridization of vertebrate embryos. . IRL Press, Oxford.

Wilkinson, D.G., Bhatt, S., Chavrier, P., Bravo, R., Charnay, P., 1989. Segment-specific expression of a zinc-finger gene in the developing nervous system of the mouse. Nature 337, 461-464.

Williams, J.B., Shields, C.O., Brettel, L.M., Napoli, J.L., 1987. Assessment of retinoid-induced differentiation of F9 embryonal carcinoma cells with an enzyme-linked immunoadsorbent assay for laminin: statistical comparison of dose-response curves. Anal Biochem 160, 267-274.

Williams, S.S., Mear, J.P., Liang, H.C., Potter, S.S., Aronow, B.J., Colbert, M.C., 2004. Large-scale reprogramming of cranial neural crest gene expression by retinoic acid exposure. Physiol Genomics 19, 184-197.

Wilson, D.G., Phamluong, K., Lin, W.Y., Barck, K., Carano, R.A., Diehl, L., Peterson, A.S., Martin, F., Solloway, M.J., 2012. Chondroitin sulfate synthase 1 (Chsy1) is required for bone development and digit patterning. Dev Biol 363, 413-425.

Wilson, L.J., Myat, A., Sharma, A., Maden, M., Wingate, R.J., 2007. Retinoic acid is a potential dorsalising signal in the late embryonic chick hindbrain. Bmc Dev Biol 7, 138.

Yajima, H., Hara, K., Ide, H., Tamura, K., 2002. Cell adhesiveness and affinity for limb pattern formation. The International journal of developmental biology 46, 897-904.

Yajima, H., Yoneitamura, S., Watanabe, N., Tamura, K., Ide, H., 1999. Role of N-cadherin in the sorting-out of mesenchymal cells and in the positional identity along the proximodistal axis of the chick limb bud. Dev Dyn 216, 274-284.

Yamada, G., Mansouri, A., Torres, M., Stuart, E.T., Blum, M., Schultz, M., De Robertis, E.M., Gruss, P., 1995. Targeted mutation of the murine goosecoid gene results in craniofacial defects and neonatal death. Development 121, 2917-2922.

Yamamoto, M., Gotoh, Y., Tamura, K., Tanaka, M., Kawakami, A., Ide, H., Kuroiwa, A., 1998. Coordinated expression of Hoxa-11 and Hoxa-13 during limb muscle patterning. Development 125, 1325-1335.

Yang, Y., Drossopoulou, G., Chuang, P.T., Duprez, D., Marti, E., Bumcrot, D., Vargesson, N., Clarke, J., Niswander, L., McMahon, A., Tickle, C., 1997. Relationship between dose, distance and time in Sonic Hedgehog-mediated regulation of anteroposterior polarity in the chick limb. Development 124, 4393-4404.

Yashiro, K., Zhao, X.L., Uehara, M., Yamashita, K., Nishijima, M., Nishino, J., Saijoh, Y., Sakai, Y., Hamada, H., 2004. Regulation of retinoic acid distribution is required for proximodistal patterning and outgrowth of the developing mouse limb. Dev Cell 6, 411-422.

Yi, S.E., Daluiski, A., Pederson, R., Rosen, V., Lyons, K.M., 2000. The type I BMP receptor BMPRIB is required for chondrogenesis in the mouse limb. Development 127, 621-630.

Yokouchi, Y., Nakazato, S., Yamamoto, M., Goto, Y., Kameda, T., Iba, H., Kuroiwa, A., 1995. Misexpression of Hoxa-13 induces cartilage homeotic transformation and changes cell adhesiveness in chick limb buds. Genes Dev 9, 2509-2522.

Yokouchi, Y., Ohsugi, K., Sasaki, H., Kuroiwa, A., 1991a. Chicken Homeobox Gene Msx-1 - Structure, Expression in Limb Buds and Effect of Retinoic Acid. Development 113, 431-444.

Yokouchi, Y., Sasaki, H., Kuroiwa, A., 1991b. Homeobox gene expression correlated with the bifurcation process of limb cartilage development. Nature 353, 443-445.

Yu, L., Liu, H., Yan, M., Yang, J., Long, F., Muneoka, K., Chen, Y., 2007. Shox2 is required for chondrocyte proliferation and maturation in proximal limb skeleton. Dev Biol 306, 549-559.

Yu, S., Levi, L., Siegel, R., Noy, N., 2012. Retinoic acid induces neurogenesis by activating both retinoic acid receptors (RARs) and peroxisome proliferator-activated receptor beta/delta (PPARbeta/delta). J Biol Chem 287, 42195-42205.

Yu, V.C., Delsert, C., Andersen, B., Holloway, J.M., Devary, O.V., Naar, A.M., Kim, S.Y., Boutin, J.M., Glass, C.K., Rosenfeld, M.G., 1991. RXR beta: a coregulator that enhances binding of retinoic acid, thyroid hormone, and vitamin D receptors to their cognate response elements. Cell 67, 1251-1266.

Zakany, J., Duboule, D., 2007. The role of Hox genes during vertebrate limb development. Curr Opin Genet Dev 17, 359-366.

Zakany, J., Zacchetti, G., Duboule, D., 2007. Interactions between HOXD and Gli3 genes control the limb apical ectodermal ridge via Fgf10. Dev Biol 306, 883-893.

Zeldin, D., Seubert, J.M., 2007. Structure, Mechanism and Regulation of Cytochromes P450. Molecular and Biochemical Toxicology, 147-172.

Zelent, A., Krust, A., Petkovich, M., Kastner, P., Chambon, P., 1989. Cloning of murine alpha and beta retinoic acid receptors and a novel receptor gamma predominantly expressed in skin. Nature 339, 714-717.

Zelent, A., Mendelsohn, C., Kastner, P., Krust, A., Garnier, J.M., Ruffenach, F., Leroy, P., Chambon, P., 1991. Differentially expressed isoforms of the mouse retinoic acid receptor beta generated by usage of two promoters and alternative splicing. Embo J 10, 71-81.

Zhang, H., Hu, G., Wang, H., Sciavolino, P., Iler, N., Shen, M.M., Abate-Shen, C., 1997. Heterodimerization of Msx and Dlx homeoproteins results in functional antagonism. Mol Cell Biol 17, 2920-2932.

Zhang, X.K., Lehmann, J., Hoffmann, B., Dawson, M.I., Cameron, J., Graupner, G., Hermann, T., Tran, P., Pfahl, M., 1992. Homodimer formation of retinoid X receptor induced by 9-cis retinoic acid. Nature 358, 587-591.

Zhao, D., McCaffery, P., Ivins, K.J., Neve, R.L., Hogan, P., Chin, W.W., Drager, U.C., 1996. Molecular identification of a major retinoic-acid-synthesizing enzyme, a retinaldehyde-specific dehydrogenase. European journal of biochemistry / FEBS 240, 15-22.

Zhao, W.F., Sala-Newby, G.B., Dhoot, G.K., 2006. Sulf1 expression pattern and its role in cartilage and joint development. Dev Dynam 235, 3327-3335.

Zhao, X.L., Sirbu, I.O., Mlc, F.A., Molotkova, N., Molotkov, A., Kumar, S., Duester, G., 2009. Retinoic Acid Promotes Limb Induction through Effects on Body Axis Extension but Is Unnecessary for Limb Patterning. Curr. Biol. 19, 1050-1057.

Zhu, J., Nakamura, E., Nguyen, M.T., Bao, X., Akiyama, H., Mackem, S., 2008a. Uncoupling Sonic hedgehog control of pattern and expansion of the developing limb bud. Dev Cell 14, 624-632.

Zhu, S., Barbe, M.F., Amin, N., Rani, S., Popoff, S.N., Safadi, F.F., Litvin, J., 2008b. Immunolocalization of Periostin-like factor and Periostin during embryogenesis. J Histochem Cytochem 56, 329-345.

Zujovic, V., Thibaud, J., Bachelin, C., Vidal, M., Deboux, C., Coulpier, F., Stadler, N., Charnay, P., Topilko, P., Baron-Van Evercooren, A., 2011. Boundary cap cells are peripheral nervous system stem cells that can be redirected into central nervous system lineages. Proc Natl Acad Sci U S A 108, 10714-10719.

Zuzarte-Luis, V., Hurle, J.M., 2002. Programmed cell death in the developing limb. Int. J. Dev. Biol. 46, 871-876.